AN ELECTROCHEMICAL STUDY ON THE CORROSION OF STEEL IN CONCRETE STRUCTURES IN SEVERE MARINE ENVIRONMENT BASED ON LONG-TERM EXPOSURE TEST

アンドゥリアミサハリマナナ, アンジャティアナ, ルシア, ブラナ

https://hdl.handle.net/2324/4496041

出版情報：Kyushu University, 2021, 博士（工学）, 課程博士
バージョン：
権利関係：

AN ELECTROCHEMICAL STUDY ON THE CORROSION OF STEEL IN CONCRETE STRUCTURES IN SEVERE MARINE ENVIRONMENT BASED ON LONG-TERM EXPOSURE TEST

A DISSERTATION

Submitted to
Kyushu University
in partial fulfillment of the requirements
for the degree of
Doctor of Engineering

by
ANDRIAMISAHARIMANANA
ANJATIANA LUCIA VOLANA

DEPARTMENT OF CIVIL AND STRUCTURAL ENGINEERING
GRADUATE SCHOOL OF ENGINEERING
KYUSHU UNIVERSITY
Fukuoka, Japan 2021

ACKNOWLEDGMENT

"Bless the LORD, O my soul, and all that is within me, bless his holy name!
Bless the LORD, O my soul, And forget not all His benefits."
Psalms 103: 1-2

A long and challenging journey has come to an end; it taught me patience and perserence but it also taught me to give up when it is necessary. From this process, I learned the importance of research and small progress. However, I could have reached this stage without the help and contributions of many. I praise my sovereign God for His providence and guidance during this journey.

I am particularly grateful to my supervisor, Prof. Hidenori HAMADA, who received me in his laboratory and has been of great support during my Ph.D. journey. I could never be thankful enough because of his tremendous help, teaching me to love and enjoy research under his precious guidance. I would like to extend my gratitude to Assoc. Prof. Yasukata SAGAWA and Assist. Prof. Takayuki FUKUNAGA for their valuable help and guidance during my study.

My sincere thanks to the doctoral advisory committee, Assoc. Prof. Shigenobu KAINUMA and Assoc. Prof. Daisuke YAMAMOTO, for their precious times, advices and suggestions for the improvement of this work.

My thanks go to all previous and present concrete laboratory members who never said no whenever I needed help and for the memorable journey I had in this laboratory.

I gratefully acknowledge the support of the Ministry of Education, Culture, Sports, Science and Technology, Japan (MEXT) by awarding the "MOMBUKAGAKUSHO SCHOLARSHIP" without which pursuing my dream to study in Japan could have never been fulfilled.

Last but most importantly, I would like to thank my beloved family who has been great support and motivations for me; listening, comforting, encouraging dispites the 11 km distances. I would like to thank my friends back in Madagascar but also the new friends I encountered here in Japan who made this journey smoother and enjoyable.

From the bottom of my heart, thank you very much!
VOLANA ANDRIAMISA
KYUSHU UNIVERSITY, JAPAN, 2021

ABSTRACT

Concrete is a long-established manufactured material in the civil engineering field worldwide. Concrete is popular due to its extensive versatility, its adaptability, and its relatively low cost. Moreover, the idea of sustainability is a growing appeal in construction fields. Due fast global population growth, the overconsumption of resources along with overproduction of waste have increased. Chloride-induced corrosion is one of the underlying reasons for the deterioration of reinforced steel concrete structures. The financial implications of concrete deterioration are considerable that a sustainable and durable method of prevention and protection is of heightened needs.

In this study, the mechanism of chloride-induced corrosion in concrete is studied. In the first part, the effect of long-term exposure of concrete to a chloride environment is presented. Prevention and repair method are presented in the second half of the thesis. This work will contribute to a comprehensive understanding of the mechanism of corrosion in concrete construction, and to give more insight into the method for repair and prevention of corrosion in concrete construction.

Chapter 1 introduces the background of the research, states the research problem, shows the objectives and the limitation of the study, and finally gives the research contribution and the outline of the dissertation.

Chapter 2 summarizes previous work related to the deterioration of concrete due to chloride attacks. This chapter summarizes the behavior, the mechanism, and the parameters affecting the corrosion of reinforcing steel in concrete. In addition, this chapter considers prevention and repair methods introduced in the past years. Finally, monitoring and assessment methods on steel corrosion in concrete are also detailed.

Chapter 3 presents the research related to concrete in the realization stage. The effectiveness of joint in severely damaged pre-stressed concrete exposed to the marine environment for more than 30 years was investigated. The visual assessment of the specimen without joint treatment reiterated the significance of the use of appropriate joint treatment. From the electrochemical and destructive tests, the outcome showed that both mortar and epoxy resin is effective in treating joints. As cracks of 0.1mm and 0.2mm were targeted for each kind of joint treatment, the results suggest that the fine cracks at the joint could be the

reason for the lower performance of the treated specimen with 0.2 mm crack width. A non-uniform formation of corrosion or macro-cell corrosion was observed with an average distance between the anode and the cathode of about 5 to 10 cm.

Chapter 4 deals with the study of the effect of concrete bleeding on the corrosion of horizontal steel bars, which is a form of deterioration that often occurs in fresh concrete. The results confirmed that the formation of interfacial gaps between the concrete and the steel bars by breezing. In addition, from the void area measurement, it was found that the void areas are more significant on the upper section and in the axial direction of each specimen as the water rise and evaporates from the concrete. The mentioned areas were more prone to corrosion, as per the electrochemical results and the visual observation. To enhance the long-term durability of reinforced concrete under severe marine environments, it is necessary to prevent the formation interfacial gap between steel surface and cement paste.

Chapter 5 proposes a solution to the corrosion of reinforcement and investigates the effectiveness of the use of calcium nitrite in the coating of reinforcement. In the case of the OPC specimen, the effect of the different concentrations of calcium nitrite in seawater mixed concrete is distinguished, unlike the GGBFS specimen. From the half-cell potential results, it is understood that the specimen with steel coating (Series 2) shows more noble potential compared to the specimen without coating (Series 1). From the polarization resistance measurement, Series 2 showed the lower current density than Series 1. In the anodic polarization curve, the effect of calcium nitrite in Series 1 and Series 2 is not distinguished. However, from the cathodic polarization curve and the oxygen permeability, the supply of oxygen in Series 2 is limited than in Series 1. From the experimental work described in this chapter, it became clear that mortar coating system on steel surface before concrete casting could prevent the gap formation and eventually contributes to the corrosion prevention of steel bars in concrete.

Chapter 6 describes the monitoring of repairs method of 40 years severely damaged reinforced concrete beams. The combination of Sacrificial Anode Cathodic Protection (SACP) in the non-patch repair area and polymer mortar in the patch repair area were used. Corrosion inhibitor was added in one of two specimens to check its effectiveness. After three years of monitoring, the results show that the depolarization in cathodic protection still reaches the 100mV criterion, which suggests that the addition of inhibitor has a good effect on the recovery of the potential. Most of the steel surface, with inhibitor showed a potential between -200 mV and -300 mV classified as in an “Uncertain” corrosion zone. On the contrary, the steel without inhibitor showed a less noble potential around the patch repair classified “Uncertain” to “90% corrosion” zone. The potential of steel bars became constant after three years. From three years monitoring of repaired reinforced concrete beams, it is clear that the steel inside concrete became stable condition even in chloride contaminated concrete.

Chapter 7 summarizes the main finding of the study described in Chapter 3 to Chapter 6 and advances recommendations for future works.

TABLE OF CONTENTS

LISTS OF FIGURES

LISTS OF TABLES

CHAPTER I

GENERAL INTRODUCTION

Concrete is a long-established manufactured material in the civil engineering field worldwide. It is popular due to its extensive versatility, its adaptability, and its relatively low cost. It is the first choice when it comes to engineering construction, especially in a wide range of construction like bridges, dams, tunnels. It is recorded to be the world's most used man-made material [Flatt et al., 2012]. It is only second to water in terms of resources, with 4.7 tons of concrete for every person in the world yearly (some 30 billion tons/year) [Mindess, 2019]. Lomborg reports that concrete has become the construction of choice for structures exposed to extreme conditions such as seismic events, weather, chemical attacks [Lomborg, 2001].

Moreover, the idea of sustainability is a growing appeal in construction fields. Due to fast global population growth, the overconsumption of resources along with overproduction of waste has increased. Consequently, coming up with the most durable and environmentally friendly construction involving a lower volume of primary materials, use of renewable energy, less waste is crucial [Georgopoulous and Minson, 2014]. Nevertheless, the manufacturing of concrete, especially Ordinary Portland cement (the most used material in the field: 4.6 billion/year [Mindess, 2019]), accounts among the most significant source of energy-intensive that releases significant percentage of global carbon dioxide emission and greenhouse gases, with nearly 0.84 tons of carbon dioxide per tons of cement [Watts, 2019; Mindess, 2019].

Secondly, water represents 20% of concrete, and the same amount is also used for curing and cleaning during concrete production. Therefore, the extensive use of freshwater will cause a tremendous issue in concrete construction, because, in the coming decades, water scarcity will become a common issue worldwide. According to the study performed by Miller et al., the production of concrete represents 9% of global industrial water (1.7% of total global water), and it is expected that by 2050, 75% of the water demand for concrete production will occur in regions facing water stress [Miller et al.,2018]. Therefore, providing an alternative for freshwater is equally urgent.

Chloride-induced corrosion is one of the underlying reasons for the deterioration of reinforced steel concrete structures. The financial implications of concrete deterioration are considerable that a sustainable and durable method of prevention and protection is of heightened needs. Recently, due to its large potential, both in quality, and accessibility, the use of seawater in concrete has been explored. However, still most existing standards forbid or restrict its usage, especially in reinforced concrete [JGC, 2007]. The principal cause of the prohibition is due to the vulnerability of concrete construction to severe environments, such as Chloride. Studies suggest the amount of chloride ions contained in seawater-mixed concrete is about 3kg/m^3, which is already exceeding the threshold values set in many countries [Otsuki et al., 2014]. If many chloride ions are present in concrete, concrete structures are more prone to corrosion leading to cracks, spalling, and eventually an early deterioration. Consequently, the improvement of the quality and the materials used for concrete construction from production to repair systems are of high importance. Japanese concrete committee reports on the use of seawater in concrete [JCI, 2015].

Several studies were performed to improve the durability of concrete and its sustainability. The use of mineral admixtures in seawater mixed concrete, such as Fly ash and ground granulated blast furnace slag, has been explored to reduce the risk of early corrosion [Adiwijaya et al. 2015; Nishida et al. 2015]. Numerous opinions are in favor of the use of seawater in concrete. However, a deep understanding of the mechanism of concrete exposed to or used with seawater is still required.

In this study, the mechanism of chloride-induced corrosion in concrete is studied. In the first part, the effect of long-term exposure of concrete to a chloride environment is presented. Then, the effect of segregation occurring in fresh concrete is discussed. Prevention and repair method are presented in the second half of the thesis. The studies were more inclined to the electrochemical parameters of the concrete rather than mechanical. This work will contribute to a comprehensive understanding of the mechanism of corrosion in concrete construction, especially exposed to a severe marine environment. In addition, it is expected to give more insight into the method for repair and prevention of corrosion in concrete construction. This study will contribute to enhancing the knowledge of parameters that should be considered before, during, and after the construction of concrete.

THESIS OUTLINE:

This study is divided into 07 chapters, detailed as followed:

Chapter 1 introduces the topic with background concerning the study. The research objectives, the limitations, the contributions of the research are stated in this chapter.

Chapter 2 reports previous works performed related to the field with an extensive literature review. Mainly, the parameters affecting the corrosion of concrete and its mechanisms, several methods for repairs and prevention, implemented, and alternative strategies to monitor and measure corrosion in concrete construction are discussed. Besides, the problems of seawater, the explored work, and the issues raised on the topics are reported.

Chapter 3 describes the study performed to evaluate the effectiveness of joint treatment on the corrosion of steel bars in prestressed concrete beams (corrosion prevention at the initial stage of construction). The presence of joints is an important parameter to be considered at the early stage of construction and casting of concrete. Different types of joint treatment are studied in this chapter and compared to construction without joint and with joints but without treatment.

Chapter 4 deals with a study on the effect of interfacial gaps caused by the settlement of the solid components of the concrete mix during casting on the corrosion of horizontal steel bars. The phenomenon called bleeding is assessed in this chapter using different shapes of horizontal steel bars.

Chapter 5 develops the investigation on the effectiveness of Calcium nitrite inhibitors in concrete. In this study, calcium nitrate is mixed with mortar and used as a coating for seawater-mixed mortar. Different concentrations of CNI are prepared and added to two series of specimens.

Chapter 6 discusses the study executed concerning the repair method of severely damaged reinforced concrete beams using Sacrificial anode cathodic protection (SACP)

Chapter 7 summarizes the output of the research performed in each chapter of this study (Chapter 3 to Chapter 6) followed by some applications and recommendations.

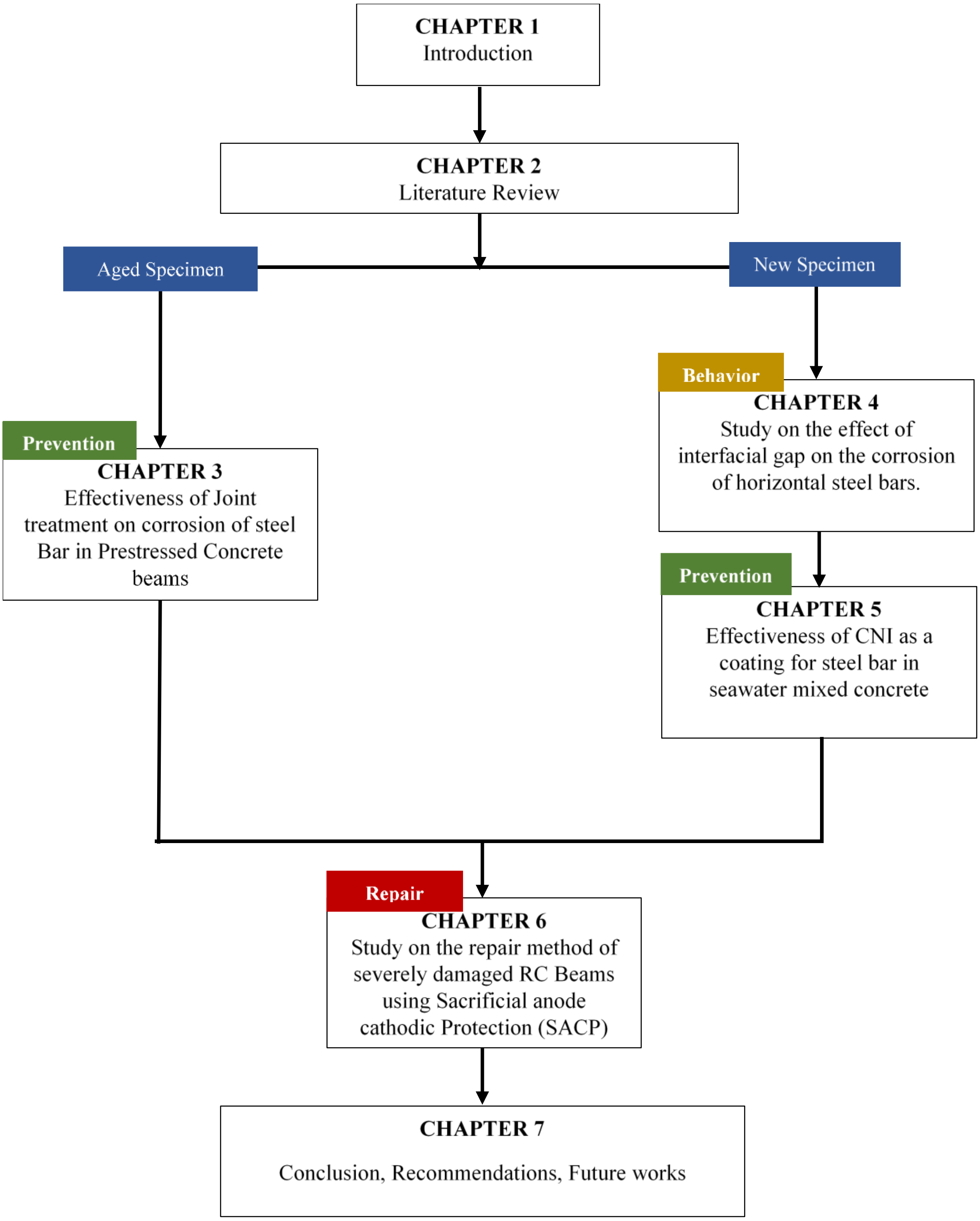

Figure 1.1 Outline of the dissertation

REFERENCES

Adiwijaya, A., Hamada, H., Sagawa, Y., and Yamamoto, D., (2015): Effect of Mineral Admixtures on Carbonation of Seawater Mixed Concrete. *The 2nd Makassar Int. Conf. on Civil Eng.*, Makassar-Indonesia.

Flatt, R.J., Roussel, N., Cheeseman, C.R., (2012): Concrete: an eco-material that needs to be improved. *J. Eur Ceram Soc* 32(11), pp. 2787–2798.

Georgopolous, G., and Minson, A., (2014) Sustainable Concrete Solutions, Wiley Backwell

JGC 16, (2007): Standard Specification for Concrete Structures, *Materials and construction*, Japan Society of Civil Engineers.

Lomborg, B., (2001): The Skeptical Environmentalist: measuring the real state of the world, *Cambridge University Press*, Cambridge, United Kingdom, pp. 512–540.

Mehta, P. K., (2002): Greening of the Concrete Industry for Sustainable Development, *Concrete Int*.

Miller, S.A., Horvath, A., and Monteiro, P.J.M., (2018) Impacts of Booming Concrete Production on Water Resources Worldwide. *Nat Sustain* 1, pp. 69–76.

Mindess, S., (2019): Developments in the Formulation and Reinforcement of Concrete, Architecture *Woodhead Publishing*, pp 3-5.

Nishida, T., Otsuki, N., Ohara, H., Garba-Say, Z. M., (2015): Some Considerations for Applicability of Seawater as Mixing Water in Concrete, *J. of Materials in Civil Eng.* 27 (7).

Otsuki, N., Hamada, H., Takeda, N., Imamoto, K., Yamaji, T., Habuchi, T., and Nishida, T., (2014): Technical Committee on the Use of Seawater in Concrete, *Technical Committee Reports 2014* – JCI-TC121A Digest Edition.

Watts. J., (2019): Concrete: the most destructive material on earth, *the guardian.*

CHAPTER II

INTRODUCTION-LITERATURE REVIEW

2.1 INTRODUCTION

In normal conditions, a good quality concrete has the potential of providing excellent protections for rebars due to the high alkalinity and provided by the concrete that works as a barrier against aggressive agents. The literature on the durability of concrete construction highly suggests that the corrosion of reinforcement has been established as the predominant determinant inducing the early deterioration of concrete construction across the globe. This issue is known to be more concerning in the case of construction nearing the coastal areas. Chloride attack is a major cause of corrosion of reinforcement. It is widely known that seawater reacts with the hydration products of the concrete leading to the corrosion of steel bars and the degradation of the concrete.

Deterioration is defined as "the process that adversely affects the performance of a structure over time due to defects and damages occurred by naturally occurring chemical, physical or biological actions repeated actions such as those causing fatigues, normal or severe environmental influences, and wear due to use, abuse and others." JSCE standard specification. In the current chapter, literature concerning the corrosion of reinforcement, namely the phenomenon of chloride-induced corrosion, established methods for investigation, the methods of prevention, and some repair strategies are summarized.

2.2 DURABILITY IN CONCRETE

2.2.1 The notion of durability in concrete

The JSCE Standard 2007 defines the durability of concrete structures as its resistance to the time-dependent deterioration of materials in the structures caused by expected aggressive agents such as the weather, the intrusion of chemicals, and erosion by chemicals (*Figure 2.1*) [JSCE, 2007]. To attain this required performance and maintain it during the designed service life of the structure, the prevention of material deformation due to aggressive environmental action has become a common practice. Durability is an essential requirement when designing concrete structures, along with strength and quality.

The resistance to corrosion of reinforcement is an additional concern in reinforced and prestressed concrete structures. Among the most common issues jeopardizing the durability of concrete structures is the effect of carbonation and chloride attack. The statistics record that 70 – 90% of the investigated cases corrosion was the dominant degradation mechanism [BCA,1997; FIB, 2011].

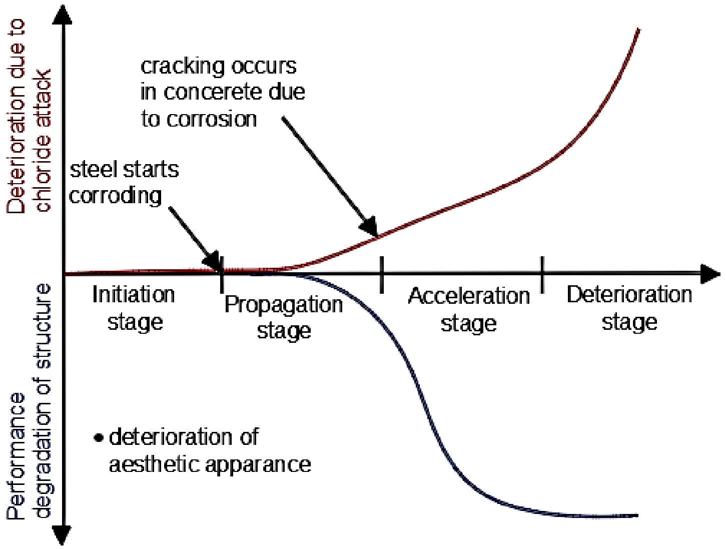

a. Focused on aesthetic appearance and landscape

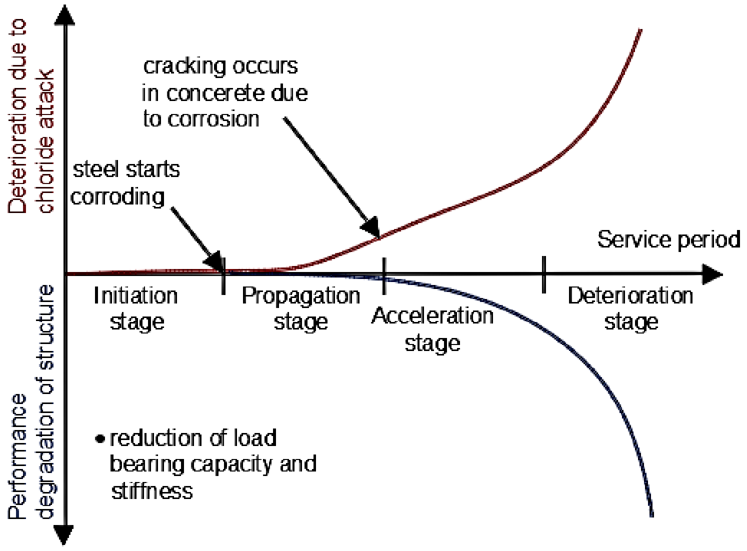

b. Focused on safety

Figure 2.1 Service life model according to the JSCE Standard 2007- Maintenance

2.2.2 Corrosion process

The Japan Society of Civil Engineers (JSCE) has classified the deterioration of concrete structures due to chloride attack into 4 distinctive stages [JSCE Maintenance, 2007].

- *Initiation:*

The stage of initiation of corrosion concerns the stage until the concentration of chloride ions on the surface of the steel reaches the marginal concentration for the occurrence of corrosion, which will lead to the break of the protective film [Bertolini et al., 2012; Poursaee, 2016]. According to the standards set by the JSCE, it is fixed at 1.2 kg/m3. The stage is determined by the number of chloride ions diffused in the concrete and the chloride initially contained in the original mix.

- *Propagation*

The stage of propagation of corrosion is marked by the initiation of the corrosion of the steel and the formation of cracks at the interface concrete-steel. Studies showed that corrosion products formed on the surface of the steel bar can generate tensile stresses until 490 MPa [Hoke et al, 1983; Hladky, 1989]

- *Acceleration*

The stage of acceleration is the stage when the steel corrodes at a higher rate. Cracks will form in several directions of the concrete due to the expansion of the volume of the corroded steel. Rust stains and cracks appear on the surface of the concrete

- *Deterioration*

As the cracks reach the surface of the concrete, the infiltration of water, oxygen, and aggressive agents are more facilitated leading to a faster corrosion rate, an eventual spalling of the concrete, and exposition of the rebar. *Figure 2.2* illustrates the progress of corrosion of reinforcement in concrete due to corrosion.

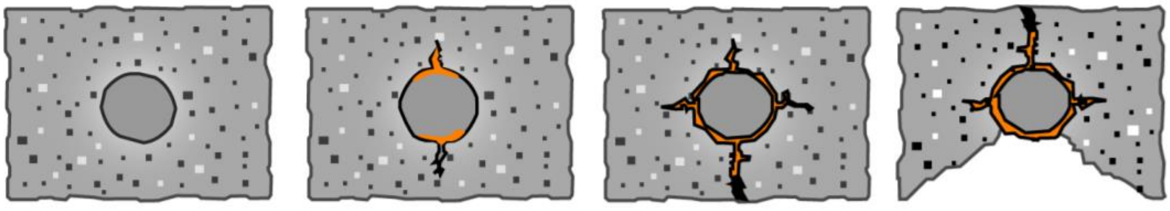

Rebar in concrete before corrosion

Build-up of corrosion products

Further corrosion: surface crack, stain appears

Eventual spalling: corroded bar exposed

Figure 2.2 Different stages of the corrosion of steel in concrete

Table 2.1 Criteria for diagnosis of deterioration degree

Evaluation points	**Deterioration Level**					
	0	**1**	**2**	**3**	**4**	**5**
Corrosion of steel bar	None	Rust spots on the concrete surface	Partial rust stains on the concrete surface	Significant rust stain	Significant floating rust	Drastic surge of the amount of floating rust
Cracking	None	Partial cracks on the concrete surface	Some cracks	Many cracks, in the range of mm or more width	Many cracks of several mm in width	-
Spalling covering concrete	None	None	Partial floating concrete	Partial spalling	Significant spalling	Drastic spalling

2.2.3 Corrosion mechanism

The sciences and engineering of steel have more than five hundred years of history, unlike other areas related to construction technology and building materials. As a result, a large number of documents are available on the topic. However, in terms of the durability of reinforced concrete, the processes are rather slow as it requires a time frame of decades to manifest, which makes the long-time documentation highly valuable [Ueli,2018]. However, as mentioned earlier, the corrosion in concrete is a lead factor in the deterioration of concrete structures. Thus, it is essential to understand its mechanism.

a. Definition

Corrosion is the phenomenon by which metals return to their mineral states. It is also defined as the destruction of metals or alloys due to chemicals and electrochemical reactions. It is the process by which the metal passes from its metal states at zero valences to its oxidized states, and electrons are released. Corrosion can be classified into two groups. Wet corrosion is corrosion that occurs in the presence of moisture, and dry corrosion takes place due to corrosive gases. The area of interest of this study is limited to the first one, as only this one is relevant in concrete structures in the marine environment.

b. Passivity film and passivation

Passivity is the state where the rate of corrosion of the steel is low following the formation of passivity film. After the casting of the concrete and if steel is embedded, a self-generated protective film, also called "*passivity film*" forms due to the reaction of hydration of concrete and its high alkalinity [Duval,1992; Saremi and Mahallati, 2002]. Nevertheless, their proprieties are not clearly understood due to their fineness and complexity in analysis.

The passivity film is a relatively fine protective ferric oxide (g-Fe2O3) or hydroxide layer, usually inferior to 10nm [Richardson, 2002; Page, 1997]. It also depends on the high alkalinity environment of the concrete at a pH of around 12 to 13 [Hunkeler, 2005; Haleem et al., 2010]. Its main action is to protect the rebar against corrosion by reducing the corrosion attack to negligible values. This passivity layer does not stop corrosion on itself; nonetheless, it significantly reduces the rate of corrosion. For steel embedded in concrete, the passive corrosion rate is at 0.1µm/year. Without the passivity film, the rate of corrosion is recorded to be 1000 times higher [ACI 222, 2001]. Besides, corrosion takes place when this film is penetrated.

The passivation of the steel in concrete is a function of potential and pH, illustrated by the diagram of Pourbaix [Pourbaix, 1973]. It is noteworthy that the steels used in concrete are generally iron-based alloys rather than pure irons. Therefore, it contains some impurities. In addition, the interstitial solution of concrete consists of different ions (Ca^{2+}, Na^{+}, K^{+}, SO_4^{2-}). However, it can be assumed that quantitatively, the passivation phenomenon is comparable for the Fer/water system and Steel/interstitial solution.

From the Pourbaix diagram of Fe-H_2O system, it shows that stable oxides resistant to corrosion are formed on the surface of the steel at a highly basic solution and that corrosion occurs after a decrease of pH [Ahmed, 2006]. *Figure 2.3* can be classified into 3 zones:

- Immunity zone: the steel is not reacting, it is in the stable state (Fe).
- Passivity zone: the ferric oxides which protect the steel are in stable condition (Fe_2O_3, Fe_3O_4).
- Corrosion zone: the steel can be dissolved in ions form (Fe^{2+} and Fe^{3+}).
- thermodynamic stability of water at atmospheric pressure: region delimited by parallel straight lines, in dotted lines.

This equilibrium diagram of the iron / H_2O system shows the formation of stable oxides on the surface of iron in solutions with strongly basic pH and can predict corrosion reactions when the pH is lowered.

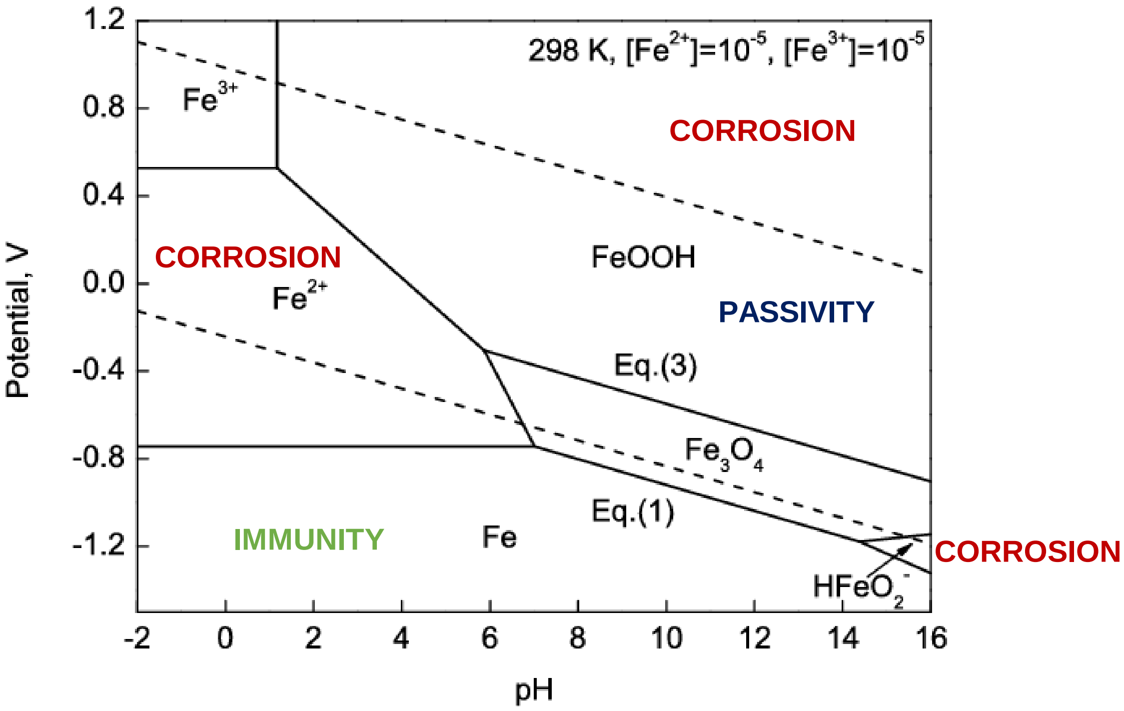

Figure 2.3 Pourbaix diagram of Fe-H_2O system at 25°C and 1atm [adapted from Pourbaix,1973]

In basic conditions (pH>8), hardened concrete provides a safe and protective environment for steel. It was shown that concrete with a pH of around 12.4 is the best condition for the formation of the passive film. In acidic conditions, steels are unprotected, and the Fe easily dissolve into Fe^{2+} et Fe^{3+}.

Table 2.2 Influence of the pH on the corrosion of steel

pH	**Condition**	**Passive state**
pH < 8	Formation of ions Fe^{2+} et Fe^{3+}	Unprotected
pH > 8	Basic condition	Protected
10>pH>12.4	Basic condition	Best condition

However, as aggressive agents accumulate, essentially chloride, the protective film is broken, and the corrosion is initiated in concrete. The reactions occur in two areas:

- *the anode*: the corroded area or at the place of metal loss
- *the cathodic area*: the passive area and the oxygen dissolved in water can accept electrons.

c. Chemical reaction:

Hunkeler [Hunkeler, 1994] summarizes the four conditions required for a corrosion process to be fulfilled and maintained as seen in *Table 2.3*.

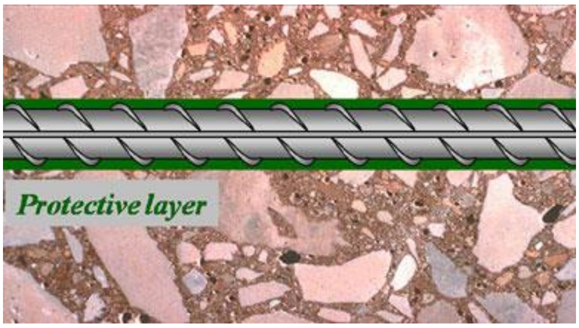

Figure 2.4 Illustration of the self-generated passivity film

Table 2.3 Conditions for corrosion of steel progress in concrete

Condition for corrosion of steel in concrete	**Requirements**
An anodic reaction is possible	The passive layer of the steel bar broke down and depassivation of the steel occurs. This can be caused by carbonation of concrete due to the decrease of pH of the pore water and ingress of chloride into the concrete, reaching a critical level.
A cathodic reaction is possible	Oxygen as the driving force of the corrosion process is available at the interface of the reinforcement in a reasonable amount.
A flux of ions between the site of the anodic reaction and the site of the cathodic reaction is possible	The environment or electrolyte between the site of the anodic reaction and the site of the cathodic reaction conducts well.
A flux of electrons is possible	There is a metallic connection between the sites of anodic and cathodic reactions. For monolithic reinforced concrete structures this condition is usually fulfilled.

Following the break of the passive film, corrosion reaction will start in concrete. In the anode, the steel in concrete oxidize and dissolves in the pore water, and gives up some electrons (*Equation 2.1*).

- $Fe \rightarrow Fe^{++} + 2e^{-}$ **(2.1)**

In the cathodic area, the electrons (2e-) released by the anodic reaction are consumed with Oxygen and water to preserve the electrical neutrality on the surface of the steel bar (Equation 2.2). From the cathodic reaction, hydroxyl ions (OH^-) are generated.

- $4e^{-} + 2H_2O + O_2 = 4OH^{-}$ **(2.2)**

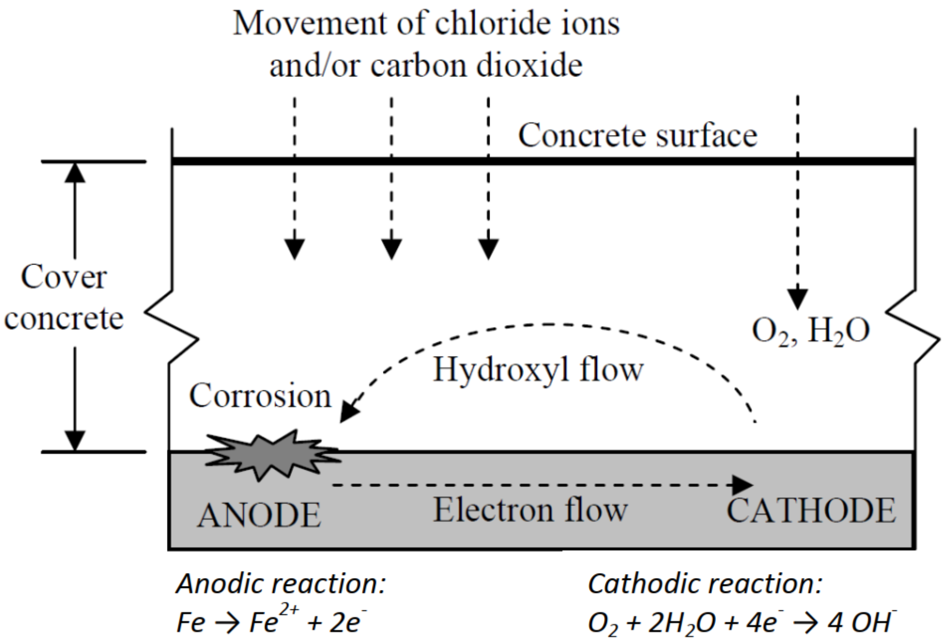

Figure 2.5 Anodic and cathodic reaction [Mackechnie et al, 2001]

Figure 2.5 illustrates the reactions occurring in the anode and cathode during the corrosion of steel in concrete. In high alkaline conditions, hydroxyl ions (OH^-) in the interstitial react with the ferrous ions (Fe^{2+}) (Equations **2.3**), and precipitate at the surface of the steel into ferrous hydroxide when the concentration of ion (Fe^{2+}) is high. Equations 2.1 and 2.2 are not enough to form rust in concrete, however, they are principal reactions in corrosion. However, the full process of corrosion leads to the formation of $\boldsymbol{Fe_2O_3}$ **(Rust)** as seen in Equation 2.5. It is noteworthy that these reactions do not progress unless water H_2O and O_2 are present in the cathodic area.

- $\boldsymbol{Fe^{2+} + 2(OH)^- \rightarrow Fe(OH)_2}$ (Ferrous hydroxide) **(2.3)**
- $\boldsymbol{4Fe(OH)_2 + 2H_2O + O_2 \rightarrow 4Fe(OH)_3}$(Ferric hydroxide) **(2.4)**
- $\boldsymbol{2Fe(OH)_3 \rightarrow Fe_2O_3.H_2O}$(Hydrated ferric oxide/rust) **(2.5)**

Red rust is the ‘normal’ product of the reaction in corrosion. In some cases, due to the lack of oxygen, and if the anode and the cathode are distant from hundred millimeters, the iron Fe^{2+} will remain in the solution. In contrast to “Red rust”, “Black rest” does not cause expansion of the volume of the steel nor crack, therefore, there is less possibility for the corrosion to be detected.

However, black rust is known to be more mechanically stable and provides better corrosion protection than red oxide (rust) Fe_2O_3. That product of corrosion is often observed in structures protected from wind and sunlight, in underproof membranes, and under water-saturated conditions.

Table 2.4 Nature of the product of corrosion

Equation	Products
$2Fe(OH)_2 + \frac{1}{2}O_2 \rightarrow Fe_2.H_2O + H_2O$	Red rust
$2Fe(OH)_2 + \frac{1}{2}O_2 + H_2O \rightarrow 2Fe(OH)_3$	
$3Fe(OH)_2 + \frac{1}{2}O_2 \rightarrow Fe_3O_4 + 3H_2O$	Black Rust
$2FeO + \frac{1}{2}O_2 + H_2O \rightarrow Fe_2O_3.H_2O$	Red rust
$2FeO + \frac{1}{2}O_2 + 3H_2O \rightarrow 2Fe(OH)_3$	
$3FeO + \frac{1}{2}O_2 \rightarrow Fe_3O_4$	Black Rust

From *Figure 2.6*, it is understood that the corrosion product $\boldsymbol{Fe_2O_3}$ has a volume about twice that of the pure iron **Fe** when fully dense. As a result, when this product is hydrated, it expands even more. This increase of volume in steel can reach up to 6 to times their initial volume. Due to the expansion in the volume of steel, cracks occur in concrete, and rust stains can be observed at the surface of the concrete [Andrade, 1989; Rodriguez, 1996].

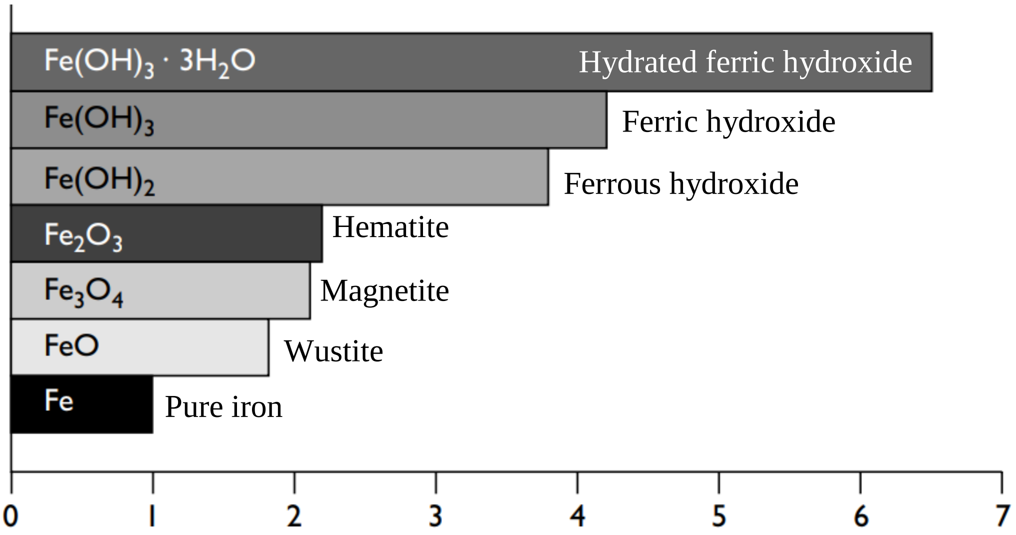

Figure 2.6 Relative volume of iron corrosion and its reaction product [modified from Mansfield, 1981]

d. Corrosion morphology

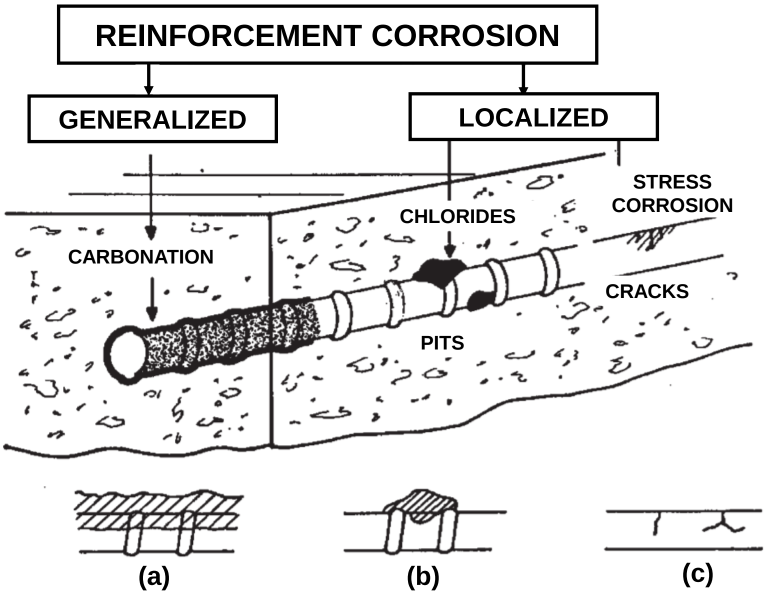

Figure 2.7 Corrosion morphology

Corrosion in steel may be presented in different forms as presented in *Figure 2.7*. First, it can be by a uniform dissolution of a large or whole surface of the steel, also called *generalized corrosion*, which is common in carbonation-induced corrosion (*Figure 2.7.a*). That form of corrosion leads to early cracking and spalling of concrete but often with comparatively little reduction of the cross-section of the steel reinforcement. The following reaction presents the loss of alkalinity in concrete due to carbonation.

- $CO_2 + Ca(OH)_2 \xrightarrow[H_2O]{} CaCO_3 + H_2O$ **(2.6)**

The second form of corrosion is called *localized corrosion*. It is frequent in steel due to chloride attack (pitting corrosion, *Figure 2.7.b*) and stress corrosion (*Figure 2.7.c*) [Andrade, 2007; Arup, 1983]. The formation of localized corrosion shows the separation of the anodic reaction and the cathodic reaction to form a macrocell [Broomfield, 1997]. Localized corrosion can, however, lead to significant loss of cross-section of the rebar before warnings of deterioration are observed on the surface of the steel.

When irons react with water and Chloride, it results in the formation of hydrochloric acid. It leads to a significant decrease in the pH to acid values, which is an aggressive environment for steel reinforcement [Arup, 1983].

- $Fe^{2+} + 2Cl^{-} + 2H_2O \rightarrow Fe(OH)_2 + 2\ HCl$ **(2.7)**

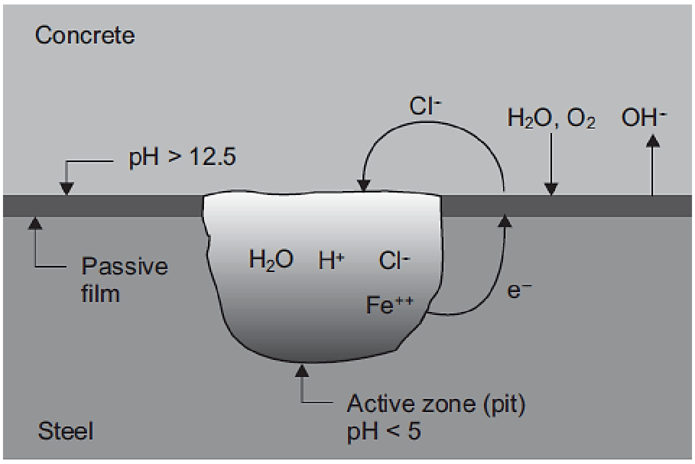

Figure 2.8 Schematic of a steel bar in Reinforced concrete exposed to Chloride [Le,2010]

2.2.4 Chloride induced corrosion

As above-mentioned, chloride is a major cause of the deterioration of steel reinforcement in concrete in many locations across the globe. Chloride ions are harmful to concrete as their accumulation leads to the disruption of the passive layer, leading to corrosion.

a. Effect of chloride attacks

Chloride ions may be present in concrete due to several reasons. On one hand, it can be incorporated from the original mix of concrete, such as contaminated aggregates, use of seawater as mixing water, or by admixtures. On the other hand, they can penetrate from outside. Marine environments and the use of deicing salt in road are claimed to be the two main sources of chloride in concrete structures [Andrade, 2007].

Generally, dry concrete absorbs salty water very rapidly due to capillary action called suction, for instance, concrete exposed to tidal or splash marine environment. Particularly, the succession of wetting and drying is accelerating the ingress of corrosion. From past studies, it was shown that the presence of an excessive amount of chloride ions in the original mix results in a more aggressive action, therefore to a higher corrosion rate than when the same amount of chlorides has infiltrated into the concrete during its service life [Lambert et al., 1991]. Hunkeler summarizes the fourfold effect of chlorides in reinforced concrete as follows [Hunkeler, 1994]:

- Destruction of the passive film of the rebar and initiation of corrosion
- Reduction of pH of the pore water as chloride reduces the solubility of $Ca\ (OH)_2$.
- Increase of the moisture content of the concrete due to the hygroscopic properties of salts present in concrete.
- Increase of the electrical conductivity of the concrete.

b. Threshold of chloride

The threshold of chloride in the *original mix* of concrete is influenced by several parameters internal and external to concrete which made the identification of a single threshold complex [Hausman, 1968]. The principal factors influencing this parameter are summarized as followed:

- The type of cement: the fineness of the cement, the C_3A content of cement, etc... C_3A content has a good effect on the threshold of chloride content. According to Hussain et al., increasing the C_3A content of cement from 2.43% to 14% raises the threshold chloride content 2.85-fold [Hussain et al., 1995]. Nonetheless, the excess of C3A in concrete can lead to other deterioration in concrete, such as sulfate-induced deterioration.
- Cementitious materials: GGBFS is known to increase the binding of chloride in concrete due to the high alumina content, which promotes the formation of Friedel's salt [Bakker 1988; Dhir, 1996]. Fly ash has the same effect by increasing the chloride binding capacity of the cement [Arya1990; Dhir and Jons, 1999]. Studies showed that partial replacement of cement to silica fume improves the passivation process of the steel and increases the corrosion resistance despite the lowering of pH value and concentration of calcium hydroxide caused by cementitious materials [Ortlolan, 2016].
- The moisture contents: as dry concrete restricts the electrolytic corrosion process, and the content of water influences the chloride concentration [Angst and Vennesland, 2007].
- The availability of oxygen: as above-mentioned, oxygen and water are essential for corrosion to progress. The transportation of oxygen through concrete is also influenced by the relative humidity of the concrete [Tuutti, 1982]. As the potential of steel reduces the limitation oxygen content, the threshold of chloride in concrete is lower in concrete in tidal or splash zone compared to dry concrete.
- The water to binder ratio: it was suggested that concrete with lower water to cement ratio has higher resistance against the penetration of chloride. As a result, it has a higher chloride threshold value [Petterson 1992, 1994; Scott, 2004].
- The pH value of the pore solution: the pH is a crucial inhibiting factor in the concrete as high pH leads to the formation of the protective film [Angst and Vennesland, 2007]. In addition, high pH values also influence the binding effect of chloride. A high value of pH (> 12.6) leads to the increase of bound chloride in concrete [Glass et al., 2000; Reddy et al., 2002].

The ACI committee limits the content of water-soluble chloride ions in the original mix as described in *Table 2.5*. Apart from the mentioned factors, the curing, and the compaction process. The literature showed that extension of wet curing preserves concrete against high corrosion rate because it reduces the ingress of aggressive agent at an early age and improves the quality of the concrete cover [Khanzadeh-Moradllo et al., 2015].

Table 2.5 Chloride threshold expressed as percentage by weight of cement [ACI 318,2002]

Concrete	**Exposure condition**	**Chloride limit**
Prestressed concrete	All	0.06
Reinforced concrete	Moist environment and exposed to external chloride	0.10
	Moist environment but not exposed to external chloride	0.15
	Dry/Protected from moisture	1.00
	Other	0.30

Japanese standards specify the threshold of chloride according to the *total chloride* content in concrete at 0.3kg/m^3 (0.1kg/m3 by weight of cement); which is rather stringent compared to other standards [JSCE, 2007; JIS A 5308, 2014]. The JSCE limits the threshold of chloride for corrosion initiation regardless of the type of concrete and its mix proportion at 1.2 to 2.4 kg/m3 [JSCE-Maintenance, 2007].

Horiguchi et al. summarize the challenges while determining the chloride threshold for *corrosion to initiate* as followed: (1) the uncertainty between laboratory simulation and the actual concrete. (2) The complexity of the determination of the actual time of corrosion initiation in concrete. (3) The variation of results even at the same setting of tests. Concerning the threshold for corrosion in Ordinary Portland cement concrete to initiate, Horiguchi et al., estimated in their study to be around 1.6kg/m3 to 3.6kg/m3 [Horiguchi et al., 2020].

c. Bound chloride

Not all forms of chloride in concrete are harmful to concrete. Through the reaction with the C3A, Calcium chloroaluminate ($3Cao.Al_2O_3$, $CaCl_2.10H_2O$), also called *Friedel's salt*, is formed in concrete which is the main form of bound chloride ions. As stated in the previous paragraph, the content of bound chloride ions depends on the content of C3A and the type of cementitious material used. Therefore, if some quantity of chloride ion is present in the concrete during mixing, they could be bound by the reaction with C3A, and become harmless. Similarly, to a small extent, this reaction can occur when chloride ingress in the concrete during the service life. Yet, these bound chlorides can be dissociated under some conditions, for instance, due to the carbonation of concrete, and become aggressive [Ho and Lewis, .1988]. The dissociation of Friedel's salt is due to the decrease in pH in the pore solution of the concrete [Glass et al., 1991].

2.2.5 Corrosion of prestressed concrete

The corrosion in Prestressed Concrete (PC) is rather scarce compared to the corrosion in Reinforced Concrete (RC). Consequently, less attention is brought to the investigation of deterioration of PC structures [Vecchi et al, 2021]. On one hand, high-strength materials are usually used in prestressed concrete, such as concrete with lower water to cement ratio and reinforcement or wire with very high strength. Therefore, the quality and resistance to corrosion are rather high.

Manning and Pfeifer et al. showed that the fundamental mechanism of corrosion in prestressed concrete structures is similar to the mechanism of corrosion in Reinforced concrete [Manning, 1988; Pfeifer, 1994]. However, if corrosion occurs in PC structures, the consequences can be more brittle and dangerous than in RC concrete. The reason for this is because, unlike RC concrete, continuous loading is applied to PC due to the prestressed effect. In addition, PC can be composed of several wires, called strands, if cross-section loss due to corrosion occurs, its failure can be easier.

In addition, unlike in RC structures, the time-lapse between some warnings or signs of corrosion and the brittle failure of the structures are relatively smaller in PC structures. Studies showed that the damages cause by the corrosion of prestressed concrete can be as significant as 4 to 5 times the damages engendered by the corrosion of reinforced concrete [Yamaoka and Tanaka, 1994]. The higher the strength of the prestressed concrete, the higher the level of damage it may cause and its sensitivity if corrosion occurs.

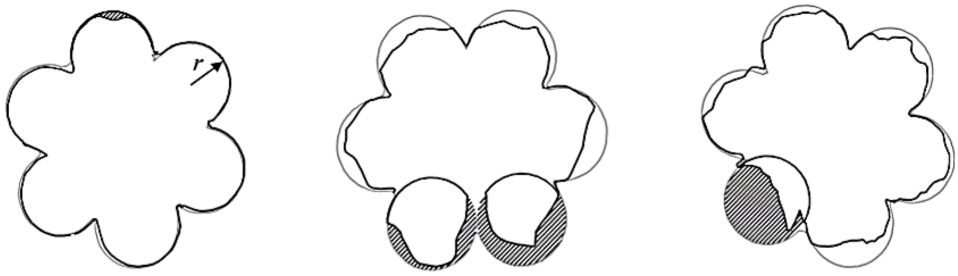

Figure 2.9 Pitting corrosion in prestressed concrete [Jeon et al., 2019]

Some studies performed by the Port and Airport Research Institute Japan showed that after 10 years of exposure to chloride environment, no change in the load-bearing capacity was observed despite the slight corrosion of the prestressing tendon and the severe corrosion of the anchorage. In addition, the corrosion prevention capacity of the prestressed beams studied was judged similar to reinforced concrete [Hamada et al., 1988].

Upon 20 years of exposure to a severe marine environment [Yokoto et al., 1999a; 1999b; Watanabe, 2001], it was shown that the compressive strength of the young modules was almost unchanged from the initial values. In addition, in terms of mechanical properties, the beams were judged to be in "good to excellent" conditions even after 23 years of exposure. Moreover, no significant effect of the application of pre-crack in the concrete was found. Nonetheless, a decrease in the load barring capacity was observed in the beams, even lower than after 10 years of exposure.

2.3 PARAMETERS AFFECTING THE CORROSION IN CONCRETE STRUCTURES

The corrosion of reinforcement in concrete depends on the properties of the steel, the concrete, and the properties existing at their interface. Environmental factors do not have direct impacts on corrosion, however, they can enhance the deterioration of the concrete. Apart from the significant effect of chloride in concrete, the presence of cracks, joints, and interfacial gaps are also significant factors influencing the corrosion of reinforced concrete.

2.3.1 Cracks

Cracks in concrete structures are the result of the effects of mechanical loadings and environmental conditions. The formation of cracks on the surface of concrete structures with a width beyond the established threshold is a leading cause of local corrosion of steel in concrete. Petterson in his study reported that macrocracks of 0.1mm to 0.8mm can significantly enhance the transportation of chloride in concrete, therefore has an impact on the chloride threshold as well [Petterson et al., 1996]. This is since the cracks in concrete facilitates the ingress of chlorides, moistures, and oxygen in the concrete as a result to foster corrosion.

Studies show that when concrete with cracks is exposed to chloride condition, the steel in the crack areas are active to corrosion while the rebar in the uncracked area remained passive [Suzuki,1999; Jaffer, 2008]. Though it is common knowledge that all reinforced concrete in service virtually shows some cracks, cracking in concrete could be controlled by accurate structural design, detailing, and construction procedures [Neville,2011].

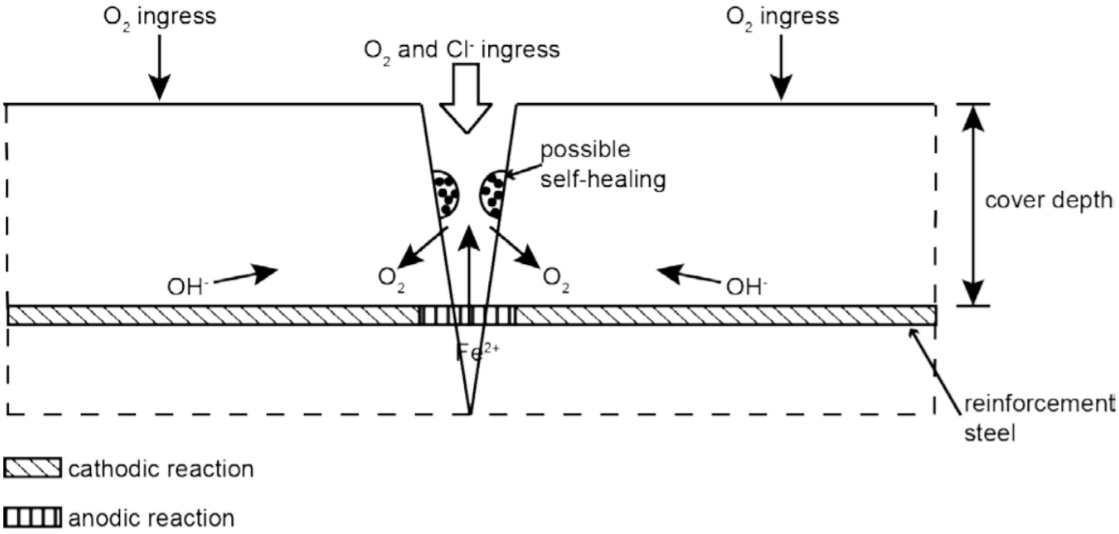

Figure 2.10 Schematic of corrosion cells formed in cracked concrete [Kathler et al., 2017]

In reinforced concrete, the Japan Society of Civil Engineering and the American Concrete Institute has limited the allowable crack width to 150 to 300 µm [JSCE, 2007; ACI 224R, 2001]. When exposed to seawater or marine environment, the maximum with of cracks permitted by the ACI is limited to 150 µm, and 180 µm for deicing chemical exposure. Other literature has set the allowable cracks to 0.1mm to 1mm [Rehm and Moll, 1964; Schiessl, 1976]. It was shown that corrosions are formed directly on the area of the crack unless the concrete is carbonate. In addition, the level of corrosion is found to increase with the increase in the width of cracks [Tuutti, 1982].

Prestressed concrete structures are designed to be cracks-free due to their higher vulnerability to corrosion and deterioration. In such concrete, the occurrence of corrosion is shown to be significantly reduced [Poston, 1984]. However, cracks will eventually occur in the long-term. Once the concrete is cracked, it becomes entirely vulnerable to atmospheric effects. In their study, Moore et al. showed that with a crack width of 0.1mm, pitting corrosion was observed on the prestressing steel [Moore et al., 1970]. In contrast, Perenchio et al. showed in their studies that severe corrosion was found on both cracked and uncracked concrete [Perenchio et al., 1989].

2.3.2 Joints

Joints in concrete are necessary for various reasons. The use of joint is not always harmful. For instance, it is an effective method of preventing the formation of virtual cracking in concrete. Sizeable structures not provided with appropriate joint to accommodate shrinkage will eventually create a joint on its own [ACI 224R-01, 2001].

Nonetheless, joints present some adverse effects on the durability of the concrete. Hamada et al. reported that, in atmospheric conditions, joints work pathways for aggressive agents into the concrete, like carbon dioxide, oxygen, and chloride. As a result, macrocell corrosion was observed nearing the joint [Hamada et al, 1987]. In terms of corrosion probability, studies showed that a significantly lower potential was observed around joints, which suggests the seriousness of the corrosion around the joint unless appropriate treatment is done [Mohammed &Hamada, 2003].

2.3.3 Interfacial gap

Bleeding is a form of segregation often occurring in fresh concrete due to the settlement of the solid composites of the concrete (aggregates, sands). Water often rises while other mixtures go down because it has the lowest specific density. Studies showed that this bleeding can reach up to 20% of the mixing water [Schwamborn, 1987]. Consequently, as the water rise, it leads to (different) types of segregation:

- Uneven water to cement ratio in the same structure, the lower part will have lower water to cement ratio, but the higher part will have a higher w/c.
- Formation of voids: as water rise, it will be trapped under horizontal steel reinforcement and other solid constituents. As the concrete hardened, the water will evaporate. However, voids will remain under the horizontal steel bar (*Figure 2.11*), especially for tall structures or rebar located at a high position. Water paths are also formed around the steel and on the surface of the structures. Because the voids will be formed in the same direction, it will result in the formation of a zone of weakness [Soshiroda, 1990].
- Corrosion of steel: because the rebar on the side of the void is not in contact with the concrete, passivity film is not formed, and corrosion can easily occur [James, 1991]. Horizontal steel bars are the main target of the effect of the corrosion of interfacial gap [Baccay, 2004, Mohammad and Hamada 2003b,2006,2008].

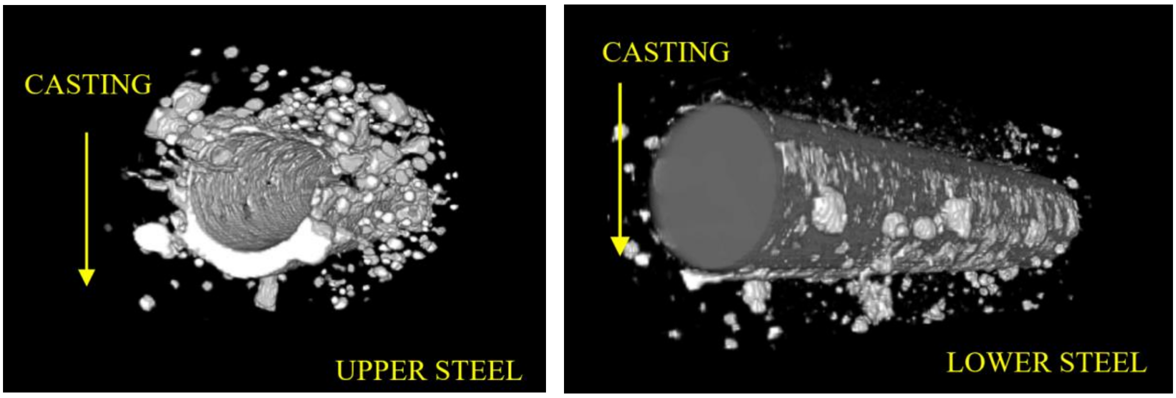

Figure 2.11 CT Scan of void under steel bar [Ikeda et al., 2013]

2.3.4 Environmental conditions

Environmental conditions are also classified as a significant factor affecting the corrosion of the steel bars, namely, environment with high exposure to moisture, carbonation, chloride, and temperatures. In his report, Tuutti showed that steels are generally protected by concrete. Therefore, only particles smaller than concrete pores can penetrate and can be considered harmful to the reinforcement [Tuutti, 1982]. Gases, liquids, and ions born by liquids are considered among the particles that can infiltrate into concretes.

2.4 CORROSION INSPECTION, ASSESSMENT, MONITORING

To detect and monitor the corrosion in concrete structures, several types of non-destructive monitoring and inspection techniques have been established, in addition to visual observations and destructive tests. The corrosion mechanism is electrochemical; thus, electrochemical methods are the most adequate to assess the risk and rate of corrosion in reinforced concrete [Andrade, 2020]. It is a standard and most used method in the monitoring of corrosion. According to the Japan concrete institute, when performed appropriately offers reliable and effective technique in maintenance and operation of real and laboratory concrete structures [JCI,2015].

The earlier the corrosion is detected, the less enormous the expenses are because suitable actions could be undertaken at the appropriate time. With time, little rusts in the reinforcement will increase, expending the initial volume of the steel bar (it can reach 8 times the initial volume of the steel), the micro-cracks in the concrete will become spalling. A proper monitor and inspections are therefore of high importance in concrete construction. During experiments, the following electrochemical measurements are mainly used: half-cell potential, polarization resistance, electrical resistivity, and polarization curve.

2.4.1 Half-cell potential

a. Definition

The corrosion potential is a measure of the ease of electron charge transfer between the steel and the cement pore water solution (half-cell, concrete) [Stratful, 1967]. Therefore, it is a property of the steel and the concrete interface not of the steel itself [Hansson, 1984].

Half-cell potential is acknowledged by many researchers and standards as the main method to detect the tendency of corrosion in concrete structures [JSCE, 2007; Song, 2007]. It determines the progress of corrosion of steel by identification of the difference in potential the steel develops on contact with the environment by nondestructive methods. In the case of reinforced concrete structures, the concrete acts as an electrolyte; conducts electric current.

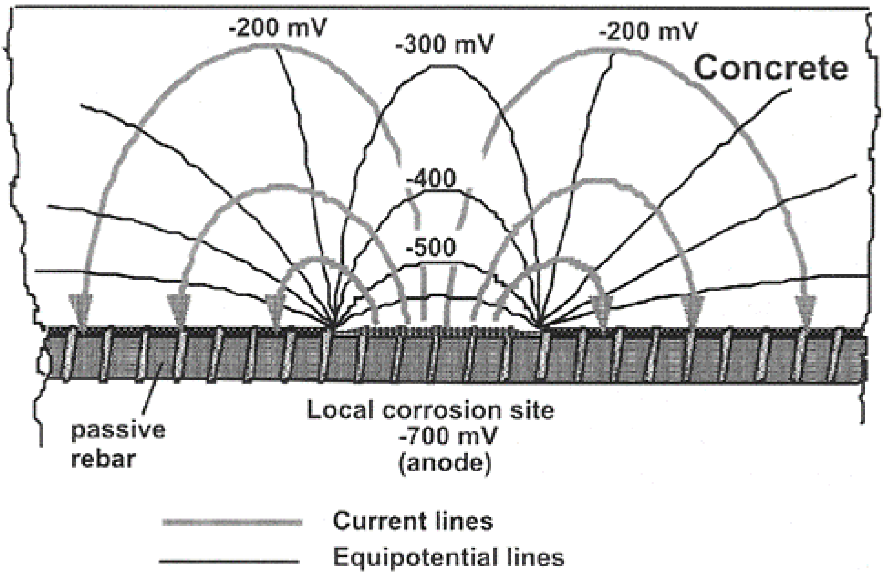

Figure 2.12 Schematic of the electric field and current flow in macrocell in concrete [Elsener, 2003]

b. Measurement methods

The measurement of Half-cell potential is usually performed using a high impedance voltmeter (at least 10MΩ) and a reference electrode, for instance, a saturated calomel electrode (SCE) [Elsener et al., 2003]. During the measurement, a water-soaked sponge is put at the connection of the electrode and the surface of the concrete to work the electrolytic connection. Sometimes, for laboratory setups, the reference electrode is immersed in the exposure solution.

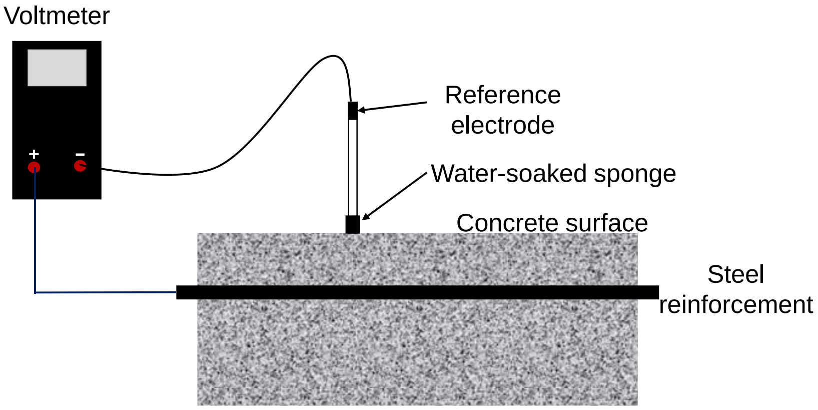

Figure 1.13 Setup of Half-cell potential measurement

Surface preparations are required for a good and stable electrical connection (adrift of potentially less than 20mV), which include the removal of rust in the connection with the rebar, cleaning of the surface of the concrete, and prior wetting of the surface of the concrete (at least 30 min, and at least 1 hour for specimen immersed in seawater). Tape water is usually used for the preparation and when available, the addition of detergent is recommended. (*Figure 2.13*) shows the setting of the half-cell potential. The steel reinforcement should be connected to the positive terminal of the voltmeter, and the reference electrode on the negative.

The potential difference between the working electrode and the reference electrode depends on the type of reference electrode used and the state of corrosion of the rebar (passive/active). Normalization was set to allow a comparison between different reference electrodes. Potentials are generally expressed versus the Saturated Calomel electrode (SCE) or standard Hydrogen Electrode (SHE). Table 2.6 illustrates the factors of conversion.

Table 2.6 Standard potentials of reference electrodes used in concrete (Vennesland 2007)

Reference Electrode	**Potential (mV vs SHE)**
Copper/Copper Sulfate, Cu/CuSO4	+316
Manganese Dioxide, MnO2	+365
Saturated Calomel	+244
Silver/Silver Chloride, Ag/AgCl	+199

Under different conditions, typical ranges of potentials are attributed to concrete as shown in Table 2.7. From a range of +50mV to -200mV, the steel in concrete exposed to atmospheric conditions is indicated to be passive. For the case of carbonated concrete, the corrosion occurs at a range of -250mV to -550mV.

In the case of chloride-induced corrosion, pitting occurs at the range of -350mV to -700mV. When small oxygen is available, the steel is passive from -400mV to -700mV [Bertolini, 2004; Arup, 1983]. However, these values are not always straightforward and there are several parameters affecting the corrosion potential. In the RILEM recommendation, Elsener et al. set the range of corrosion potential as followed:

Table 2.7 Typical Range of potentials of steel in concrete (Elsener et al., 2003)

Concrete condition	**Moisture condition**	**Potential (mV CSE)**
Concrete without oxygen	Water saturated	-900mV to -1000mV
Chloride contaminated	Wet	-400mV to -600mV
Chloride free concrete	Humid	+100mV to -200mV
Carbonated concrete	Humid	+100mV to -400mV
	Dry	+200mV to 0mV
Concrete	Dry	+200mV to 0mV

c. Influencing factors

Among the few factors influencing the results of the half-cell potential are the cover thickness, the concrete resistivity, the moisture, and the availability of oxygen. For instance, for concrete fully immersed in seawater, saturated with water, no oxygen is available, the potential is often significantly low (lower than 70mV), however, the corrosion rate is rather slow [Arup,1983]. It was found that the optimum relative humidity for corrosion to progress is at 70 to 80%. When the relative humidity is higher, the diffusion of oxygen in concrete is significantly limited [Neville, 2011]. Contrastingly, when the concrete is dry, corrosion does not occur.

d. Interpretation

The result obtained from the measurement of the half-cell potential allows:

(1) the determination of the probability of corrosion in the concrete,

(2) the location of the most corroded area in the structure,

(3) the elaboration of a corrosion map and the quantification of corroded area.

The ASTM standard has set a standard for the different ranges of the potential of different corrosion conditions, summarized in Table 2.8 [ASTM C876, 2015]. A RILEM recommendation on the measurement of potential was published [Elsener, 2003].

Table 2.8 Half-cell potential range related to corrosion probability (ASTM C876)

Half-Cell Potential (E_{corr}) (mV;CSE)	**Half-Cell Potential (E_{corr}) (mV;SCE)**	**Probability of Corrosion**
E_{corr} >-200 mV	E_{corr} >-125 mV	10%
-350<E_{corr}<-200	-275<E_{corr}<-125	Uncertain
E_{corr}<-350	E_{corr}<-275	90%
E_{corr}<-500	E_{corr}<-425	Severe corrosion

In a passive state, the steel would usually show a potential between -50 to -200 mV and categorized as a zone of “90% Corrosion”. When corrosion is initiated, the potential decreases, from -200 to -350 mV, the potential is classified as “uncertain” of corrosion. Under 500mV, the corrosion is estimated to be “severe”. Equation (1) converts the measured value from SCE electrode to SCE electrode.

$$E_{CSE} = E_{SCE} - 74 - 0.66 \times (t - 25) \qquad \textbf{(2.8)}$$

Where,

E_{CSE} : Potential value in CSE (mV)
E_{SCE} : potential value in SCE (mV)
t : temperature (ºC)

e. Challenges and limitation

The challenges for this method of interpretation of potential are on the fact does it not applicable for universal cases as the parameter affecting the corrosion, such as the concrete cover, the concrete type, are not considered in the measurement. Reliable results are difficult in the case of electrically isolated steel such as epoxy-coated steel bars, or concrete coated surfaces. Nonetheless, when combined with other electrochemical measurements, it can give reliable information on the condition of corrosion.

2.4.2 Corrosion rate

a. Definition

The corrosion rate is determined through the monitoring of the relation between the electrochemical potential. *Polarization* is the change caused by the change in the open circuit potential. *Polarization resistance* is the ratio between the change in voltage and the change in the applied current per unit area of electrodes [Andrade and Alonso, 1996].

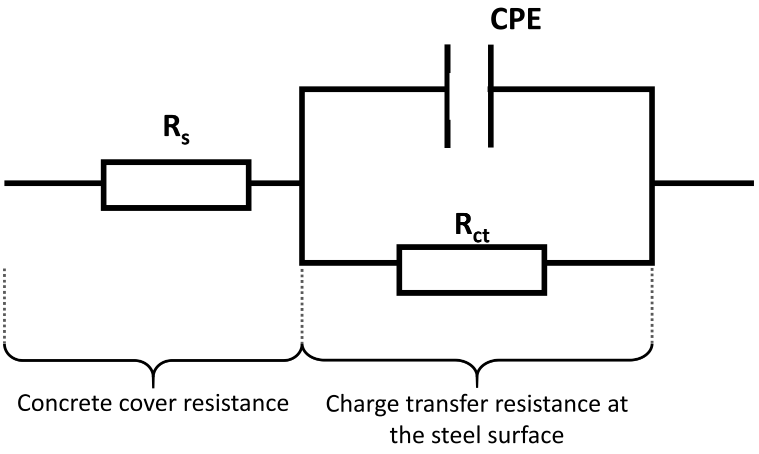

Figure 2.14 Equivalent circuit of corroding system

Linear Polarization Resistance is a non-destructive and electrochemical method of determination of the corrosion rate in concrete. It is known to be the simplest, fastest, reasonable-priced, and widely used technique that directly assesses the rate of corrosion in real-time [Kumar et al., 2013]. Furthermore, studies stated that the measurement of linear polarization is the most reliable method to assess the corrosion current density. Stern-Geary equation (Equation 2.9) describes the polarization resistance as an inversely proportional value to the corrosion current [Stern and Geary, 1957].

$$R_p = \frac{B}{i_{corr}} \tag{2.9}$$

R_P : Linear polarization resistance (Ω)
i_{corr} : Corrosion current density (μA/cm^2)
B : the Tafel constants (mV)

$$B = \frac{\beta_a \cdot \beta_c}{2.303(\beta_a + \beta_c)};\ \beta_a = \frac{2.303\ RT}{\alpha_a nF} \tag{2.10}$$

B contains the Tafel constants of the anodic (β_a)and cathodic curve β_c. In corroding steel reinforcement, a value of 26 mV is taken and recommended for the constant B in case of active steel reinforcement and 52mV for passive steel bar. [Andrade and Gonzalez, 1978; Andrade et al., 2004].

b. Procedure of Measurement

The measurement of polarization resistance is also straightforward. Surface preparation is required before the testing, including the cleaning and the pre-wetting of the surface. A portable corrosion meter is usually used; equipped with a sensor and an incorporated reference electrode and counter electrode.

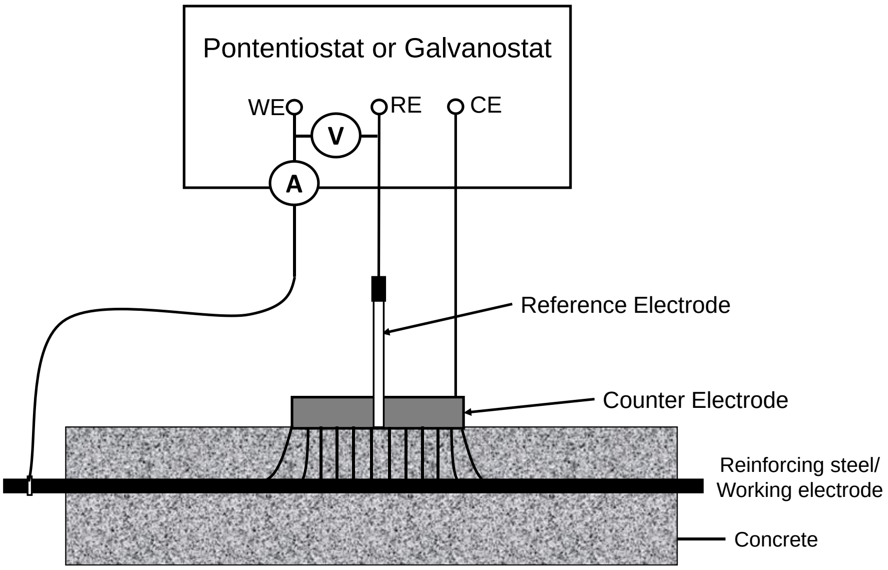

Figure 2.15 Schematic of the setup of Linear polarization measurement [Bertolini, 2004]

c. Interpretation

Several qualitative standards were set to determine the rate of corrosion from the linear polarization resistance measurement as summarized in Table 2.9.

Table 2.9 Corrosion rate from linear polarization resistance [Andrade and Alonso, 1996; CEB, 1998]

Corrosion Current Density [i_{corr}; μA/cm^2]	**Corrosion Penetration rate [μm/year]**	**Corrosion rate**
< 0.2	< 2	Passive/ Very low
0.2 – 0.5	2 – 6	Low/ Moderate
0.5 – 1.0	6 – 12	Moderate/Low
> 1.5	> 12	Very high

2.4.3 Electrical resistivity

a. Definition

The electrical resistivity of concrete is one of the properties of concrete through which the concrete structures can be monitored or/and inspected [Polder et al., 2000]. From the electrical resistivity, the ability of concrete to withstand the passage of electrical current.

From this method, the following can be determined:

- Risk of early corrosion damage, particularly for concrete exposed to chloride environment. A low resistivity in concrete is generally associated with a rapid chloride diffusion and high corrosion rate.
- Possible maintenance actions in case the corrosion has already started in the concrete.

Application of electrical resistivity according to the RILEM.

- Estimation of the risk of corrosion: by the assessment of the range of the concrete resistivity of concrete structures.
- Definition of other investigations, treatment, or protection from the localization of the most permeable section of the concrete.
- Localization of the area with the most severe exposure to water and aggressive agents.
- Designing a system for cathodic protection and other electrochemical treatments.
- Determination of the quality of concrete.

b. Methods of measurement

The four-point Wenner probe is a widely used technique. It is a non-destructive method, simple and fast [Wenner, 1916]. It consists of 4 aligned and equidistant electrodes. The two electrodes on the side apply Alternating Current (AC) to the concrete and the two inner electrodes measure the electrical potential created (*Figure 2.16*). It is recommended to measure one surface up to five times and take the average.

In addition, the measurements are to be performed as far from the rebar as possible due to their influence. Also, pre-wetting of the concrete surface is required before each measurement. As the degree of saturation is significantly impacting the results, the specimens are to be equally and fully saturated during the measurement [Layssi et al., 2015].

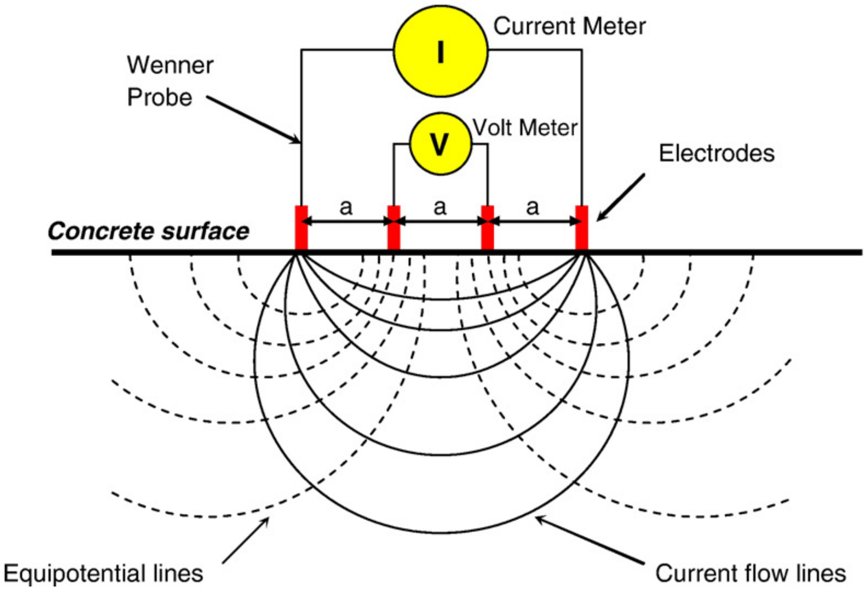

Figure 2.16 Schematic representation of the Wenner probe method for determination of Electrical resistivity

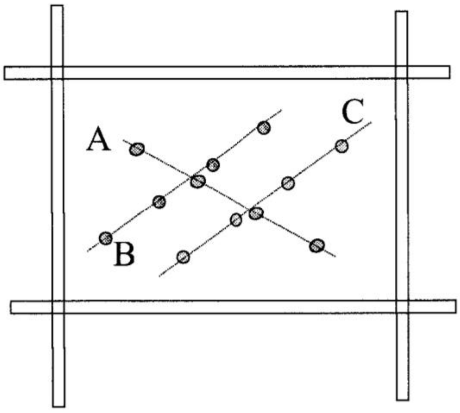

Figure 2.17 Resistivity measurement using Wenner probe method.

c. Parameters affecting the resistivity of concrete

The measurement of electrical resistivity can be performed at any temperature above 0ºC. A change of temperature of 1 ºC may result in a 3% change of electrical resistivity. This is because a higher temperature decreases the resistivity [Elkey, 1995]. In addition, according to previous studies, the electrical resistivity of concrete can vary over a wide range from 101 to 106 Ωm and is significantly impacted by the environment (moisture) and the composition of the concrete [Gjørv & Vennesland, 1977, Tuutti, 1982]. For instance, dry concrete shows higher resistivity than wet concrete.

d. Interpretation

The data obtained by the electrical measurement are useful in assessing the risk of corrosion, compared with the classification set by [Langford et al, 1987; Andrade, 1988] and the corrosion rate with the classification of [Broomfield et al., 1993] (*Table 2.10*). When performed appropriately, this method was shown to give consistent results and convenience for concrete testing [Layssi et al., 1993]. Because the permeability of concrete to chloride has a linear correlation with the resistivity, it was made possible to estimate the diffusion of chloride [AASHTO, 2014], as presented in *Table 2.11*.

Table 2.10 Electrical resistivity range related to corrosion risk level and corrosion rate level

Corrosion Risk		**Corrosion Rate**	
Resistivity (ρ) (kΩ.cm)	**Corrosion Risk Level**	**Resistivity (ρ) (kΩ.cm)**	**Corrosion Rate Level**
>100	Negligible	>20	Low
50 - 100	Low	10 - 20	Low to moderate
10 - 50	Moderate to high	5 - 10	High
<10	High	<5	Very High

Table 2.11 Electrical resistivity range related to chloride ion penetration

Resistivity (ρ) (kΩ.cm)	**Chloride ion penetration**
>254	Negligible
34 - 254	Very low
21 - 37	Low
12 - 21	Moderate to high
<10	High

From the electrical resistivity measurement, it is not possible to understand the passivity or activity of the steel in concrete to corrosion. As a result, this method is often used with other electrochemical methods, such as the potential mapping and the polarization resistance measurement. However, if the steel is active to corrosion, it is possible to determine the most affected area from the electrical resistivity methods.

2.4.4 Polarization curve

a. Definition

Figure 2.18 also called the Evans diagram, shows a simplified anodic polarization curve (oxidation reaction) and cathodic polarization curve (a reduction reaction). The corrosion reaction in concrete consists of two half-cells, anodic and cathodic half-cells which polarize at the same corrosion potential E_{corr} and current I_{corr}. Therefore, the corrosion working condition can be determined. The oxygen supply is determined from the anodic curve and the state of the corrosion of the steel from the anodic.

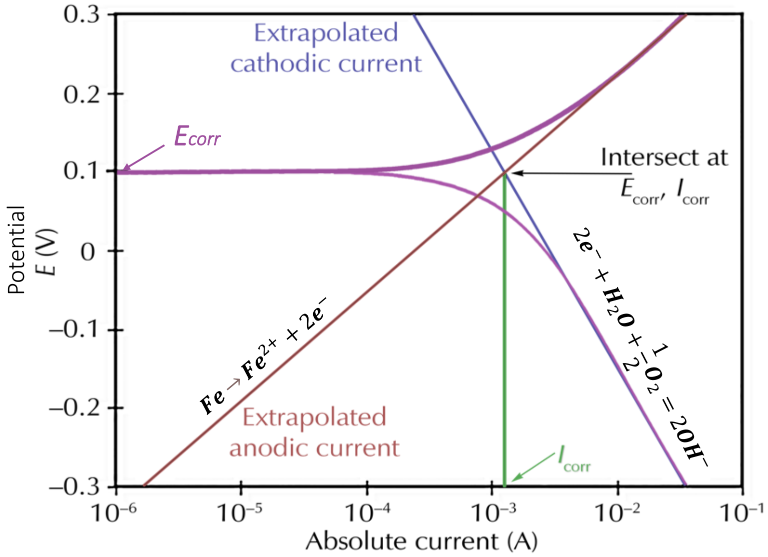

Figure 2.18 Simplified anodic and cathodic polarization curve (Tafel)

b. Methods of measurement

There are two different ways of conduction the polarization curve measurement:

(1) Immersion method [Otsuki et al., 1985]: It consists it immersing the sample into water and connecting the specimen to the potentiostat (*Figure 2.19*). This method of measurement is only applicable to specimens with a relatively small size and laboratory experiments.

(2) Contact method [Hamada et al., 2010]: Instead of immersing the concrete specimen into water, a double layer counter electrode is used and placed on the surface of the concrete structures (*Figure 2.20*). This method is applicable to site monitoring and assessment and specimen on a large scale.

(3)

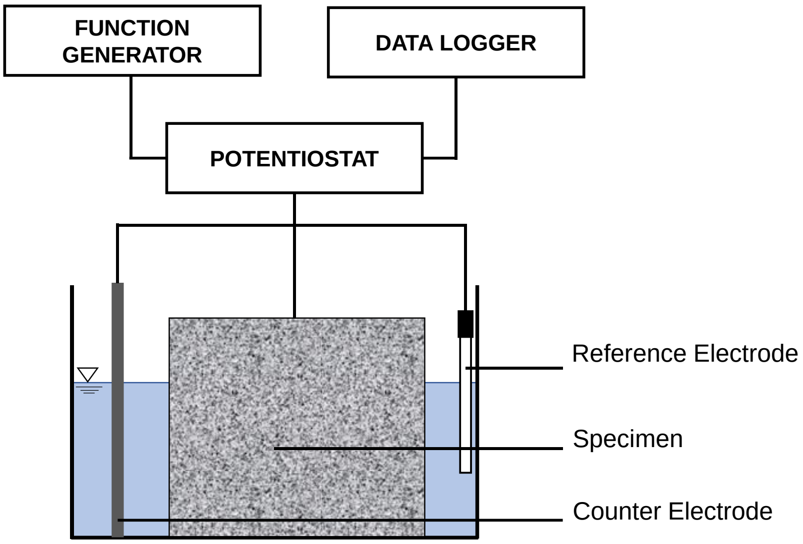

Figure 2.19 Schematic of the measurement of anodic-cathodic polarization curve (Immersion method)

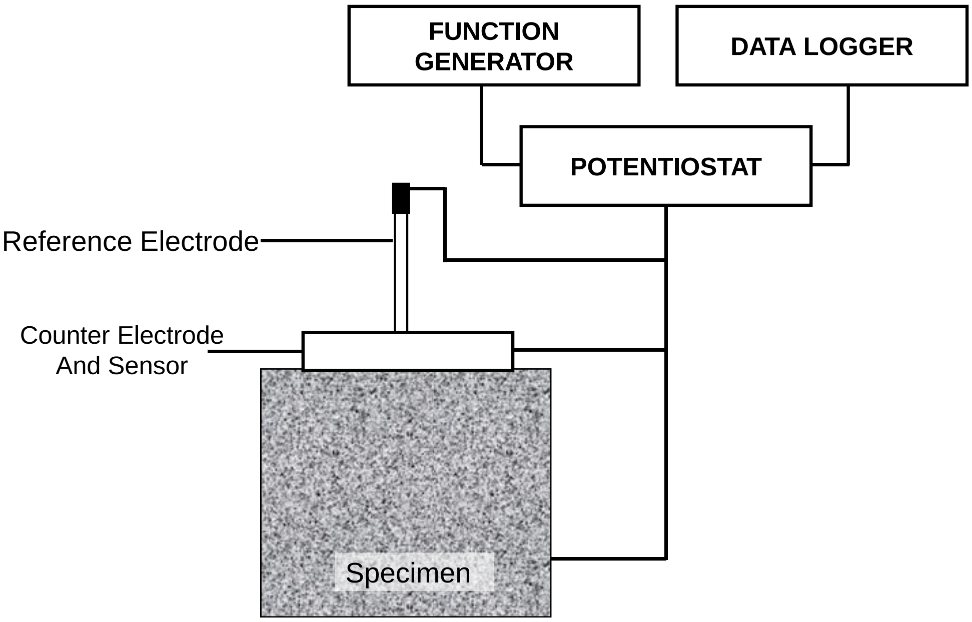

Figure 2.20 Schematic of the measurement of anodic-cathodic polarization curve (Contact method)

For both methods of measurement, a function generator, a data logger, a counter electrode, and a reference electrode (Ag/AgCl) are used. The measurement lasts about 45 min (15min for anodic curve, and 15 min for cathodic curve), is conducted at a potential range of ±700mV at a rate of 50 mV/min.

c. Interpretation

The anodic and cathodic polarization curves were interpretated according to the classification of Otsuki. The state of the grade of passivity of the steel can be judged from grade 0 to 5, function to the potential between "(E_{corr}) + 200 mV" and "(E_{corr}) + 600 mV" and the current density. As the curve is shifted to the right, the state of the passivity is getting worse.

- **Grade 0** indicates that no passivity exists when the current is over 100 µA/cm^2.
- **Grade 1** indicates a certain passivity film (less than grade 3 and 2) when the anodic current is within 10 µA/cm^2 and 100 µA/cm^2.
- **Grade 2** represents a certain degree of passivity when the current is over 10 µA/cm^2 at least at one point.
- **Grade 3** indicates a certain degree of passivity when the current is between 1 µA/cm^2 and 10 µA/cm^2.
- **Grade 4** shows a good passivity; a certain degree (better than Grade 1 to 3) of passivity is still present in the rebar when the current is 1 µA/cm^2 at least one point.
- **Grade 5** represents an excellent passivity: the current is inferior to 1 µA/cm^2.

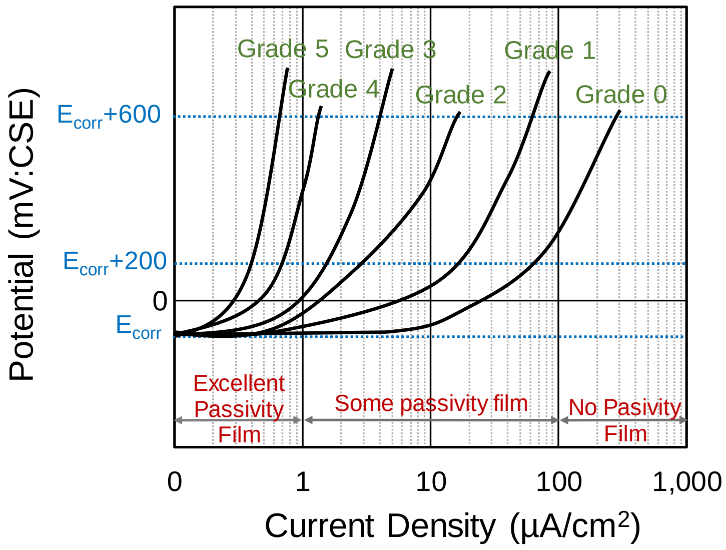

Figure 2.21 Grade of passivity from the anodic polarization curve (Otsuki et al., 1985)

Table 2.12 Grade of passivity function of potential and current density

Grade	Potential	Current density	Passivity state
0	E_{corr}+200mV to E_{corr}+600mV	$I_{corr}>100\mu A/cm^2$ at least one time	No Passivity Film
1		$10<I_{corr}<100\mu A/cm^2$	Some Passivity Film
2		The anodic curve cut the 10 $\mu A/cm^2$	
3		$1<I_{corr}<10\ \mu A/cm^2$	
4		The anodic curve cut the $1\mu A/cm^2$	
5		$I_{corr}<1\mu A/cm^2$	Excellent Passivity Film State

Oxygen permeability: From the same apparatus, the oxygen diffusion can be determined, using the constant current density [Takumi, 2018]:

$$\frac{dQ}{dt} = \frac{i_{lim}}{n.F} \tag{2.10}$$

Where,
dQ/dt : Oxygen supply ($mol/cm^2/s$)
i_{lim} : Current density ($A/\ cm^2$)
n : Number of electron (4)
F : Faradays constant (96,500 coulombs/mol)

The potential range is set at -1000mV at a rate of 10 mV/sec. The measurement lasts for about 24 hours.

2.5 CORROSION PREVENTION AND REPAIR

From the report of the NACE, about 50% of structures require major repair within ten years after construction [NACE, 2016]. Once corrosion is initiated in concrete, its progression is not inevitable. Thus, to increase the service life of concrete structures, or to avoid early corrosion in concrete; various prevention and repair methods have been developed over the last decades. Those methods include the use of membranes to cover the concrete surface, coating of reinforcement [Wang et al., 2021], cathodic protection [Bertolini, 1998; Zainal, 2020; Jeong, 2013], and corrosion inhibitors [Angst et al., 2018; Venkatesh et al., 2019; Lee et al., 2020].

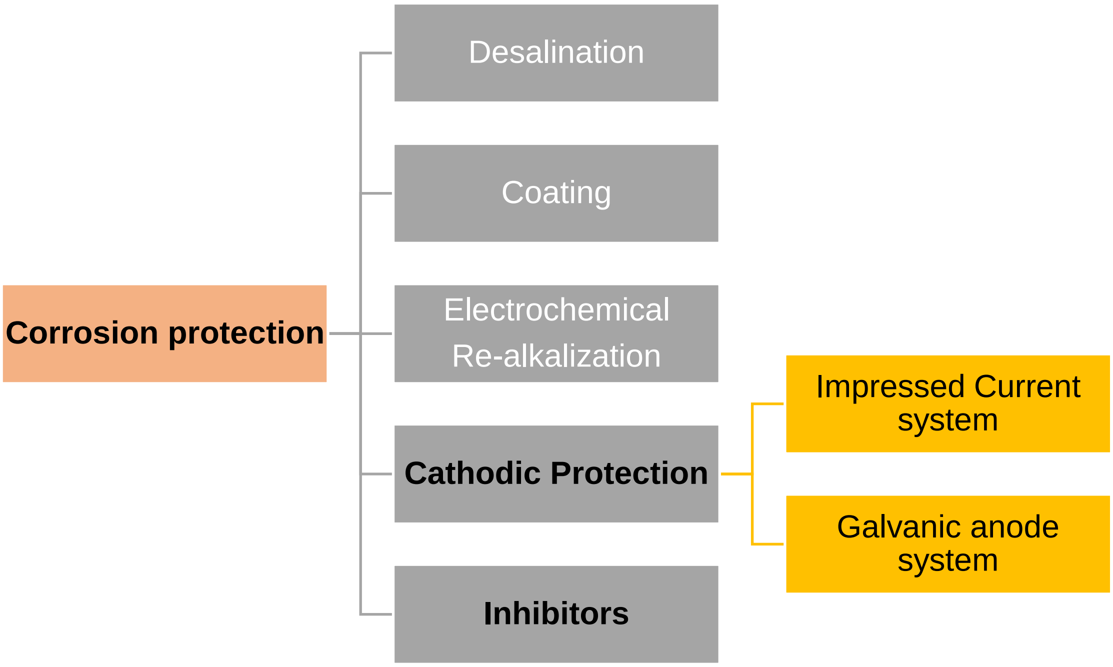

Figure 2.22 Different corrosion prevention and repair in concrete structures

Additional protection measures have also been suggested for a durable concrete structure and summarized in Table *2.13* and Table *2.14*. [Hunkeler 2000; Hunkeler et al 2001]:

Table 2.13 Different types of measures for corrosion prevention and repair (1)

Measures	Advantages	Disadvantages
MODIFICATION OF CONCRETE		
Increasing the concrete cover of the reinforcement:	- Cost-effective - Easy to realize - Experience - Higher critical chloride content for corrosion	- Limitation in the possibility of increase of the cover - Reduction of the static height

Table 2.14 Different types of measures for corrosion prevention and repair (2)

Measures	**Advantages**	**Disadvantages**
COATING		
Surface protection systems (Hydrophobic impregnation, coatings, tiles)	- Effective if properly used - Availability of a large variety -Modifiable appearance of surface (colors)	- Costs - Handling, possibility of damages during work - require monitoring of the efficiency - change of the fair-faced concrete
Zinc-coated steel	- Cost-effective - Handling - Performance in carbonated concrete	- limited efficiency and durability in chloride-contaminated concrete and cracks - None to slight influence on the critical chloride content
Epoxy-coated steel	-Costs -Deliverability	-Handling, possibility of damages during work -Mixture between the coated and non-coated steel critical - No proven long-term efficiency and durability (contradictory experience) -Minim influence on the critical chloride content
Stainless steel	- Handling - Higher critical chloride content for corrosion -Mixture with ordinary steel	- costs - restricted deliverability, availability -Experience
OTHER		
Cathodic Protection	- Efficiency	- Handling (complex) - Costs -Requiring monitoring
Waterproofing Membranes	- Efficiency - Experience	- Handling (risk of damages) - Costs -Not always applicable
Use of more tight concrete (Less porous)	- Cost-effective - Partly easy in handling - Experience (partly)	- Limitation in the reduction of w/c ratio, workability.
Inhibitors as admixtures	- Handling - Higher critical chloride content for corrosion -Cost-effectiveness	-No proven long-term efficiency and durability

2.5.1 Corrosion inhibitors

a. Definition:

Due to the merits that corrosion inhibitors offer, such as their costs, ease in handling, and their effectiveness [Söylev et al., 2008], they have been of high interest in recent decades. The ISO 8044-89 defines corrosion inhibitors of steel in concrete as chemical substances that reduce the corrosion of the steel without decreasing the concentration of corrosive agents [ISO 8044, 2015]. Corrosion inhibitors are to be distinguished from other substances added to concrete to enhance the corrosion resistance by reducing chloride ingress into concrete [Broomfield, 1999]. As per NACE international, "a corrosion inhibitor is a substance when added to an environment, either continuously or intermittently to prevent corrosion by forming a passive film on the metal" [NACE, 1965].

Using inhibitors, a decrease in the rate of reactions either anodic or cathodic will directly lead to a decrease in the rate of corrosion, and a surge in the level of the threshold level of the chloride-induced corrosion [Xu et al., 2013]. They are known to be effective in small quantities. Corrosion inhibitors can also delay the onset of corrosion, for a long period and without influencing the mechanical properties of concretes.

They work by influencing the corrosion process by:

- Forming a protective film or inhibiting layer on the surface of the steel [Hansson, 1998]
- Reducing the movement of ions of the steel surface, therefore, they reduce the corrosion rate [ISO 8044, 2015];
- Increasing the anodic or/ and cathodic polarization behavior; for instance, by stopping the diffusion or reducing the effect of oxygen dissolved in the pore solution of the concrete.
- Increasing the electrical resistance of the steel surface.

b. Classification of corrosion inhibitors

Corrosion inhibitors are generally classified according to [Jamil et al., 2004, Söylev et al., 2008]:

- The method of their application.
- Their natures (organic and inorganic inhibitor);
- the inhibited electrochemical reaction (Anodic inhibitor, cathodic inhibitor, or mixte);
- The reaction mechanism involved (absorption or formation of film)

However, some inhibitors can present at the same time several characteristics listed above.

c. Nitrites

Studies showed that nitrite-based inhibitors show better performance than other inhibitors by decreasing the corrosion current density by 1.6 to 6.7 times (amine carboxylate or amino alcohol-based inhibitors) [Al-Sodani, 2018]. Nitrites show fewer drawbacks on the properties of concrete as it is compatible with the reaction of hydration of cement and concrete [Saricimen, 2002]. In addition, it is a low-cost inhibitor but effective in delaying or stopping chloride-induced corrosion in concrete structures [Ormellesse, 2006; Reou and Ann, 2008]. Nitrites are extensively used in Japan and the USA due to their effectiveness. Berke and Rosenberg investigated the mechanism of nitrite as inhibitor in steel bar. They found that the nitrite did not react with the ion Fe or Fe^{++} but according to the reaction (2.12). [Berke and Rosenberg, 1989, James et al., 2004].

Reaction of the dissolution of ions in steel:

- $\boldsymbol{Fe \rightarrow Fe^{++} + 2e^-}$ **(2.11)**

Reaction of ferrous ion with chloride

- $\boldsymbol{Fe^{++} + Cl^- \rightarrow FeCl^- + OH^- \rightarrow FeO(H_2O)_x + Cl^-}$ **(2.12)**

Reaction of Nitrite with Ferrous ion (Anodic reaction)

- $\boldsymbol{2Fe^{++} + 2OH^- + 2NO^- = 2NO \uparrow + Fe_2O_3 + H_2O}$ **(2.13)**

Or:

- $\boldsymbol{Fe^{++} + OH^- + NO_3{}^- = NO \uparrow + \gamma - FeOOH}$ **(2.14)**

The role of the nitrite ions is to prevent ferrous ions to migrate to the cathodic area. The Ferrous oxide Fe_2O_3 formed by the reaction between ferrous ion and the nitrite, precipitates to form barriers [Hopwood,1988]. The reactions are competitive therefore, calcium nitrite should be in sufficient amount to be effective ($[NO2^-]/[Cl^-] > 0.5$) [Berke and Sunberg, 1989].

d. Calcium Nitrite

In the use of calcium nitrite as corrosion inhibitor, several adequate concentration of Calcium nitrites was given for optimum results, as summarized in the *Table 2.15*.

Table 2.15 Concentration of calcium by weight of cement from literature

Reference	Calcium nitrite concentration	Exposure condition	Effectiveness
[Berke, N. S. et al., 1989]	2% - 4%	-	Effective
[Al Moudi et al., 2003]	2% - 4%	0.8% Cl/ Seawater	Effective in short time (Until 125 days)
[Batis et al., 2004]	4%	3% NaCl	Effective on a long-term exposure
[Ormellesse et al., 2006]	2.5%	3.5% NaCl (dry-wet cycle for 3 years)	Effective
[Reou and Ann, 2008]	1% -2%- 3%	3% Sodium Chloride	Low effect at 1% and good result at 3%
[Abosrra, L. et al., 2011]	2% - 4%	3% NaCl and Impressed current	2% was not enough

From the literature, some limitations, and negative results on the use of nitrite was stated:

- A concentration under the minimum required will lead to the acceleration of corrosion.
- Their effectiveness depends on many factors, such as the presence of chloride, the change of Temperatures, and the pH [Hansson, 1998].
- Not effective in carbonated concrete with some level of chloride [Alonso and Andrade, 1990]

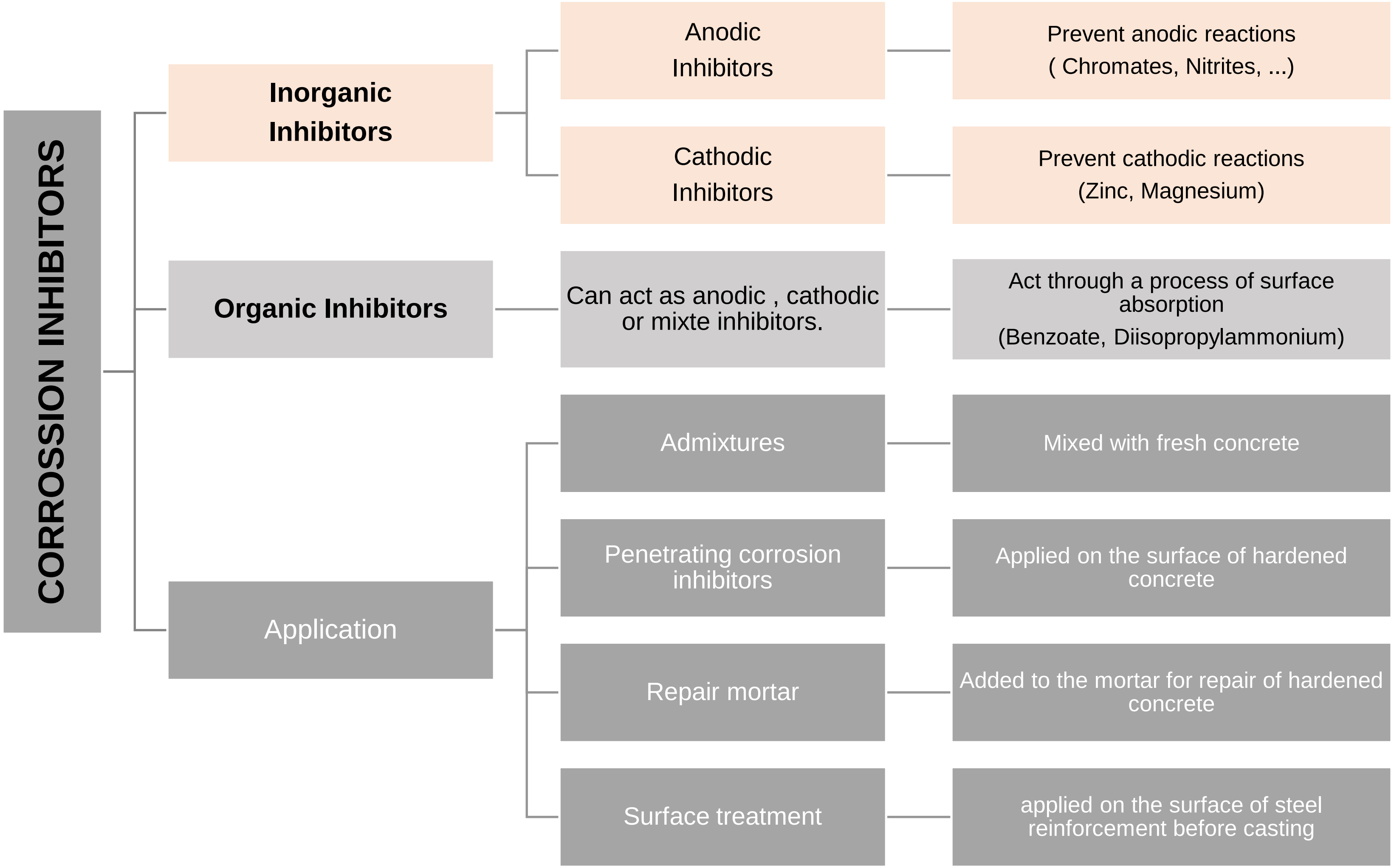

Figure 2.23 Classification of corrosion inhibitors

2.5.2 Cathodic protection

Cathodic protection is a method used to stop the corrosion of steel reinforcement in concrete. It has been demonstrated to be the most effective method able to control the corrosion in concrete structures, even exposed to chloride environment [Page, 1997; Pedeferri, 1996; Parthiban, 2018]. Cathodic protection is used in new construction for prevention, in old structures for repair, and marine environment structures.

The principal mechanism of cathodic protection is to polarize to metal to be protected or repaired from its free corrosion potential to where corrosion is less likely to occur [Pourbaix, 1974]. Current is forced on the surface of the steel, the protected steel becomes the cathode and constrains the transfer of electrons to stop corrosion [Goyal, 2019]. One of the advantages of cathodic protection is that it can be used even in prestressed concrete without risk of embrittlement of the high-strength steel of tendons. The technology of CP can be classified into 2 types:

- Sacrificial anodes cathodic protection (SACP)
- Impressed current cathodic protection (ICCP)

a. Sacrificial anodes cathodic protection

During the application of patch repair (alone), the repair process can lead to an undesirable product called “Halo effect”, which is a new corrosion site formed outside the patch repair [Sergi and Page, 1999; 2000]. The application of sacrificial anode such as galvanic anode is a solution to tackle this issue by controlling the formation of the anode and stopping the corrosion [Sergi et al., 2008; Sergi, 2011].

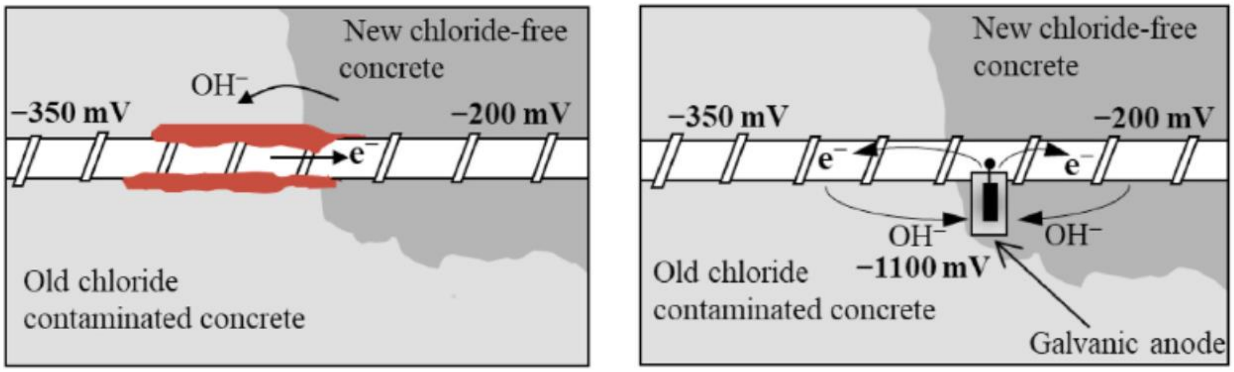

(a) Halo effect – when CP is not used **(b) Prevention of halo effect – when CP is used**

Figure 2.24 Patch repair with and without cathodic protection [Krishnan et al, 2021)

One of the features of an SACP is that it does not require the application of an external power supply. They consist of anodes (zinc-based alloys or aluminum) which are directly embedded in the concrete or connected to the rebar. The used anode is a less noble metal compared to the reinforcing steel and is consumed differently, which generates the cathodic protection current.

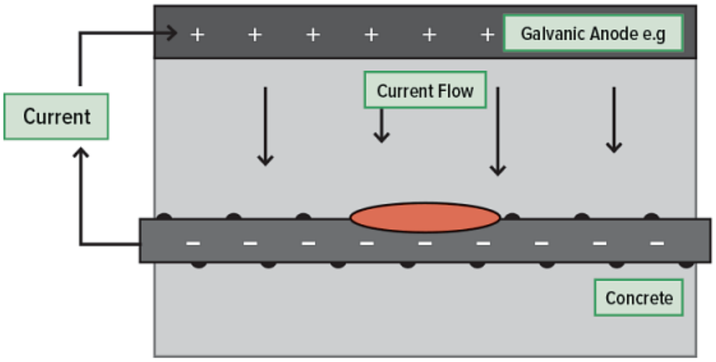

Figure 2.25 schematic of the system of Impressed current cathodic protection [Broomfield, 2014]

b. Impressed current cathodic protection (ICCP)

This method of cathodic protection mainly contains three parts: an external power supply (DC power supply), the steel reinforcement embedded in the concrete, and an external anode system [Pedeferri, 1996]. To transform the surface of the protected rebar to the cathode and stop corrosion, an external anode is connected to the rebar, and a direct negative current is passed to the rebar. The ICCP technology is acknowledged to be effective in stopping corrosion even in chloride-contaminated structures [Bertolini, 1998].

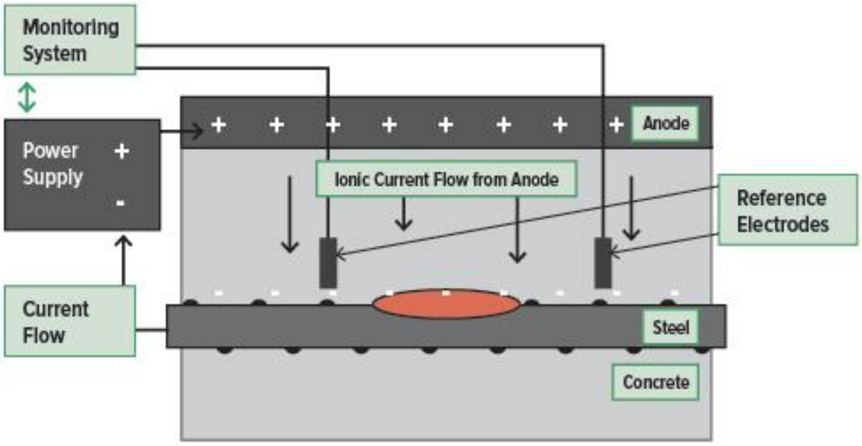

Figure 2.26 schematic of the system of Impressed current cathodic protection [Broomfield, 2014]

2.6 PROBLEMS ADDRESSED IN THIS STUDY

With regards to the durability of reinforced and prestressed concrete, the severity of the effect of chloride and exposure to the marine environment are dominant influencing factors. That is because their primary action leads to the corrosion of the steel embedded in concrete. During the phase of realization of structures, further factors to be considered are the presence of joint and interfacial gap caused by the settlement of solid materials in fresh concrete, as they can be a weak section of the concrete promoting the ingress of aggressive agents and accelerating corrosion. In addition, exploiting seawater as an alternative to fresh water and tackle the issue of corrosion in the marine environment has also become of high interest due to the extensive consummation of concrete. Finally, finding a suitable method of repair for old structures is equally essential to extend the service life of concrete construction.

Long-term PC beams exposed to the severe marine environment are studied in **Chapter 3**. Specifically, the electrochemical behavior of the corrosion of PC is studied along with the effect of joint treatment used. **Chapter 4** studies the issues of bleeding induced corrosion of horizontal steel bars in concrete. In **Chapter 5** a solution to the issue of the interfacial gap is suggested which is also a preventive method against seawater-mixed concrete, exposed to marine environment. **Chapter 6** reports on the updates on the use of repair methods by sacrificial anode cathodic protection in view of the extension of the service life of concrete structures. Finally, **Chapter 7** Summarizes the essential point of investigations performed in this research and advances some recommendations for a durable concrete structure exposed to marine environment.

2.7 REFERENCES

AASHTO TP 95, (2014): Standard Test Method for Surface Resistivity of Concrete’s Ability to Resist Chloride Ion Penetration, *American Association of State Highway and Transportation Officials*, Washington, DC.

Abossra, L., Youseffi, M., and Ashour, A. F., (2011): Effectiveness of Calcium Nitrite in Retarding Corrosion of Steel in Concrete, *International Journal of Concrete Structures and Materials*, 5, No.1, pp.65-73.

ACI Committee 222, (2001): ACI 224R-01, Control of Cracking in Concrete Structures.

ACI Committee 222, (2001): ACI 222R-01, Protection of Metals in Concrete Against Corrosion.

ACI Committee 318, (1996): ACI 318-95, Building Code Requirements for Structural Concrete, ACI Manual of Concrete Practice, Part 3: Use of concrete in Building-Design, Specifications, and Related Topics, pp. 345

ACI Committee 318R, (2002): Building Code Requirements for Structural Concrete (ACI 318-99) and Commentary (ACI 318R-99), *American Concrete Institute*, Farmington Hills, Michigan.

Ahmed, Z., (2006): Chapter 2 - Basic Concepts in Corrosion, Principles of Corrosion Engineering and Corrosion Control, pp. 415-425.

Al-Moudi, O. S. B., Maslehuddin, M., Lashari, A. N., and Almusallam, A. A., Effectiveness of Corrosion Inhibitors, *Cement and Concrete Composites*, 25, pp. 439-449.

Alonso, C., and Andrade, C., (1990): Effect of Nitrite as a Corrosion Inhibitor in Contaminated and Chloride-free Carbonated Mortars, *ACI Materials Journal*, 87, No.2, pp.130–137.

Alonso, C., Andrade, C., Rodríguez, J., and Díez, J.M., (1998): Factors Controlling Cracking of Concrete Affected by Reinforcement Corrosion, *Materials and Structures*, 31, pp. 435–441.

Al-Sodani KAA, Maslehuddin M, Al-Amoudi OSB, Saleh TA, and Shameem M., (2018): Efficiency of Generic and Proprietary Inhibitors in Mitigating Corrosion of Carbon Steel in Chloride-Sulfate, *Environment Science,* 7,11443.

Andrade, C., and Gonzalez, J.A., (1978): Materials and Corrosion, 29, pp. 515-519.

Andrade, C., Alonso, C. and Rodriguez, J., (1989): Remaining Service Life of Corroding Structures, *IABSE Symposium on Durability*, Lisbon, September, pp. 359–363.

Andrare, C., and Alonso, C., (1996): Corrosion Rate Monitoring in the Laboratory and on-site, Construction and Building Materials, 10 (5), pp.315-328

Andrade, C., Alonso, C., Gulikers, J., Polder, R., Cigna, R., Vennesland, O., Salta, M., Raharinaivo, A., Elsener, B., (1998): Materials and Structures, 37 (2004), pp. 623-624.

Andrade, C., Alonso, C., and Sarría, J., (2002): Corrosion Rate Evolution in Concrete Structures Exposed to the Atmosphere, *Cement and Concrete Composites*, 24, pp. 55–64.

Andrade, C., (2020): Electrochemical Methods for on-site Corrosion Detection. Structural Concrete, 21(4), pp.1385-1395.

Angst, U. M., (2018): Challenges and Opportunities in Corrosion of steel in Concrete, *Materials and Structures*, 51 4RILEM 2018.

Angst, U. M., Büchler, M. M., Schlumpf, J., Marazzani, B., (2016): An Organic Corrosion-inhibiting Admixture for Reinforced Concrete: 18 years of Field Experience, *Materials and Structures*, 49(7), pp. 2807-2818.

Angst, U. M., Buchler, M., Schlumpf, J., and Marazzani, B., (2016): An Organic Corrosion-Inhibiting Admixture for Reinforced Concrete: 18 years of field experience. Materials and Structures/Materiaux et Constructions, 49(7), 2807–2818.

Angst, U., and Vennesland, (2007): Critical Chloride Content – State of the art. SINTEF report, COIN – *Concrete Innovation Centre*, Trondheim, Norway, pp. 1-54.

Arligue G., T., Chaussadent, G., Grimaldi, V., Pollet, A., Raharinaivo, and Taché, G., (1998): Corrosion and Protection of Steel in Concrete, *Presses de l'école nationale des Ponts et Chaussées*. (In French)

Arup, H., (1983): The Mechanism of the Protection of Steel by Concrete, Corrosion of Reinforcement in Concrete Construction, *Crane A P (ed)*, Ellis Horwood, p. 151-157.

Arya, C., Buenfeld, N.R., and Newman, J.B., (1990): Factors Influencing Chloride-Binding in Concrete, *Cement and Concrete Research,* 20, pp. 291-300.

ASTM C876-15, (2015): Standard Test Method for Corrosion Potentials of Uncoated Reinforcing Steel in Concrete, *ASTM Int.*

Baccay, M. A., Nishida, T., Otsuki, N., Hamamoto, J., and Chin, K., (2004): Influence of Bleeding on Minute Properties and Steel Corrosion in Concrete Journal of Advanced Concrete Technology, 2, pp. 187–199.

Batis, G., Sideris, K. K., and Pantazopoulou, P., (2004): Influence of Calcium Nitrite Inhibitor on the Durability of Mortars under Contaminated Chloride and Sulphate Environments, *Anti-Corrosion Methods and Materials*, 51, No. 2, pp. 112–120.

Berke, N. S., and Rosenberg, A., "Technical Review of Calcium Nitrite Corrosion Inhibitors in Concrete," Transportation Research Record, No. 1211, Washington, 1989, pp. 18-27.

Berke, N. S., Sundberg, K. M., (1989): The Effect of Calcium Nitrite and Microsilica Admixtures on Corrosion Resistance of Steel in Concrete, *Performance of Concrete*, pp. 269.

Berke, N. S.,(1987): The Effects of Calcium Nitrite and Mix Design on the Corrosion Resistance of Steel in Concrete (Part 2, Long-Term Results), Corrosion 87 Conference, 132, National Association of Corrosion Engineers, Houston, TX, pp, 1-11.

Bertolini, L., Bolzoni, F., Pedeferri, P. et al., (1998): Cathodic protection and cathodic prevention in concrete: principles and applications. *Journal of Applied Electrochemistry* 28, pp. 1321–1331.

Bertolini, L., Elsener, B., Pedeferri, P., and Polder, R., (2004): Corrosion of Steel in Concrete – Prevention, Diagnosis and Repair, 1st edition, Wiley-VCH, Weinheim, Germany.

British Cement Association (BCA), Development of an holistic approach to ensure the durability of new concrete construction, British Cement Association Crowthorne

Broomfield, J. P., Rodriguez, J., Ortega, L. M., and Garcia, A. M., (1993): Corrosion Rate Measurement and Life Prediction for Reinforced Concrete Structures, P*roc. Structural Faults and Repair 2*, Engineering Technical Press (University of Edinburgh, Scotland), pp. 155.

Broomfield, J., (1999): Corrosion Inhibitors for Steel in Concrete, *Concrete International,*44, 7.

CEB, Strategies for Testing and Assessment of Concrete Structures, Bulletin No. 243, 183 pp.

Collepardi, M., Fratesi, R., Moriconi, G., Corradetti, C., and Coppola, L., (1990): Proceeding of the International RILEM Symposium on Admixtures for concrete—Improvement of Properties, Barcellona, Chapman and Hall, London UK (1990), pp. 279-288.

Dhir, R.K., and Jones, M.R., (1999): Development of Chloride-resisting Concrete using Fly Ash, Fuel, 78, pp.137-142.

Duval, R., (1992): The durability of steel and Concrete Cover, Presses des Ponts et Chaussées, pp. 173-226. (in French)

Elkey, W., and Sellevold, E.J., (1995): Electrical Resistivity of Concrete, *Norwegian Road Research Laboratory*, Oslo, Norway, pp. 11-13.

Elsener, B., (2001): Half-cell Potential mapping to Assess Repair Work on RC Structures, *Construction and Building Materials*, 15, No. 2-3, pp. 133–139.

Elsener, B., Andrade, C., Gulikers, J., Polder, R., and Raupach, M., (2003): Half-cell Potential Measurements - Potential Mapping on Reinforced Concrete Structures, *Materials and Structures,* 36, 7, pp. 461-471.

Federation International du Beton (FIB), (2011): Condition Control and Assesement of Reinforced Concrete Exposed to Corrosive Environments, *FIB Bulletin*, No. 59.

Ghods P., O. B. Isgor, J. R. Brown, F. Bensebaa, et D. Kingston, « XPS depth profiling study on the passive oxide film of carbon steel in saturated calcium hydroxide solution and the effect of chloride on the film properties », Applied Surface Science, vol. 257, no 10, p. 4669 4677, mars 2011

Gjørv, O. E., Vennesland, Ø., and El-Busaidy, A. H. S., (1977): Electrical Resistivity of Concrete in the Oceans, *9th Annual Offshore Technology Conference*, paper 2803, Houston.

Glass, G.K., Page, C. L., and Short, N. R., (1991): Factors Affecting the Corrosion Rate of Steel in Carbonated Mortars, *Corrosion Science,* 32, No. 12, pp. 1283-1294.

Glass, G.K., Reddy,B., and Buenfeld, N.R., (2000): The Participation of Bound Chloride in Passive Film Breakdown on Steel in Concrete. *Corrosion Science,* 42, pp. 2013-2021.

Goyal, A., Pouya, H.S., Ganjian, E., Olubanwo, A.O., and Khorami, M., (2019): Predicting the Corrosion Rate of Steel in Cathodically Protected Concrete using Potential Shift, Construction Building Materials, 194, pp. 344-349

Haleem, A. E., Abd, El. Aal. E. E., Abd. El. Wanees., S.; Diab, A., (2010): Environmental Factors Affecting the Corrosion Behaviour of Reinforcing Steel: I. The Early Stage of Passive Film Formation in Ca(OH)(2) Solutions, *Corrosion Science,* 52 (12), pp. 3875-3882.

Hamada, H., Haramo, M., Otsuki, N., (1987): Ten Years Test on the Effect of Joints on the Durability of Concrete in Marine Environment, *Japan concrete Institute*, 9, pp. 147-154.

Hamada, H., Otsuki, N., and Haramo, M., (1988): Durabilities of Concrete beams under Marine environments, exposed in Sakata and Kagoshima (after 10 year's exposure), Technical Note of the Port and Airport Research Insitute, 614, pp.3-43.

Hamada, H., Sagawa, Y., Ikeda, R., and Morikawa, R., (2010): Several factors affecting the Anodic Polarization Curve of Steel Bars Embedded in Mortar, Sixth International Conference on Concrete Under Severe Conditions: Environment and Loadings, pp. 201-208.

Hansson, C. M., (1984): Comments on Electrochemical Measurements of the Rate of Corrosion of Steel in Concrete, *Cement and Concrete Research,* 14, (4), pp. 574-584.

Hansson, C. M., Mammoliti, L., and Hope, B. B., Corrosion inhibitors in concrete - Part I: The principles. Cement and Concrete Research, 28 (12), pp. 1775-1781.

Hansson, C. M., Mammoliti, L., Hope, B. B., (1998): Corrosion Inhibitors in Concrete - Part I: The Principles, *Cement and Concrete Research,* 28 (12), pp. 1775-1781.

Hausam, D.A., (1968): Criteria of Cathodic Protection of Steel in Concrete, *24th Conf. of NACE*, Cleveland.

Hladky, K., John, D.G., Dawson, J.L., (1989): Development in Rate of Corrosion Measurements for Reinforced Concrete Structures, *Corrosion,* 89, No. 169, *National Association of Corrosion Engineers*, Houston, Texas.

Hoke, J.H., Chama, C., Rosengarth, K., (1983): Measurement of Stresses Developing during Corrosion of Embedded Concrete Reinforcing Bars, *Corrosion*, 83, No. 168, *National Association of Corrosion Engineers*, Houston, Texas.

Horiguchi, k., Yamaguchi, T., Maruya, T., and Koji, T., (2020): Study on the Method of Measuring the Chloride Threshold Value of Corrosion and Estimation of the Values in Durability Design of Concrete Structures. *Journal of Advanced Concrete Technology*, 18, pp. 571-587

Huet B., L'Hostis, V., Miserque, F., and Idrissi, H., (2005): Electrochemical behavior of mild steel in concrete: Influence of pH and carbonate content of concrete pore solution, *Electrochimica Acta*, 51, No. 1, pp. 172-180.

Hunkeler, F., (2000): Einsatz von nichtrostenden Bewehrungsstählen im Betonbau',Eidg. Departement für Umwelt, Verkehr, Energie und Kommunikation (UVEK), Bundesamt für Strassen, FA 89/00, Bericht VSS 543

Hunkeler, F., (2001), Use of inoxidable reinforcng steel in concrete structure, Departement federal de l'environnement, des transports, de l'energieet de la communication, Office Federale des Routes, FA 95/00, Rapport VSS 558. (In French)

Hunkeler, F., (2005): Corrosion in Reinforced Concrete: Processes and Mechanism, Techincal research and consulting on cement and concrete, Woodhead Publishing.

Hussain, R. R., (2014): Passive Layer Development and Corrosion of Steel in Concrete at the Nanoscale, *Journal of Civil and Environmental Engineering*, 4, No.3, pp. 1-4.

Hussain, S. E., Rasheeduzzafar, Al-Musallam, A., Al-Gahtani, A.S., (1995): Factors Affecting Threshold Chloride for Reinforcement Corrosion in Concrete, *Cement and Concrete research*, 25, 7, pp. 1543-1555.

Ikeda, T., Hamada, H., Sagawa, Y., Funahashi, M., (2013): Experimental Investigation of Air Void Formed around Steel Bar using X-Ray CT Scanning, *Proc. of the 7th int. conf. on concrete under severe condition* -Envi and loading, 1, pp. 742-748.

Jaffer, S.J., Hansson, C.M., (2008): The Influence of Cracks on Chloride-induced Corrosion of Steel in Ordinary Portland Cement and High-Performance Concretes Subjected to Different Loading Conditions, *Corrosion Science*, 50 (12), pp. 3343–3355.

James, J., (1991): Interface Durability Correlation in Concrete, *Bulletin of Materials Science*, 14 (5), pp. 1183-1195.

James, M., and Gaidis, (2004): Chemistry of Corrosion Inhibitors, *Cement and Concrete Composites*, 26, pp. 181-189.

Jamil, H. E., Shriri, A., Boulif, R., Bastos, C., Montemor, M. F., and Ferreira, M. G. S., (2004): Electrochemical Behaviour of Amino Alcohol-based Inhibitors used to Control Corrosion of Reinforcing Steel, *Electrochimica Acta* , 49 (17-18), pp. 2753-2760.

Japan Concrete Institute (JCI), (2015): Technical Committee report of systematization of Electrochemical Measurement Techniques based upon Physicochemical interpretation, DVD, 2015.

Jeon, C.H., Lee, J.B., Lon, S., and Shim, C.S., (2019): Equivalent material model of corroded prestressing steel strand, J. Material Ressources Technologies, 8, pp. 2450-2460.

Jeong, J.A., Chung, W.S. and Kim, Y.H., (2013): Electrochemical measurements of cathodic protection for reinforced concrete piles in a marine environment using embedded corrosion monitoring sensors. Met. Mater. Int. 19, pp. 445–452.

Käthler, A. C. B., Angst, U. M., Wagner, M., Larsen, C. K., and Elsener, B., (2017): Effect of Cracks on Chloride-induced Corrosion of Reinforcing Steel in Concrete – A Review, *Staten Vegvesen Rapporter,*No. 454.

Khanzadeh-Moradllo, M., Meshkini, M.H., and Eslamdoost, E., (2015): Effect of Wet Curing Duration on Long-Term Performance of Concrete in Tidal Zone of Marine Environment, *International Journal of Concrete Structures and Materials* 9, pp.487–498.

Koch, G.,Varney, J., Thompson, N.O., Moghissi, O., Gould, M., Payer, J.H., (2016): NACE International Impact Report, NACE Int 1–3.

Krishnan, N., Kamde, D. K., Veedu, Z. D., Pillai, R. G., Shah, D., and Velayudham, R., (2021): Long-term Performance and life-cycle Costs benefits of Cathodic Protection of Concrete structures using Galvanic Anodes, Journaml of Building Engineering, 42.

Kumar, V., Singh, R. & Quraishi, M., (2013): A study on Corrosion of Reinforcement in Concrete and Effect on Inhibitor on Service Life of RCC, *Journal of Material and Environmental Science*, 4(5), pp. 726-731.

Langford, P., and Broomfield, J., (1987): Monitoring the Corrosion of Reinforcing Steel, *Construction Repair*, 1 (2), pp. 32-36.

Layssi H, Ghods P, Alizadeh A and Salehi M 2015 Electrical resistivity of concrete Concrete Int. 37 pp 41-46

Lee, H. S., Saraswathy, V., Kwon, S. J., and Karthick, S., (2018): Corrosion Inhibitors for reinforced concrete: A review. In Corrosion inhibitors, principles, and recent applications.

Leonhardt, F., (1988): Cracks and Cracks Control in Concrete Structures, Special reports, *PCI journal*, pp. 124-145.

Liu, Y., Presuel-Moreno, F. J., and Paredes, M. A., (2015): Determination of Chloride Diffusion Coefficients in Concrete by Electrical Resistivity Method, *ACI Materials Journal*, 112 (5), pp. 631-640.

Manning, D. G., (1988): Durability of Prestressed Concrete Highway Structures, NCHRP Synthesis of Highway Practice 140, *Transportation Research Board*.

Mansfield, S., (1981): Corrosion, 37 (5) pp. 301-307.

Mohammed, T. U., and Hamada H., (2003a): Effect of Construction Joint Preparation on Corrosion of Reinforcing Bars Under Atmospheric Environment, *Durability of concrete*, pp. 260-277.

Mohammed, T. U., and Hamada, H., (2003c): Durability of Concrete made with Different Water Reducing Chemical Admixtures in Tidal Environment, *ACI Materials Journa*l, 100(4), pp. 265-273.

Mohammed, T. U., and Hamada, H., (2006): Corrosion of Horizontal Bars in Concrete and the Method to Stop Earlier Corrosion, *ACI Materials Journal*, 103 (5), pp. 303-311.

Mohammed, T. U., and Hamada, H., (2008): Corrosion of Steel Bar in Concrete-facts from the Long-term Exposure Tests, *JCI Concrete journal*, 46(4), pp. 23-26.

Mohammed, T. U., Hamada, H., and Otsuki, N., (2003b): Several Factors regarding Sustainability of Marine Concrete Structures, *Durability of Concrete,* pp. 23-44.

Mohammed, T. U., Yamaji, T., Toshiyuki, A., and Hamada, H., (2002): Marine Durability of 15-year Old Concrete Specimens Made with Ordinary Portland, Slag and Fly ash Cements, *Journal of materials, concrete structures and pavements,* Japan Society of Civil Engineers, pp. 201–214.

Moore, D. G., Klodt, D., and Hensen, R. D., (1970): Protection of Steel in Prestressed Concrete bridges, NCHRP Report, 90.

NACE, (1965): Glossary of Corrosion Terms, *Materials Protection,* 4, pp. 79-80.

Nelson, S., (2013): Chloride Induced Corrosion of Reinforcement Steel in Concrete,Threshold Values and Ion Distributions at the Concrete-Steel Interface, C*halmers University of Technology.*

Neville, A. M., (1995): Chloride Attack of Reinforcement-An Overview, *Materials, and structures*, 28, No. 176, pp. 63-70.

Neville, A. M., (2011): Properties of Concrete Pearson Education Limited (Harlow United Kingdom) pp 207-208 chloride attack of reinforcement-an overview, Materials, and structures, 28, No. 176, pp 63-70.

Ormellese, M., Berra, M., Bolzoni, F., and Pastore, T., (2006): Corrosion Inhibitors for Chlorides Induced Corrosion in Reinforced Concrete Structures, *Cement and Concrete Research,* 36, pp. 536-547.

Ortolan, V.K., Mancio, M., and Tutikian, B.F., (2016): Evaluation of the Influence of the pH of Concrete Pore Solution on the Corrosion Resistance of Steel Reinforcement, *J. Builduing Rehabilitation*, pp.1-10.

P. Pedeferri, Construct. Build. Mater. 10 (1996) 391

Page, C.L., (1997): Cathodic Protection of Reinforced Concrete -Principales and Applications, *Proc. Int. Conf. on Repair of concrete structures*, Scolvaer, Norway, pp, 123-132.

Page, C.L., Sergi, G., (2000): Developments in Cathodic Protection applied to Reinforced Concrete. Journal Materials in Civil Engineering, Sp. Issue, Durability of Construction Materials, pp. 8-15.

Page, C.L., Short, N.R., and El Tarras, A., (1981): Diffusion of Chloride ions in Hardened Cement Pastes, *Cement and Concrete Research,* 11, pp. 395–406.

Parthiban, G.T., Parthiban, T., Ravi, R., Saraswathy, V., Palaniswamy, N., Sivan, V., (2008): Cathodic Protection of Steel in Concrete using Magnesium Alloy Anode, *Corrosion Science*, 50 (12), pp. 3329-3335

Pedeferri, P., (1996): Cathodic Protection and Cathodic Prevention, Construction Building Material, 10, pp. 391-402.

Perenchio, W. F., Fraczek, J., Pfeifer, D. W., (1989): Corrosion Protection of Prestressed Systems in Concrete bridges, Materials Science, NHRP Report.

Pettersson, K., (1992): Corrosion Threshold Value and Corrosion Rate in Reinforced Concrete. CBI report 2:92., S*wedish Cement and Concrete Research Institute*, pp. 1-43.

Pettersson, K., (1994): Chloride induced Reinforcement Corrosion, *status report. Högpresterande Betongkonstruktioner,* CBI, Report M1:5.

Pettersson, K., (1995): Chloride threshold Value and the Corrosion Rate in Reinforced Concrete, *Proc. of the Nordic Seminar. Lund,* pp. 257-266.

Pfeifer, D., McDonald, D. and Krauss, P., (1994): Rapid Chloride Permeability Test and its Correlation to the 90-day Chloride Ponding Test, *PCI J.*, pp. 38-47.

Pourbaix, M., (1973): Lectures on Electrochemical Corrosion, *NewYork: Plenum Press,* 29.

Pourbaix, M., (1974): Atlas of Electrochemical Equilibria in Aqueous Solution, 307, NACE.

Poursaee, A., (2016): Corrosion of Steel in Concrete Structures, *Elsevier*.

Raja, P.B., Ghoreishiamiri, S., Ismail, M., (2015): Natural Corrosion Inhibitors for Steel Reinforcement in Concrete – A Review, *World Scientific Publishing Company,*22, pp.68-75.

Reddy, B., Glass, G.K., Lim, P.J., and Buenfeld, P., (2002): On the Corrosion Risk presented by Chloride Bound in Concrete, *Cement and Concrete Composites, 24*, pp. 1-5.

Rehm, T. R., and Moll, A. J., (1964): Attempts to Study the Influence of the Crack Width on the Rust Formation on the Reinforcement of Reinforced Concrete Components. DAfS, Heft 169. Berlin.

Reou, J. S. and Ann, K. Y., (2008): The Electrochemical Assessment of Corrosion Inhibition Effect of Calcium Nitrite in Blended Concretes, Material Chemistry and Physics, 109, pp. 526-533.

Richardson, M. G., (2002): Fundamentals of durable reinforced concrete, *CRC Press*.

Rodriguez, J., Ortega, L.M., and García, A.M., (1994): Assessment of Structural Elements with Corroded Reinforcements, *Int. Conference on Corrosion and Corrosion Protection of Steel in Concrete,* Sheffield, UK, ed. R.N. Swamy, pp. 171–185, 1994.

Saremi, M., Mahallati, E., (2002): A study on Chloride-induced Depassivation of Mild Steel in Simulated Concrete Pore Solution, *Cement and Concrete Research*, 32 (12), pp. 1915-1921.

Saricimen, H., Mohammad, M., Quddus, A., Shameem, M., and Barry, M. S., (2002): Effectiveness of Concrete Inhibitors in Retarding Rebar Corrosion, Cement and Concrete Composites, 24, pp. 89-100.

Sato, N., (1981): Comprehensive Treatise of Electrochemistry, vol. 4. New York: Plenum Press.

Schiessl, P., (1976): On the Question of the Permissible Crack Width and the Required Concrete Cover in Reinforced Concrete Construction with Special Consideration, the Carbonation of Concrete. DAfS, Heft 255. Berlin.

Schiessl, P., and Raupach, M., (1997): Laboratory Studies and Calculations on the Influence of Crack Width on Chloride-induced Corrosion of Steel in Concrete. American Concrete Institute. 94(1), pp. 56-62.

Scott, A. N., (2004): The Influence of Binder Type and Cracking on Reinforcing Steel Corrosion in Concrete, Cape Town: *Department of Civil Engineering University of Cape Town*.

Scwamborn, B., (1987): About the Bleeding of Fresh Concrete*, Proc. of a colloquium, Frischmortel, Zementleim, Friscbeton (University of Hanover)* 55, pp. 283-297

Sergi, G., Page, C.L., (1999): Sacrificial Anodes for Cathodic Protection of Reinforcing Steel around Patch Repairs applied to Chloride-contaminated Concrete, Proc. Eurocode 99, European Corrosion Congress, Aachen, Germany.

Song, H., and Saraswathy, V., (2007): Corrosion Monitoring of Reinforced Concrete Structures—A Review," *International Journal of Electrochemical Science*, 2, pp. 1–28,

Soshirada, T., (1990): Effect of Bleeding and Segregation on the Internal Structures of Hardened Concrete, *Proprieties of fresh concrete*, Ed H J Wierig, pp. 253-60.

Soylev, T. A., Richardson, M. G., (2008): Corrosion Inhibitors for Steel in Concrete: State-of the-art report, *Construction and Building Materials*, 22 (4), pp. 609-622.

Söylev, T.A., and Richardson, M.G., (2008): Corrosion Inhibitors for Steel in Concrete: State-of-the-art report. *Construction and Building Materials*, 22 (4), pp. 609-622

Stern, M., and Geary, A., (1957): Electrochemical Polarization: A theoretical analysis of the shape of polarization, *Journal of the Electrochemical Society*, 104(1), pp. 56-63.

Subramaniam, K. V., and Bi, M., (2010): Investigation of Steel Corrosion in Cracked Concrete: Evaluation of Macrocell and Microcell Rates using Tafel Polarization Response, *Corrosion Science*, Elsevier, 52, pp. 2275-2735.

Suzuki K., Ohno, Y., Praparntanatorn, S., and Tamura, H., (1990): Mechanism of Steel Corrosion in Cracked Concrete International, Symposium on Corrosion of Reinforcement in Concrete Construction (3rd), *Elsevier, Applied Science*, Wishaw, England.

Takumi Haruna, II. Fundamental Electrochemical Methods for Corrosion - Corrosion Potential Zairyo to Kankyo, Vol.67, No. 1, pp. 2-8, 2018 Jan. (in Japanese)

The International Organization for Standardization, ISO 8044, (2015): Corrosion of Metals and Alloys – Basic terms and definitions.

Tuutti, K., (1982): Corrosion of Steel in Concrete, CBI Research Report 4:82, *Cement and Concrete Research Institute,* Stockholm, pp. 1-469.

Tuutti, K., (1982): Corrosion of Steel in Concrete, *CBI Stockholm.*

Venkatesh, C., Mohiddin, S.K., Ruben, N., (2019): Corrosion Inhibitors Behavior on Reinforced Concrete—A Review. In: Das B., Neithalath N. (eds*) Sustainable Construction and Building Materials*, Lecture Notes in Civil Engineering, 25. Springer, Singapore.

W. Medford, "Testing calcium nitrite corrosion inhibitor in concrete," Transportation Research Record, vol. 1795, pp. 62–65, 2014.

Wang, J.,Lu S., (2021): Review of Short-Term and Long-Term Bond Properties between Epoxy-Coated Reinforcement and Concrete, IOP Conference Series: Earth and Environmental Science,719(212), 7th International Conference on Environmental Science and Civil Engineering, ESCE,2021.

Watanabe, H., Hamada, H., Yokota, H., and Yamaji, T., (2001): Long Term Performance of concrete and Reinforced Concrete under Marine Environment, Proc. of the 3rd conference on concrete under Severe Conditions, The University of British Columbia, Vancouver, Canada.

Wenner, F., A (1916): Method of Measuring Earth Resistivity, *Bulletin of the Bureau of Standards*,12, No.4, pp.469–478.

Xu, J., Jiang, L., Wang, W., Tang, L., Cui, L., (2013): Effectiveness of Inhibitors in Increasing Chloride Threshold Value for Steel Corrosion, *Water Science and Engineering*, pp.354-363.

Yamaoka, Y., and Tanaka, Y, (1993): Comparison of the Mechanisms of Hydrogen Embrittlement and Stress Corrosion Cracking of High Carbon Steel Wire, *Int. Workshop on Prestressing Wire*, Denver, Colo.

Yokota, H., Akiyama, T., and Hamada, H., (1999a): Effect of degradation of Concrete on Mechanical Properties of Reinforced Concrete Beams Exposed to Marine Environment (for 20 years in Sakata), Report of the Port and Airport Research Institute, 38 (22).

Yokota, H., Fukute, T., Hamada, H., and Akiyama, T., (1999b): Structural assessment of deteriorated RC and PC beams exposed to marine environment for more than 20 years, Wakachiku Kensetsu Doboku Gijitsu Nenpo, 8, pp. 78-84.

Yu, B., Yang L., Wu, M., and Li, B., (2014): Practical Model for Predicting Corrosion Rate of Steel Reinforcement in Concrete Structures, *Construction and Building Materials,* 54, pp. 385-401.

Zainal, F.F., Zin, N.M., Razak, S.A.A., Rahmat, A., Hussin, K., and Abdullah, M.M.A.B., (2020): Corrosion Control by Using Zinc as Sacrificial Anode Cathodic Protection in Geopolymer Concrete. In: The Minerals, Metals & Materials Society (eds) TMS 2020 149th Annual Meeting & Exhibition Supplemental Proc. The Minerals, Metals & Materials Series. Springer, Cham.

CHAPTER III

EFFECTIVENESS OF JOINT TREATMENT ON CORROSION OF STEEL BAR IN PRESTRESSED CONCRETE BEAMS

-- Observation of Severely Damaged Specimens under Marine Conditions for More than 35 years –

3.1. INTRODUCTION

The use of prestressed concrete is very popular in civil engineering construction due to its numerous benefits, such as the increase of load-bearing capacity, the better control of cracks, and the slenderness of elements. Prestressed concrete differs from Reinforced Concrete by the fact that initial compression is applied to the concrete through a high-strength steel wire (or bar) also called “tendons”. In post-tension systems, the prestressing load is applied after the concrete reaches a certain strength after a determined curing period. Ducts (galvanized or polyethylene steel) are usually imbedded in such kind of concrete with grout which is usually made of Portland cement paste.

Like in reinforced concrete, the degradation due to corrosion must be given high consideration as their damages are significant. According to previous studies, Corrosion is the main cause of the collapse of bridges and concrete pipes [Singh, 2000; Bertolini et al., 2004; Essamin and Holley, 2004]. According to the past studies, the cause of the collapse of more than 7% of bridges between 1980 and 2012 was due to environmental degradation [Di Prisco, 2019] and the vast majority of poor performance was due to certain construction practices and improper designs [Burdekin and Rothwell, 1981]. The ingress of aggressive agents like chlorides and carbon are among the most prevalent deterioration factors of corrosion and decrease the service life of structures [Ann et al., 2009].

Generally, the fundamental mechanism of corrosion observed in prestressed concrete (PC) structures are essentially like the mechanism seen in reinforced concrete (RC) members [Manning, 1988; Pfeifer et al., 1994]. The ACI 222 provides extensive coverage of the fundamental mechanism of corrosion of metal imbedded into concrete [ACI 222-2R, 2001]. The presence of grout in PC concrete provides a highly alkaline environment in the concrete and bond between concrete tendons that protects against corrosion similarly to reinforced concrete. In addition, the type of concrete and steel used in prestressed concrete are designed to have higher strength compared to reinforced concrete. Therefore, they are renowned to be more durable [Freyermuth, 1991].

Yet, if corrosion occurs the primary effect of the corrosion of steel in prestressed concrete is more serious than in RC concrete [Coronelli et al., 2009; Li and Yan, 2013]. For instance, when the loss of cross-section in RC beams may lead to cracks, spalling, and other serviceability related issues long before its failure, in PC members that could lead to the increase of the net stress in the prestressing leading to a yielding and fracture, as 55 to 65% of its ultimate tensile strength is continuously applied to the steel. The damages caused by the corrosion of prestressed concrete could be quantified to about 4 to 5 times the damage in reinforced concrete. Besides, there is relatively little superficial warning immediately before the failure of the prestressed structures [Yamaoka and Tanaka, 1993].

Numerous are the reasons for the occurrence of corrosion in concrete but the most common cause in post tension, particularly in the bonded post tension, is the result of the inappropriate ground injection. During the injection of grout, it is essential that the grout is fully filled to avoid the corrosion of the duct leading to corrosion of the steel. Another factor affecting the corrosion of the prestressed concrete steel is the presence of joints and its location. Due to various reasons such as the impossibility of continuous casting, joints are inevitable. Joints in concrete promote the ingress and accumulation of chloride in the vicinity of the rebar [Hamada et al., 1987]. When exposed to a severe marine environment, due to the attack of chlorides and the moistures, the PC structures are more vulnerable than the RC concrete, and the use of protection is imperative. Protection against corrosion in new construction is set to limit the ingress of chloride in the prestressing system.

For the past few years, several studies where done to ameliorate the durability of prestressed concrete; nonetheless, due to its complexity, the literature accessible about the latter is not as common as in the reinforced concrete. The corrosion of prestressing steel is more complex and affected by many factors. As a result, the study of the behavior of prestressed concrete has steel left some gaps in the concrete field when it comes to corrosion.

In this study, the durability of beams exposed to severe environments after 30 years is studied. Previous studies have almost exclusively focused on specimens at an early age of exposure [Miyazato, 2021]. Therefore, the results of this study will be beneficial to fill the gap in the literature concerning long-term exposures. The effectiveness of different types of joints treatment applied to severely damaged PC beams was evaluated using non-destructive, destructive, and visual observation. Besides, the phenomenon of macrocell corrosion is also assessed as a secondary objective.

The main parts of a bonded prestressing steel

Prestressed concretes are beforehand subjected to compressive stresses that oppose the stresses created by external loads, once the structure is in service.

- **Prestressing ducts** is a passageway, made of non-corroding plastics or galvanized steel used to provide a cavity in the concrete along the profile of the prestressing steel or cable to inject the grout and bond the system together.
- **Prestressing steel** (wire, strands, or bar) is to which the strength is applied during construction and the lifespan of the structure.
- **Grouts** are generally Portland cement paste, used to bond the prestressing steel for the rest of the construction.
- **Anchorages** are the elements of the post-tensioning system that anchor the tendons into the concrete and are used to transfer the stressing force to the concrete once the stressing proceed is complete.

3.2 TEST PROGRAMS

3.2.1 Specimen Outline

To bring out this study, 4 types of post tensioned beams specimens were used, consisting of: 01 specimen with joint and without treatment (J1), 01 specimen without joint (N1), 02 specimen with joint treated with the same mortar as the concrete (M1, M2), and 02 specimen with joint treated with Epoxy resin with 5 mm thickness (E1, E2).

Beams with dimension of 120 x 150 x 1200mm were prepared for experimental works. Bending loads were applied to each of the specimen, targeting respectively 0.1 and 0.2 mm of cracks. Concerning the mix proportion, due to the old age of the specimens, no data were available concerning its mixed proportion besides the fact that the specimens were cast using the same water to cement ration concrete. However, the quality of the concrete was assessed.

Table 3.1: Specimen outlines

Specimen	**Joint**	**Treatment type**	**Crack (mm)***
N1	No Joint		
J1	With Joint	No Treatment	0.1
M1	With Joint	Mortar treatment	0.1
M2	With Joint	Mortar treatment	0.2
E1	With Joint	Epoxy Resin Treatment	0.1
E2	With Joint	Epoxy Resin Treatment (5mm)	0.2

- *Targeted cracks under bending loads in mm.

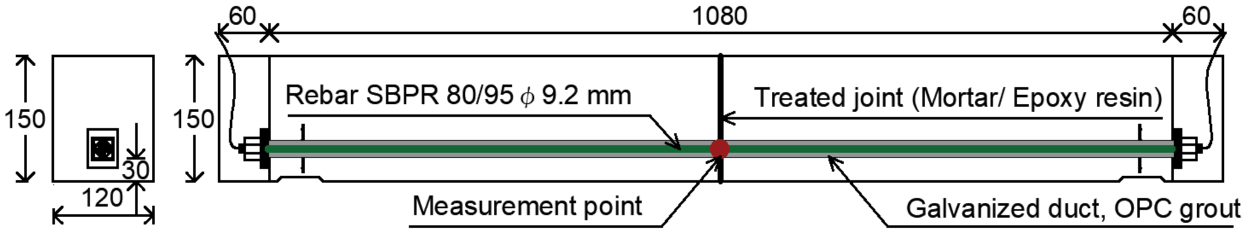

Figure 3.1 Outline of the specimen

3.2.2 Materials

Round high strength steel bars (SBPR 80/95 with Ø9.2 mm diameter) were used for the application of compressive force to the beams, and two layers of galvanized prestressing ducts were incorporated in the prestressing system. Ordinary Portland Cement (OPC) with a concrete density of 2400 kg/m^3. The duct of prestressing system was filled with Portland cement grout.

3.2.3 Specimen Exposure condition

The specimens were cast in the Port and airport Research Institute, Japan, where it was exposed to severe environmental conditions for about 30 years. After, the specimens were moved to Kyushu University and exposed to atmospheric conditions for 7 years (2014-2021)

- 1982-2014 (32years) Port and Harbor Research Institute (PHRI) in severe tidal environments under bending loads.
- 2014-2021 (7 years): Kyushu university in the atmosphere condition without bending loads. From 2020, electrochemical measurements and visual observation were performed, and the specimens were crushed for destructive tests afterward.

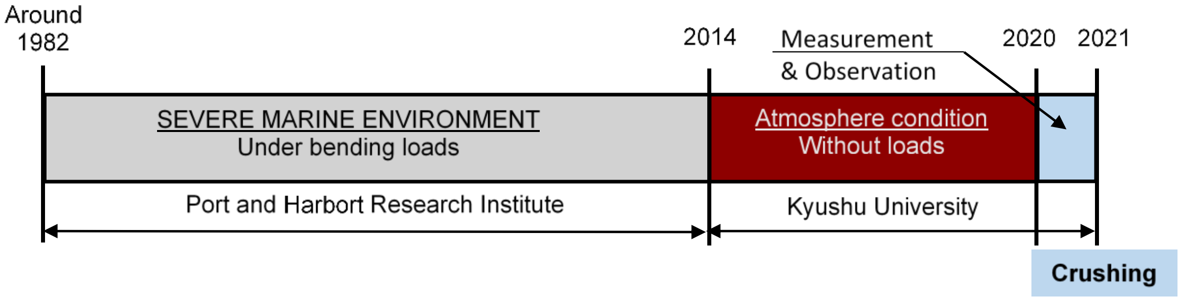

Figure 3.2 Exposure condition of the specimens

3.2.4 Experimental Methods

(1) *Visual observation*

Visual observations were performed in 2 steps in this study.

The first observation concerns the investigation of the outward appearance of the beams, such as the presence of cracks, rust, spalling, and the assessment of the quality of the concrete.

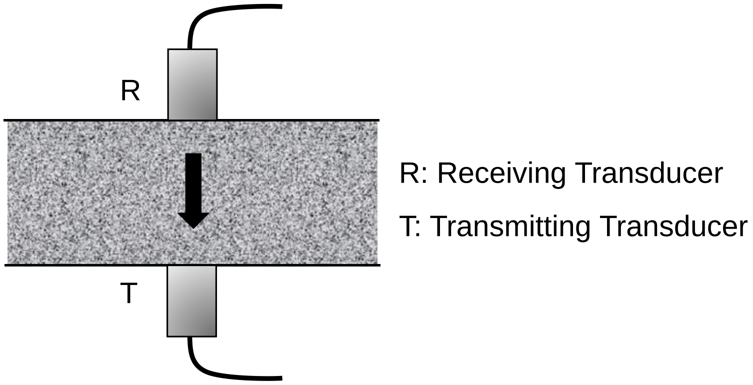

Figure 3.3 Pulse Velocity measurement setting using a direct transmission method

Ultrasonic Pulse Velocity (UPV) has been widely recognized in terms of reliability especially in high-strength concrete as the precision is even more accurate with the increase of strength [Jones, 1969, Soutsos et al., 2011]. In this study, it was used to estimate the quality of the concrete and the depth of the cracks according to the EN 12504 regulation [EN 12504-4, 2004]. The Velocity Pusle V is determined by the ratio of length (L:m) and the measured time (Δt: sec) and qualitatively compared with the classification of Whitehurst (Table 3.2) [Whitehurst, 1951].

Table 3.2 Concrete quality according to ultrasonic pulse velocity

Ultrasonic Pulse Velocity [m/s]	**Concrete quality**
> 4500	Excellent
3500-4500	Good
3000-3500	Doubtful
2000-3000	Poor
<2000	Very poor

The second series of visual observations were done to assess the inner condition of each specimen. Core samples were taken for different sections of each beam and the specimens were crushed afterward. The condition of corrosion inside of the concrete was assessed and the corrosion of the steels are also quantified by the measurement of the cross-section loss of each steel.

(2) *Electrochemical measurement*

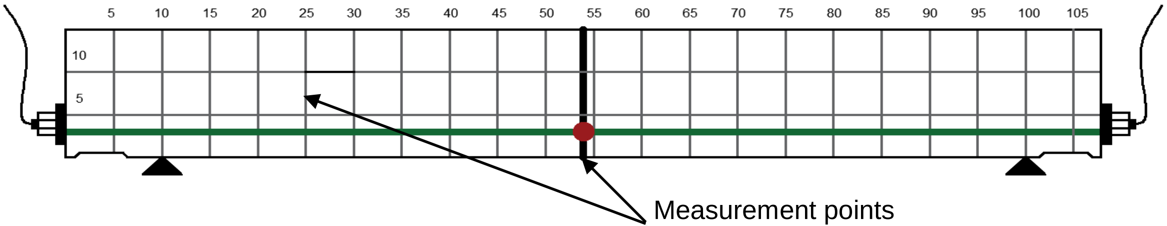

Figure 3.4 Measurement point for nondestructive testing

Several electrochemical measurements were used to assess to corrosion of the steel reinforcement. Electrochemical methods are widely used in concrete as the reaction occurring in concrete during the corrosion process is mostly electrochemical [Lambert et al., 1991; Elsener, et al., 2003]. 5 cm grids were drawn on the surface of the beams and the half-cell potential was measure at every 5 cm of the beams as shown in *Figure 3.4*. The current density, the polarization resistance and polarization curve, electrical resistivity, and diffusion of oxygen were performed directly at the joint. Finally, electrical resistivity is measured at the section without rebar [Wenner, 1916].

Half-cell potential was measured to assess the corrosion probability level in every 5cm of the specimen. Impedance voltmeter and silver/silver chloride (Ag/AgCl) reference electrode were used. The probability of corrosion was determined following the ASTM Standard in table [ASTM, C872, 2015].

Table 3.3. Half-cell potential range related to corrosion probability (ASTM C876)

Half-Cell Potential (E_{corr}) (mV;CSE)	**Probability of Corrosion**
E_{corr} >-200 mV	10%
-350<E_{corr}<-200	Uncertain
E_{corr}<-350	90%
E_{corr}<-500	Severe corrosion

Polarization resistance measurement was done to assess the risk and the rate of corrosion using a portable corrosion meter and silver/silver chloride reference electrode (Ag/AgCl). The CEB standard was used to quantitatively assess the results [CEB, 1998].

Table 3.4 Corrosion rate according to the CEB Standard

Corrosion Current Density	**Corrosion Rate**
$i_{corr} < 0.2$ µA/cm^2	Passivity state/ very low
$0.2 < i_{corr} < 0.5$ **µA/cm^2**	Low to moderate
$0.5 < i_{corr} < 1$ **µA/cm^2**	Moderate to High
$i_{corr} > 1.5$ **µA/cm^2**	Very high

Polarization curve to assess the oxygen permeability and the grade of passivity of reinforcements following the qualitative standard developed by Otsuki et al. [Otsuki et al., 1985], owing to the size of the specimen, the contact method was opted [Hamada et al., 2010]. A potentiostat, a reference electrode, and a sensor with a counter electrode are used for the measurement. A data logger was connected to the sensor to collect the data.

Table 3.4: Grade of passivity function of potential and current density

Grade	**Potential**	**Current density**	**Passivity state**
0	E_{corr}+200mV to E_{corr}+600mV	$I_{corr} > 100$µA/cm^2 at least one time	No Passivity Film
1		$10 < I_{corr} < 100$µA/cm^2	Some Passivity Film
2		The anodic curve cut the 10 µA/cm^2	
3		$1 < I_{corr} < 10$ µA/cm^2	
4		The anodic curve cut the 1µA/cm^2	
5		$I_{corr} < 1$µA/cm^2	Excellent Passivity Film State

Potential step to assess the supply of oxygen at the joint section. In this experiment, a first attempt of the use of contact method was performed. Oxygen diffusion has been determined using the immersion method, however, this method is restricted to specimen in a relatively small scale. Potentiostat, data logger, silver/silver chloride reference electrode, and contact sensor equipped with a counter electrode were used. The beams were wetted, wrapped in wet towels and plastic wraps for 1 month for the specimen to be well wetted (*Figure 3.5*). During the measurement, all surfaces of the specimen were wrapped with a wet towel, and the sensor was fixed to the beams using clamps as seen in *Figure 3.6*.

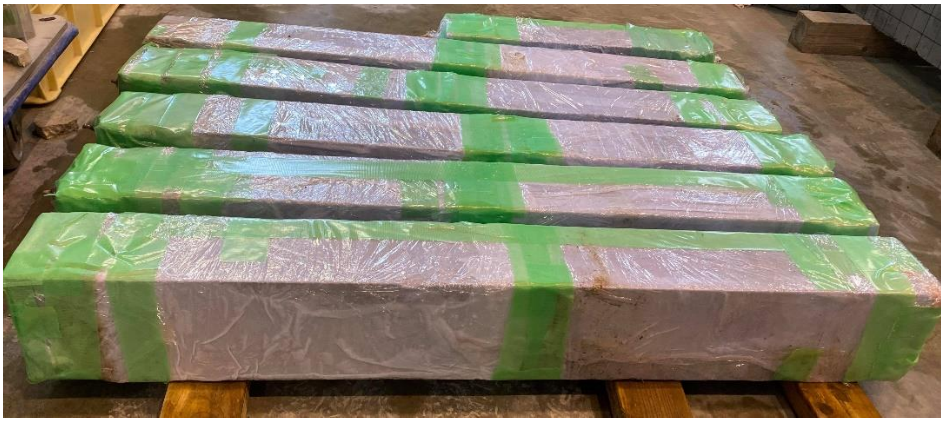

Figure 3.5 Condition of the specimen wrapped in wet towel

Figure 3.6 Potential step using contact method procedure

The potential was set and hold at 1000 mV and the measurement was held on for 24 hours like in the immersion method, in the first trial. However, it was observed that the current is stabilized after 4 hours of measurement, therefore, the measurements were stopped after 5 hours. The cathodic current density I_{lim} was used to calculate the diffusion of oxygen [Nagataki, 1996].

$$\frac{dQ}{dt} = \frac{i_{lim}}{n.F} \tag{3.1}$$

Where,

dQ/dt : Oxygen supply (mol/cm^2/s)

i_{lim} : Current density (A/ cm^2)

n : Number of electron (4)

F : Faradays constant (96,500 coulombs/mol)

(3) *Destructive test*

Series of destructive tests were also done to assess the parameters which may affect the corrosion of steel bars in the concrete. For this purpose, 9 samples of 50 mm x 120 mm were taken from each specimen as seen in *Figure 3.8* below.

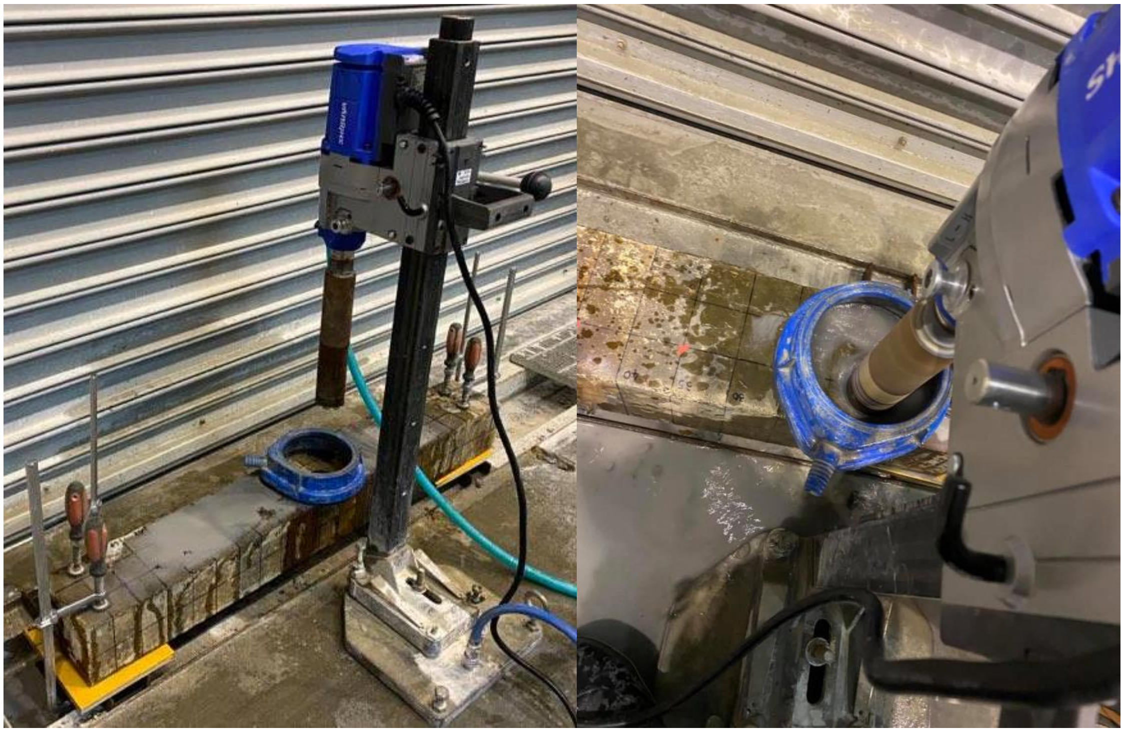

Figure 3.7: Core drilling process

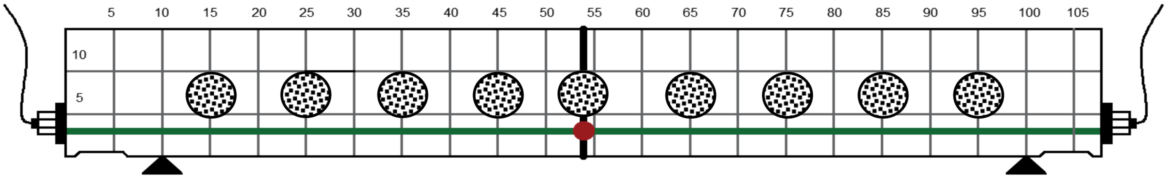

Figure 3.8 Core sampling points

First, **Chloride concentration** tests were done at different depths of the concrete using 2 core samples for each specimen. The drilled cores are sliced in 5mm thickness at 5 different depths at the surface, 3cm, 6cm, 9cm, and 12cm. Afterward, they were crushed and milled. The powders were kept for 24hours in clean plastic containers. The powders were dissolved, and the titration process was done based on the JIS 1154 using a potentiometer titrator AT-700 [JIS A 1154, 2020].

Sliced specimen Specimen after crushing Dissolution Samples

Figure 3.9 Process of the preparation for titration test

Figure 3.10 AT-700 Automatic potentiometer titrator

Compressive strength was performed on 5 samples from each specimen (*Figure3.12*). The tests were performed according to the JIS A 1108 [JIS A 1108; 2018]. The cores were trimmed and polished to have a section about 100mm and a diameter of 50mm (error ± 1mm). The diameter and the height were measured in three directions each.

The compression strength test was calculated using the following formula:

$$f_c = \pi . P . \frac{d^2}{4} \tag{3.2}$$

With:

- fc: Compression strength (N/mm^2)
- P: Maximum load (N)
- d: Diameter (mm)

Figure 3.11: Compressive strength test

3.3 RESULTS AND DISCUSSIONS

3.3.1 Specimen assessment

3.3.1.1 Ultrasonic pulse velocity (UPV)

The UPV of the concrete was measured using the direct transmission method and qualitatively judged using Whitehurst classification. Table 3.6 shows the average of the measured UPV for each specimen. The concrete is judged “good” (3500-4500) and “excellent” (4500m/s and above)

Table 3.6 Ultrasonic pulse velocity results [Whitehurst, 1951]

	N1	**J1**	**M1**	**M2**	**E1**	**E2**
UPV [m/s]	4528	4528	4454	4494	4428	4651

3.3.1.2 Appearance of the beams

- Cracks and rust stains

Cracks, rust stains, and stalling were observed in all the specimens. *Figure 3.13* shows the conditions of the beams without joint treatment. One of its sections has spalled due to the corrosion of the prestressing system and the rebar was exposed. Failures occurred in the steel reinforcement. Spalling did not happen in the other section; however, the degree of cracks is already very severe. *Figure 3.14* shows the conditions of the specimen without joint (N1). Some cracks parallel to the steel reinforcement are observed with some rust stains. Nonetheless, the beam is still in better conditions than the specimen without a joint. *Figure 3.15* displays the states of the treated specimens. The beams show some cracks and rust stains. However, the mortar treated specimen (M2) shows larger areas of rust stain coming out of the horizontal cracks.

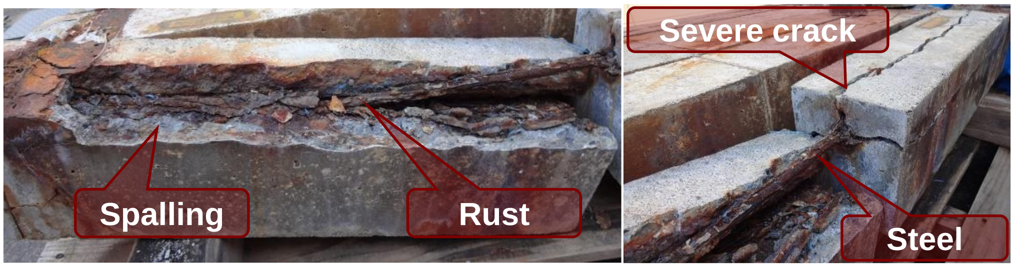

Figure 3.12 Condition of the specimen without treatment (J1)

Figure 3.13 Condition of the specimen without joint (N1)

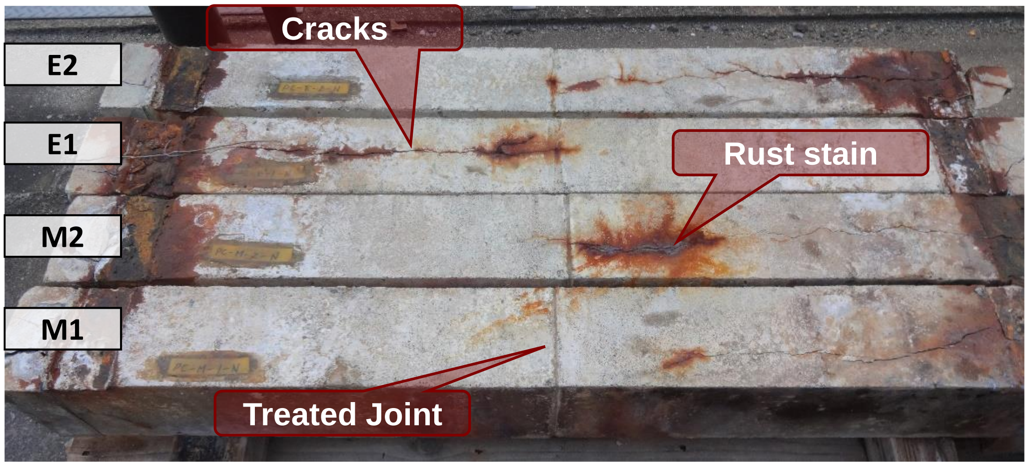

Figure 1.15 Conditions of the specimen with joint treatment, a view from the tensile side

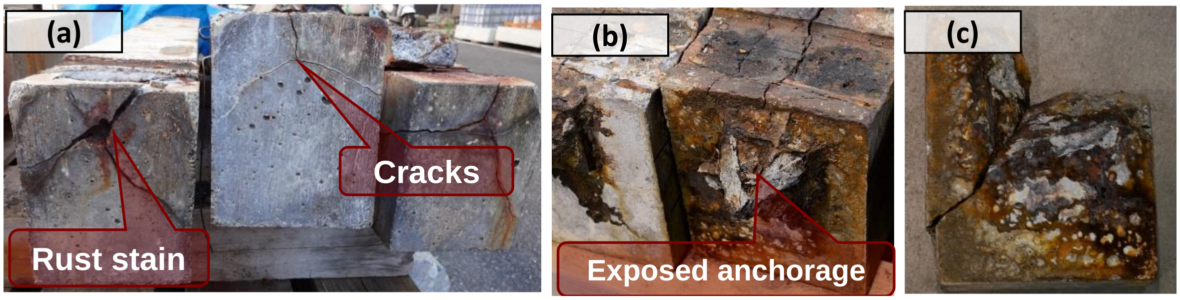

Figure 3.15 Condition of the anchor of the post tensioning system

- Anchorage

The condition of the anchorage of the post tensioning system is also shown in *Figure 3.16*. Due to the corrosion of the anchorage spalling occurred in both end abutments. The corrosion of the anchorage is a factor promoting the ingress of moisture and chloride into the prestressing system [ACI 222-2R, 2001]. In case of the presence of void in the duct, this may lead to an even more severe condition as moisture and aggressive agents can easily move along the tendon. Because of the corrosion of the anchorage, further cracks are observed approximately to the anchorage as seen in *Figure 3.17b* [Isecke, 1990; Dickson et al., 1993]. The lack of protection of anchorage is also influencing the corrosion of the beams as shown in previous researches [Ahmad et al, 2016; 2018].

- Bending cracks

As mentioned earlier in this chapter, bending loads were applied to all specimens with joints targeting a bending crack of 1 mm and 2 mm parallel to the joints (at the joint), for E1, M1, and E2, M2, respectively. However, as illustrated in the figures that follow, no apparent crack can be seen for the specimen targeting 1mm crack (E1, M1). However, for the specimens aiming 2 mm cracks (E2, M2), hairy cracks are seen in E1 and the crack is slightly wider in the case of the mortar specimen M2.

Figure 3.16 Mortar treated joint condition due to the bending load (Tensile side)

Figure 3.17 Epoxy treated joint condition due to the bending load E1-E2(Tensile side)

- <u>Crack mapping</u>

Part of the visual observation, the width, and the depth of the cracks in each PC beams were measured. The details of the cracks for each PC beam are shown in the following pages.

Figure 3.18 illustrated the cracks of the specimen without a joint (N1). Cracks are seen from two extremities of the beams on the trajectory of the rebars. A maximum crack width of 7 mm is seen on the tensile side of the beam with a maximal depth of 5.25 mm. That shows that the crack has reached the reinforcement. In addition, cracks are observed on the side of N1. *Figure 3.19* shows the crap mapping of the specimen without treatment (J1) which shows wide cracks in different directions from the rebar.

A common trend observed in the treated specimen is the formation of crack, only on one side of the beams unlike in beam (N1). Most of the horizontal cracks were observed on the tensile side of the beams and few on the sides, whereas almost no crack was seen on the compression side of the beams. M1 shows a maximum crack width of 1.70 mm and crack depth of 4.25 mm (Figure 3.18). M2 displays fewer cracks compared to M1 on the side. Nonetheless, a maximal horizontal crack of 3.00mm width and 4.25 mm of depth is seen on its tensile surface (Figure 3.19). Figure 3.21 and Figure 3.22 show the crack mapping of the epoxy treated specimen. E1 shows no apparent crack on the side. However, longitudinal crack with until 4 mm is observed with a depth of 4.25. The maximal crack depth of E1 has not reached the rebar. Finally, E2 displays crack up to 2.5mm with a depth of 5.25mm. In addition, cracks are seen on the other section of the beams and the side, unlike E1.

The results from the crack assessment show the importance of adequate treatment as the non-treated specimen (J1) was in the worst condition. Among the treated beams, beam E1 shows the least crack. Comparing the treated specimen and the specimen without joint, the treated specimens are in better condition, this may imply that the use of effective treatment is efficient in mitigating corrosion in reinforced structures. Previous research suggests that the mere presence of cracks is enough the estimate that corrosion has already occurred in the concrete. However, it was confirmed from several researches that generally the type of corrosion occurring in prestressed concrete is “localized corrosion”. Thus, the occurrence of cracks in one section cannot represent the whole rebar [Schupack, 1994]. As a result, it is important to deal with other methods of investigation to understand the condition of the beams.

❖ Specimen without Joint (N1)

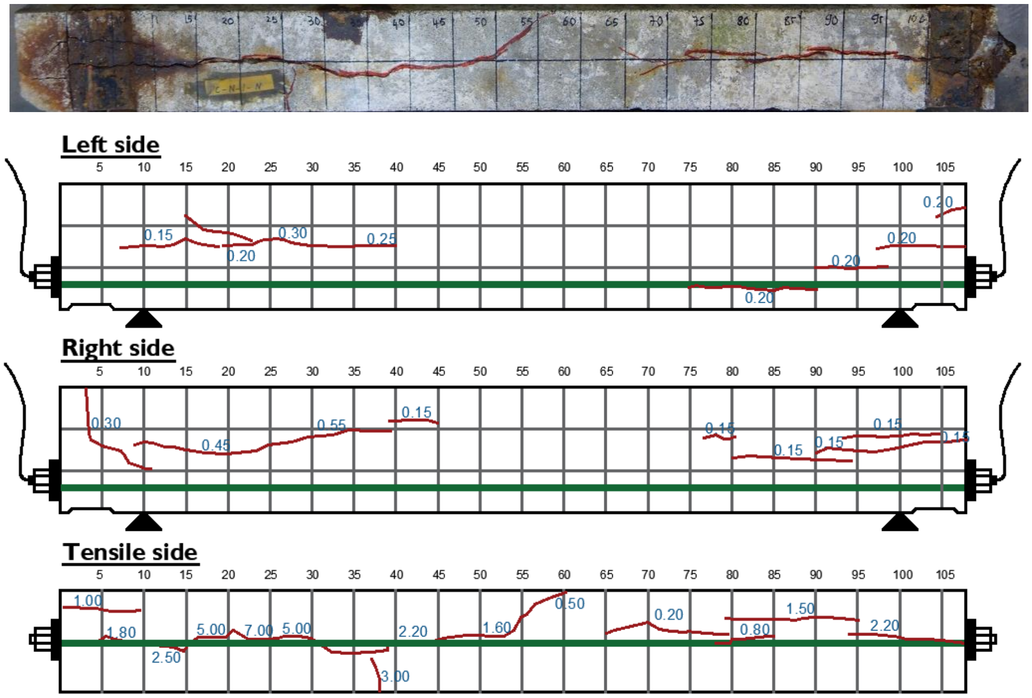

Figure 3.18 Appearance and crack mapping of N1

❖ Specimen without treatment:(J1)

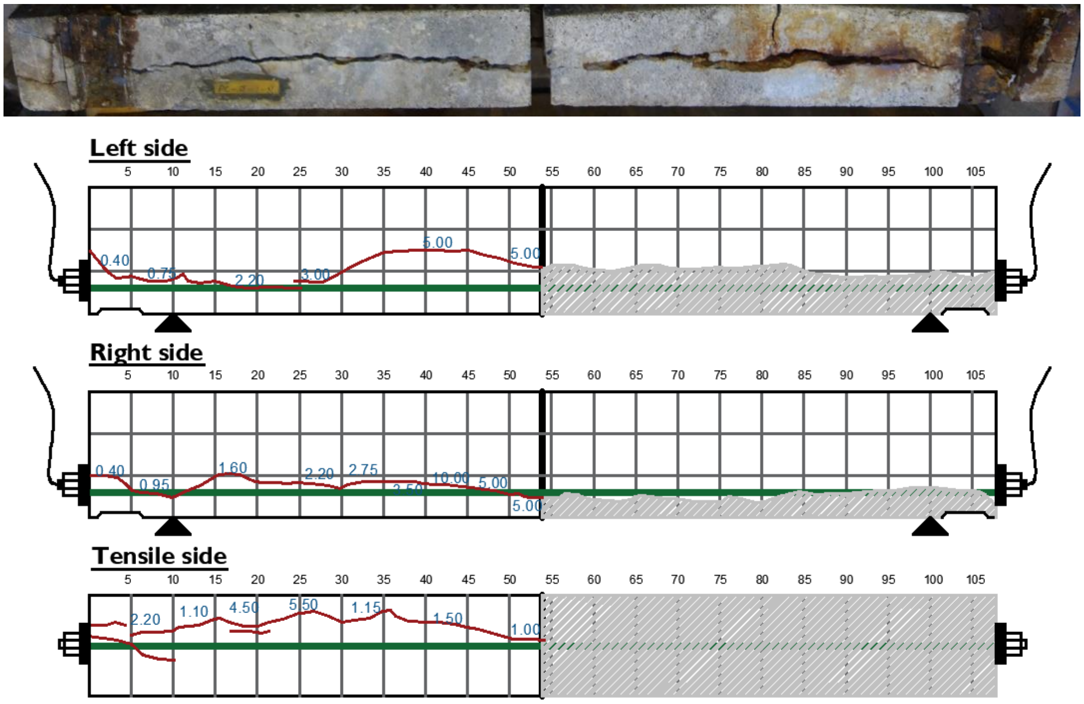

Figure 3.19 Appearance and crack mapping of J1

❖ Specimen without Joint (M1)

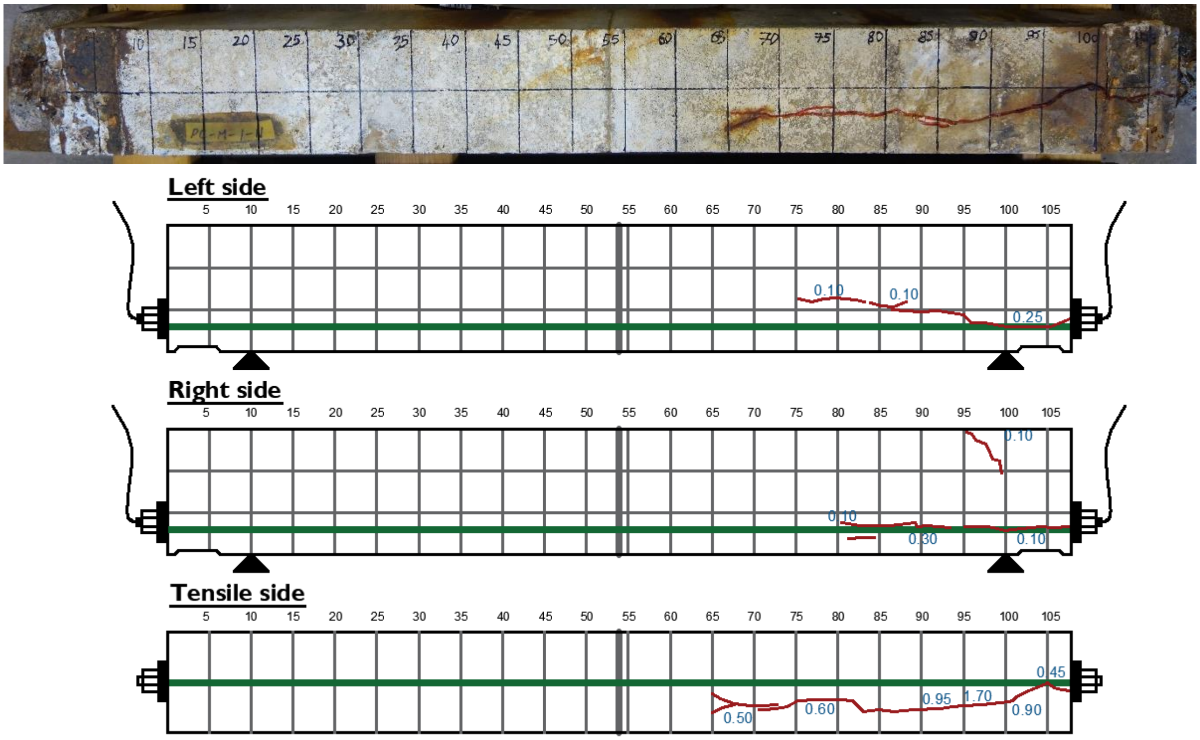

Figure 3.20 Appearance and crack mapping of M1

❖ Specimen without Joint (M2)

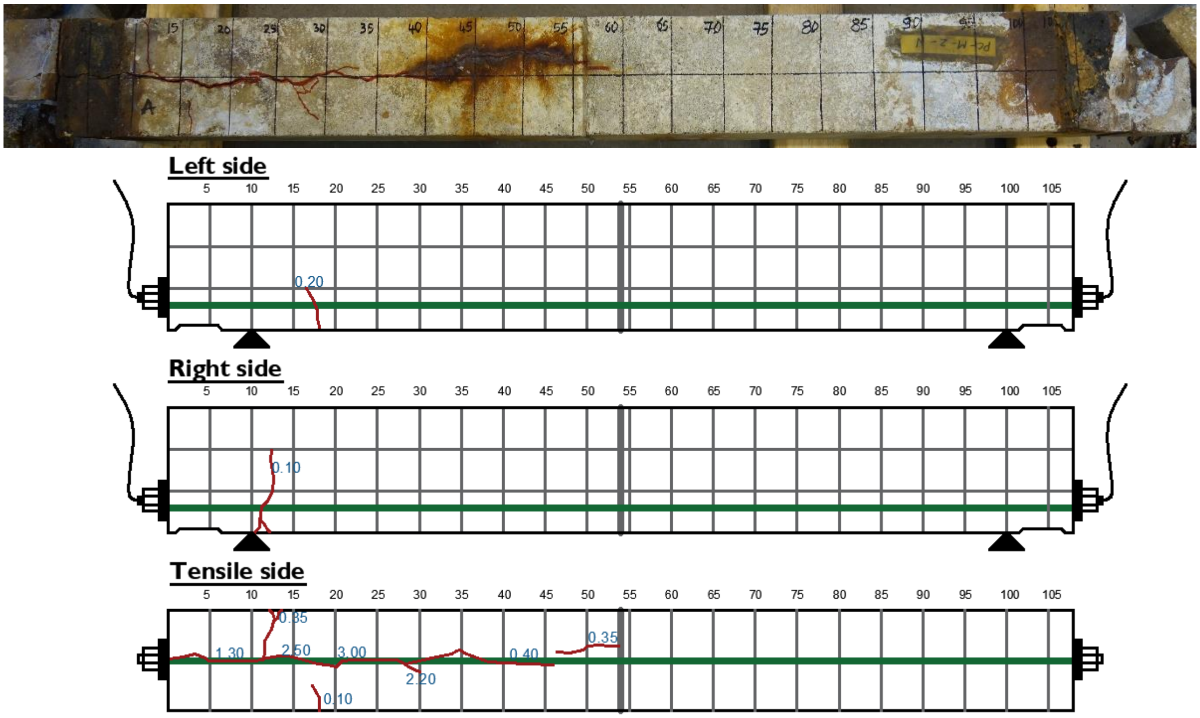

Figure 3.21 Appearance and crack mapping of M2

❖ Specimen without Joint (E1)

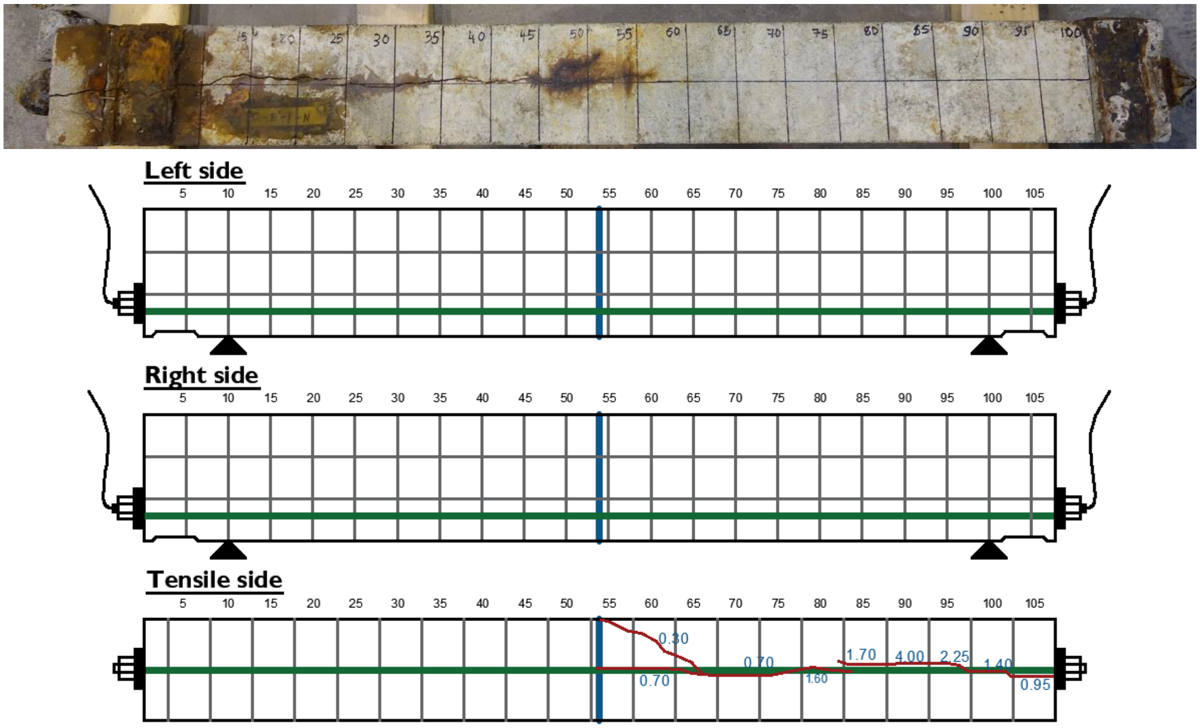

Figure 3.22 Appearance and crack mapping of E1

❖ Specimen without Joint (E2)

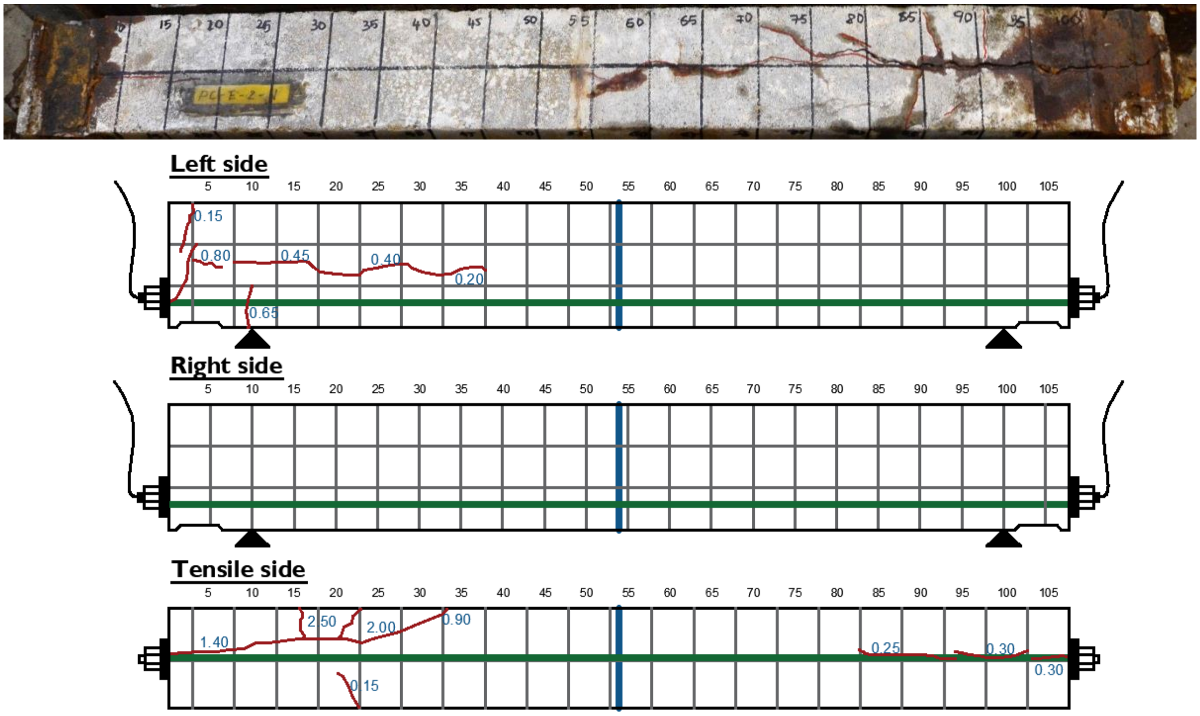

Figure 3.23 Appearance and crack mapping of E2

3.3.2 Electrochemical Measurement

3.3.2.1 Half-cell potential

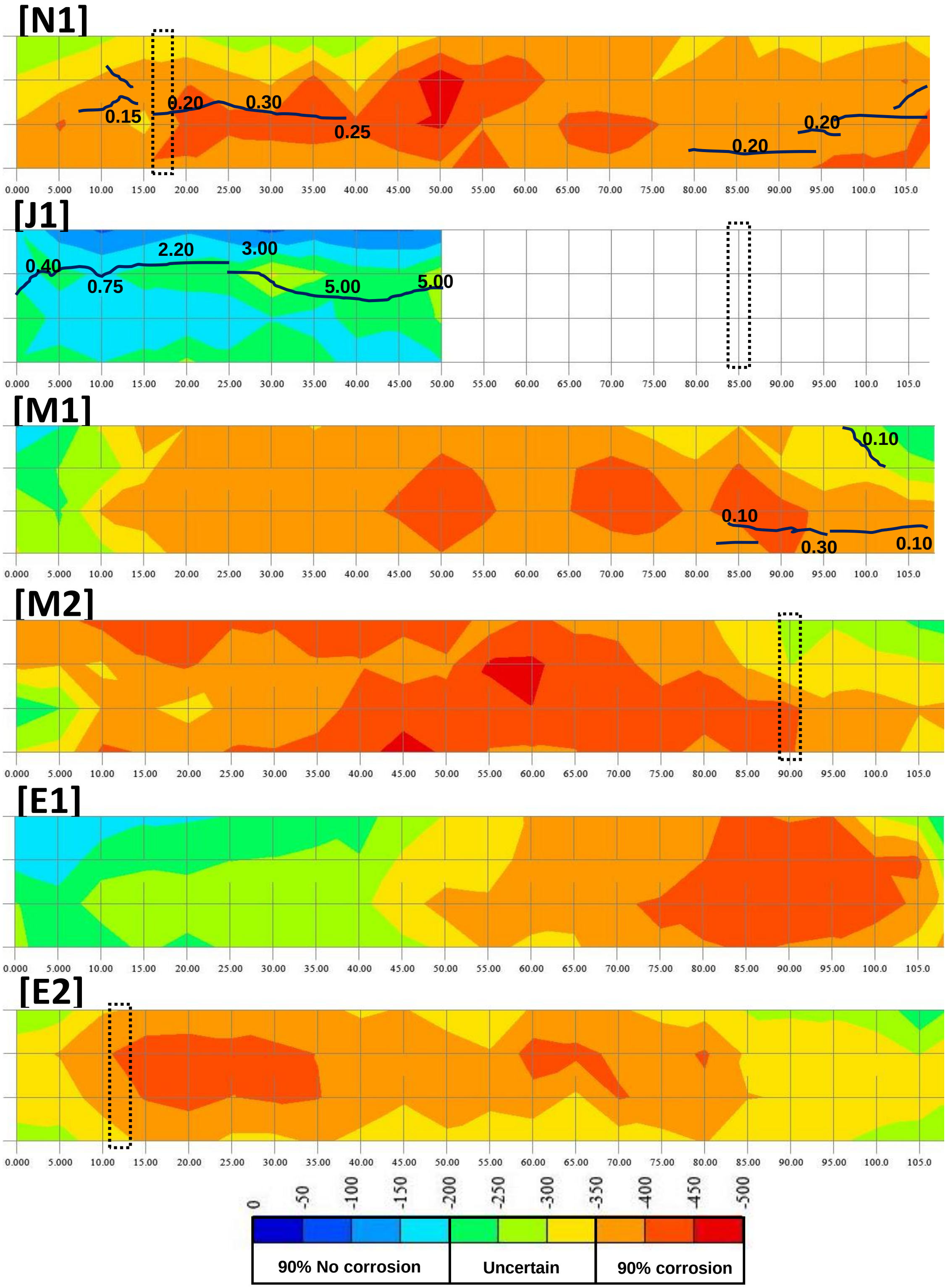

Figure 3.24 Corrosion mapping [mV]

Half-cell potential was measured to draw the corrosion map of each specimen using the ASTM C876 standard [ASTM C876, 2015], as represented in *Figure 3.24*. The measurement was performed after wetting all the specimens for about 1 hour using wet towels and tap water. The measurements were done following the grid lines drawn every 5 cm in each sample, and the side with the fewest cracks was chosen for the measurement (right side).

The corrosion of the specimens is classified as “uncertain” corrosion (−200mV to −350mV) to “90% corrosion” (−350mV to −500mV). The level of corrosion in each specimen is not constant on all the surfaces of the steel, which is a common trend for the beams. The corrosion map also shows that the steel nearing the cracks shows less noble corrosion, which is in line with previous [Suzuki, 1999; Jaffer, 2008]. The specimen without joint N1 and the mortar-treated specimen shows the most surface potential under -350mV.

The results of J1 are not accurate as the large crack width has created electrical isolation between the concrete and the rebar. Nerveless, the visual observation shows that the specimen without treatment is in the worst condition.

3.3.2.2 Polarization resistance

Figure III.24 illustrates the results of the polarization resistance measurement at the joints. It shows that the rebars in specimen M1 and E1 are still in passivity state (R_P>130kΩ.cm^2), whereas, specimen N1, M2, and E2 have lower polarization resistance. The rate of corrosion is also understood, M1 and E1 have a “very low” corrosion rate while other beams have “Low to Medium” rate. It shows that the resistance of the specimen with joints is comparable to the specimen without joint N1.

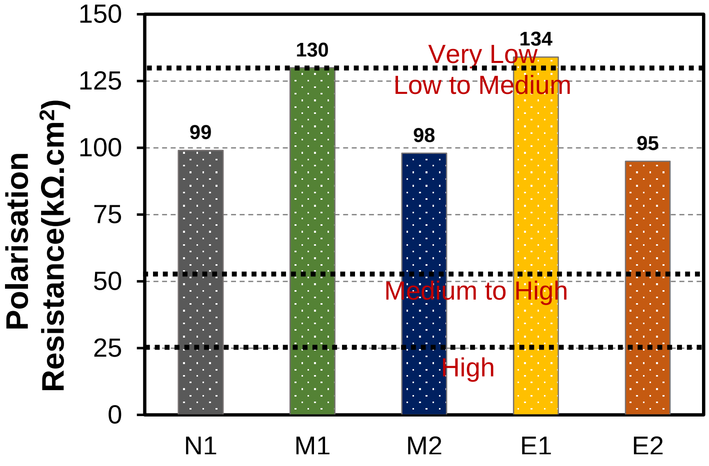

Figure 3.25 Polarization resistance results

3.3.2.3 Polarization curve

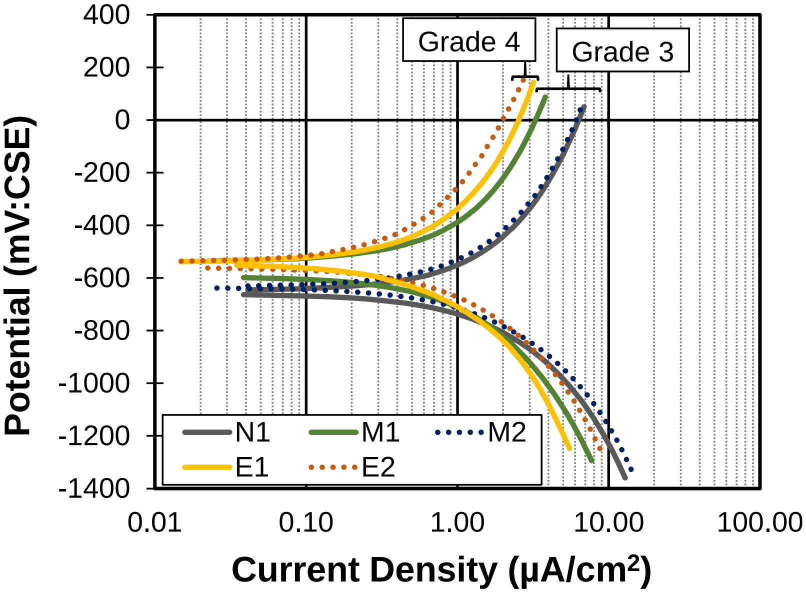

Figure 3.26 Anodic-cathodic polarization curve

The anodic-cathodic polarization curve was measured, and the results were interpreted using the grade of passivity by Otsuki [Otsuki, 1985]. From *Figure 3.26*, it is understood that a "certain grade of passivity" still exists in each beam. The difference between the curves is not significant. Nonetheless, the specimen with epoxy resin treatment shows a better condition of passivity film ("good": grade 4). The specimen without joint and the specimen with mortar treatment have

3.3.2.4 Oxygen permeability tests

The diffusion of oxygen at the joints was measured using potentials-step methods. The outcome shows a slight difference in the permeability of oxygen at the joint section of the rebar. That suggests that the treatments used, epoxy and mortar, are as effective as the specimen without joint to limit the permeability of oxygen to the structure. The limitation of oxygen is a significant factor as the electrochemical reaction at the cathodic zone depends on it. Table 3.7 represents the results of the measurement of oxygen supply in mol/cm^2/s.

Table 3.7 Oxygen supply at the joint in 10^{-12} mol/cm^2/s

Beams	**N1**	**M1**	**M2**	**E1**	**E2**
O_2 Supply [10^{-12} mol/cm^2/s]	37.2	39.6	33.9	40.3	34.2

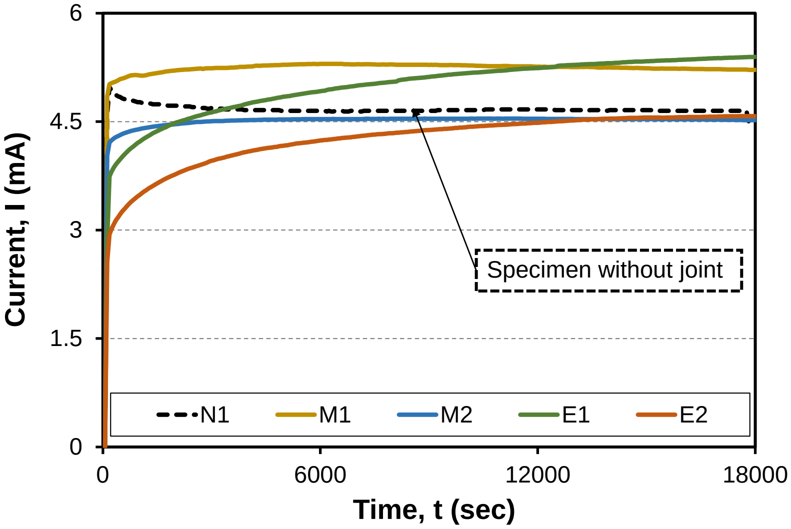

Figure 3.27 Potential step results at the joint

3.3.3 Destructive tests

3.3.3.1 Chloride concentration

In this study, the titration method was used to assess the chloride concentration at different depths of each specimen. 02 core samples (Ø 50 mm, 120mm) were taken from each PC beam for this purpose. The 06 samples were taken at different depths of each core as seen in *Figure 3.28*.

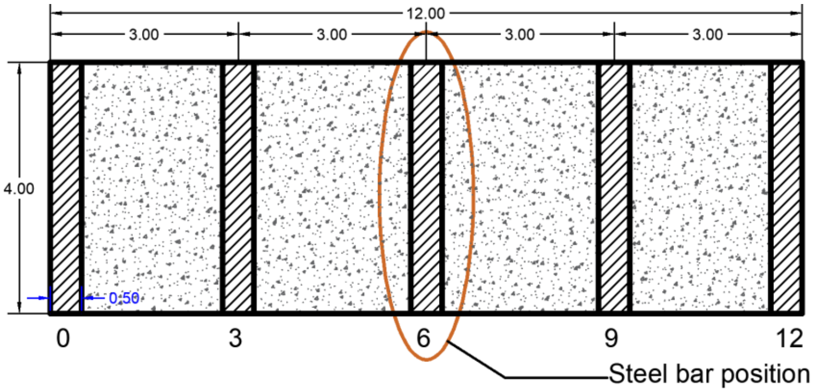

Figure 3.28 Sampling for the chloride distribution test

The result of the chloride concentration test at different depths of the beams is presented in Figure 3.29. From the JSCE standard, the allowable chloride concentration in concrete structures is limited to 1.2 to 2.4 kg/m^3. However, in the case of the study, the average value has already reached more than 8 times that threshold. It shows that there is no significant difference due to the different types of joints. Therefore, it may suggest that the joint is as effective as the specimen without joint to mitigate the ingress of chloride in the concrete.

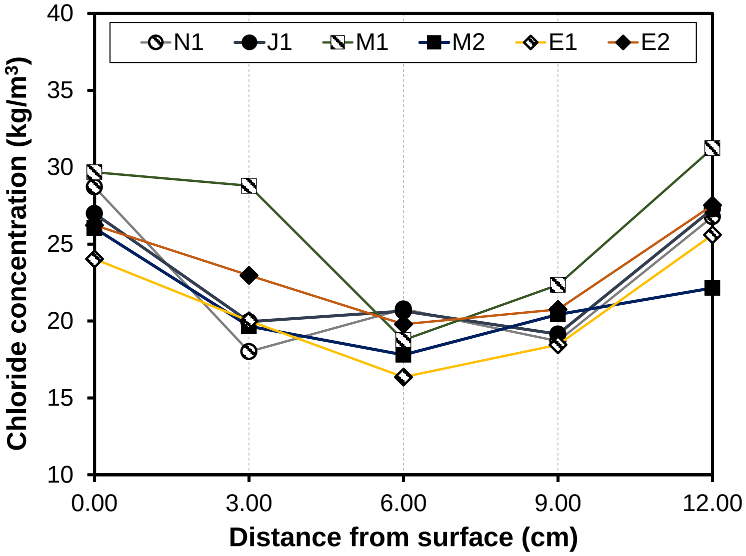

Figure 3.29 Chloride concentration at different depth of each beam

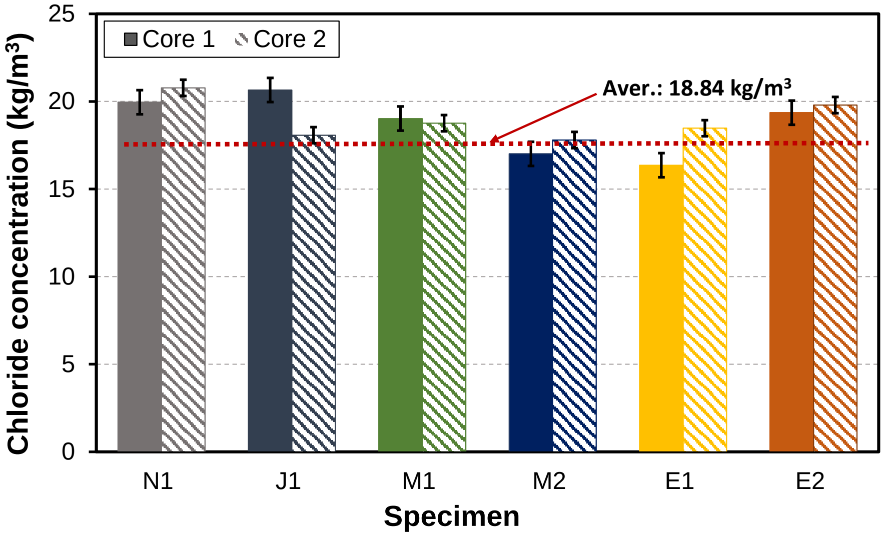

Figure 3.30 Chloride concentration at the depth of the steel bar (6cm)

3.3.3.2 Compression strength

Compression strength and elastic modulus was measured using 50mm diameter and 100mm height core. The average results are summarized in *Table 3.8*. Due to the lack of initial data, comparison, such as the decrease of strength with age, could not be done. However, it can be concluded that even after more than 30 years of exposure in severe marine environment, the concrete is still considered to be in good quality, which is in line with the ultrasonic velocity test. Besides, it meets the design code of the Japan Society of Civil Engineering to be classified as high strength concrete (>80MPa) [JSCE; 2007]. In addition, since beam J1 shows the highest strength, therefore, it can be inferred that the deterioration of J1 was not due to the poor quality of the concrete.

Table 3.8 Average compression strength and Elastic Modulus

Type	**Compressive strength [MPa]**	**Elastic Modulus [GPa]**
N1	88.3	39.8
J1	**93.1**	**41.1**
M1	89.9	40.7
M2	90.5	38.5
E1	87.4	38.9
E2	83.3	38.8

3.3.3.3 Physical Analysis

- Condition of the type of joints

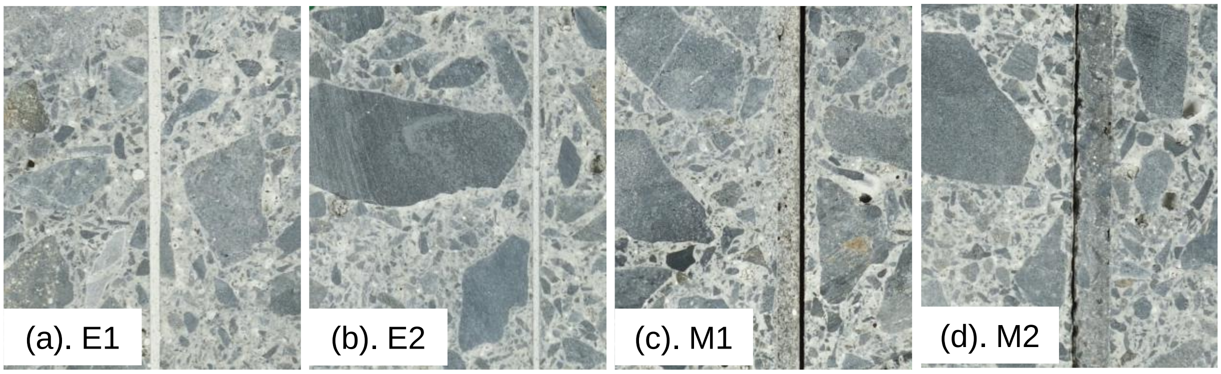

Figure 3.31 Condition of each joint treatment

Cores were taken at the joint section of each specimens in order to observe the condition of the joint. As seen in *Figure 3.31* (a) and (b), the epoxy specimen remained intact even after crushing the specimen. However, the mortar joint fell apart during the core drilling. It shows that the epoxy treatment has better bond strength with the concrete, nevertheless, the effect of this was not significant in the corrosion of the beam.

- Corrosion of the ducts

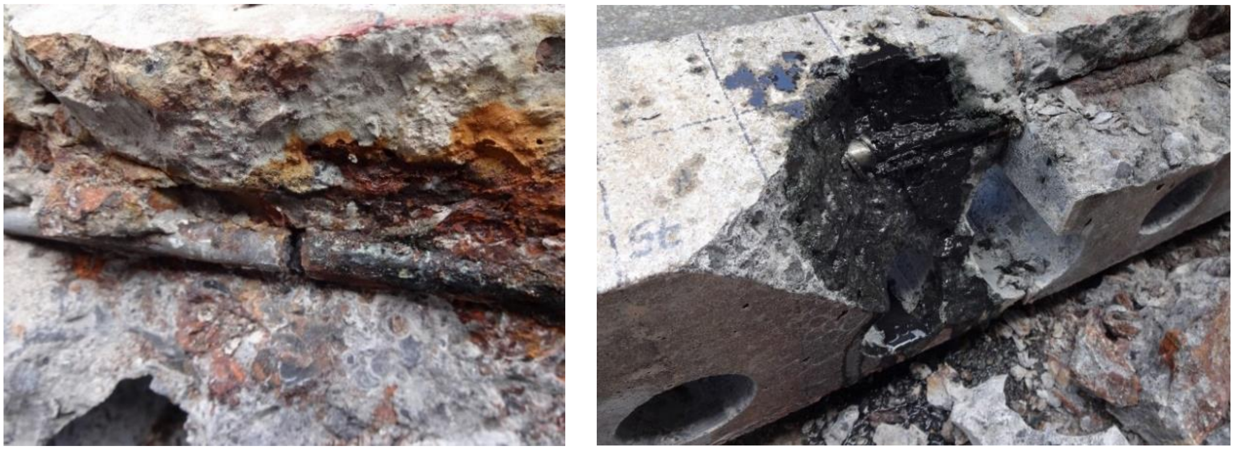

Figure 3.32 (a) Corrosion condition at the failure of the bar, (b) Blackish liquid from the duct

Figure 3.32 (a) shows the condition of the bar at the failure. The rebar was already broken prior to the crushing of the concrete. The continuous stress applied to the concrete and the loss of cross section could have caused a brittle failure of the rebar, though the cut area is not in severe corrosion condition. While crushing the beam, blackish liquid rust flowed out of the duct (*Figure 3.32(b)*). These suggest that water might have penetrated the duct through cracks or through the anchorage. In wet conditions, the product of corrosion is rust in the form of γ-FeOOH. However, the rust is black rather than red (Fe2O3); which suggests the presence of Fe3O4 due to the absence of wind and sunlight in the duct and an eventual limitation of the supply of oxygen [Takaya, 2021].

- Location of the failure

Figure 3.33 shows the states of the rebars after crushing. In the specimen M1 and E1, failure has not occurred yet, while the four other rebars are broken. The location of the failure occurred in one section and was found at about 9.5cm to 22.2 cm from the anchorage. Unlike in the reinforced concrete, the split of the rebar did not occur in the most corroded section of the rebar.

Figure 3.33 Location of the failure of the rebar (E1, M1, J1, E2, M2, N1)

- *Visual observation of the steel bars*

Prior to the measurement of the cross section and the weight loss, the steel bars were cleansed using 10% diammonium hydrogen citrate ($C_6H_{14}N_2O_7$) solution. The bars were immersed in the solution for 48hours and placed in a 40ºC temperature room chamber at a relative humidity of 60%. The rusts were removed by brushing the rebars with a metallic brush and rinsed with tap water.

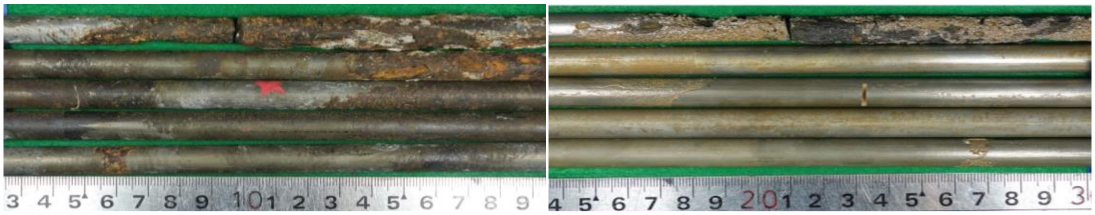

Before rust removal **After rust removal**

Figure 3.34 Condition of the rebar before and after rust removal

- *Type of corrosion on the steel bars*

Many types of corrosion were observed on the surface of the rebar, namely elliptical and mild pitting corrosion, and general corrosion, as seen in Figure 3.34. Nevertheless, pitting corrosion was dominant in the beams.

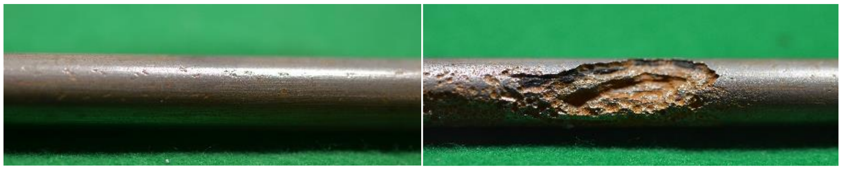

(a) No corrosion (b) Elliptical pitting corrosion

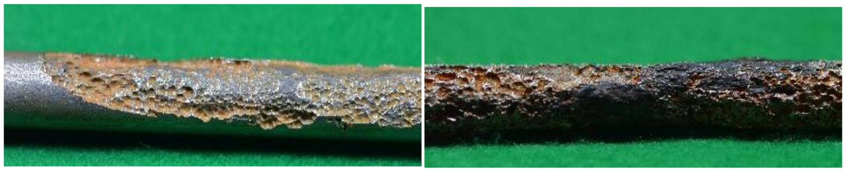

(c) Wide mild pitting corrosion (d) Generates corrosion

Figure 3.35 Condition of the corrosion of the steel after rust removal

- *Conditions of the steel bars at the failure*

Figure 3.35 shows the condition of each prestressing bar at the fracture section. For E1 and E2, the surface of the fracture is smoother and straighter. This could suggest that the failure happened more recently compared to the specimen without joint and the specimen without treatment. The fracture surface of specimen N1, and particularly J1 was severely attacked by corrosion as well.

(a) Specimen N1 (b) Specimen J1

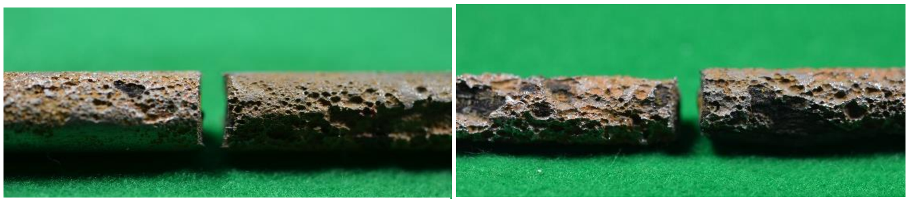

(c) Specimen M2 (d) Specimen E2

Figure 3.36 Condition of the prestressing bar at the failure

3.3.3.4 Corrosion cross section area.

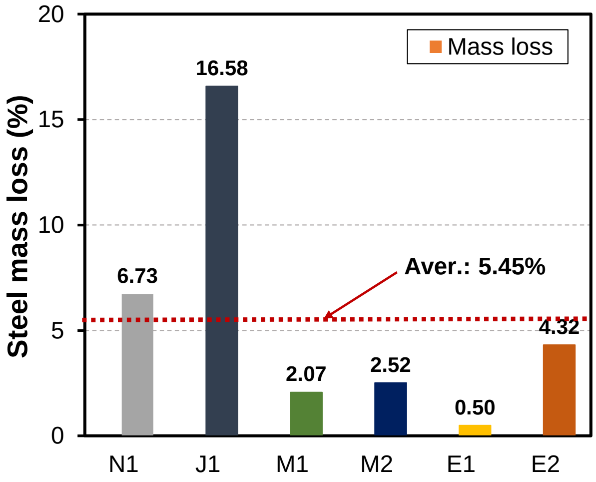

Figure 3.37 Mass loss of the prestressing bars due to corrosion

The rusts of the surface of the prestressing bar were removed using 10% Diammonium hydrogen citrate solution. After cleaning, the weight of each rebar was measured to estimate to a loss of weight due to corrosion. The result is summarized in *Figure 3.36*. The specimen without joint shows the most significant mass loss with 16.58 % loss which represents about 2.5 times the mass loss in the specimen without joint N1. In contrast, the specimens with joint treatments show even lower mass loss compared to the N1. From this, it can be understood that the presence of adequately treated joints, and without bending cracks could be a good corrosion prevention in prestressed concrete structures.

To quantify the loss of cross section in the steel, measurements were performed every 5 cm for each steel. A non-uniform formation of corrosion is found on the surface of the rebar. On average, the distance between the joint-corroded area and corroded- non-corroded areas varied from 5 cm to 10 cm. From the visual observation, the surfaces of the steels around the joints are less corroded compared to other sections, for all specimens. These outcomes provide evidence that the joint works as the cathode by supplying oxygen to the steel surface. Therefore, the failure of the rebars was found in one section of the beams rather than at the joints, similar to the specimen without joint N1. It was measured from 28 cm to 40 cm from the joint. These results are consistent with the outcomes of the half-cell potential, showing the formation of macrocell corrosion. *Figure 3.37* shows that severe corrosion has occurred on the totality of the surface of J1 because the rebar was exposed and unprotected after eventual spalling. *Figure 3.38* indicates that in some sections of specimen N1, corrosion has not yet occurred.

However, generated corrosion has occurred in the first half of the rebar, leading to its failure. Based on the observation, Specimen M1 shows mild and wide pitting corrosion, but the majority of its surface is not corroded yet (*Figure 3.39*). The visual assessment confirmed that no failure of rebar occurred in mortar specimens. In specimen M2, circular pitting corrosion was identified at about 10 cm from the joint (*Figure 3.40*). In addition, the corrosion has spread on the surface of the rebar. Corrosion has initiated even at the joint. General and severe corrosion are detected surrounding the failure point of M2.

Beam E1 shows a better performance compared to other beams (*Figure 3.41*). Similar to M1, failure has not occurred yet in specimen E1, nevertheless, some general shallow corrosion has formed. The total surface is less rusted in E2, but severe elliptical pitting corrosion is found (*Figure 3.42*). In addition, failure has occurred in E2, and the surface surrounding the failure point is also in serious condition. These results indicate that the specimens with 0.1mm cracks (E1 and M1) show better performance among the six specimens. After observation, the reinforcements in specimens N1, M2, and E2 were broken long before the crushing of the specimen.

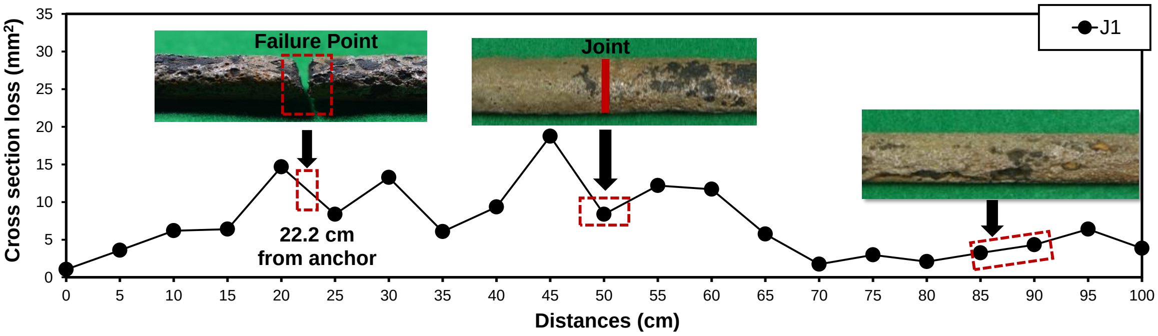

Figure 3.38 Section loss and corrosion condition of the specimen without treatment J1

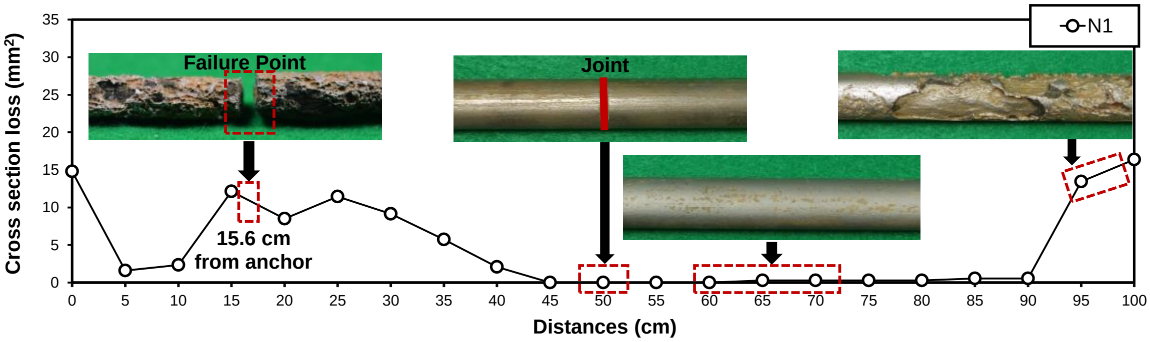

Figure 3.39 Section loss and corrosion condition of the specimen without joint N1

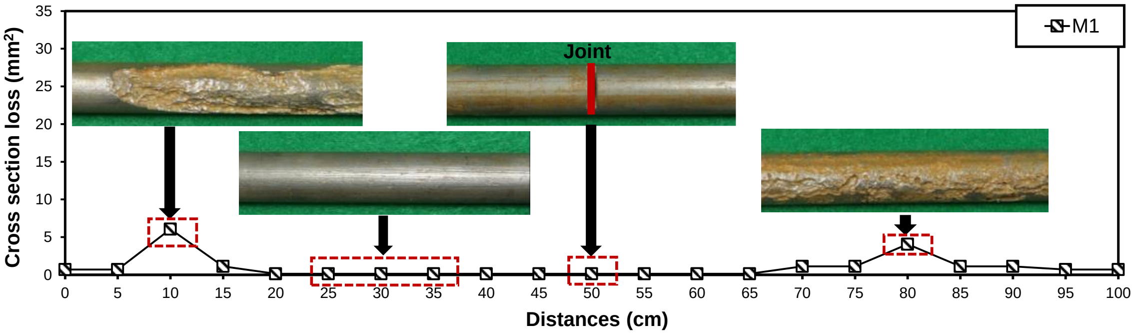

Figure 3.40 Section loss and corrosion condition of the specimen mortar treatment M1

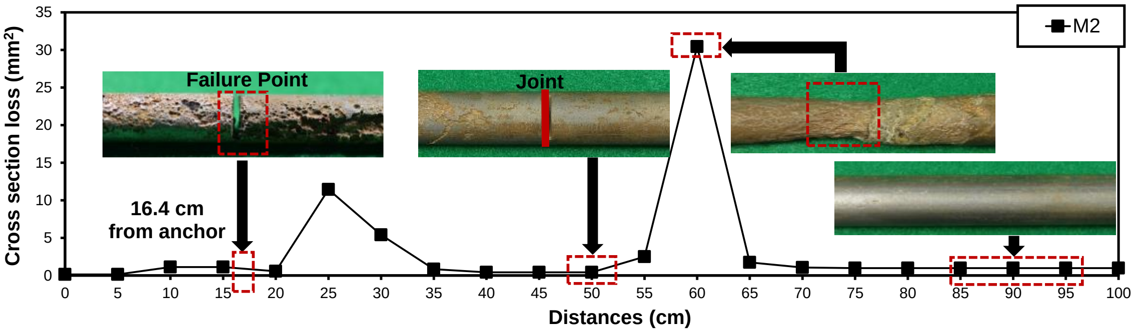

Figure 3.41 Section loss and corrosion condition of the specimen mortar treatment M2

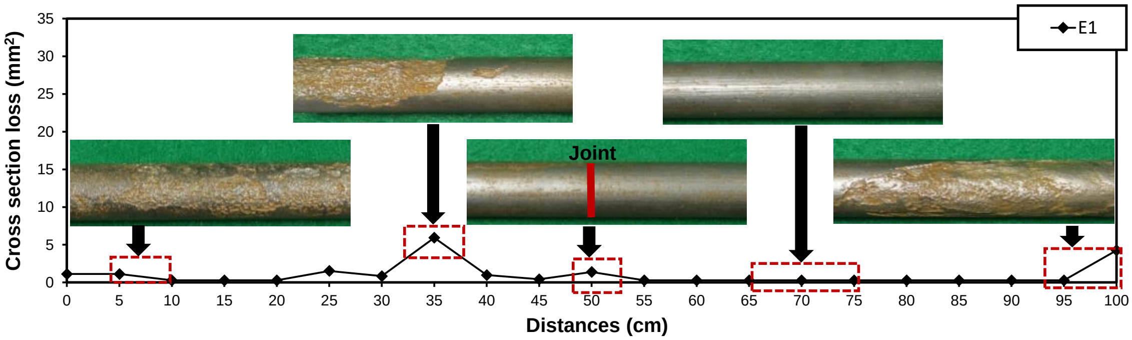

Figure 3.42 Section loss and corrosion condition of the specimen Epoxy treatment E1

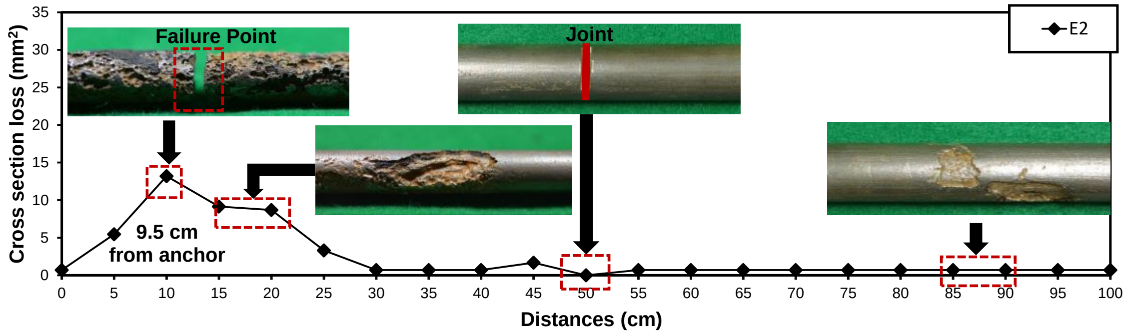

Figure 3.43 Section loss and corrosion condition of the specimen Epoxy treatment E2

3.4 CONCLUSIONS

In this study, the effectiveness of different joint treatments in prestressed beams, exposed to marine environments for more than 30 years, was assessed. Mortar and epoxy resin were chosen as a treatment, and their effectiveness was compared with the specimen without joint and the specimen with a joint but without treatment. Electrochemical methods, visual observations, and destructive methods were used during the experiments. The results showed:

- The importance of effective joint treatment and a good anchorage as the specimen without treatment was in critical condition compared to the specimen without joint and the treated specimen.
- The electrochemical measurement revealed that the epoxy-treated specimen E1 and the mortar specimen M1 are in the best condition. The results show that both chosen treatments are effective in mitigating the corrosion of prestressed concrete. Though it is not clear, their performance compared to M2 and E2 can be attributed to the effect of the loading cracks applied targeted in the specimens. In addition, the treatments were able to limit the diffusion of oxygen at the joint and keep the steel around the joint passive to corrosion. The area with cracks showed less noble potential.
- From the destructive test, the compression strength tests revealed that the beams are classified as high-strength concrete. Correlation between the concentration of chloride and the type of joint treatment could not be observed, as the beams had similar chloride content, which highlights the effectiveness of the joint treatment. From the crashing of the specimen, the distance between the anodic area and cathodic area was observed and was measured around 5 to 10 cm. The failure of the steel in the PC was observed at a similar distance from the anchorage (from 9.5 to 22.5 cm from the anchorage). The steel bar in the prestressed concrete broke even if the steel was not in a very severe condition.
- This study enhances the importance of adequate joint treatment and repair methods for structures, especially those exposed to severe marine environments. Further study is still required to assess to use of electrochemical in post-tensioned prestressed concrete and assessing the behavior of prestressed concrete contaminated with chloride.

3.5 REFERENCES

ACI Committee 222.2R-01, (2001): Corrosion of prestressing steels, American Concrete institute.

Ahmad, I., Suksawang, N., Sobhan, K., Corven, J.A., Sayyafi, E. A., Pant, S., and Martinez, F., (2016): Develop Epoxy Grout Pourback Guidance and Test Methods to Eliminate Thermal/Shrinkage Cracking at Post-Tensioning Anchorages: Phase II, Final Report, Contract No. BDV29-977-13, Florida Department of Transportation.

Ann, K.Y., Ahn, J.H., and Ryou, J.S., (2009): The Importance of Chloride Content at the Concretesurface in Assessing the Time to Corrosion of Steel in Concrete Structures, Construction and Building Materials, 23, pp. 239–245.

Belletti, B., Rodrìguez, J., Andrade, C., Franceschini, L., Sànchez, J., and Vecchi, F., (2020): Experimental tests on shear capacity of naturally corroded prestressed beams, *Structural Concrete*, 21, pp. 1777–1793.

Belletti, B., Vecchi, F., Bandini, C., Andrade, C., Sanchez, J., (2020): Numerical Evaluation of the Corrosion Effects in Prestressed Concrete Beams without Shear Reinforcement Structural Concrete., 21, pp.

Bertolini, L., Elsener, B., Pedeferri, P., and Polder, R.P., (2004): Corrosion of Steel in Concrete, (1st ed.), WILEY-VCH, Morlenbach.

Burdekin, F. M., ant Rothwell, G. P., (1981): Survey of Corrosion and Stress Corrosion in Prestressing Components used in Concrete Structures with Particular Reference to Offshore Applications, Publication 15.632, Cement and Concrete Association.

CEB, (1998): Strategies for Testing and Assessment of Concrete Structures, Bulletin No. 243, 183 pp.

Coronelli, D., Castel, A., Vu, N., and François, R., (2009): Corroded Post-tensioned Beams with Bonded Tendons and Wire Failure, Eng. Struct., 31, pp.1687-1697.

Di Prisco, M., (2019): Critical Infrastructures in Italy: State of the art, case studies, rational approaches to select the intervention priorities, Proceedings of the fib symposium: Concrete-Innovations in Materials, *Design and Structures*, Krakow, Poland, pp.49–58.

Dickson, T. J., Tabatai, H., and Whiting, D. A., (1993): Corrosion Assessment of a 34 Years old Precast Post-tensionned Concrete Grider, PCI Journal, 38, No. 6, pp. 44-51.

Domaneschi, C., Pellecchia, M., De Iuliis, E., Cimellaro, G.P., Morgese, M., Khalil, A.A. et al., (2020): Collapse Analysis of the Polcevera Viaduct by the Applied Element Method, Engineering Structures, 214, p. 110659,

Elsener, B., Andrade, C., Polder, R., and Raupach, M., (2003): RILEM TC 154-EMC - Electrochemical for Measuring Metallic Corrosion Materials and Structures, 36, pp. 461-471.

EN 12504-4. Testing concrete- Part 4: Determination of ultrasonic pulse velocity; 2004.

Essamin, O., Holley, M., Great Man Made River Authority (GMRA), (2004): The Role of Acoustic Monitoring in the Management of the World’s Largest Prestressed Concrete Cylinder Pipe Project, In: Proceedings of the ASCE pipeline division specialty congress – Pipeline engineering and, construction, pp.283–290.

Freyermuth, C. L., (1991): Durability of Post-tensioned Prestressed Concrete Structures, Concrete International, 13, No. 10, pp. 58-65.

Hamada, H., Haramo, M., and Otsuki, N., (1987): Ten Years Test on the Effects of Joints on the Durability of Concrete in Marine Environment, Japan Concrete Institute, 9, pp. 147-154.

hmad, I., Suksawang, N., Sobhan, K., Corven, J.A., vallier, R., Sayyafi, A. E., and Pant, S., (2018): Developing Guidelines for Epoxy Grout Pourback Systems for Controlling Thermal/Shrinkage Cracking at Post-Tensioning Anchorages: Full-Scale Testing and Numerical Analysis, Transportation Research Record, pp. 1-10.

Jaffer, S.J., Hansson, C.M., (2008): The Influence of Cracks on Chloride-induced Corrosion of Steel in Ordinary Portland Cement and High-Performance Concretes Subjected to Different Loading Conditions, *Corrosion Science*, 50 (12), pp. 3343–3355.

Japan Society of Civil engineers (JSCE), (2007): Standards specifications for concrete structures-design, No.15, pp 128-145.

JIS A 1108, (2018): Method of Test for Compressive Strength of Concrete, Japanese Standard Association.

JIS A 1154, (2020): Methods of Test for Chloride ion content in Hardened concrete, Japanese Standard Association.

Jones, R., (1969): Proceedings, International Symposium on Nondestructive Testing of Concrete and Timber, Institution of Civil Engineers, London, pp.1-7.

Lambert, P., Page, C. L., and Vassie, P. R. W., (1991): Investigations of Reinforcement Corrosion Electrochemical Monitoring of Steel in Chloride-contaminated Concrete Materials and Structures, 24, 143, pp. 351-358.

Li, F., and Yuan, Y., (2013): Effects of Corrosion on Bond Behavior Between Steel Strand and Concrete, Construction and Building Materials, 38, pp. 413-422.

Li, F., and Yuan, Y., Li, C.Q., (2011): Corrosion Propagation of Prestressing Steel Strands in Concrete Subject to Chloride Attack, *Construction and Building Material*, 25, pp. 3878-3885,

Manning, D. G.: Durability of prestressed concrete highway structures, NCHRP Synthesis of Highway Prac-tice 140, Transportation Research Board, 1988.

Miyazato, S., (2021): Countermeasure by shielding against macrocell corrosion after patch repair, Concrete J., Vol.59, No.5, pp.452-455. (in Japanese)

Nagataki, S., Otsuki, N., Moriwake, A., and Miyazato, S., (1996): Experimental Study on Corrosion Mechanism of Reinforced Concrete at Local Part, Journal of Materials, Concrete Structures and pavement, n. 544, pp. 109-119 (in Japanese).

Oleiwi, H.M., Wang, Y., Curioni, M. et al., (2018): An Experimental Study of Cathodic Protection for Chloride Contaminated Reinforced Concrete Materials Structure,51, 148.

Otsuki, N., (1985): A Study of effectiveness of the Chloride on Corrosion of Steel Bar in Concrete, Report of Port and Harbor Research Institute, 127-134.

Page, C.L., Sergi, G., (2000): Developments in Cathodic Protection applied to Reinforced Concrete. Journal Materials in Civil Engineering, Sp. Issue, Durability of Construction Materials, pp. 8-15.

Pfeifer, D., McDonald, D. and Krauss, P., (1994): Rapid Chloride Permeability Test and its Correlation to the 90-day Chloride Ponding Test, PCI J., pp. 38-47.

Suzuki K., Ohno, Y., Praparntanatorn, S., and Tamura, H., (1990): Mechanism of Steel Corrosion in Cracked Concrete International, Symposium on Corrosion of Reinforcement in Concrete Construction (3rd), *Elsevier*, *Applied Science*, Wishaw, England.

Schupack, M., (1994): Durability Study of a 35 Years Old Post-Tensioned Bridge, Concrete International, 16, No, 2, pp. 54-58.

Sergi, G., Page, C.L., (1999): Sacrificial Anodes for Cathodic Protection of Reinforcing Steel around Patch Repairs applied to Chloride-contaminated Concrete, Proc. Eurocode 99, European Corrosion Congress, Aachen, Germany.

Singh, S.K., (2000): Corrosion Studies on Prestressing Steel Wire, Ph.D. thesis. Imperial College, University of London.

Soutsos, M.N., Breysse, D., Garnier, V., Goncalves, A., and Monteiro, A.V., (2011): Estimation of on-site Compressive Strength of Concrete, Non-Destructive Assessment of Concrete Structures: Reliability and Limits of Single and Combined Techniques-State-of-the-Art Report of the RILEM Technical Committee 207-INR, 1, pp.119-186.

Takaya,S., Sato, S., Shiomi, H., Yamamoto, T., (2021): Maintenance method focusing on environmental dependence of corrosion products, Concrete J., Vol.59, No.5, pp.398-403. (in Japanese)

Whitehurst, E.A., (1951): Sonic tests concrete structures, Ameri-can Concrete Institute, J. proc., Vol. 47, pp. 433-444.

Yamaoka, Y., and Tanaka, Y., (1993): Comparison of the mechanisms of hydrogen embrittlement and stress corrosion cracking of high carbon steel wire, Int. Workshop on Prestressing Wire, Denver, Colo.

CHAPTER IV

EFFECT OF INTERFACIAL GAP ON THE CORROSION OF HORIZONTAL STEEL BAR

4.1 INTRODUCTION

Bleeding is the segregation on the microlevel of the concrete, as it is the result of the separation of the mixing water and the cement particles. During the setting time of concrete, downward settlements of the solid constituents, coarse and fine aggregates, in the mix usually occur. Consequently, as being the constituent with the lowest specific density, the mixing water rises on the surface of the members. The phenomenon of “bleeding” or also “water gain” which a form of segregation in concrete. Literature also mentions that the excess in air content of entrained or the lack of fine element in the mix could be also a cause of bleeding

In most cases, this rise of water will lead to uneven water to cement ratio in the concrete. As a result, the quality of the members, especially near the top layer, will become more defective while the inferior part will increase in strength [Scwamborn, 1987]. Previous studies have emphasized that in extreme cases, the bleeding water can reach 20% of the total settlement per unit weight of cement or the percentage of the mixing water [Nevile, 2011]. The bleeding phenomenon occurs from the placement of the concrete until the concrete has hardened.

In some cases, bleeding can be beneficial to the concrete depending on its usage as it increases the strength of the structure when the excessive water is properly removed. Especially in the case where the rate of evaporation of water from the concrete is equivalent to the rate of bleeding. Some form of bleeding is nevertheless unavoidable; especially, for tall concrete members such as columns. In fresh concrete, some of the bleeding water moving upward does not reach the surface of the structure but stagnates under the horizontal steel bars and the coarse aggregates. Thus, voids are created on the lower surface of the steel bar in hardened concrete as the water evaporates.

However, the void or air pocket formed can as well results in the formation of a zone of a poor bond between the paste and the solid elements in the mix. In addition, as the void is also formed in the same direction, the permeability of the concrete in the horizontal direction is also influenced and the zone of weakness can be also formed. Besides, the presence of such voids facilitates the accumulation of chloride ions in the vicinity of the steel bar, which is a significant factor promoting the corrosion of steel bar when high concentration of oxygen is present. Hence, a more significant localized corrosion, greater than the corrosion created due to the formation of cracks, could be observed at the interfacial gap area [Mohammed et al., 2002]. Besides, it was suggested that several chemical reactions can occur at the gap created between the cement mortar and the reinforcement which contribute to alter or improve the integrity between both components. The interfacial bond strength is crucial in determining the mechanical properties and service life of concrete structures [James, 1991]. Views were also further expressed that the durability of the horizontal steel bar could be highly diminished by the bleeding of fresh concrete [Baccay et al., 2004].

Nevertheless, a detailed study is still necessary for a better understanding of the effect of water gain on the mortar, especially around horizontal steel bars. In addition, the relationship between the electrochemical characteristics of steel bar and the voids formed under the latter remains to be further addressed. This experimental study aims at examining the effect of the bleeding on the mortar in fresh concrete, as well as the steel corrosion in the hardened concrete. The tendency of occurrence of bleeding is significantly dependent on the properties of the cement used in the concrete but the increase in the quantities of fine aggregate is also a way to reduce the quantity of the bleeding water. The objective of this structure is to assess the macrostructure around the rebar and the macrostructure of mortar affected by bleeding.

4.2 EXPERIMENTAL PROGRAM

4.2.1 Specimen overview

Reinforced concrete specimens with a dimension of 150x 150 x 500mm (Series 1) and 200 x 200 x 500mm (Series 2) were prepared for the testing, as shown in *Figure 4.1* and *Figure 4.2*. The mix proportions of the mortar are presented in *Table 4.1*. Water/cement ratio of 50% was used for each mixture and coarse aggregates were not incorporated into the mix to eliminate its effect on the bleeding mentioned in the previous section [Yim et al., 2014].

Table 4.1. Mix proportions of mortar specimen

Specimens	**W/C [%]**	**Unit Weight（kg/m³）**			**Cl⁻ Concentration [%]**
		W	**C**	**S**	
Series 1	50	255	510	1508	0.2
					0.5
Series 2	50	263	530	1446	0.2
					0.4
					0.6

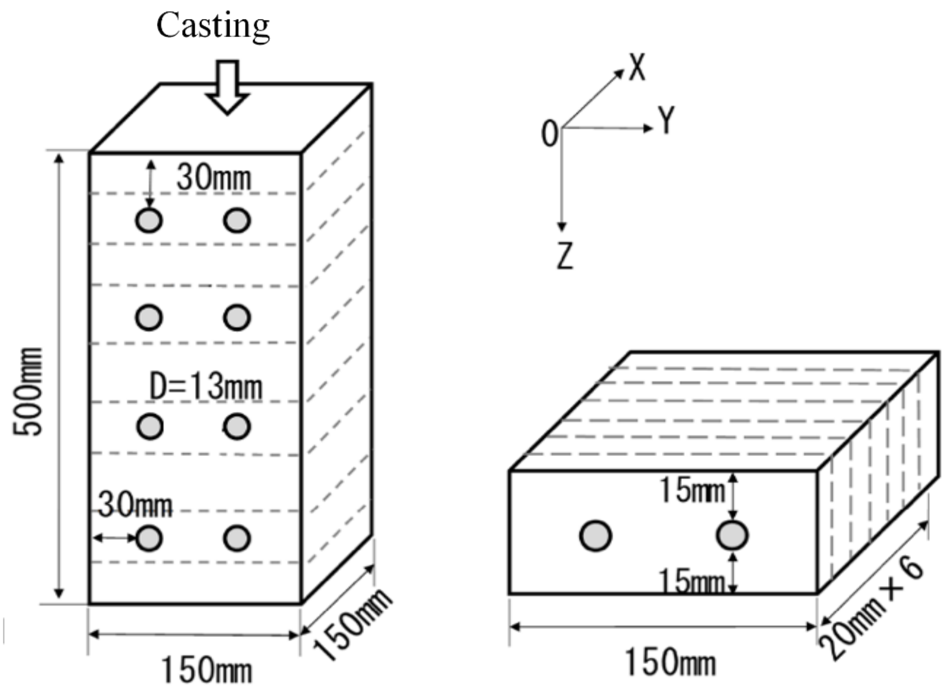

Figure 4.1. Specimen outline and cutting Series 1

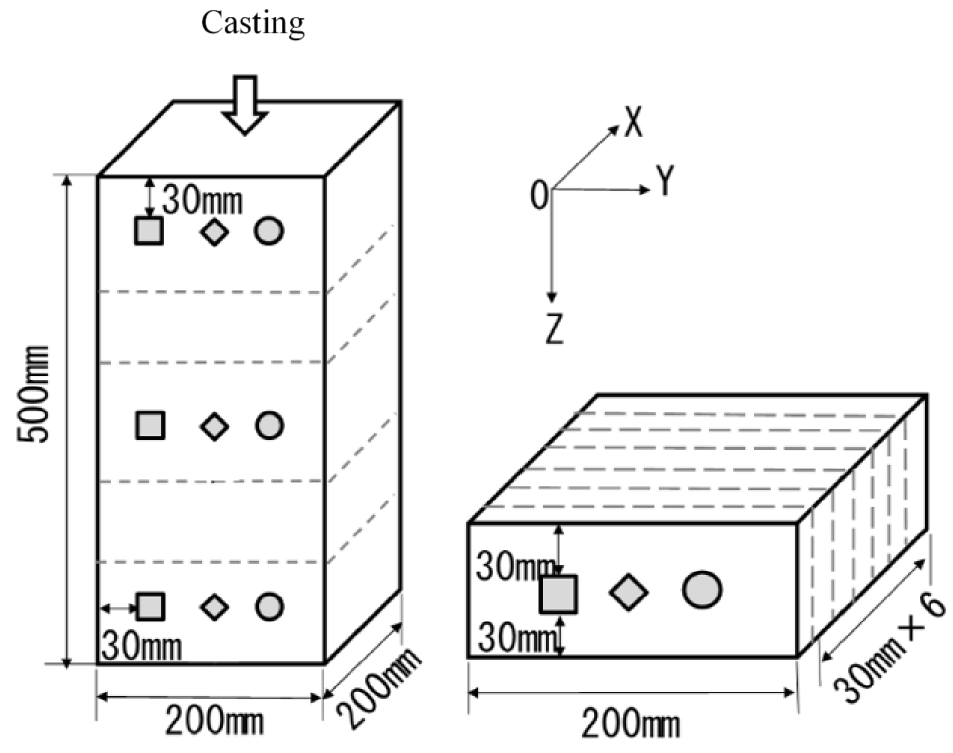

Figure 4.2. Specimen outline and cutting Series 2

4.2.2 Material outlines

The properties of the materials utilized are detailed in Table 2. For the mortar mix, Ordinary Portland cement with a density of 3.16 g/cm³ and washed sea sand of a saturated surface area of 2.57 g/cm³ for Series 1 and 2.54 g/cm³ for Series 2 were used. In Series 1, 13mm diameter of steel bar SGD 400 was embedded in the mortar. Whereas in Series 2, different shape of steel bars was chosen: namely, a circular steel SS 400 of 13mm diameter, rectangular steel SS 400 of 13mm x 13mm, and a diamond-shape SS 400 steel of 9.52mm x 9.52mm.

Table 4.2. Properties of the materials used

	Ordinary Portland Cement		**Sea sand**	**Reinforcing bar**	
	Density **[g/cm³]**	Specific Surface area **[cm²/g]**	Saturated Surface Dry **[g/cm³]**	Shape - **Grade**	Dimension **[mm]**
Series 1	3.16	3250	2.57	Round - **SGD 400**	13
Series 2	3.16	3250	2.54	Round - **SS 400**	13
				Square - **SS 400**	13 x 13
				Diamond - **SS 400**	9.52 x 9.52

For Series 1, the specimens were demolded a day after casting and were cured (moisture curing) at 100% of relative humidity with a temperature controlled at 20°C for 28 days. The specimens were afterward stored in a room at a temperature of 20°C with a relative humidity of 60%. Series 1 was cast in 2012, therefore the specimen was 7 years when Series 2 was prepared. For Series 2, the demolding was performed 5 days after the casting prior to curing at a temperature of 20°C until the 28th day. Wet fabrics were used to wrap the specimen using 3% of NaCl solution for the curing process in such a way that the concentration of chloride in the mix is conserved for series 2.

Different level of chloride concentration dissolved from NaCl was added to the mixing water of each specimen to simulate aggressive environment condition, to ensure and to accelerate the corrosion of steel bar. Even though no universally valid threshold content of chloride ions is set for corrosion to be initiated in the concrete, several standards and previous researches have set a total amount of chloride in the mix to about 0.4% by mass of cement. Furthermore, chloride in the original mix is mentioned to be more aggressive than the ingress chloride during service life. The different concentration of chloride was set to ensure that there is no corrosion, uncertain corrosion, and sure probability of corrosion in the concrete, respectively for 0.2% and 0.5% in Series 1 and 0.2%, 0.4% and 0.6% in Series 2.

Table 4.3 Chloride concentration and specimen age

Series	**Chloride concentration [%]**	**Specimen age [years]**	**Specimen age [Unit]**
Series 1	0.2	9 years (2012)	2
	0.5		2
Series 2	0.2	2 years (2019)	1
	0.4		1
	0.6		1

The specimens were cut in the parallel direction to the reinforcing bar after the macro-cell test was performed. For Series 1, each cut segment was then labeled as "upper", "middle upper", "middle lower" and "lower" respectively. In Series 2, the segments were named: "up", "middle" and "low". The five surfaces of each segment were coated with Epoxy resin, except on the lower surface which corresponds to the bottom side of the steel bar. All specimens were kept in 40°C chamber with a relative humidity of 80%, to expose them to a more severe condition and further accelerate the corrosion of the reinforcing bar.

4.2.3 Measurements methods

Electrochemical non-destructive methods were performed to determine the condition of corrosion in the concrete owing to the fact that the reactions occurring in concrete during corrosion are electrochemical [Lambert et al., 1991; Elsener et al., 2003]. However, due to its limitations, several electrochemical methods were used.

Half-cell potential was measured according to the ASTM C876 to determine the risk of corrosion in the concrete [ASTM C876, 2015]. Like in the previous chapter, high impedance voltmeter and Saturated Calomel Electrode (SCE) were used in the measurement.

The development of the current density time dependently was assessed using a portable corrosion meter. The corrosion rate was compared to the value set by the CEB standard [CEB, 1998].

Electrical resistivity was measured using the four-point probes introduced in chapter 2. The risk of corrosion and the rate of corrosion was evaluated using the standard set by Langford et al., and Broomfield et al. [Langford et al.,1987; Broomfield et al. 1993].

Table 4.4. Electrical resistivity range related to corrosion risk level and corrosion rate level

Corrosion Risk		**Corrosion Rate**	
Resistivity (ρ) (kΩ.cm)	**Corrosion Risk Level**	**Resistivity (ρ) (kΩ.cm)**	**Corrosion Rate Level**
ρ>100	Negligible	ρ>20	Low
50>ρ>100	Low	10>ρ>20	Low to moderate
10>ρ>50	Moderate to high	5>ρ>10	High
<10	High	ρ<5	Very High

The macrocell corrosion was measured to evaluate the influence of the height location of the steel and its shape on the formation of macrocell current. During testing, the rebars were connected in pairs by outer lead wires to measure the total macrocell current using a zero-resistance ammeter [Jäggi et al., 2001].

The porosity of the mortar under the rebar was measured using a mercury porosimeter (penetration methods). The specimens were cut into 5mm cubes, voids were removed by immersion into acetone and by a vacuum pump. The sample was put in freeze dryer for 48hours before the penetration test.

The chloride concentration of each specimen was measured using titration methods [JIS A 1154, 2020]. The specimens were cut into fine piece under the steel bar (around 15mm) in order to assess the influence of bleeding on Potentiometer titrator AT-700 was used.

Void area under the rebar was calculated by using image J software. Photographs of the mortar section were taken from single lens reflex camera and were analyzed with image J software to measure the quantity of the voids due to the bleeding effect.

Finally, the specimens were crashed, and visual observation of the rebar was done to assess the actual state and compare with the electrochemical results.

4.3 RESULTS AND DISCUSSIONS

4.3.1 Half-cell potential

Figure 3.3 and *Figure 3.4* show the time dependent evolution of the potential in the round steel bars (Series 1 and Series 2). In Series 1, the effect of the difference in concentration of the chloride and the location of the steel bar was not distinguished. Corrosion has not yet occurred in Series 1 as the potential is more than -200mV (90% no corrosion zone). For Series 2, the effect of the height and the location of the steel is slightly observed. The rebars on the upper section have lower potential. Compared to Series 1, Series 2 shows lower potential. The potentials of Series 2 are mostly in the uncertain zone of corrosion.

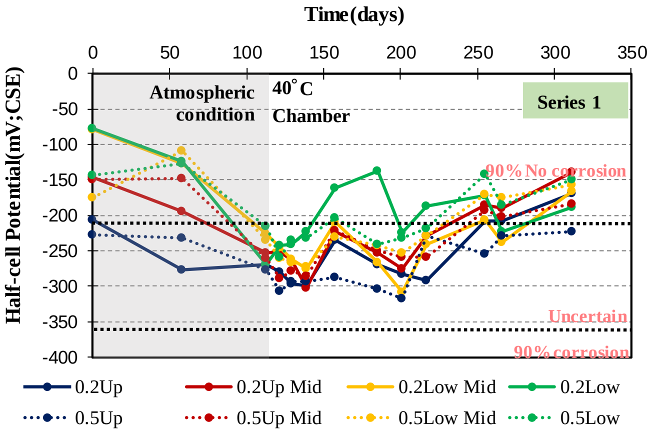

Figure 4.3 Half-Cell Potential – Series 1

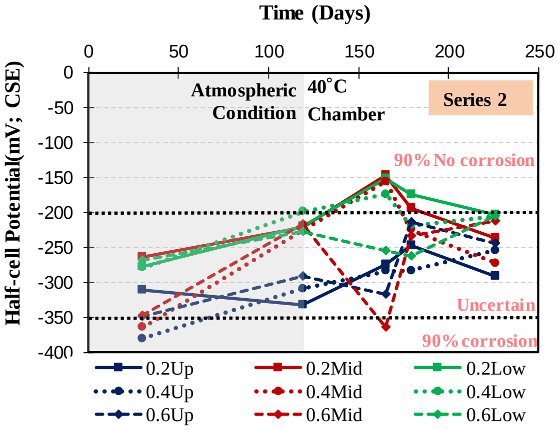

Figure 4.4 Half-Cell Potential – Series 2

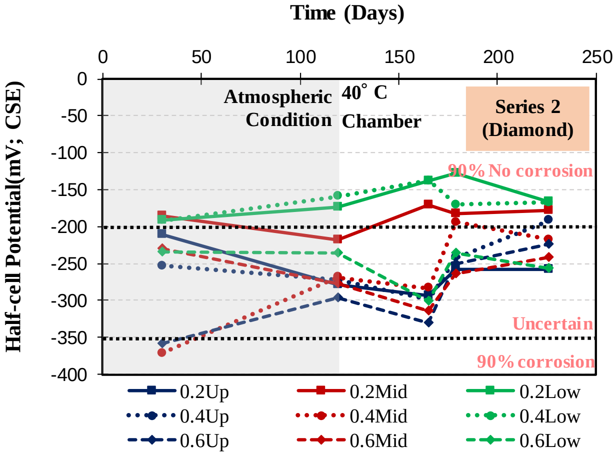

Figure 4.5 Half-Cell Potential – Series 2 (Diamond)

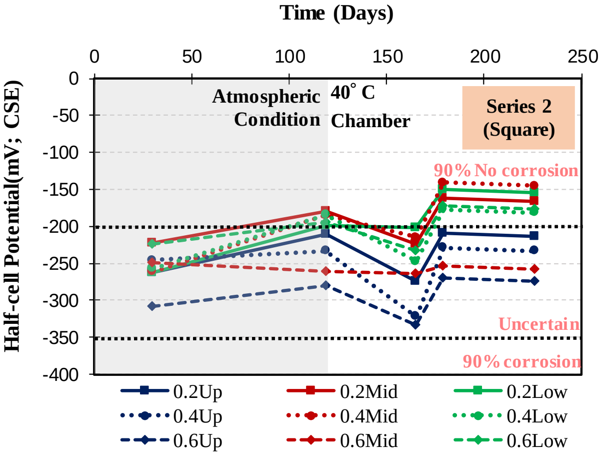

Figure 4.6 Half-Cell Potential – Series 2 (Square)

Figure 4.5 and *Figure 4.6* shows the trends of the potential of the Diamond-shaped and the square shaped steel bar in Series 2. Both square-shaped and diamond-shaped steel bar are in the zone of uncertain corrosion and 90% corrosion (-150mV to -300mV). The effect of the chloride concentration and the location of the rebar is distinguished in the square shaped steel bar. The specimen with the highest content of chloride (0.6%) located at the upper section shows the lowest corrosion. The corrosion is more affected by the location of the rebar more than the level of chloride content.

- **Relationship Half-cell potential- rebar position-chloride concentration**

Figure 4.7 illustrates the relationship between the height location of the steel bar, the half-cell potential, the shape of the rebar and the different concertation of chloride in the Series 2. A common trend observed in all the specimen in that the rebar in the lower section shows more noble potential compared to the rebar in the middle and the upper section.

From the concentration of chloride, the mortar with 0.6% of chloride and positioned in the higher section shows the lowest potential. And the specimen with 0.2% of chloride concentration positioned in lower section presents the lowest potential.

Regarding the shape of the steel bar, the round steel bar seems to have the lowest potential, especially with 0.2% and 0.4% of chloride content. In the mortar with 0.6% of chloride, the square-shaped rebar shows the lowest potential. Therefore, on average the specimen with diamond rebar show the best performance in terms of potential.

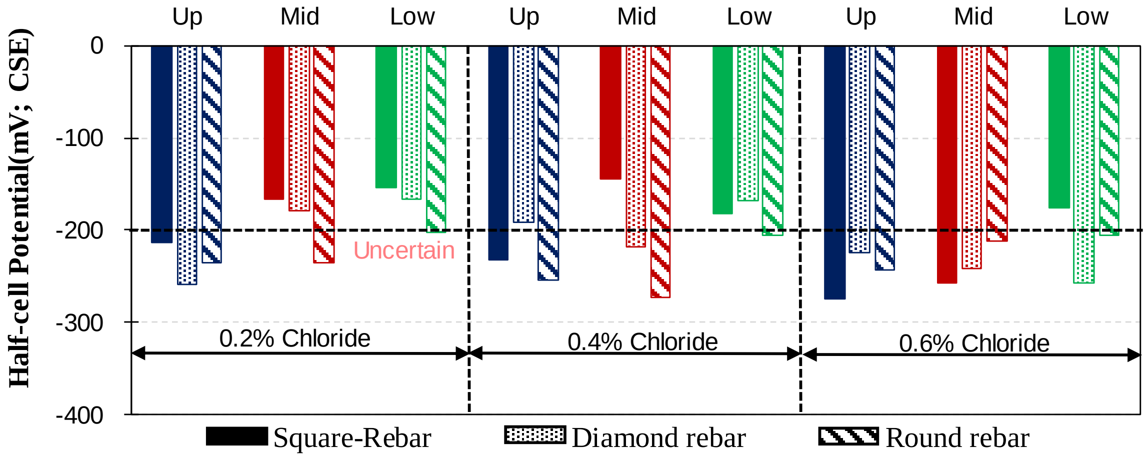

Figure 3.7 Chloride concentration – Half-cell Potential – Series 2

4.3.2 Polarization resistance

The polarization resistance of the steel bar was measured in every Series. The rate of corrosion in each specimen is classified as “negligible” as the polarization resistances are higher than 130kΩ.cm^2. In Series 1, the specimen located in the upper section has the lowest polarization resistance while the specimen located in the lower section shows higher polarization resistance (*Figure 4.8*). These results agree with the result of the half-cell potential, giving further evidence of the vulnerability of the rebar located in the upper section to corrosion. Similarly, in Series 2, the difference is not significant however, the rebar in the upper position shows lower resistance as well.

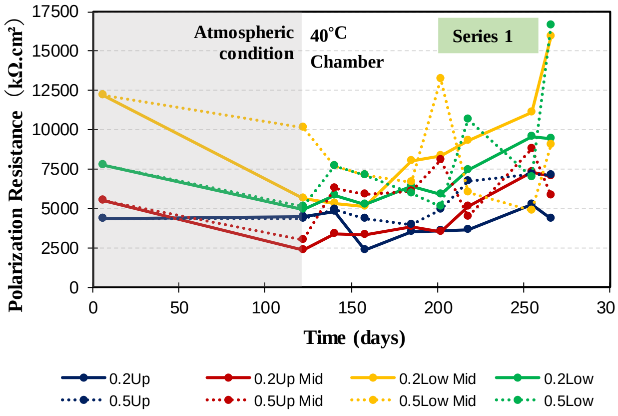

Figure 4.8 Polarisation Resistance -Series 1

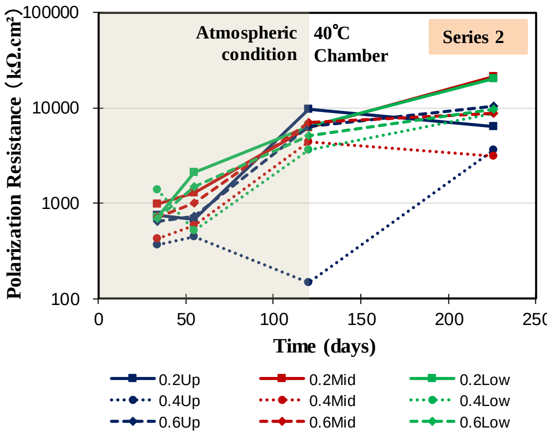

Figure 4.9 Polarization Resistance- Series 2 (Round)

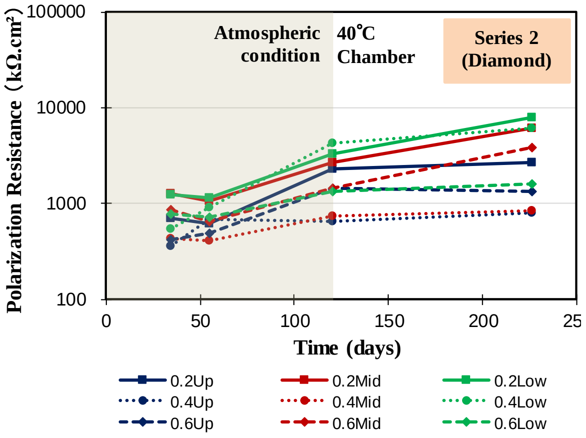

Figure 4.10 Polarisation Resistance -Series 2 (Diamond)

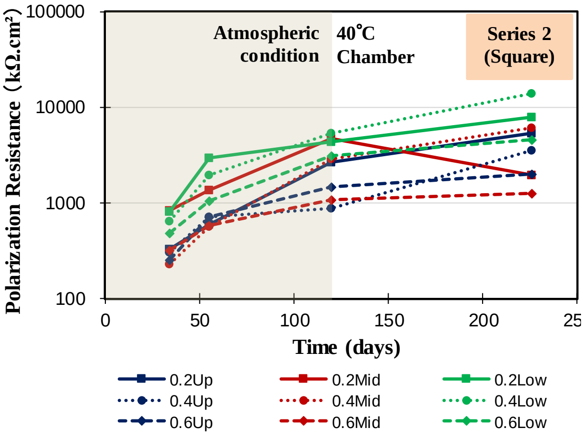

Figure 4.11 Polarisation Resistance -Series 2 (Square)

4.3.3 Electrical Resistivity

The results demonstrate that the electrical resistivity of the upper part tends to be lower in most of the specimens, as illustrated *Figure 4.12* and *Figure 4.13*. In both specimens, the risk of corrosion can be classified as “moderate to high” as the electrical resistivity values are between 10 to 50 kΩ.cm. The value is even less in the upper rebar of the Series 2; classified as “high” corrosion rate. The results seem to depend on the larger void located on the upper zone of the specimens. As far as the corrosion risk is concerned, the risk is high on the up and middle part of the specimen Series 2 and moderate to low in the other locations as well as Series 1, which is in line with the results of the experiment conducted in this study.

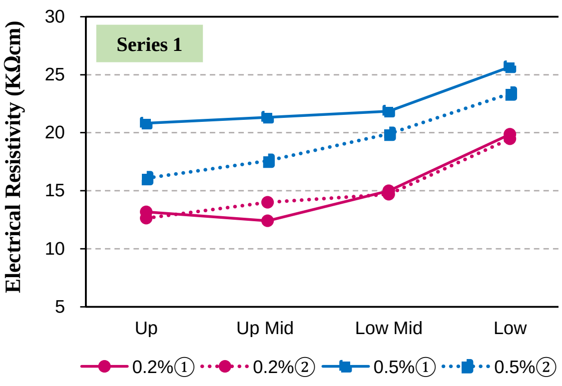

Figure 4.12 Electrical Resistivity -Series 1

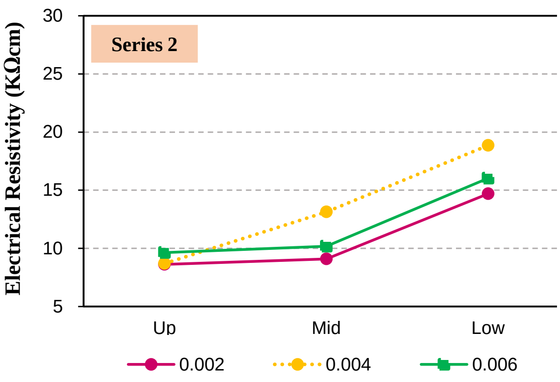

Figure 4.13 Electrical Resistivity -Series 2

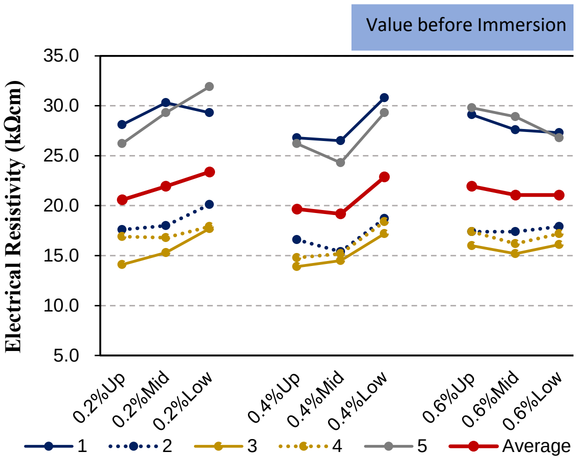

Figure 4.14 Electrical Resistivity Before Immersion

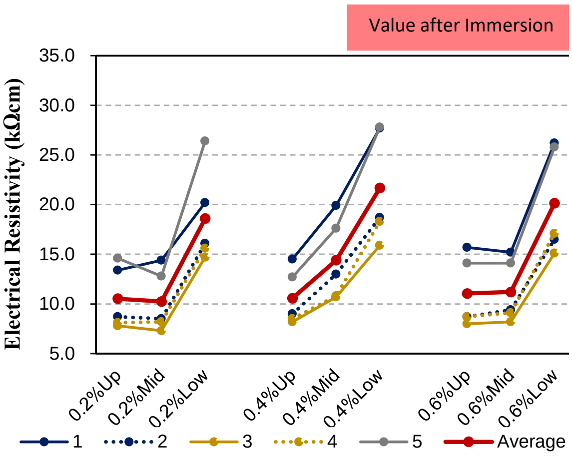

Figure 4.15 Electrical Resistivity After Immersion

4.3.4 Moisture and electrical resistivity

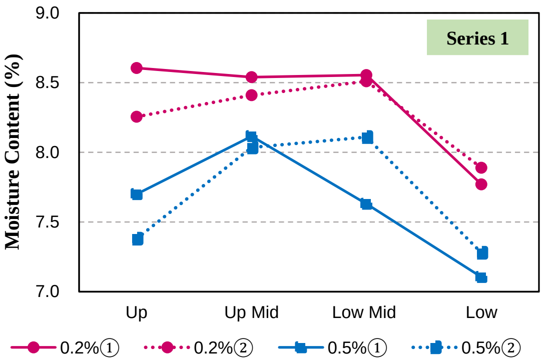

Figure 4.16 Moisture Content – Series 1

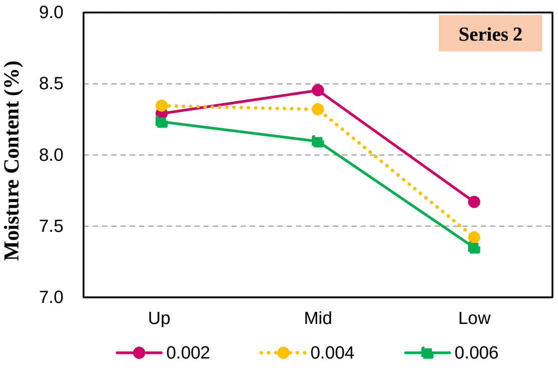

Figure 4.17 Moisture Content – Series 2

The moisture content of the specimen was also measured. The result shows that the moisture content is lower in the lower section of the specimen and higher in the middle and the higher section. It can be assumed that the higher section of the specimen absorbs more water than the lower section.

4.3.5 Macro-cell corrosion

Prior to the cutting of the specimen, macro-cell measurement was performed on the specimen Series 2. First, the lower bar was considered as the anode when performing the measurement, and afterward the middle rebar was considered to be the anode because it could only be confirmed after the measurement, as represented in *Figure 4.18*. The result revealed that the macro-cell corrosion current is significantly higher when the middle rebar is acting as the anode. That reveals that the middle rebar might be more corroded than the up rebar. Similarly, the macro-cell corrosion current is lower when the middle bar is assumed to be the anode, as shown in *Figure 4.19*, which implies that the corrosion in the upper steel bar is higher than in the middle bar. These results are broadly in line with prior studies [Baccay et al., 2004]. Besides, a common trend can be observed in both graphs, showing the rise of the macro-cell current pattern over time.

Similarly, the macrocell between the different shapes of the rebar was measured and the results are seen in *Figure 4.20* and *Figure 4.21*. However, the results show an opposite trend seen in the half cell potential. The diamond shape appears to be more sensitive to the flow of current.

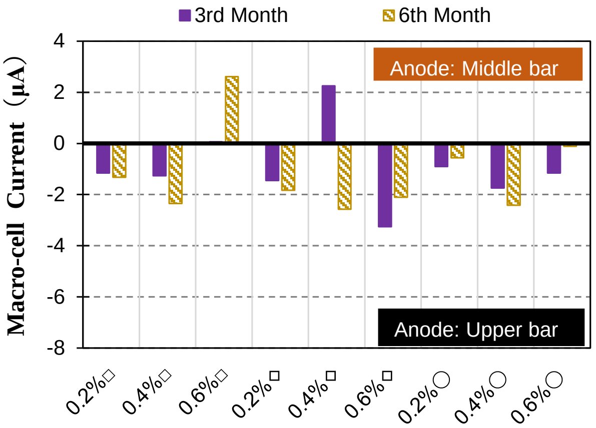

Figure 4.18 Macro-Cell Middle Bar – Upper Bar

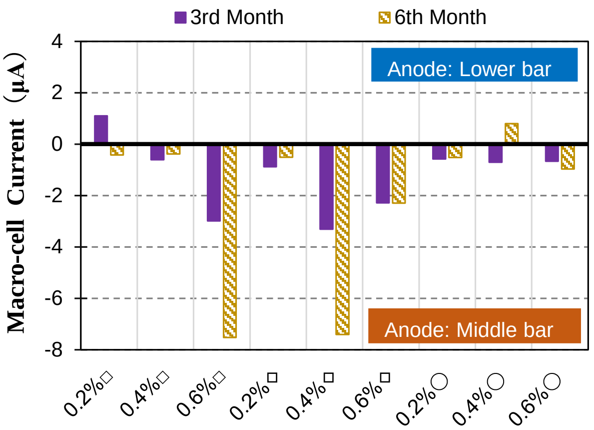

Figure 4.19 Macro-Cell Middle Bar – Lower Bar

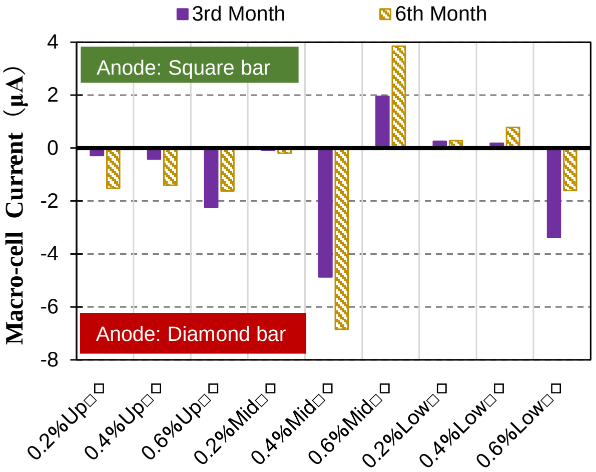

Figure 4.20: Macrocell Corrosion Square-Diamond Rebar

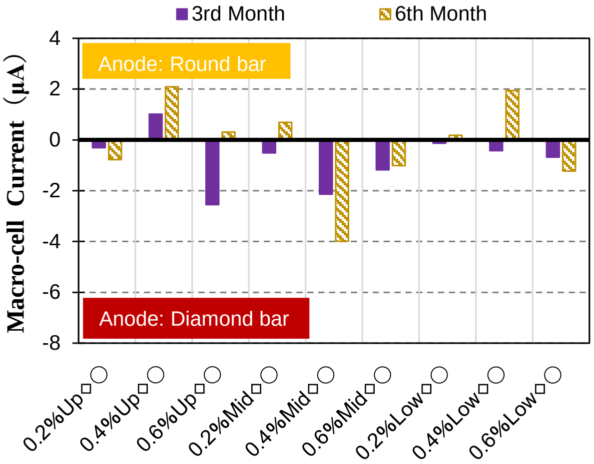

Figure 4.21 Macrocell Corrosion Round-Diamond Rebar

4.3.6 Chloride concentration

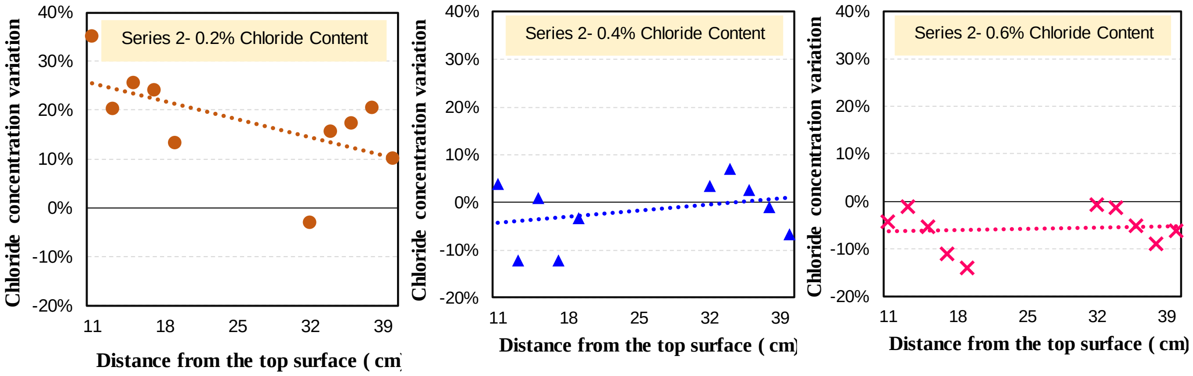

Figure 4.22: Effect of water rise on the concentration of chloride

4.3.7 Void area under the rebar.

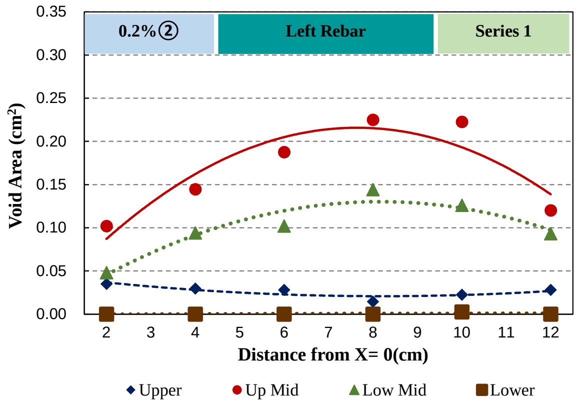

Figure 4.23 Void Area Under Rebar 0.2% Round – Series 1

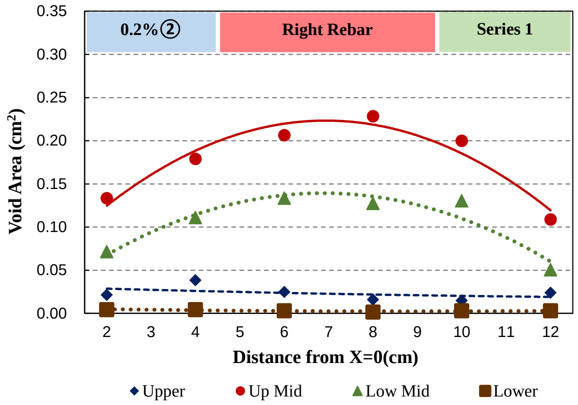

Figure 4.24 Void Area Under Rebar 0.2% Round – Series 1

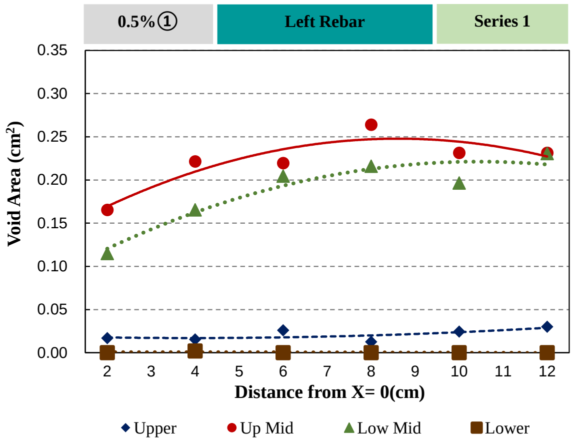

Figure 4.25 Void Area Under Rebar 0.5% Round – Series 1

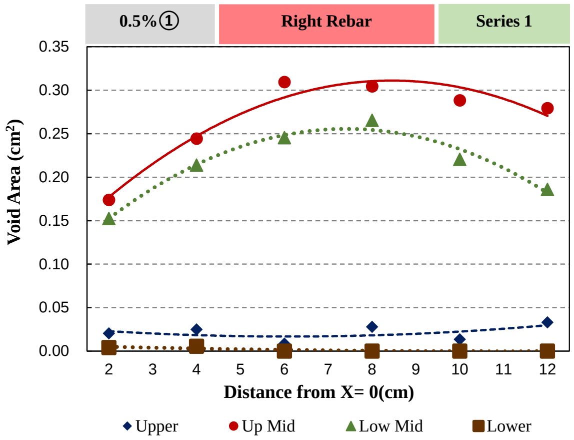

Figure 4.26 Void Area Under Rebar 0.5% Round – Series 1

Describing the trend observed in *Figure 4.23* and *Figure 4.35*, the curve of the graphs displays a peak near the center of both specimens and the lowest values found on the edge side of each specimen. Under certain assumptions, this can be explained by the fact that the bleeding water could easily travel upwards along the forms [Neville, 2011]. As a result, the water at the edge of the specimen moves up faster while the water in the interior of the concrete may take longer. On the other hand, while in Series 2, the quantity of void area is highest on the top layer, followed by the middle layer. In contrast, in Series 1, there is a tendency that the void area in the middle section (upper middle and lower middle) is larger compared to the upper section. That low value could be possibly because in some cases, the water on the top surface could evaporate if the surface is not disturbed, leading to the decrease of the effective water to cement ratio in that area. As a result, the strength of the concrete is increased in that area as well [Neville, 2011].

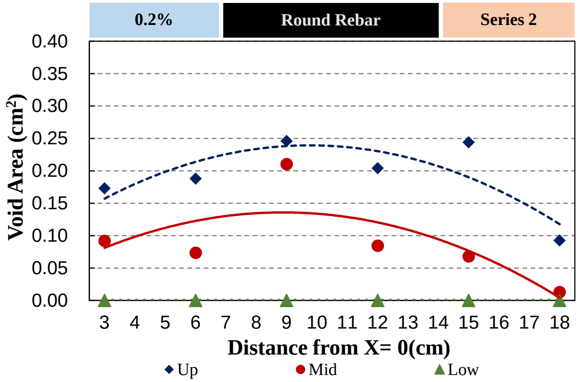

Figure 4.27 Void Area Under Rebar 0.2% Round – Series 2

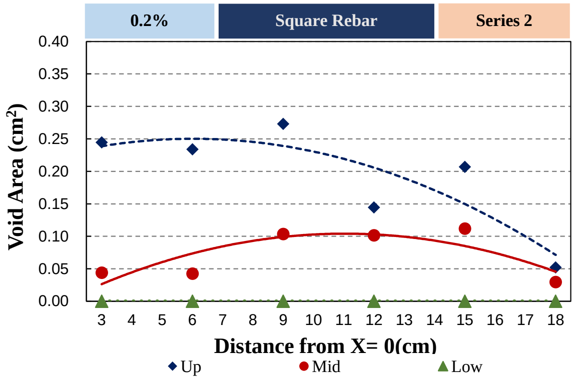

Figure 4.28 Void Area Under Rebar 0.2% Square – Series 2

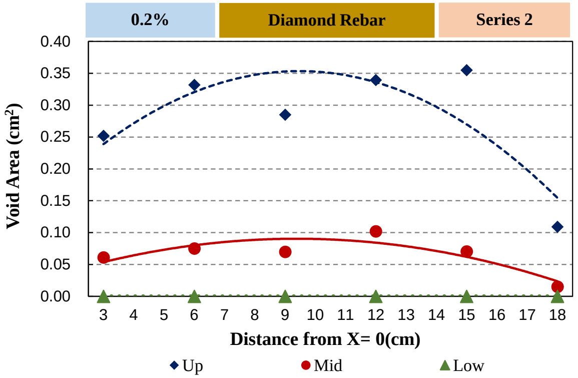

Figure 4.29 Void Area Under Rebar 0.2% Diamond – Series 2

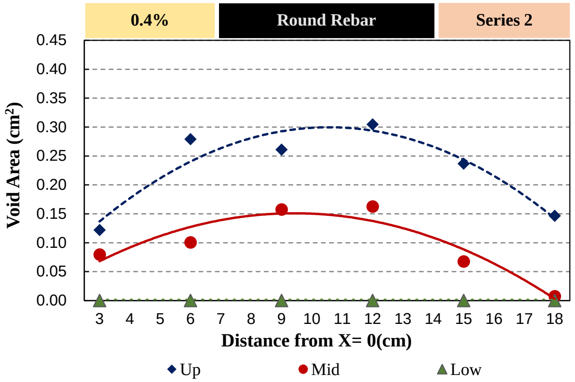

Figure 4.30 Void Area Under Rebar 0.4% Round – Series 2

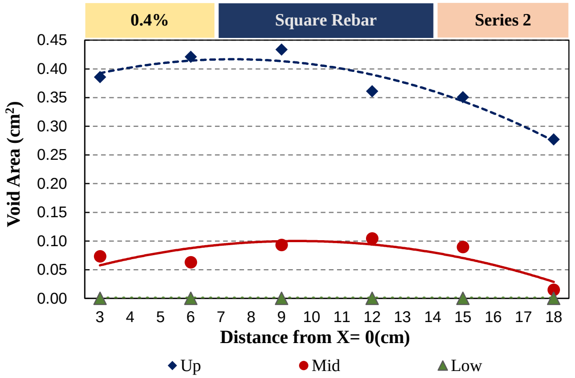

Figure 4.31 Void Area Under Rebar 0.4% Square – Series 2

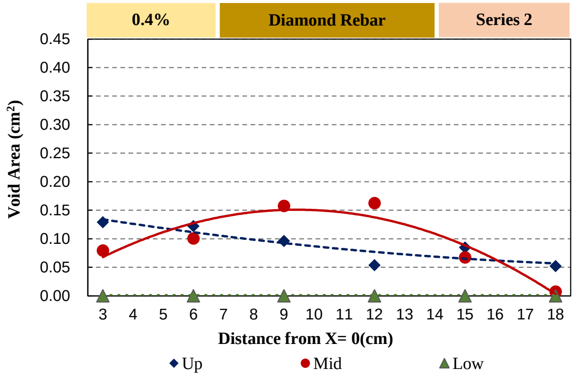

Figure 4.32 Void Area Under Rebar 0.4% Diamond – Series 2

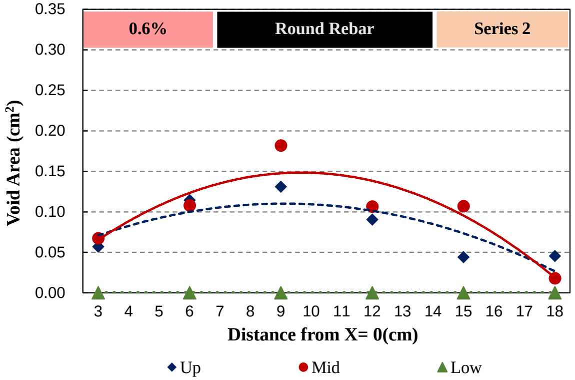

Figure 4.33 Void Area Under Rebar 0.2% Square – Series 2

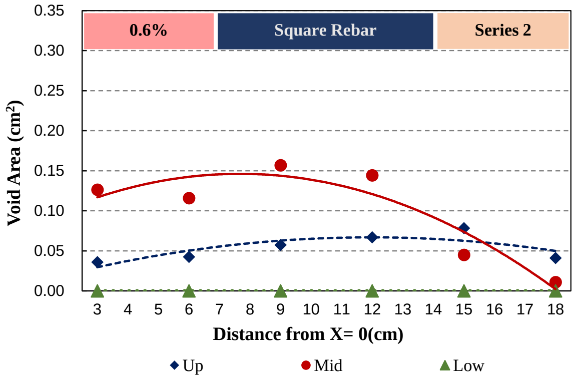

Figure 4.34 Void Area Under Rebar 0.6% Square – Series 2

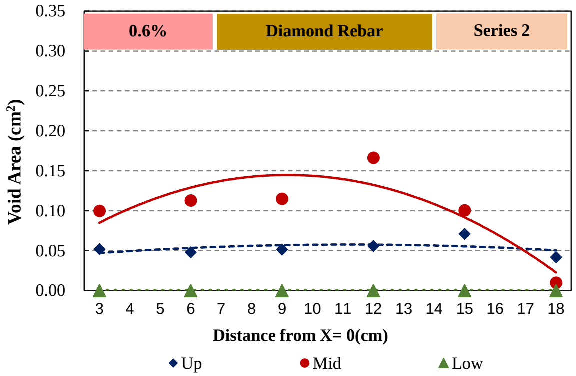

Figure 4.35 Void Area Under Rebar 0.6% Diamond – Series 2

4.3.8 Visual observation

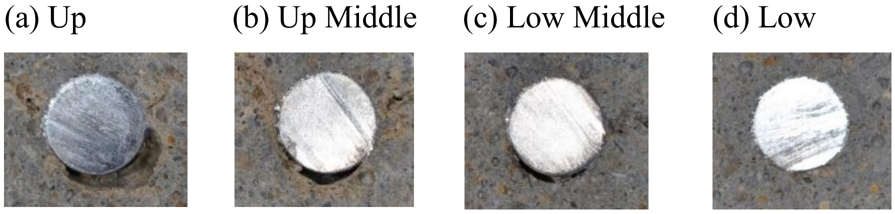

(a) Up (b) Up Middle (c) Low Middle (d) Low

Figure 4.36 Void Under the Horizontal still bar – Series 1

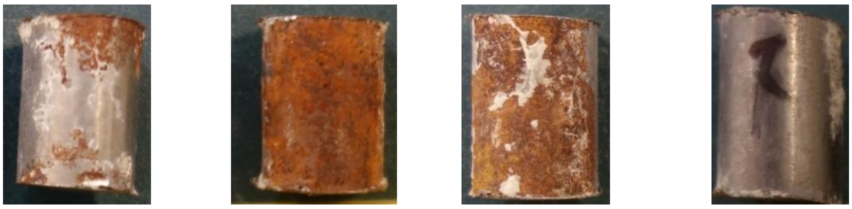

Figure 4.37 Visual observation of the specimen reinforcing steel (Series 1. 0.2% chloride content)

Figure 4.36 shows distinctively the void under each reinforcing steel of Series 1 with 0.2% of chloride content owing to the bleeding. It clearly pictures an increase in the quantity of the void area when the position of the steel becomes higher. These results provide more evidence on the effect of the bleeding water on the macrostructure of the concrete. There are reasons to believe that the higher the position of the bar, the more the water quantity is cumulated on the undersurface of the horizontal steel bar resulting in the surge of the surface of the void. By comparing with the electrical resistivity results, a relation could be set as when the void area increases, the electrical resistivity decreases as well, leading to higher risk and higher rate of corrosion.

To confirm the state of corrosion in each specimen, the reinforcing bars at the middle of the specimen were removed from the mortar. It can be seen in *Figure 4.37* that the upper rebar is not as corroded as the upper middle, which is the most corroded, and the lower middle, whereas the lower steel bar is completely free of corrosion. This best support the results received from the void measurement, the area where the void areas are found to be significant, the corrosion appears to be more significant as well, mainly on the upper middle and the lower middle rebar. Besides the lower void quantity on the upper steels seems to make a substantial difference on the corroded surface. Finally, as void was not observed in the inferior rebar, the rebar appears to be in a passive state.

The bleeding did not only created voids, but water paths, also called vertical bleed channels, were also created in the interior of the mortar around some steel bar, as shown in *Figure 4.38*. The water path was mainly generated on the upper and the middle steel bar when some water stagnating under the rebar tried to escape. However, this could promote the ingress of aggressive agents inducing damage to the concrete, like carbon dioxide and chloride since the permeability of the concrete will be declined.

Figure 4.38 Water drainage path

4.4 CONCLUSION

In this study, the effect of bleeding on the corrosion of the reinforcing steel was investigated. The results are summarized as followed:

- The visual observations and the void measurements showed that the bleeding had a substantial effect on the quantity of the void areas under the steel bar. As a general trend, the higher the location of the steel, the higher the quantity of voids. However, in this study, in some specimens, the highest steel bar did not show the largest void. This phenomenon is estimated to be due to that the bleeding water could move upward through the side surface of steel bars which is the water drainage path.
- The electrochemical measurements also revealed that the higher section of the beams shows lower potential and a higher rate of corrosion which is presumed to be the effect of the interfacial gaps as the formation of passivity film could not take place.
- In this experimental work, the study was focused on the electrochemical proprieties and visual observation, therefore mechanical effect such as the load bearing capacity is outside of the scope of the research, though important it may be. Further research on the effect on the air bubble formed owing to the bleeding water needs to be carried out as well.

4.5 REFERENCES

ASTM C876-15, (2015): Standard Test Method for Corrosion Potentials of Uncoated Reinforcing Steel in Concrete, ASTM International.

Baccay, M. A., Nishida, T., Otsuki, N., Hamamoto, J., and Chin, K., (2004): Influence of Bleeding on Minute Properties and Steel Corrosion in Concrete, Journal of Advanced Concrete Technology, 2, pp. 187–199.

Broomfield, J. P., Rodriguez, J., Ortega, L. M., and Garcia, A. M., (1993): Corrosion Rate Measurement and Life Prediction for Reinforced Concrete Structures, Proc. Structural Faults and Repair 2 Engineering Technical Press (University of Edinburgh, Scotland) pp. 155

Elsener, B., Andrade, C., Polder, R., and Raupach, M., (2003): RILEM TC 154-EMC Electrochemical for Measuring Metallic Corrosion, Materials and Structures, 36, pp. 461-471.

Hooton, R. D., Geiker, M. R., and Bentz, E. C., (2002): Effects of Curing on Chloride Ingress and Implications on Service Life, ACI Material Journal, 99, pp 201–206

Hooton, R. D., Geiker, M. R., and Bentz, E. C., (2002): Effects of Curing on Chloride Ingress and Implications on Service Life, ACI Material Journal, 99, pp. 201–206.

Jäggi, S., Elsener, B., and Böhni, H., (2001): Macrocell Corrosion of Steel in Concrete – Experiments and Numerical Modelling (Riva di Garda, Italy), Associazione Italiana Metallurgia Milan CD.

James, J., (1991): Interface Durability Correlation in Concrete, Bulletin of Materials Science, 14 (5), pp. 1183-1195.

Lambert, P., Page, C. L., and Vassie, P. R. W, (1991): Investigations of Reinforcement Corrosion Electrochemical Monitoring of Steel in Chloride-contaminated Concrete, Materials and Structures, 24 (143), pp. 351-358.

Langford, P., and Broomfield, J., (1987): Monitoring the Corrosion of Reinforcing Steel, Construction Repair, 1(2), pp. 32-36.

Layssi, H., Ghods, P., Alizadeh, A., and Salehi, M., (2015): Electrical Resistivity of Concrete, Concrete Int., 37, pp. 41-46.

Liu, Y., Presuel-Moreno, F. J., and Paredes, M, A, (2015): Determination of Chloride Diffusion Coefficients in Concrete by Electrical Resistivity Method, ACI Materials Journal, 112 (5), pp. 631-640.

Mohammed, T. U., Otsuki, N., Hamada, H., and Yamaji, T., (2002): Chloride-induced Corrosion of Steel Bars in Concrete with Presence of Gap at Steel-Concrete Interface, ACI Materials Journal, 99 (2), pp. 149–156.

Mohammed, T. U., Yamaji, T., Toshiyuki, A., and Hamada, H., (2002): Marine Durability of 15-year Old Concrete Specimens Made with Ordinary Portland, slag and fly ash cements Journal of materials, concrete structures and pavements Japan Society of Civil Engineers, pp. 201–214.

Neville, A. M., (2011): Properties of Concrete Pearson Education Limited (Harlow United Kingdom), pp. 207-208.

Scwamborn, B., (1987): About the Bleeding of Fresh Concrete, Proc. of a colloquium, Frischmortel, Zementleim, Friscbeton (Univerisity of Hanover), 55, pp. 283-297.

Yim, H. J., Kim, J. H., and Kwak, H. G., (2014): Experimental simulation of bleeding under a high concrete column, Cement and Concrete Research, Elsevier, 57, pp. 61-69.

CHAPTER V

EFFECTIVENESS OF CALCIUM NITRITE COATING FOR STEEL BAR AS CORROSION INHIBITOR IN SEAWATER-MIXED MORTAR

5.1. INTRODUCTION

The problems raised due to the shortage of water have become increasingly considerable for the past decades and are expected to increase in the next coming decades. However, the use of concrete in construction demands huge quantities of water for mixing, cleaning, and curing. Statistics suggest the water required in concrete production is about 20% of the volume of concrete [Miller et al., 2016; 2018]. For the past few years, the use of seawater as concrete mixing water has been considered owing to its large potential in terms of accessibility and quantity. However, another challenging problem, which arises in the use of seawater is the fact that it adds to the total volume of chloride in the original mix proportion of concrete. According to JIS A 5308, the total volume of chloride allowable in the original mixed is limited to 0.30kg/m^3 or less than 0.60kg/m^3 for civil engineering concrete construction [JIS A 5308, 2019]. However, the content of chloride comprised in seawater-mixed concrete is around 3kg/m^3[Otsuki et al., 2014]. In addition, previous researches have proven that the degradation engendered by chloride contamination into the original mix is even more severe than that the same quantity of chloride ingress during the service life [Lambert, 1991]. As a result, the usage of seawater is still forbidden in most of existing standard, when it is used as mixing water.

To remediate these issues, studies on the addition of cementitious materials, such as Ground Granulated Blast Furnace Slag (GGBFS) and Fly Ash (FA) admixtures, have been explored for the past few years. Prominent results were achieved as attempts to improve the quality of concrete. Adiwijaya et al showed that seawater has an effective effect on the strength of concrete when mixed with ground granulated blast furnace slag and when air curing is opted [Adiwijaya, 2017].

Neville showed in his study that the use of seawater is possible to use seawater as mixing water under 2 circumstances: (a) for concrete kept completely dry during its service life, and (b) for a construction build with the sea or completely immersed in seawater [Neville, 2001]. In their research, Akashi et al. showed that the use of seawater is reducing the quantity of bleeding in concrete [Akashi et al., 1965], because the setting time tends to be faster. When freshwater is used, it takes 2.6 hours for the concrete to reach the final setting time from the initial setting time, while this only takes 1.8 hours when seawater is used due to the coagulation effect of the NaCl [Hasaba et al. 1974; Hasaba et al. 1975]. Nonetheless, previous studies have shown that, when exposed to marine environmental conditions, even concrete of good quality does not always withstand the attack of chlorides.

Corrosion inhibitor is one of the numerous alternatives for corrosion prevention methods developed to deal with the matters of corrosion. Recently, the use of Calcium Nitrite Inhibitor has been of interest for its simplicity in usage, its cost-effectiveness, and its appreciated effect [Page et al., 2000]. As an anodic inhibitor, it is claimed that its effect is more pronounced. (ACI 222). Corrosion inhibitor can be added to fresh concrete as admixtures [Shi et al. 2009; Elsener, 2001; Elsener and Cigna, 2002], or applied on the surface of hardened concrete and penetrates through the microstructures of the concrete to reach the rebar [Faustine et al. 2014; Elsener and Cigna, 2002; Page et al., 2000].

Anodic nitrite-based inhibitor has a long history in terms of corrosion prevention. Research concerning nitrite started in the sixties, both in the fields of texting and laboratory, showing prominent results on their effectiveness [Berke, 1992;2004].

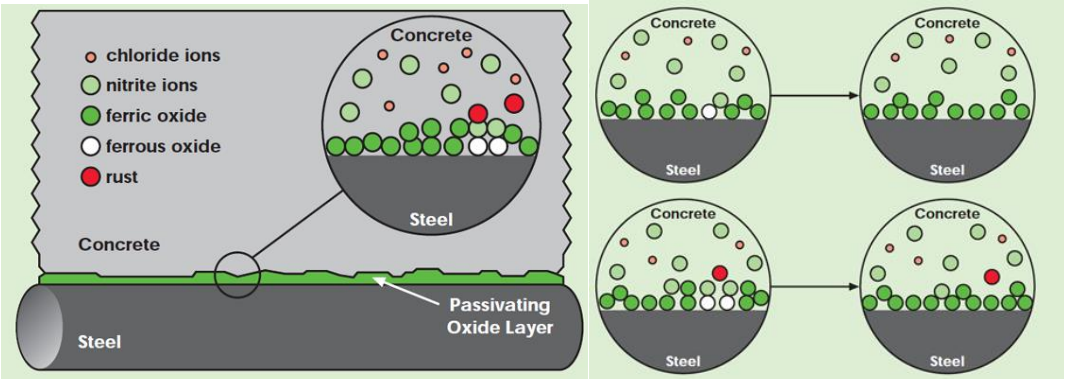

Figure 5.1 Schematic of the action of calcium nitrite as corrosion inhibitor [GCP, 2021]

Some concerns were raised on the toxicity, possibility of increase of corrosion rate in case of low dosage, and the solubility of nitrite. The nitrite ion was shown to oxidize to ferrous ions to ferric ions. As a result, it blocks the passage of ferrous ions from the steel and delays the attack or chloride in concrete [Gaidis and Rosenberg, 1979].

The purpose of this study was to investigate the effectiveness of Calcium Nitrite as coating for steel bars in see water mixed concrete. It was analyzed whether the use of different concentrations of CNI in seawater mixed concrete has effects on the prevention of corrosion after about 3 years of exposure to dry-wet conditions. Besides, the difference because of the use of CNI as a coating is investigated.

5.2. TEST PROGRAMS

5.2.1 Specimen Materials

In this experiment, 2 Series of 12 specimens with a dimension of 120 mm x 135 mm x 135 mm were used. For both Series, Ordinary Portland cement (OPC) and Ground Granulated Blast Furnace Slag (GGBFS) were used as a binder and sea sand as fine aggregates. Two reinforcing bars of 13mm were imbedded into each specimen, with a concrete cover of 50mm. Epoxy resins were applied to 5 surfaces of each specimen. One surface was not coated for measurement purposes. The properties of each material used in the mix are detailed in *Table 5.1*. The mortar casting was done in the direction parallel to the rebar.

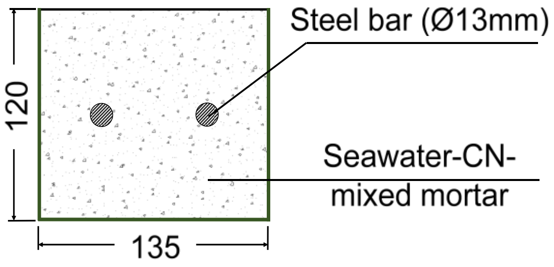

Figure 5.2 Series 1 – CNI -mortar specimen

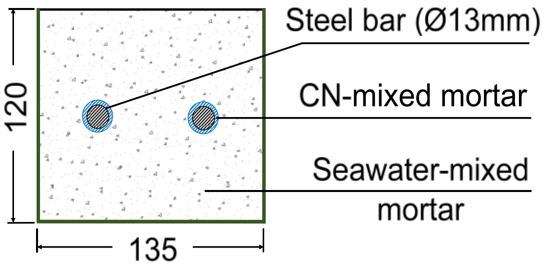

Figure 5.3 Series 2- CNI – Coating Specimen

5.2.2 Mix proportion

Table 5.1 Properties of materials

Material	**Physical properties**	
Ordinary Portland cement	Density, [g/cm^3]	3.16
GGBFS	Surface area, [cm^2/g]	4000
Fine Aggregate (Sea sand)	Density, [g/cm^3] (SSD condition)	2.54
	Water Absorption, [%]	1.09
Round steel Bar	SS400 (Ø 13 mm)	
AE Water Reducer	Polycarboxylate ether-based	
AE Agent	Alkylcarboxylic type	

As mentioned above, two Series of specimens are used. Series 1 consists of specimens in which different concentrations of Calcium Nitrite were added to the entire seawater mortar mix with a water to cement ratio of 50% as presented in Fig. 2. The mix proportion and the calcium nitrite concentration are presented in *Table 5.2* and Table *5.3*.

In Series 2, Calcium Nitrite was applied to the mortar for coating alone using tap water as mixing water, with water to binder ratio of 40% as seen in Fig. The thickness of the coating was about 3 mm. For the core of the specimen, seawater was used as the mixing water with water to binder ratio of 50%. For both Series of specimens, respectively 1.5 liters/m^3 and 3 liters/m^3 of Calcium Nitrite solution were used containing 20-30% of Calcium Nitrite. Series 1 and Series 2 were prepared in 2019 (Series 1= 31 months; Series 2= 30months). In addition, both Series contain a Series with OPC specimens and GGBFS specimens.

Table 5.2 Mix proportion of the mortar - Series 1 and Series 2

Specimen Name		**CNI** **（l/m^3）**	**W/C** **(%)**	**Unit Weight（kg/m^3）**			
				Seawater	**OPC**	**GGBFS**	**Sand**
Series 1	0N	0	50	255	510	-	1525
	1.5N	1.5					
	3N	3					
	0B	0	50	255	255	255	1515
	1.5B	1.5					
	3B	3					

Table 5.3 Mix proportion of the coating mortar - Series 2

Specimen Name		CNI (l/m³)	W/C (%)	Unit Weight（kg/m³）			
				Tap Water	OPC	GGBFS	Sand
Series 2	0NN	0	40	232	581	-	1508
	1.5NN	1.5					
	3NN	3					
	0BB	0	40	232	291	291	1514
	1.5BB	1.5					
	3BB	3					

T*able 5.4* shows the chemical properties of the seawater used for the Mixing, curing, and the immersion (Dry-wet cycle) of the specimen. The seawater was taken from Shimakeya, Itoshima, Fukuoka, Japan. The concentration of chloride in the mix is about 4.77 kg/m^3.

Table 5.4 Chemical content of seawater

Specific Gravity	pH	Chemical Composition (g/l)					
		Cl^-	SO_4^{2-}	Ca^{2+}	Mg^{2+}	K^+	Na^+
1.020	7.71	18.72	2.37	0.36	1.2	0.35	9.9

Figure 5.4:Shimakeya, Itoshima, Japan (seawater used for the experiment)

5.2.3 Casting Process, Curing method and Exposure condition

a. Series 1 Exposure conditions

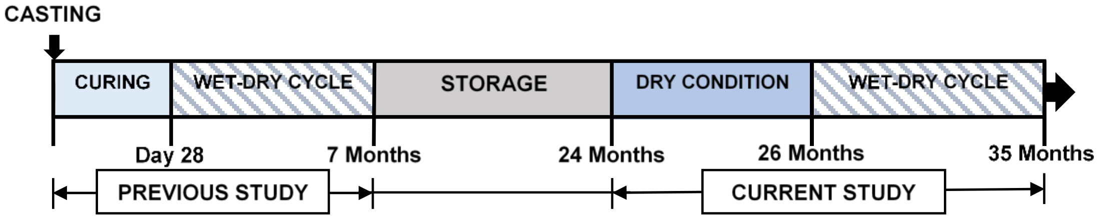

Figure 5.5: Chronological exposure condition of Series 1 (Until Mai 2021)

A day after casting, Series 1 was demolded. The curing process was then processed for 28 days at 20ºC room temperature, and 60% of relative humidity. Wet towels were used to preserve the concentration of Calcium Nitrate and the seawater. After 28 days of curing, the specimens were put under wet-dry cycles. It was performed by immersing the sample in seawater for 2 days, and the specimens were dried for 5 days. Electrochemical measurements were performed at the end of each wet cycle.

During the wet-dry cycle, the specimens were exposed to the atmospheric conditions of the laboratory room. After 7 months, the specimens were stored at in the laboratory room condition for 17 months. To assess, the condition of the specimens after several months, the specimens were kept in a dry condition at 20ºC, and testing were performed. After 26 months, the wet-dry cycle process was restarted in the laboratory room condition.

b. Series 2, Exposure condition

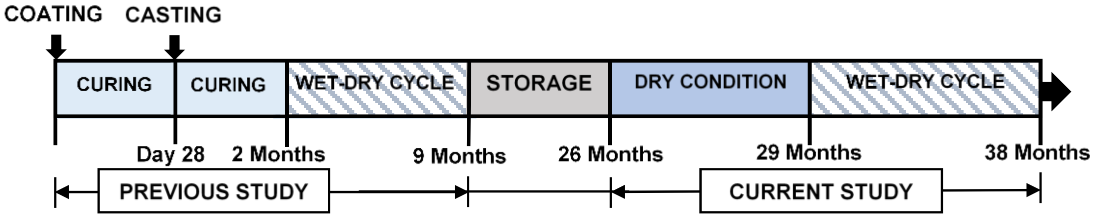

Figure 5.6 : Chronological exposure condition of Series 2 (Until Mai 2021)

Figure 5.7. Dry-wet cycle through immersion in seawater

Figure 5.8. Steel coating and curing - Series 2

For the preparation of Series 2, first, the steel bar was coated with CNI mixed mortar using tap water. The coated steels were afterward cured using a wet towel as illustrated in *Figure 5.8*, using the same room condition as Series 1. After the 28 days of curing was over, the specimens were cast with the coated steel bars. After the curing process, Series 2 was put under the same condition as Series 1. The curing process of both Series was done by wrapping with wet towels, then they were stored in a controlled room maintained at 20º C for 28 days.

After curing, the specimens were put under a dry-wet cycle for the first 7 months for Series 1 and eight months for Series 2 and the progress of corrosion was monitored at the laboratory room conditions. Dry-wet cycle, performed by immersing the specimens in seawater, was used to simulate aggressive marine environments and to accelerate the initiation and progression of corrosion of steel bars. Then, both Series specimens were stored in the laboratory at room conditions for 17 months and the actual conditions of the specimen were measured for 2 months under room conditions at a constant temperature of 20ºC. The specimens were subjected again to 5 days of dry and 2 days wet cycle under atmospheric conditions (*Figure 5.8)*.

5.2.4 METHODS

Non-destructive, electrochemical methods were used to monitor the effectiveness of calcium nitrite as a corrosion inhibitor in seawater-mixed concrete. Because sweater was used, the specimen were immersed in seawater, seawater was cleaned, and the specimen were wetted for at least one hour.

Half-cell potential was measured at the end of each dry-wet cycle, every 1 to 2 weeks. Impedance multimeter and Ag/AgCl reference electrode were used. The evaluation of corrosion was done as per the ASTM C85 standard [ASTM, 2015].

Table 5.5. Half-cell potential range related to corrosion probability (ASTM C876)

Half-Cell Potential (Ecorr) [mV; CSE]	**Probability of Corrosion**
Ecorr >-200 mV	10%
-350<Ecorr<-200	Uncertain
Ecorr<-350	90%

The rate of corrosion for each specimen was monitored using corrosion meter. The current density was measured at the end of 2 cycles and evaluated according to the CEB standard [CEB, 1998].

Table 5.6. Corrosion rate classification (CEB Standard)

Corrosion Current Density [i_{corr}; μA/cm^2]	**Corrosion rate**
< 0.2	Passive/ Very low
0.2 – 0.5	Low/ Moderate
0.5 – 1.0	Moderate/Low
> 1.5	Very high

To assess the state of the passivity grade and the permeability of oxygen in the specimen, Potentiostat method was used and performed at the end of 4 cycles. Owing to the small size of the specimen, the immersion method was opted [Otsuki et al., 1992]. The grade of passivity was qualitatively compared with the classification of Otsuki as seen in *Table 5.7*.

Table 5.7. Grade of passivity function of potential and current density

Grade	Potential	Current density	Passivity state
0	E_{corr}+200mV to E_{corr}+600mV	I_{corr}>100µA/cm^2 at least one time	No Passivity Film
1		10<I_{corr}<100µA/cm^2	Some Passivity Film
2		The anodic curve cut the 10 µA/cm^2	
3		1<I_{corr}<10 µA/cm^2	
4		The anodic curve cut the 1µA/cm^2	
5		I_{corr}<1µA/cm^2	Excellent Passivity Film State

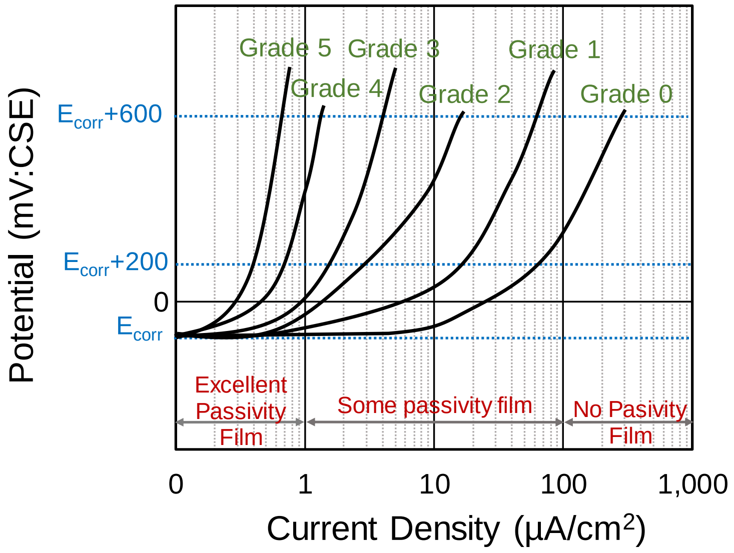

Figure 5.9. Grade of passivity from the anodic polarization curve (Otsuki et al., 1985)

The supply of oxygen was measured according to the method of potential step, through the immersion method. The measurements were run for 24 hours until the current density value is constant. The oxygen diffusion was calculated from the following formulation [Nagataki, 1996]:

$$\frac{dQ}{dt}=\frac{i_{lim}}{n.F}$$

Where,
dQ/dt : Oxygen supply (mol/cm^2/s)
i_{lim} : Current density (A/ cm^2)
n : Number of electron (4)
F : Faradays constant (96,500 coulombs/mol)

5.3. RESULTS AND DISCUSSION

In this section, the results from several months of monitoring using electrochemical methods namely the half-cell potential, current density, anodic-cathodic polarization curve, and the oxygen diffusion detailed.

5.3.1 Half-cell Potential

Half-cell potential was measured and assessed according to the ASTM standard [ASTM, 2015]. *Figure 5.11* and *Figure 5.12* show the time-dependent data from day 0 (from demolding) to 200 (about months) and day 700 to day 1050 (35 months) of the uncoated specimen. *Figure 5.13* and *Figure 5.14* show the time-variant change of the data in Series 2, from the day of demolding until 250 days, then the data of 750 days to 1100 days.

Two different trends are observed in the potential, for the uncoated specimen the potential at the early is almost equal -200 mV, then gradually decreases during the hydration process until it becomes rather constant. This trend is also seen in the previous results, depicting a drop in potential until about 28 days [Al-moudi et al., 2003]. Contrastingly, the potential in the uncoated specimen is significantly low after demolding with a minimum of -434 mV for the OPC specimens and -553mV for the GGBFS specimens and gradually recovers until 85 days where it becomes rather constant after a slight decrease. The absence of drop of potential is possibly due to the dense interface present between the steel and the concrete.

Until the 200 and 250 days for Series 1 and 2 respectively, the data were contained in the "uncertain" zone of corrosion with a potential between (-200 mV and -300mV). The potentials of the GGBFS are more scattered for both Series, while the potentials in the OPC specimen are more similar. The effect of the concentration was not yet clear for both Series. After being stored under laboratory conditions for several months, the monitoring was resumed. First, the specimens were put under 20 ºC room under dry conditions to assess their actual conditions and measurement were done once a week. After 2 months, it was subjected under wet and dry cycle again. From the second monitoring until the current condition, the potential is steel increasing in all specimen. When the dry condition, potential was still under the "uncertain" zone of corrosion for all specimens.

The dry-wet cycle was resumed, and the progress of potential was monitored over time. Surprisingly, the potentials are still increasing in both Series. The effect of the concentration of nitrite is observed in the Series 1- OPC specimen; the specimen with 3 l/m^3 of CNI shows the noblest data and has exceeded the -200mV. Therefore, it is now considered to be in the zone of "90% no corrosion". The specimen containing less CNI concentration (1.5 l/m^3) is still in the zone of "uncertain" corrosion however, it shows better results compared to the specimen without CNI (0N). These results agree with previous studies on the effectiveness of CNI as a corrosion inhibitor [Ann et al., 2006].

The trend is not straightforward in the GGBFS specimen Series 1 as in the OPC (*Figure 5.12*), nonetheless the specimen with the highest CNI content (3B). A sudden drop of potential is observed in one of the rebars with 1.5 l/m^3 concentration of CNI after it was subjected to dry-wet cycle. The potential is in the lower range of the "uncertain" zone of corrosion, nevertheless, this may imply that corrosion might have initiated in the specimen or some defects have occurred.

As observed in *Figure 5.13* and *Figure 5.14*, the potentials of all specimen in Series 2 -OPC are beyond the -200mV boundary, thus, the potential is qualified as "90% corrosion" with a maximum potential of -92 mV. The effect of the concentration of CNI is not however distinguished. Similarly, in the Series 2 – GGBFS, the potentials are higher than -200mV for the specimen without CNI and with 1.5 l/m^3. Nonetheless, the specimen with 3 l/m^3 shows the lowest data and is between the zone of uncertain corrosion. This might suggest that the combination of GGBFS, the coating, and the CNI does not have positive effects on the corrosion of seawater mixed mortar. A similar result was found in previous studies, showing that the performance of CNI strongly depends on the type of cementitious material used [Sideris et al., 2005].

Moreover, from both Series, the trend of the effect of temperature is also observed. The half-cell potential decreases with increasing temperature and increases as the temperature drops. A similar result was reached in previous research. These results show that the CNI-coating specimens are more effective compared to the CNI-mortar specimens [Alhozaraimy et al., 2020]. It can be assumed that the use of lower water to binder ratio and taper water has a role to play in this result along with the use of CNI.

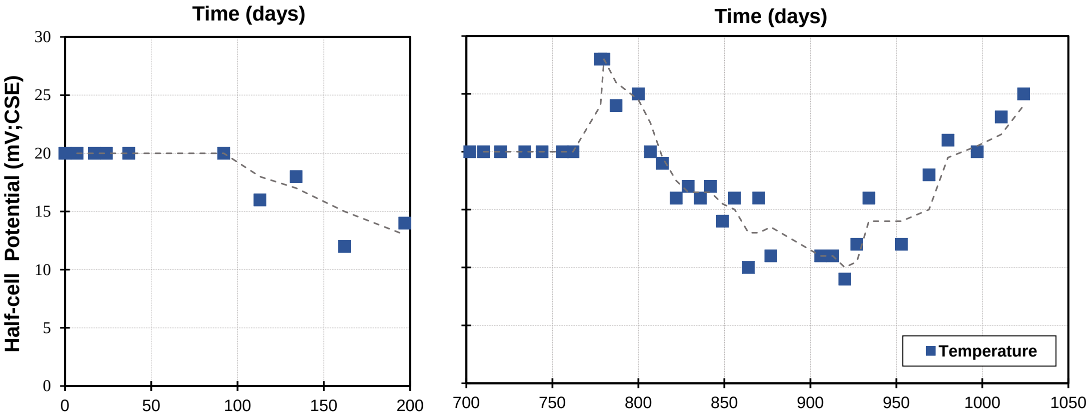

Figure 5.10 Temperature Variation with time

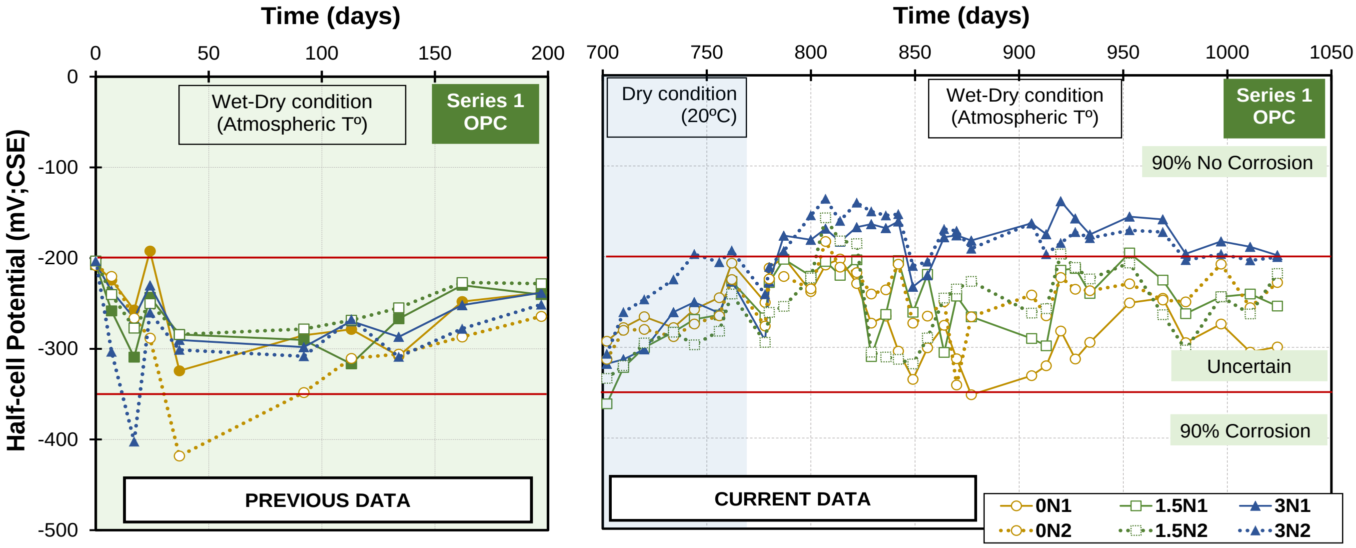

Figure 5.11 Half-cell Potential Series 1-OPC

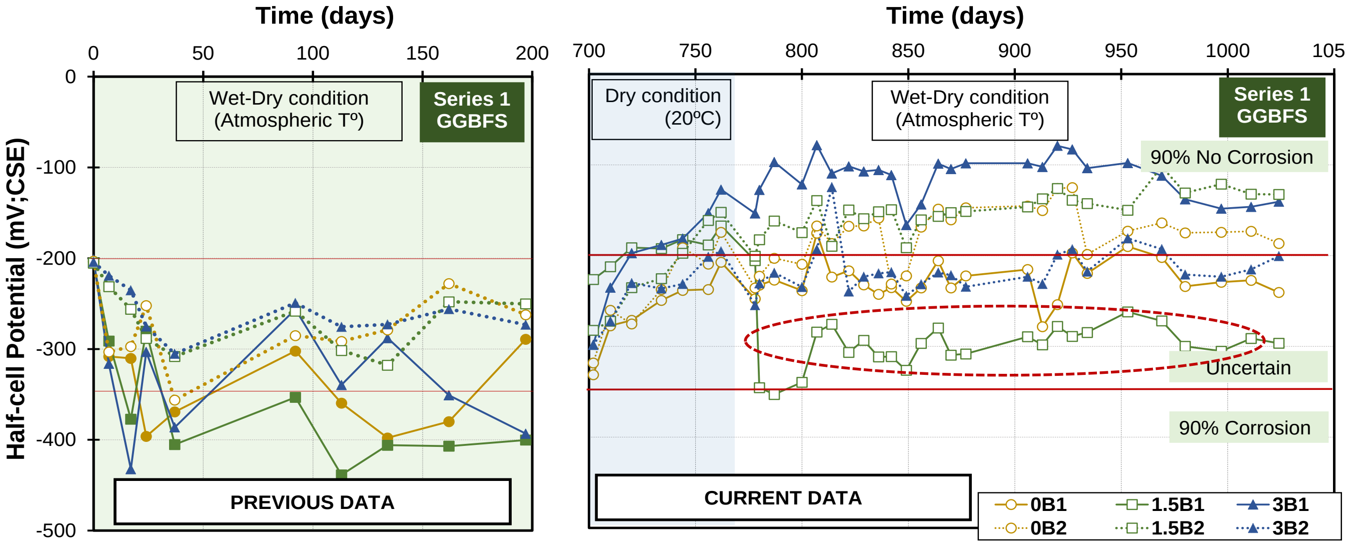

Figure 5.12 Half-cell Potential Series 1-GGBFS

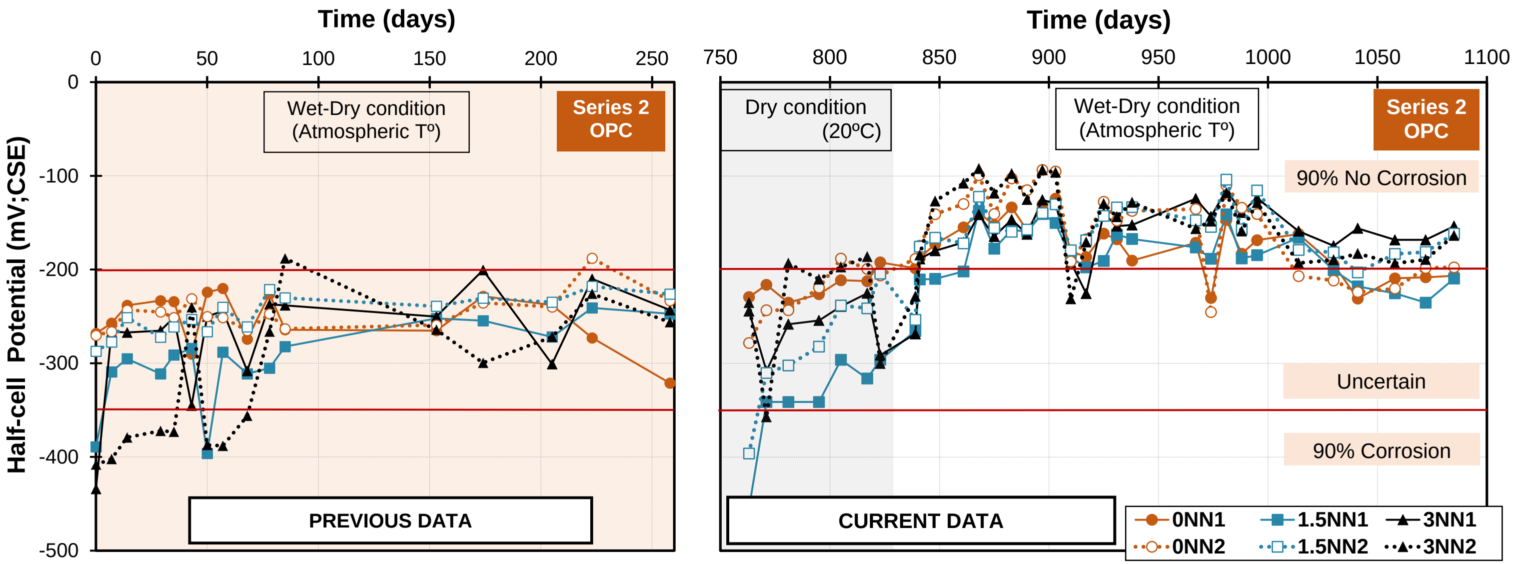

Figure 5.13: Half-cell Potential Series 2-OPC

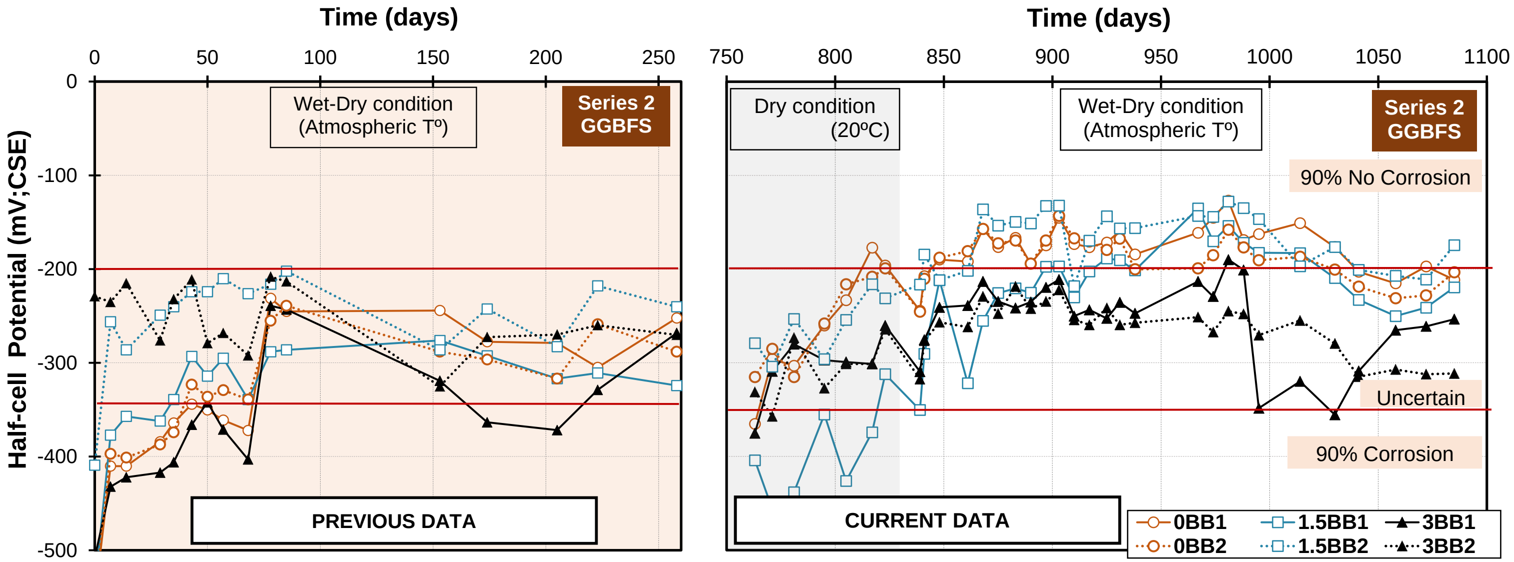

Figure 5.14. Half-cell Potential Series 2-GGBFS

5.3.2 Polarization Resistance

The current density of the steel reinforcement was measured at the end of 4 cycles of dry-wet and the rate of corrosion was determined using the CEB method. *Figure 5.15* shows the results at 7 months for Series 1 and 9 months for Series 2, whereas *Figure 5.16* illustrates the last data at 35 months and 39 months for Series 1 and Series 2 respectively.

The results show that the current and previous data are under 0.2μA/cm2, which indicates a "very low" rate of corrosion. From the previous data, the corrosion rate has decreased with time. The specimen coated shows lower current density compared to the uncoated, however, the use of GGBFS and the effect of the CNI is not observed. From the current density as well, the use of coating shows better results than the non-coated specimen.

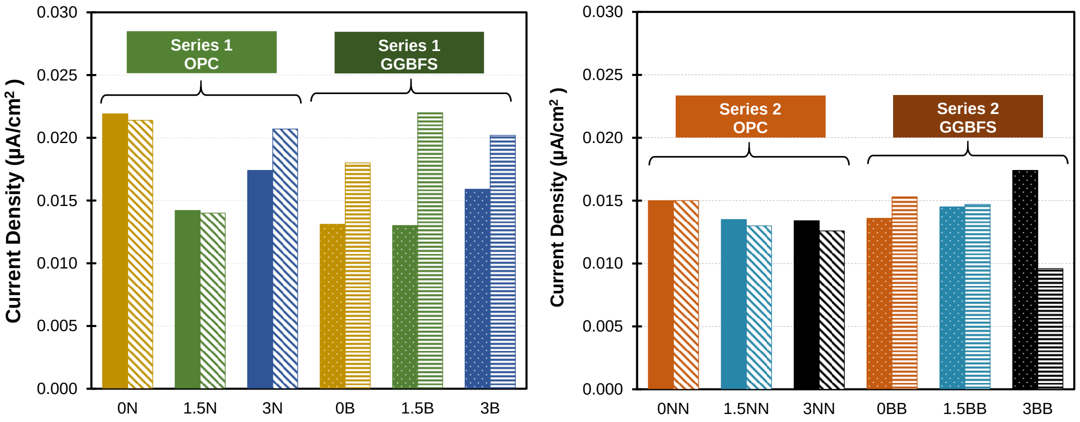

Figure 5.15 Current Density Series 1 (7 months) – Series 2 (9 months)

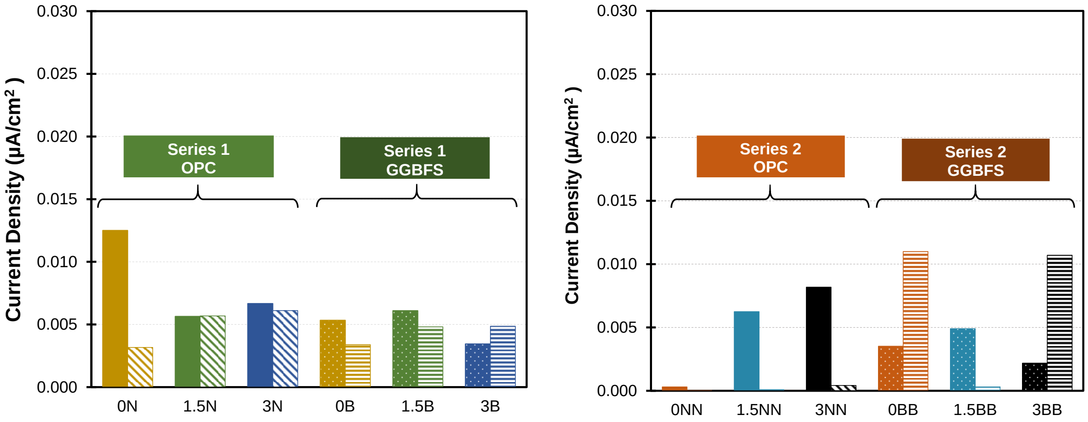

Figure 5.16 Current Density Series 1 (35 months) – Series 2 (38 months)

5.3.3 Polarization Curve

The anodic and cathodic polarization curves of the specimens were measured at the end of 4 dry-wet cycles (every month), to monitor the evolution of the grade of passivity of the steel reinforcement. For qualitative comparison, the state of the passivity grade of the rebars were was evaluated from the anodic polarization curve [Otsuki et al., 1992].

Figure 5.17 illustrates the data from the previous data; at 7 months and 9 months, respectively for Series 1 and Series 2. *Figure 5.18* shows the last data from this study (35 months for Series 1 and 38 months for Series 2).

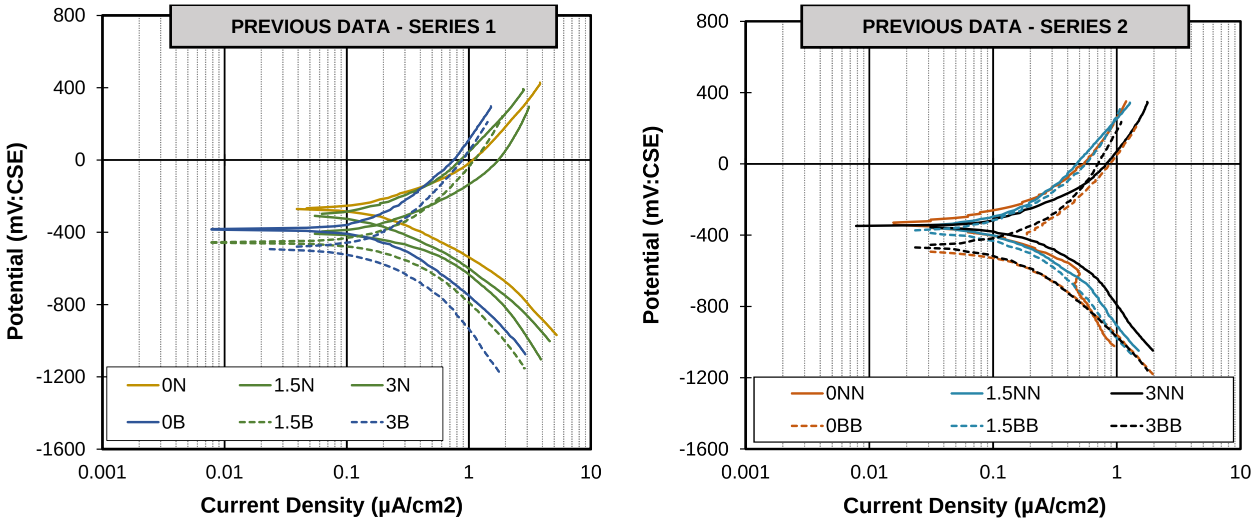

Figure 5.17. Anodic polarization curve (Previous data)

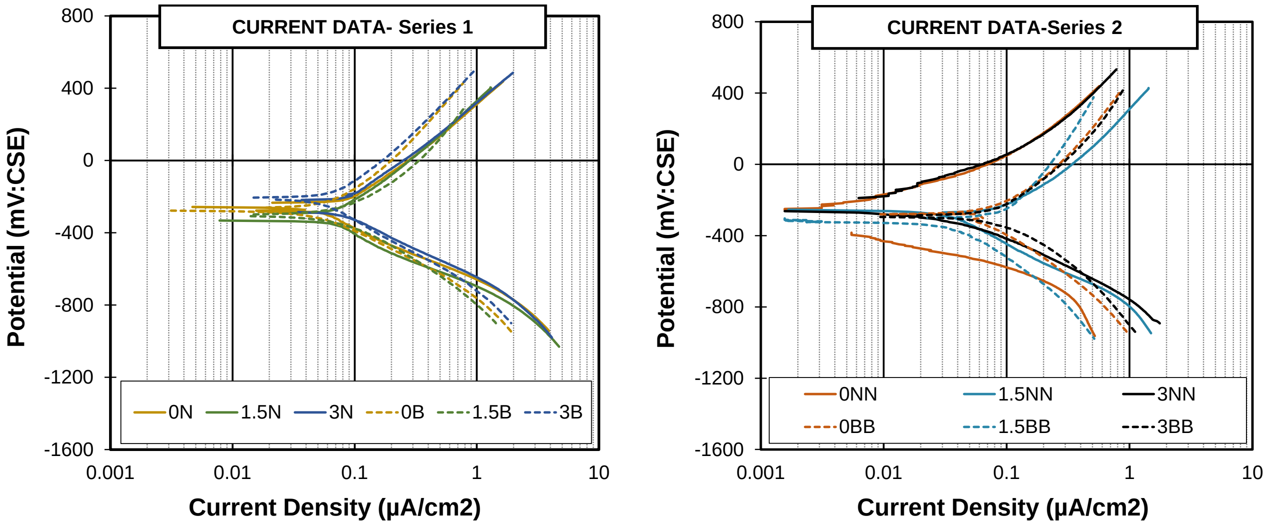

Figure 5.18. Anodic polarization curve (Current data)

The data shows that after more than 3 years of exposure in seawater conditions, corrosion has not yet initiated for both Series regardless the quantity of the calcium nitrite. The grade of passivity is judged to be 5, which shows the presence of excellent passivity film protection in the rebar. Comparing the data from the previous data (7 months and 9 months) and the current data (35 months and 39 months), a slight shift to the left is observed in both Series of specimen OPC and GGBFS. This suggests that the formation of the ferric oxide film is still ongoing in the specimen. At this point in time, there is no evidence of the effectiveness of the CNI in both specimen as the trend of the anodic polarization curve is almost similar for the Series with coating and without coating or with GGBFS or OPC.

Concerning the cathodic polarization curve, if compared to the previous data, the diffusion of oxygen has slightly decreased in the current data. An important finding from this data is a diffusion of oxygen in the coated specimen is remarkably reduced compared to the uncoated steel bar. This shows the effectiveness of the coating to reduce/ mitigate the activity of corrosion in the concrete as oxygen is an important element required in the reduction reaction of corrosion. Oxygen is called by the literature as the "governing factor" that influences the rate of propagation of corrosion in the presence of a minimum relative humidity [Tuutti, 1982; Raupach, 1996; Hussain, 2011].

5.3.5 Oxygen permeability

The diffusion of oxygen in each specimen was measured using the potentiostat in immersed method. The oxygen supply was estimated from the calculation of i_{lim} [Takumi, 2018]. Fig and Fig show the results of the calculation of the oxygen diffusion.

The average value of the oxygen diffusion is each Series are 6.00x10^{-12} m^2/s, 2.40x10^{-12} m^2/s, 1.84x10^{-12} m^2/s, and 0.82x10^{-12} m^2/s, respectively for Series 1-OPC, Series 1-GGBFS, Series 2-OPC and Series 2-GGBFS. From these results, a significantly lower oxygen diffusion is seen in the coated specimen (Series 2) compared to the uncoated Series. By adding coating on the steel bar, the diffusion is reduced by 69% in the OPC specimen and by using GGBFS and coating, a reduction of 65.85 % of the diffusion of oxygen is reported.

These results are consistent with the results obtained from the cathodic polarization curve, showing a further evidence of the effectiveness of the coating in limiting the diffusion of corrosion. From the past studies, the presence of coating or dense steel-concrete interface does not only reduces the diffusion of oxygen but it does also contribute significantly in constraining the ingress of chloride to the steel bar [Mohammed et al., 2002; Mohammed and Hamada, 2003; Otsuki et al., 2007; Mohammed et al., 2015].

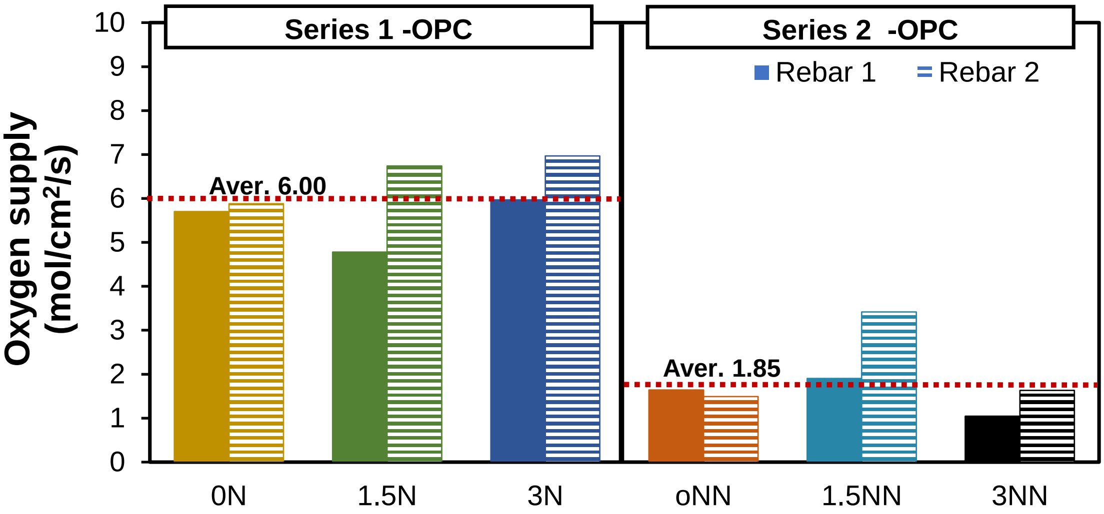

Figure 5.19 Oxygen diffusion for OPC specimen Series 1 and Series 2 (10^{-12} cm^2/s)

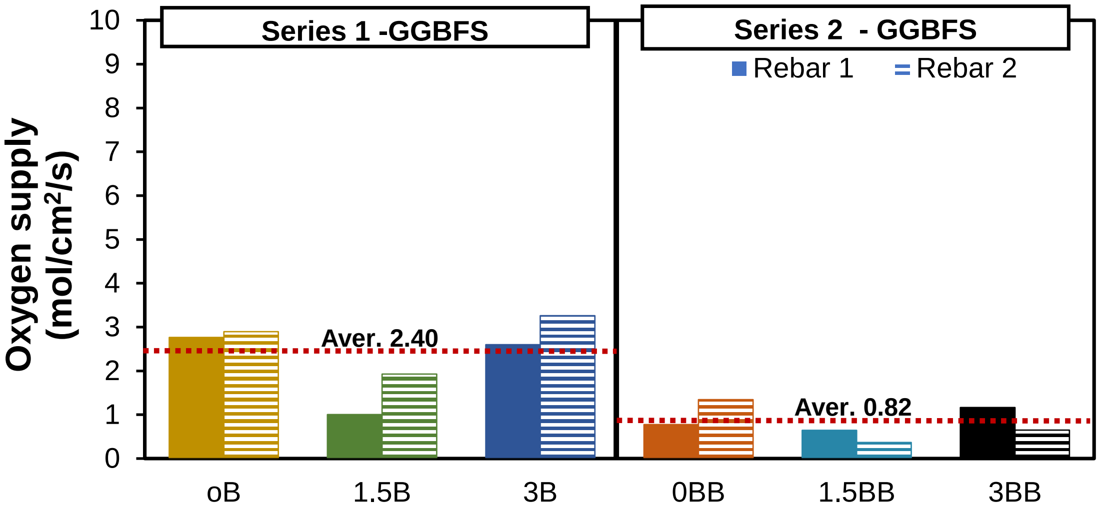

Figure 5.20 Oxygen diffusion for GGBFS specimen Series 1 and Series 2 (10^{-12} cm^2/s)

5.4 CONCLUSION

The effectiveness of calcium nitrite as an admixture in the mortar coating for steel reinforcement was investigated in this research. The results from the electrochemical measurements are summarized as follows:

From the half cell potential, the difference in the level of concentration is observed in the OPC seawater mixed concrete, showing positive performance. In addition, a slight distinction is observed in the OPC coated specimen. Nevertheless, the effect of the CNI nitrite is not observed in the GGBFS specimens (coated and uncoated). Overall, the OPC coated specimen showed the noblest specimen. Then, from the current density results, the performance of mortar coating is displayed. The rate of corrosion is significantly reduced using coating, however, the effect of the concentration of CNI was not observed. Contrariwise, the coated OPC specimen showed the best performance in reducing the corrosion rate. Moreover, the passivity film of all the specimens is in excellent states, as seen from the polarization curve results. The cathodic polarization curve shows that the coating is significantly reducing the diffusion of oxygen in the concrete. This result is in line with the results of the oxygen diffusion measurement as the diffusion of oxygen is reduced by 69% in the OPC specimen and 65.85 % when GGBFS is used. This could be a good technology for a durable concrete as the reduction of oxygen is a key point for the reduction of the rate of corrosion.

On one hand, the quantity of CNI might not have been sufficient to compete with the chloride. If that is the case, the corrosion is not yet initiated, therefore, it cannot be confirmed but the insufficiency of CNI may lead to an increase in corrosion rate. That is because, in the presence of CNI, the ingress of chloride to the depth of the steel reinforcement is relatively higher [Ann and Buenfeld, 2004]. Enough concentration of CNI promotes the formation of a stable ferric oxide film on the steel and restrains the ingress of aggressive agents which react with the ferrous ions of the steel. Therefore, an increase in the concentration of CNI could be more likely to bring a more prominent result, while making sure not to alter the long-term compression strength of the specimen. For instance, a study showed that for a chloride concentration of 3.6 kg/m^3, 10l/m^3 of calcium nitrite (30% solution) should be used [Berke and Hicks, 2004]. On the other hand, calcium nitrite might have not been compatible with the use of GGBFS [Sideris et al., 2005], however, the use of GGBFS as a coating shows good results. On the other hand, some previous research showed that in some cases, especially in the case of chloride contaminated concrete, calcium nitrite does not show any effect even after increasing the concentration.

For a better understanding of this research, a long-term investigation is necessary as there is not a sign of corrosion initiation yet in the specimen even after 3 years of exposure.

5.5 REFERENCES

Adiwijaya, A., Hamada, H., Sagawa, Y., and Yamamoto, D., (2017): Influence of Seawater Mixing and Curing on Strength Characteristics and Porosity of Ground Granulated Blast-Furnace Slag Concrete. *IOP Conf. Ser.: Mater. Sci. Eng. 271*

Otsuki, N., (1985): A study of effectiveness of chloride on cor-rosion of steel bar in concrete, Report of Port and Harbor Research Institute, pp.127-134. (in Japanese)

Akashi, T., Yamaji, F., Michikiyo, Y., and Hikada, K., (1965): Fundamental Study on Properies of mortar using Seawater, Cement science and concrete technology, 19, pp. 233-236. (In Japanese)

Al-Amoudi, O. S. B., Maslehuddin, Mohammed, Lashari, A. N., and Almussallam, A. A., (2003): Effectiveness of Corrosion Inhibitor in Contaminated Concrete, Cement & Concrete Composite, 25, pp 439 - 449.

Alhozaraimy, A., Hussain, R. R., and Al-Negheimish A., (2020): Electro-chemical investigation for the effect of rebar source and surface condition on the corrosion rate of reinforced concrete structures under varying corrosive environments", Construction and Building Materials, 244.

Ann, K.Y., and Buenfeld, N.R., (2004): The Influence of Calcium Nitrite on the Initiation of Chloride-induced Corrosion of Steel in Concrete, *Concrete Under Severe Conditions*, Consec,4, pp. 287.

ASTM C876-15, (2015): Standard Test Method for Corrosion Potentials of Uncoated Reinforcing Steel in Concrete, ASTM Int.

Berke, N.S., and Hicks, M.C., (2004): Predicting Long-term Durability of Steel Reinforced Concrete with Calcium Nitrite Corrosion Inhibitor, *Cement and Concrete Composites*, 26, pp. 191-198.

Berke, N.S., and Weil, T.G., (1992): World-wide Review of Corrosion Inhibitors in Concrete, *Advances in Concrete Technology*, pp. 899-924

CEB, (1998): Strategies for Testing and Assessment of Concrete Structures, Bulletin No. 243, 183 pp.

Elsener, B., (2001): Corrosion of Reinforcement in Concrete: Mechanisms, Monitoring, Inhibitors and Rehabilitation Techniques, EFC 38, *Woodhead Publishing*, Cambridge, UK.

Elsener, B., and Cigna R., (2002): Surface Applied Inhibitors, in COST 521: Corrosion of Steel in Reinforced Concrete Structures, R. Wydert, Ed., *European Cooperation in Science and Technology*, Luxembourg City, Luxemburg.

Faustino, P., Bras, A., and Ripper, T., (2014): Corrosion Inhibitors Effect on Design Service Life of RC Structures, *Construction and Building Materials*, 53, pp. 360–369.

Gaibis, G. M., and Rosenberg, A. M., (1979): The mechanism of Nitrite Inhibitors of Chloride Attack on reinforcing Steel in Alkaline Aqueous Environments, *Materials Performance*, 18, No. 11, pp. 45-48.

Gaidis, J.M., (2004): Chemistry of corrosion inhibitors, *Cement and Concrete Composites*, 26, pp. 181-189.

Hasaba, S., Kawamura, M., and Yamada, Y., (1974): The Properties of Concrete using Seawater, *Proc. Of annual conference of the Japan Society of Civil Engineers*, 29, No. 5, pp. 97-98 (In Japanese)

Hasaba, S., Kawamura, M., Yamada, Y., and Takakuwa, J., (1974): Several Preperties of concrete using seawater as Mixing water, J. of the Society of Materials Science, Japan, 24, No. 260, pp. 425-431.

Hussain, R.R., (2011): Effect of Moisture Variation on Oxygen Consumption Rate of Corroding Steel in Chloride Contaminated Concrete, *Cement and Concrete Composites*, 33, pp. 154-161.

Japanese Industrial standard JIS A 5308 (2019): Ready-mixed Concrete, *Japanese Standard Association* (Translated from Japanese)

Lambert, P., Page, C. L., and Vassie, P.R.W., (1991): Investigation of Reinforcement Corrosion, 2. Electrochemical Monitoring of Steel in Chloride-contaminated Concrete, *Materials and Structures*, 24, No.143, pp. 351-358

Miller, S.A., Horvath, A., Monteiro, P.J.M., (2016): Readily Implementable Techniques can cut annual CO2 emission from the production of concrete by over 20%, Environ. Res. Lett., 11, Article 074029

Miller, S.A., Horvath, A., Monteiro, P.J.M., (2018): Impacts of booming concrete production on water resources worldwide, *Nat. Sustain.*, 1, pp. 69-76

Mohammed, T. U., and Hamada, H., (2003): Relationship Between Free Chloride and Total Chloride in Concrete, Cement and Concrete Research, 33(9), pp. 1487-1490.

Mohammed, T. U., Hamada, H., and Yamaji, T., (2003): Marine Durability of 30-year Old Concrete Made with Different Cements, Journal of Advanced Concrete Technology, 1(1), pp. 63-75.

Mohammed, T. U., Hamada, H., Hasnat, A., and Manum, M. A., (2015): Corrosion of Steel Bars on Concrete with the Variation of Microstructure of Steel-Concrete Interface, *Journal of Advanced Concrete Technology*, 13, pp. 230-240.

Nagataki, S., Otsuki, N., Moriwake, A., and Miyazato, S., (1996): Experimental Study on Corrosion Mechanism of Reinforced Concrete at Local Part, *Journal of Materials, Concrete Structures and pavement*, n. 544, pp. 109-119 (in Japanese).

Neville, A., (2001): Seawater in the mixture, *Concrete Int*., 2, No. 1

Otsuki, N., Hamada, H., Takeda, N., Imamoto, K., Yamaji, T., Habuchi, T., and Nishida, T., (2014): Technical Committee on the Use of Seawater in Concrete, *Technical Committee Reports 2014* – JCI-TC121A Digest Edition.

Otsuki, N., Nishida, T., and Madlangbayan, (2007): Considerations on the threshold Chloride Content Values on the Corrosion of Steel Bars in Concrete, Proc. Of the 32nd conference on our world in concrete and structures, Singapore.

Page, C. L., Ngala, V.T., and Page, M. N., (2000): Corrosion Inhibitors in Concrete Repair Systems, *Magazine of concrete research*, 52, No. 1, pp. 25 - 37

Raupach, M., (1996): Investigations on the Influence of Oxygen on Corrosion of Steel in Concrete - Part I, Materials Structures, 29, pp. 174-184.

Shi, X., Yang, Z., Nguyen,T. A., Suo, Z., Avci, R., and Song, S., (2009): An Electrochemical and Microstructural Characterization of Steel in Mortar Admixed with Corrosion Inhibitors, *Science in China Series E: Technological Sciences*, 52, no. 1, pp. 52–66, 2009.

Sideris, K. K., and Savva, A.E., (2005): Durability of mixtures containing Calcium Nitrite Based Corrosion Inhibitor, Cement and Concrete Composites, 27, pp. 277-287.

Takumi, H., (2018): II. Fundamental Electrochemical Methods for Corrosion - *Corrosion Potential –, Zairyo to Kankyo*, 67, No. 1, pp. 2-8. (in Japanese)

TB-0909, (2021): GCP applied Technologie.

Tuutti, K., (1982): Corrosion of steel in concrete, report No. 4, *Swedish Cement and Concrete Research Institute*, Stockholm.

CHAPTER VI

REPAIR METHOD OF SEVERELY DAMAGED REINFORCED CONCRETE BEAMS USING SACRIFICIAL ANODE CATHODIC PROTECTION (SACP)

6.1. INTRODUCTION

Many decades ago, the technology of cathodic protection has been applied to halt the corrosion of steel reinforcement in concrete structures. Studies have shown that cathodic protection is the most effective technology able to control the corrosion of steel reinforcement at any amount of chloride in concrete [Broommfield, 1992; Bertolini et al., 1993; Parthinan et al., 2007]. The process of application of cathodic protection consists of imposing a current on the surface of reinforcing steel. Next, the section of the steel that is protected becomes the cathode. Therefore, by preventing the transfer of electrons on the surface of the steel, the corrosion process is effectively stopped [Goyal et al., 2019].

Two distinguished types of cathodic protection technology have been established over the last several decades, namely: Sacrificial Anode Cathodic Protection (SACP) and Impressed Current Protection (ICP). Both technologies are proven to be effective for the protection of steel in marine environment. The use of sacrificial anode in cathodic protection has become a common practice around the world. Unlike ICP method, SACP is suitable in small corrosion protection range. However, an advantage of SACP is first that it does not require external power, therefore, the occurrence of overprotection and hydrogen embrittlement of steel is rare unlike in ICP [Zhang et al., 2018; Yan et al., 2019]. Besides, the current density applied to the protection of steel in SACP (0.58 to 1.6 mA/m^2 of the concrete surface [Bertolini et al., 2002]) is usually far lower. In addition, SACP is known to be easy in handling with a good price-performance ratio. Among galvanize cathodic protection for concrete structures, Zinc-based anodes are well known to be a conventional material. Studies showed that zinc alloy shows good electrochemical stability and performance as a sacrificial anode [Wang et al., 2020]. By applying zinc sacrificial anode cathodic protection and corrosion inhibitor, the effectiveness of repair method on severely damaged reinforced concrete beams is investigated in this study.

6.2. TEST PROGRAMS

6.2.1 Specimen Materials

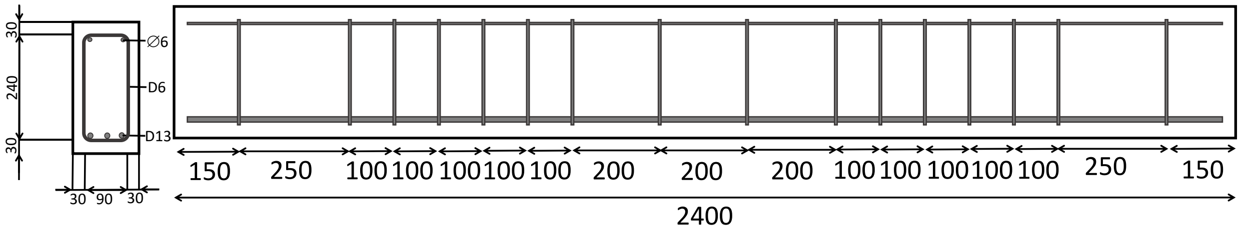

Figure 6.1 Outline of the beam

The corrosion of 2 reinforced concrete beams with a dimension of 150mm x 300mm x 2400mm is monitored in this study. The details of the beams are shown in Figure 1. Table 1 details the proprieties of the aggregates used for the mixing. Ordinary Portland cement (OPC) was used as a binder. The proprieties of the material are identic to the proprieties mentioned by Dasar et.al 2017. The beams consist of three round tensile rebar with a diameter of 13mm and a tensile strength of 363 MPa. Round steel bar of a diameter of 6 mm was used for the compressive rebars and the stirrups. The spacing of the stirrups is shown in Figure 1 as well.

Table 6.1 Properties of aggregates

Aggregate	Specific gravity	Fineness modulus
Fine river sand	2.25	2.84
Coarse-Crushed stone	2.75	6.63

Table 6.2 Mix proportion of existing concrete

MSA	Slump	Air	w/c	s/a	Unit weight [mm]				
[mm]	[mm]	[mm]	[mm]	[mm]	W	C	S	G	Adm.
20	12±2	4±1	68	47	204	300	793	964	1.2

6.2.2 Exposure conditions

The exposure conditions of the beams during their service life are presented in Figure 6.2. The beams were cast in 1974, then they were moisture-cured for a day, and demolded before they were air-cured. From 1975 to 1995, the beams were exposed to natural marine environment at the Sakata Port, Japan.

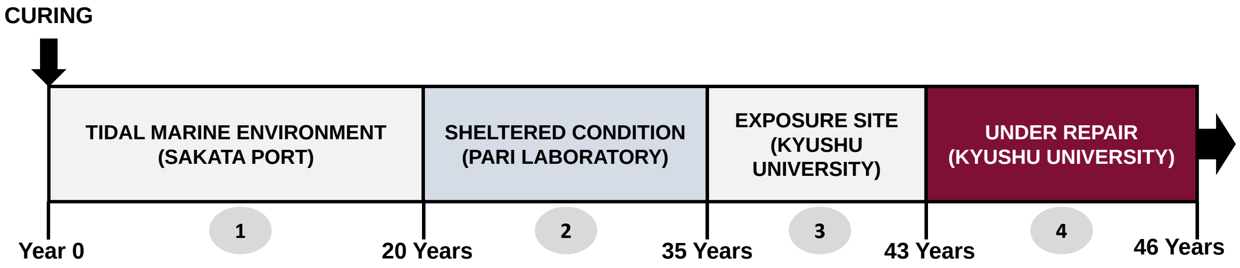

Figure 6.2 Exposure outline of the specimen

(1) (2) (3)

Figure 6.3 Exposure situation of the beams [(1) Sakata port; (2) PARI Laboratory; (3) Kyushu University]

From 1995-2010, they were sheltered at the Port and Airport Research Institute laboratory (PARI), Yokosuka, Japan [Hamada et al., 1988; Yokota et al., 1999]. The specimens were moved to Kyushu University exposure site from 2010. The repair was implemented from 2018 and being monitored. This chapter presents the data until Mai 2021.

6.2.3 Pre-repair investigation

The preliminary work and the 2 first years of monitoring of this experiment are reported in the thesis of Dr. Astuti, 2020. Investigations about the quality and the appearance of the concrete were performed prior to the repair. The ultrasonic velocity tests were performed, and the quality of the concrete was determined as per the ASTM standard [ASTM C597; 2002]. The quality of the concrete was classified as “good quality” as the UPV results for the two beams were in the range of 4000-5000 m/s. Rebound Hammer test was performed to estimate the compressive strength of the beams. From the results, the average compressive strength of the beams after 44 years was estimated to be on average equal to 34 MPa.

6.2.4 Previous work and RC condition before repair

6.2.4.1 Appearance investigation

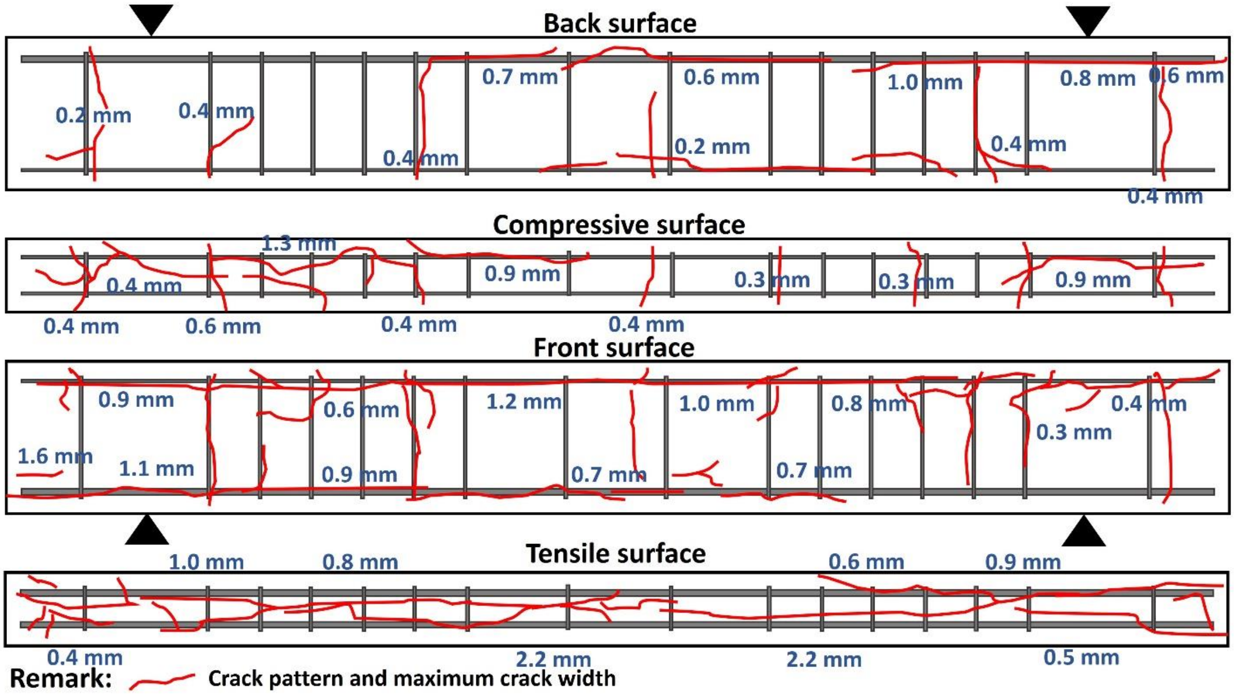

Figure 6.4: Crack pattern of beam RC3

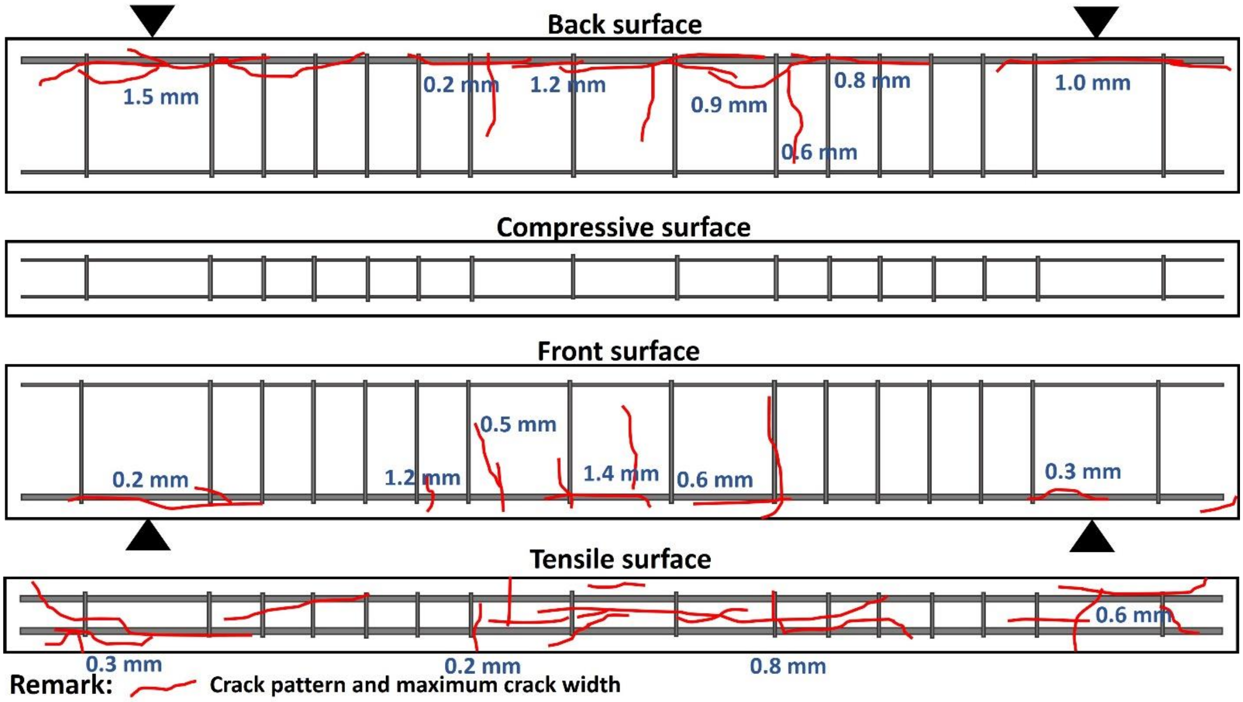

Figure 6.5: Crack pattern of beam RC4

Cracks were observed on the fours sides of both beams RC3, whereas no crack was detected on the compressive side of RC4, as represented in *Figre 6.4* and *Figure 6.5*. Transversale cracks and longitudinal cracks parallele to the tensile and compressive rebars were found on the rebars. Maximal cracks of 2.2 mm was found in RC3 and 1.5 mm for RC4 with some air bubbles of 1 to 17mm of diameters. The beam RC3 was judged to be in the worst condition [Astuti et al., 2018].

Figre 6.6 and *Figure 6.7* shows the condition before repair of RC3 and RC4, respectively. The zone in '90% corrosion' for RC3 and RC4 is very similar; with 20% for RC3 and 21% for RC4. However, the zone included in -200mV and -300mV is larger in RC4 compared to RC3. From, the potential mapping the condition of the beams are considered similar with slightly better condition in RC4.

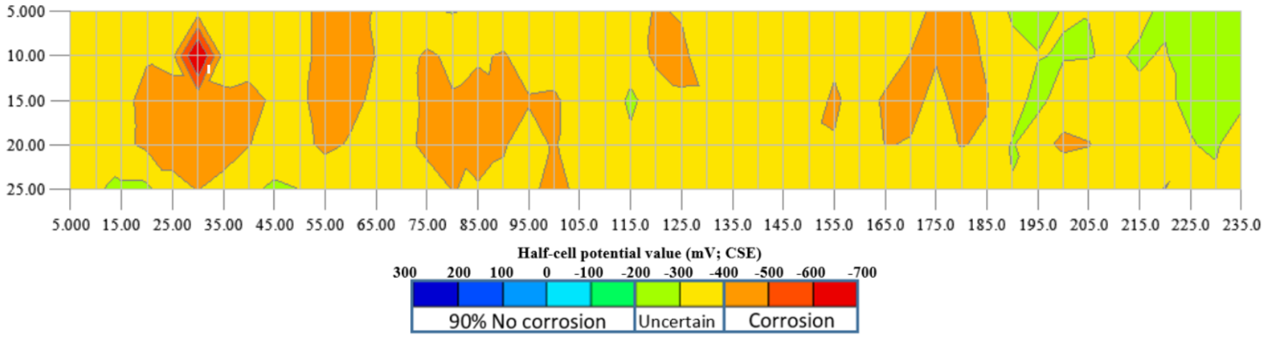

Figure 6.6: Corrosion map of RC3 before repair

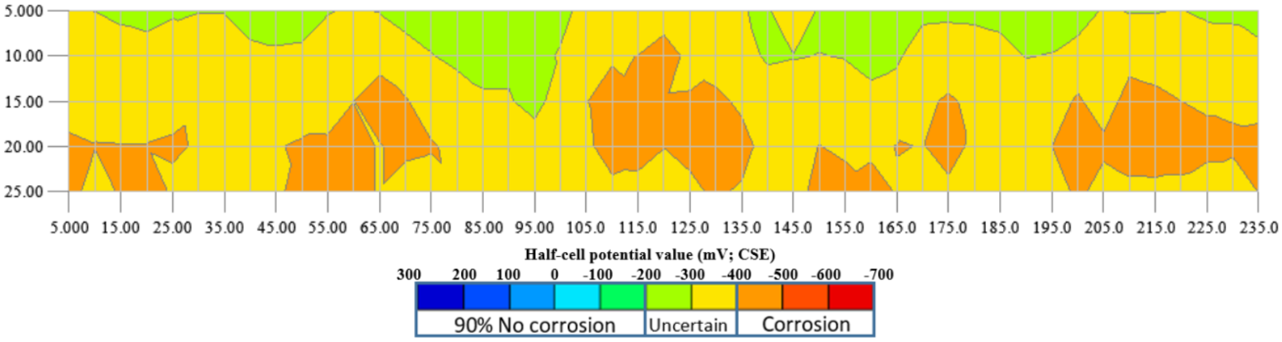

Figure 6.7: Corrosion map of RC4 before repair

6.2.4.2 Repair method

From the outcomes of the primary work, cracks formed on the tensile side of the specimen, and the condition of the specimen was judged to be at high risk. Therefore, patching method with corrosion inhibitor and sacrificial anode was used to mitigate the corrosion in the beams. Two kinds of measures were applied:

- Sacrificial anode cathodic protection in the non-patch repair (RC3) (Figure 6.3)
- Sacrificial anode cathodic protection in the non-patch repair and corrosion inhibitor in the patch repair (RC4) (Figure 6.4)

Polymer mortar was used at the tensile side of the beams and Vinyl Acetone/ Ethylene copolymer emulsion as an adhesive material coating between the parent concrete and the patch repair. Cylindrical ribbed sacrificial anode with a diameter of 30mm and 139 mm of height was placed in the non-repair area and LiOH cementitious coating was applied as a protection of the anode [Rincon et al, 2008]. The anode was placed at 0.38 m from each other. Literature showed that a spacing of 0.45m is sufficient to protect corroding steel in any exposure conditions [Redaelli, 2014]. For RC4, modified epoxy paint was applied as a corrosion inhibitor on the surface of the rebar after rust removal.

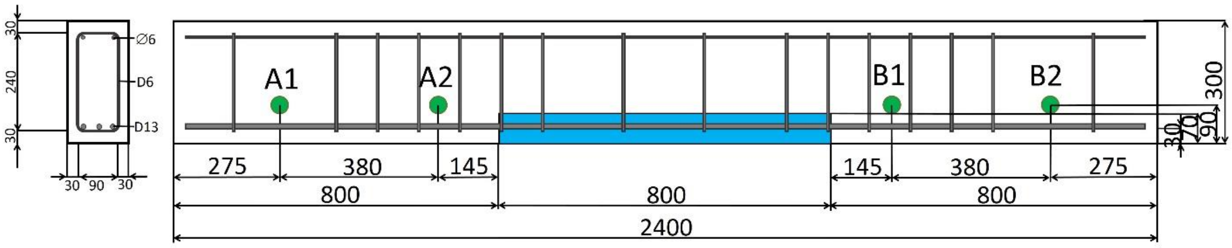

Figure 6.8: Repair design of the specimen with sacrificial anode (RC3)

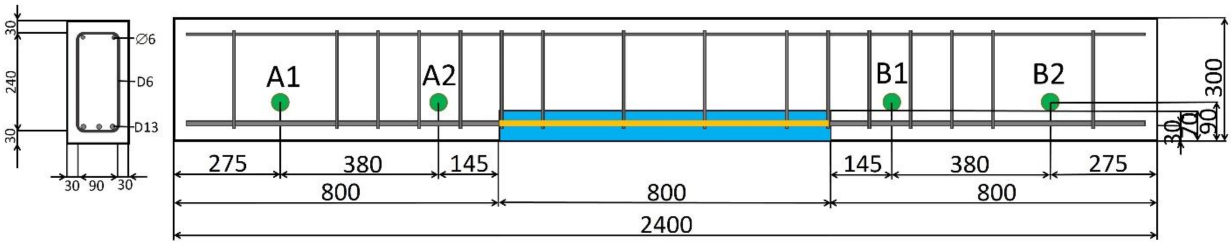

Figure 6.9 Repair design of the specimen with inhibitor and sacrificial anode (RC4)

Figure 6.10 (a) Ribbed cylindrical SACP; (b) Modified polymer mortar

6.2.5 Measurement method

Half-cell potential: The potential of the rebars and the sacrificial anodes were monitored using the half-cell potential method as per the ASTM C876-15 [ASTM C876, 2015]. Like in the previous chapters, high impedance voltmeter and saturated calomel reference electrode (SCE, Ag/AgCl) were used during the experiment. Corrosion maps were drawn after qualitative comparison to the ASTM C876 corrosion probability.

Depolarization (*figure 6.11*) was measured to assess the performance of the cathodic protection. 100 mV potential decay was used as a criterion to assess the effectiveness of the method. The half-cell potential of the rebar and the anodes were measured in 3 steps:

- Potential (E_{on}): measurement under protection.
- Instant off potential (E_{ioff}): measurement immediately after disconnection.
- Rest potential (E_{rest}): measurement after 24 hours reconnection.

Protective current density. The current density ($\mu A/m^2$), the current flow generated by the sacrificial anode (μ) per surface of the steel bar (m^2), was measured using a high impedance ammeter. The British standard threshold 0.2 $\mu A/m^2$ was used as a minimum current flow generated by the sacrificial anode [BS EN 1504; 2005]. The current flow was measured immediately after switching off the connection.

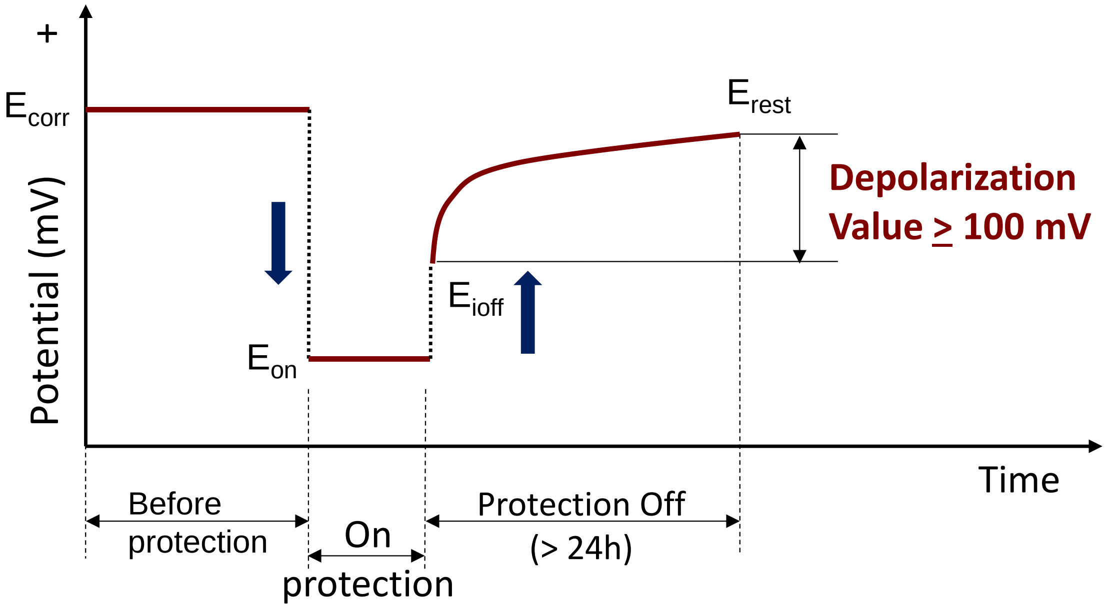

Figure 6.11 Schematic of the depolarization method.

Corrosion current density was measured using a portable corrosion meter and the Stern-Geary formula was used to calculate the corrosion current density (I_{corr}) [Stern and Geary, 1957; Andrade and Gonzalez, 1978]. And the current density was compared to the CEB standard as seen in the previous chapter [CEB standard; 1998].

$$I_{corr} = \frac{B}{R_P} . 10^6$$

- I_{corr}: corrosion current density(µA/m^2)
- Rp: polarization resistance (Ω.cm^2)
- B: constant (B= 26V in active corrosion)

Anodic-cathodic polarization curve. The state of the passivity film and the diffusion of oxygen were determined using the method developed by Otsuki et al. [Otsuki et al., 1985]. The potential was measured at a range of corrosion of ±700mV from the initial potential at a rate of 50mV/min.

6.3. TEST RESULTS

6.3.1 Potential development of the steel bar

Figure 6.12 and *Figure 6.13* illustrate the development of the corrosion in RC3 and RC4. In the first month of measurements, some areas of the beams show potential under -600mV. Previous studies showed that corrosion could be mitigated when it shows a potential less than -600mV to -705mV [Takewaka, 1993; Shi et al., 2011]. With time, the area under -400 mV has gradually decreased. At 37 months, the corrosion in RC3 is classified as “Uncertain” corrosion. For RC4, the area under -300mV has almost disappeared. The potential gradient is progressively disappearing. Overall, RC4 shows better results than RC3, which can be attributed to the application of inhibitor in the patch repair of RC4.

With regard to the depolarization, the concrete in the patch repair area of RC3 is no longer under protection after 37 months of application, while the parent concrete surrounding the anode is still under protection. However, all the surfaces of RC4 are still under protection with higher protection surrounding the anodes.

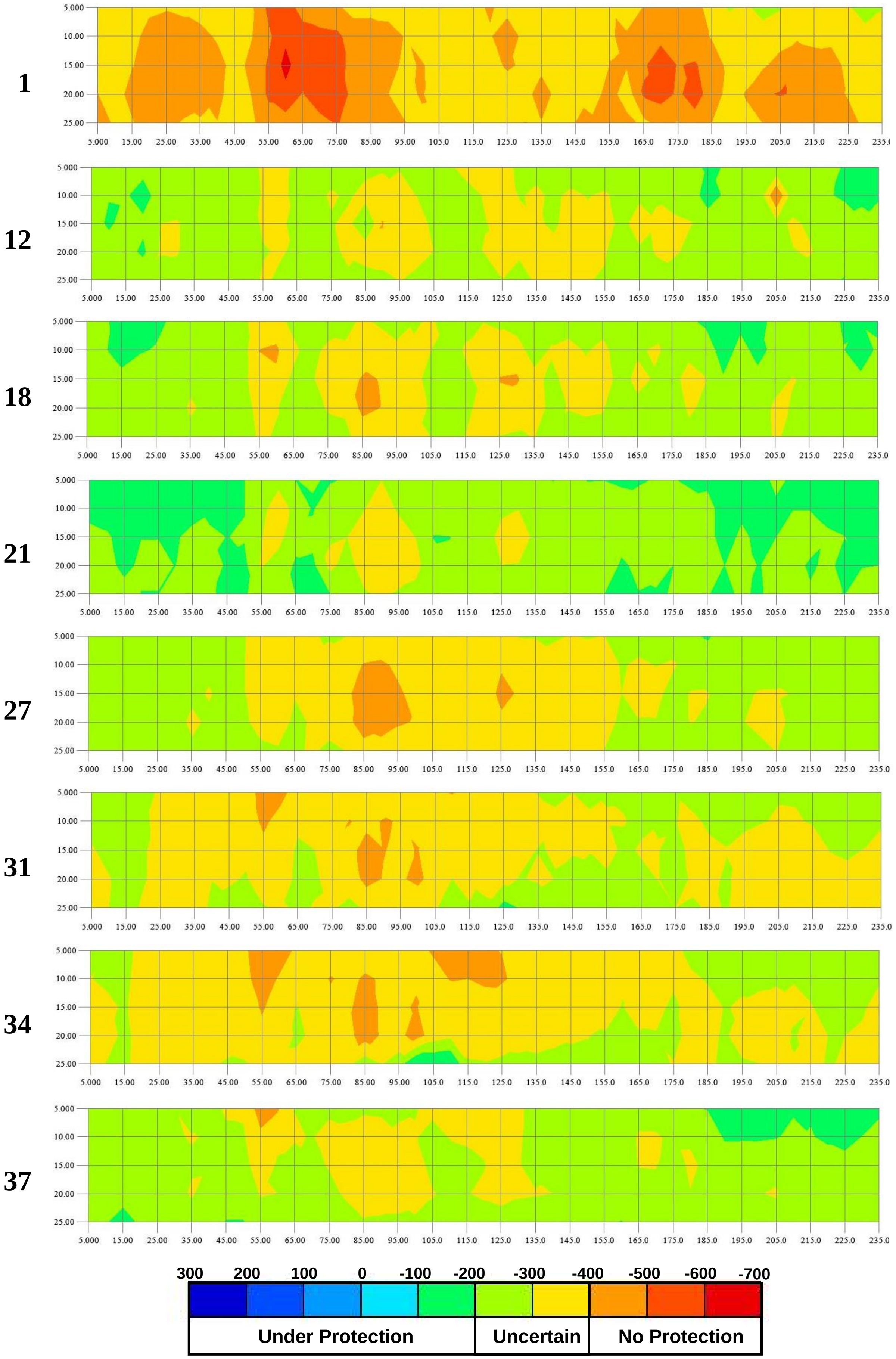

Figure 6.12: Corrosion development map during repair of RC3

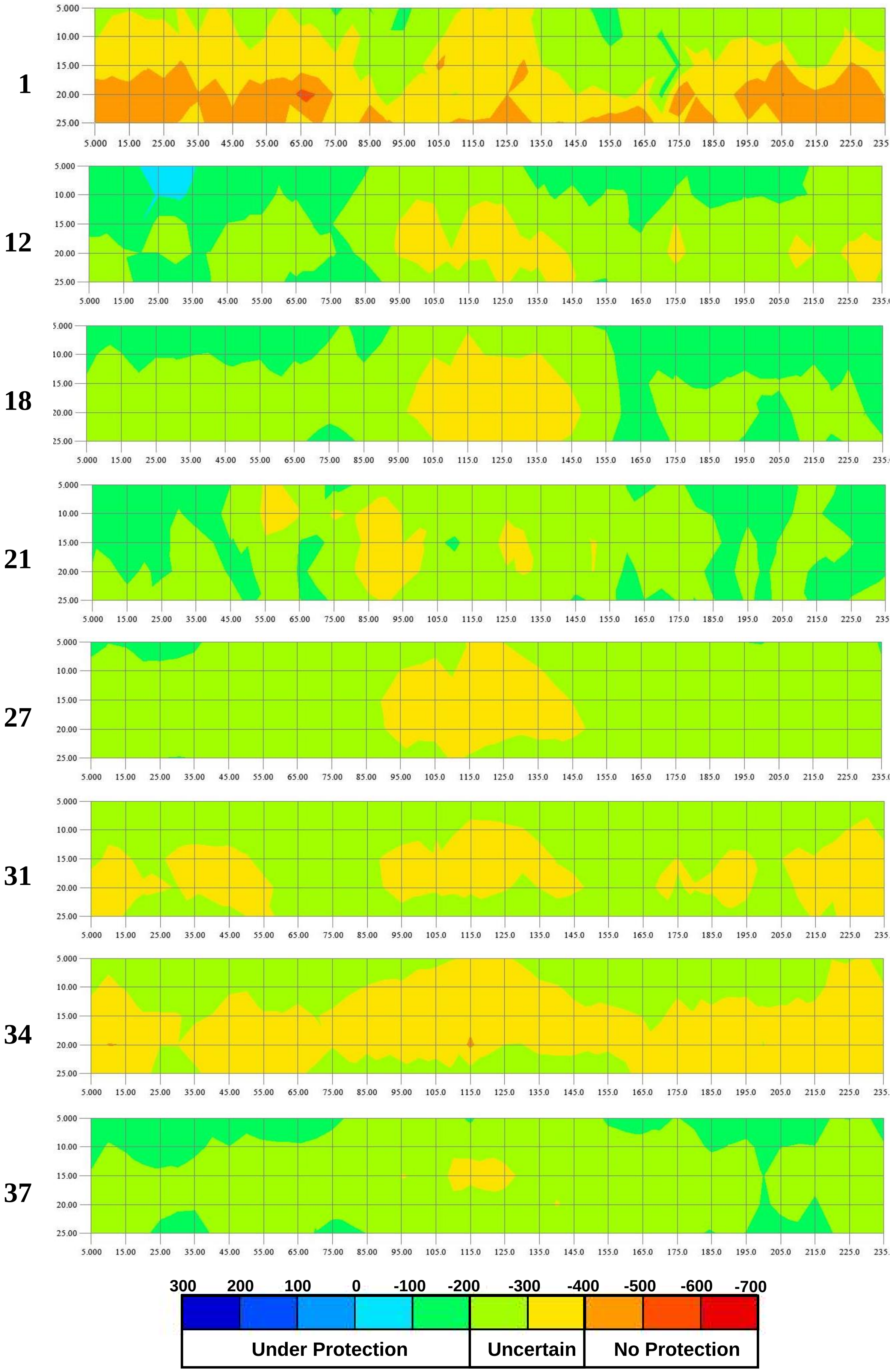

Figure 6.13: Corrosion development map during repair process of RC4

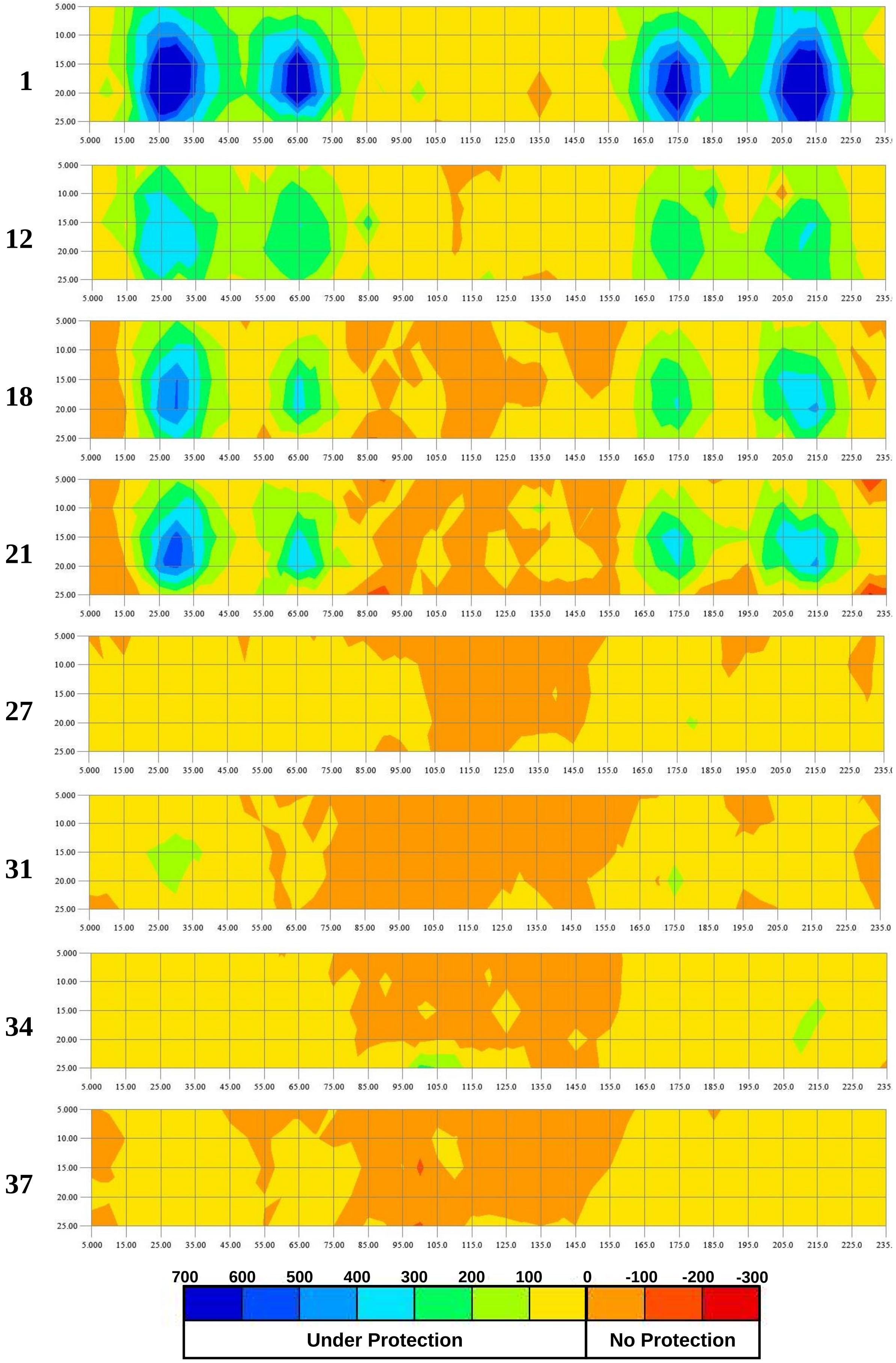

Figure 6.14: Depolarization development mapping of RC3

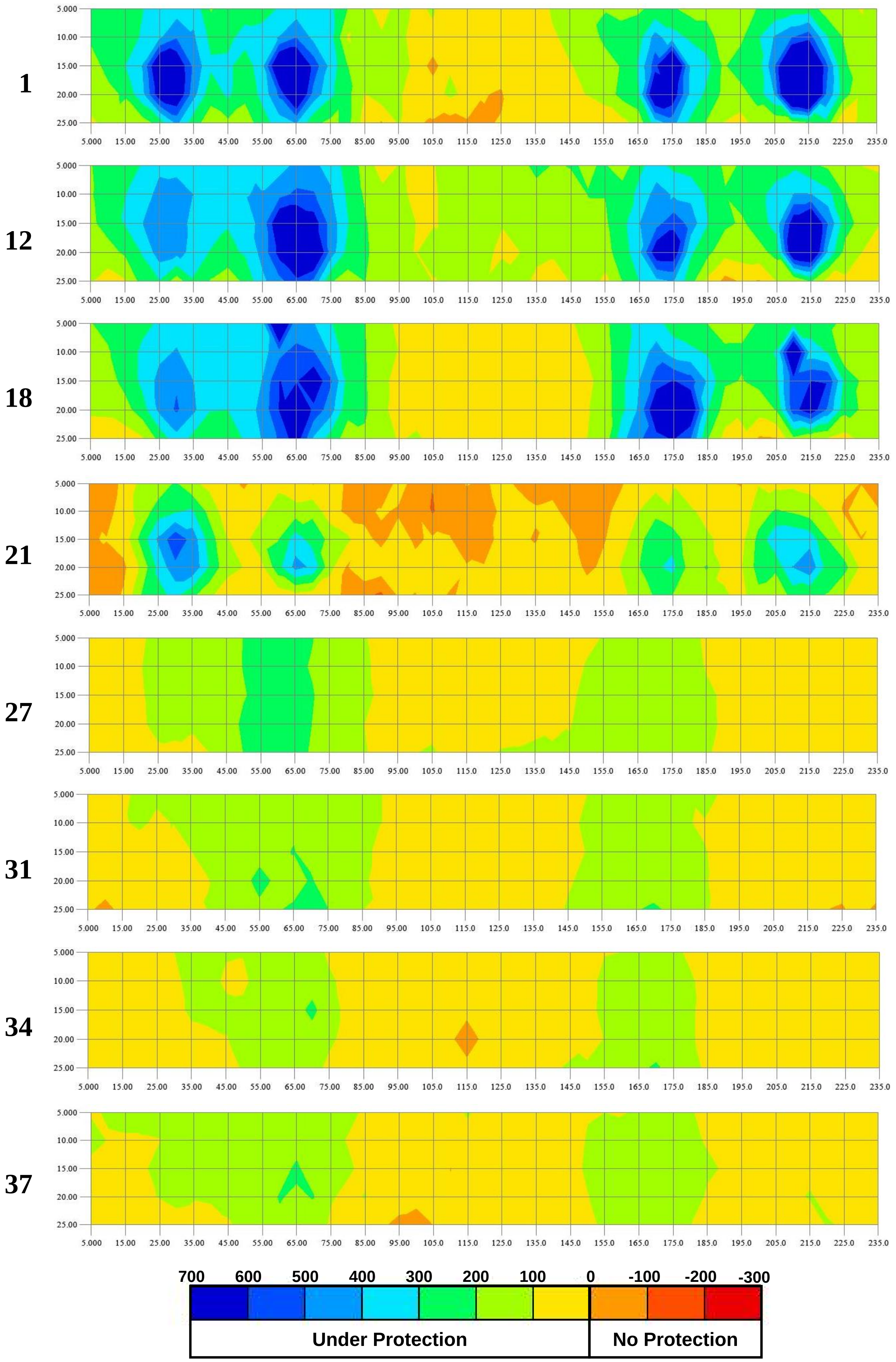

Figure 6.15: Mapping of the development of the depolarization of RC4

To monitor the effectiveness of the sacrificial anode cathodic protection, the potential of the rebar under connection, the instant-off potential, and the depolarization of the rebar were measured. The potentials were monitored *Figure 6.16* and *Figure 6.17* show the time-dependent improvement of the instant of potential of the rebar. From the first month of the application of the sacrificial anodes, the potential shows a significantly low value, particularly in the anodes (-600mV to -1000mV). The EN ISO 12696 standards specify that the E_{ioff} should be higher than -1100mv to avoid the occurrence of oxygen embrittlement in the concrete. Therefore, both beams meet the requirement.

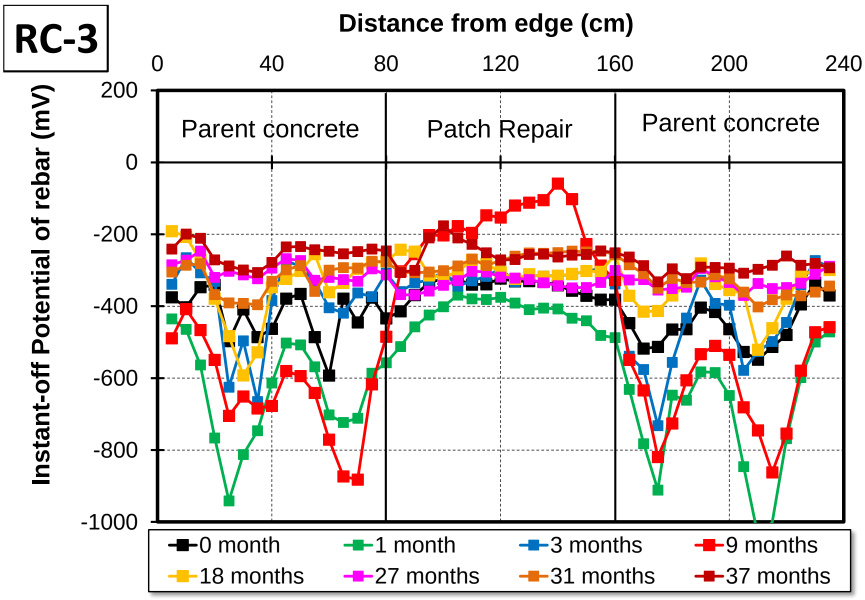

Figure 6.16: Instant-off of rebar (RC 3)

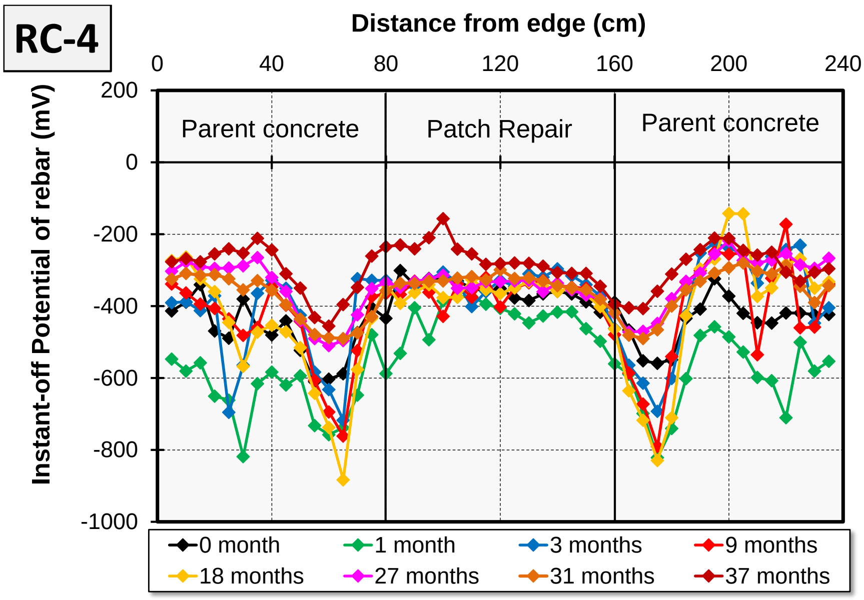

Figure 6.17: Instant-off of rebar (RC 4)

The patch repair shows a higher value of potential with of potential of about -400 mV. Especially in RC4, the potential of some sections of the rebar has reached the -200mV (zone of 90% no corrosion). In RC3, the potential has significantly increased after 37 months of exposure however it is still classified in the zone of “uncertain” corrosion. With time, the potential of the rebar becomes constant along the rebars. One of the purposes of the cathodic protection is to reduce the potential gradient [NACE; 2000], therefore the method can be concluded as effective until now.

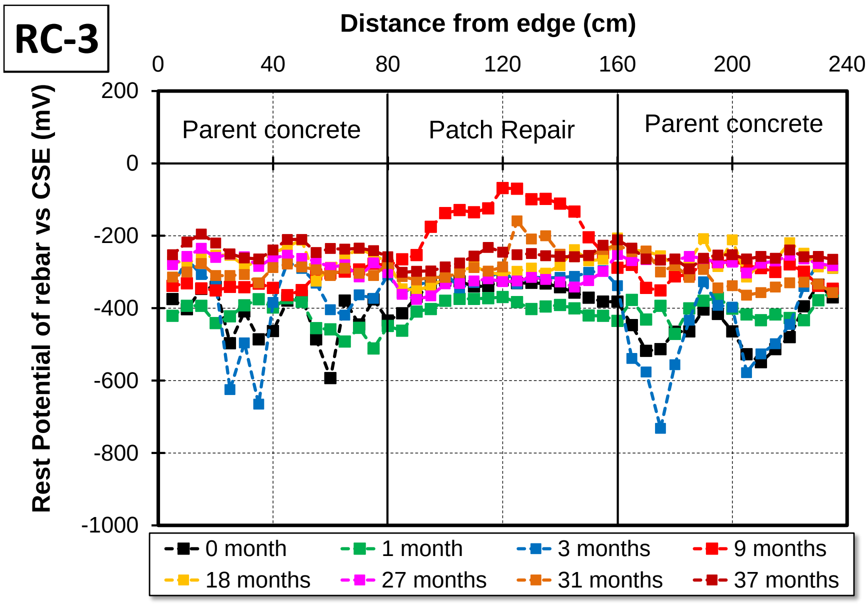

Figure 6.18: Rest potential of the rebar (RC3)

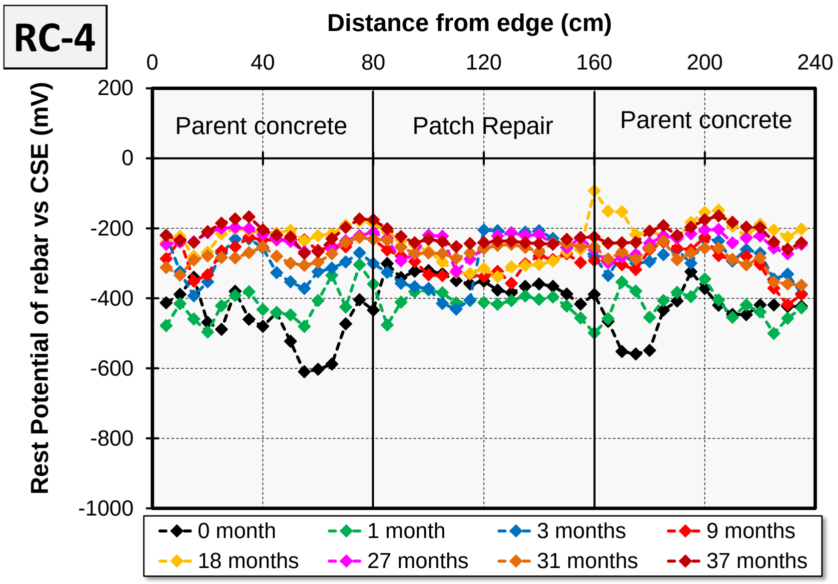

Figure 6.19: Rest potential of the rebar (RC4)

The depolarization of the rebar has significantly exceeded the -100mV criterion, however, its effect has decreased with time. At 37 months, the depolarization in RC3 has drastically decreased with some negative value at the patch repair area (Figure 6.14). The RC4 is slightly higher (Figure 6.15). The effectiveness of the method is observed from the potential monitoring however, it is difficult to reach the 100mV criterion along all the surfaces of the rebar.

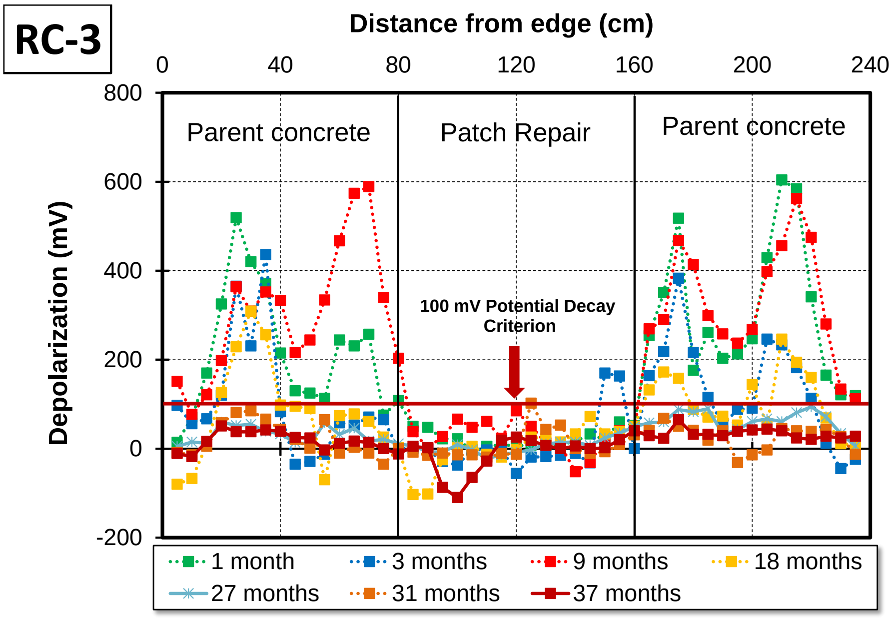

Figure 6.20: Depolarization of the rebar (RC3)

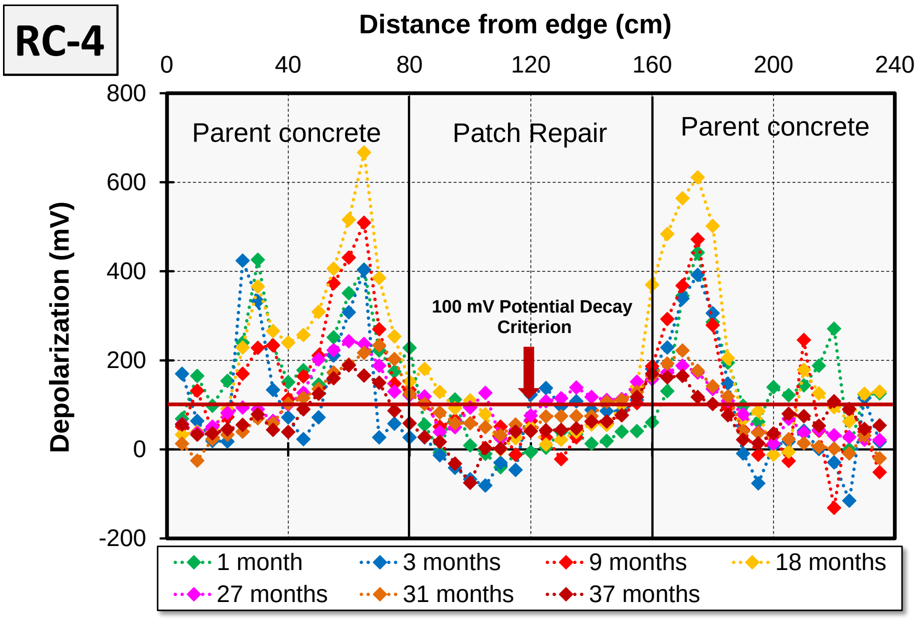

Figure 6.21: Depolarization of the rebar (RC4)

6.3.2 Anodic-cathodic polarization curve

The passivity grade of the rebar was monitored using polarization curve method. The result was qualitatively compared to the classification of Otsuki [Otsuki, 1985]. Figure 6.22 illustrates the change in the anodic-cathodic polarization curve of the tensile rebar of RC3 at 80cm (at the boundary) and 120 cm (patch repair area) from the edge.

Figure 6.23 shows the results from the measurement of RC4. The results of the passivity grade are summarized in *Figure 6.24*, *Figure 6.25*, *Figure 6.25*, and *Figure 6.27*. It shows that the treatment did not have a substantial effect on the passivity state of the compression steel (RC3). The grade remained at grade 2 and 3 (presence of a slight passivity film). In the tensile side however, the grade of passivity has moved from grade 2 to grade 3 (at the boundary) and grade 4 at the patch repair area, which shows the presence of certain to good passivity.

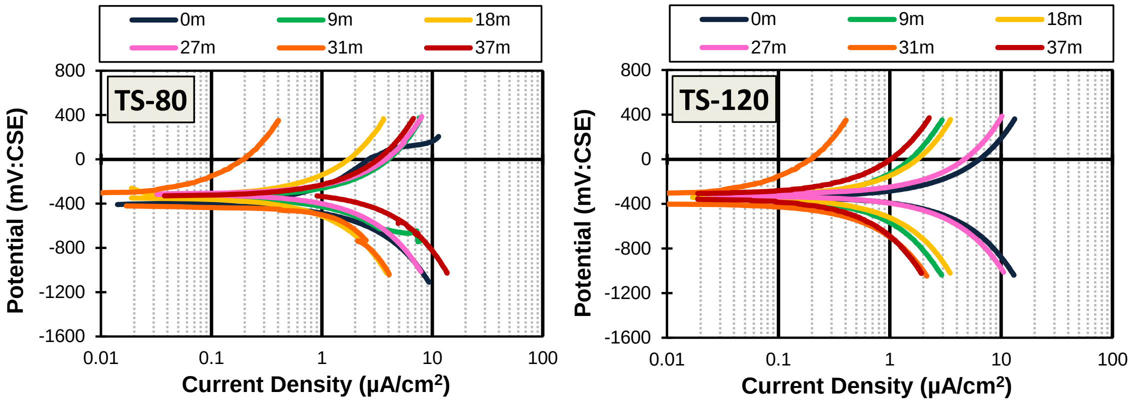

Figure 6.0.22: Anodic-cathodic polarization of the tensile side of RC3

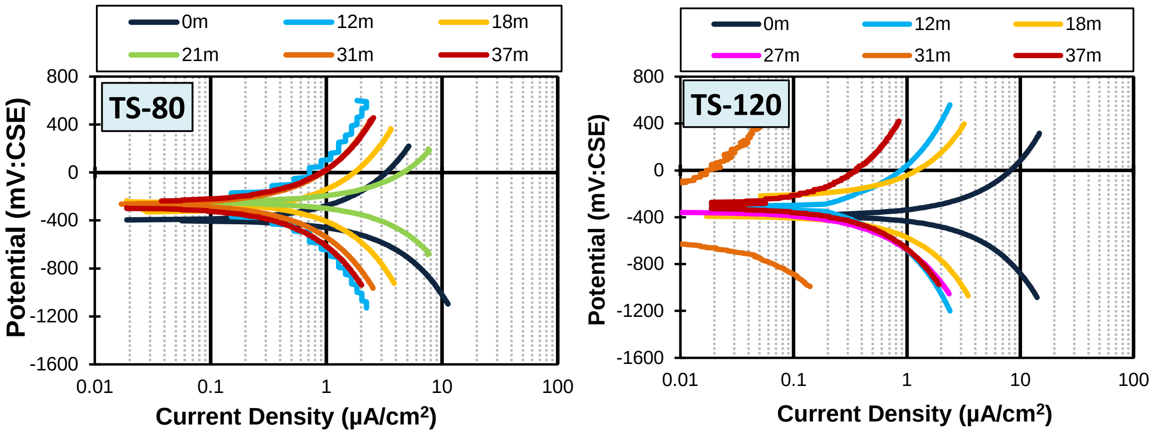

Figure 6.0.23: Anodic-cathodic polarization of the tensile side of RC4

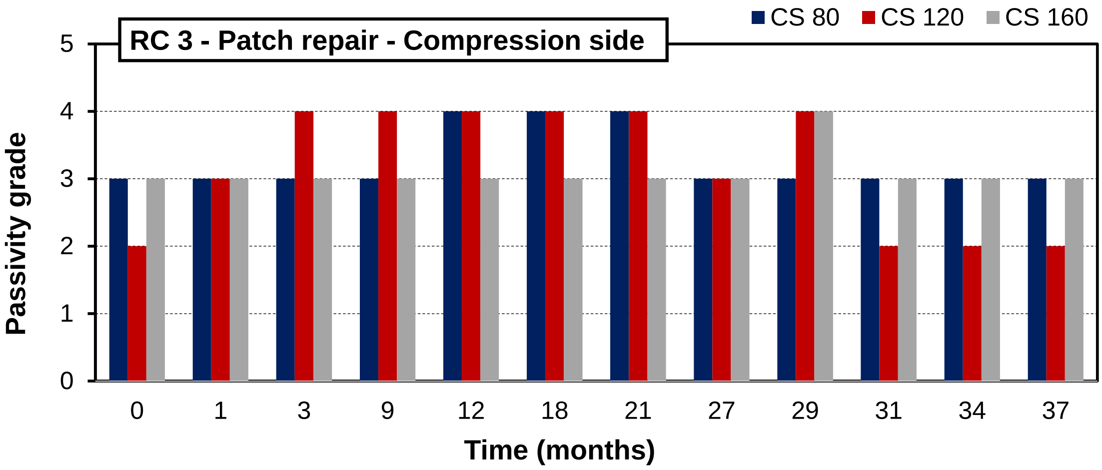

Figure 6.24: Development of the passivity film in the compressive steel (RC3)

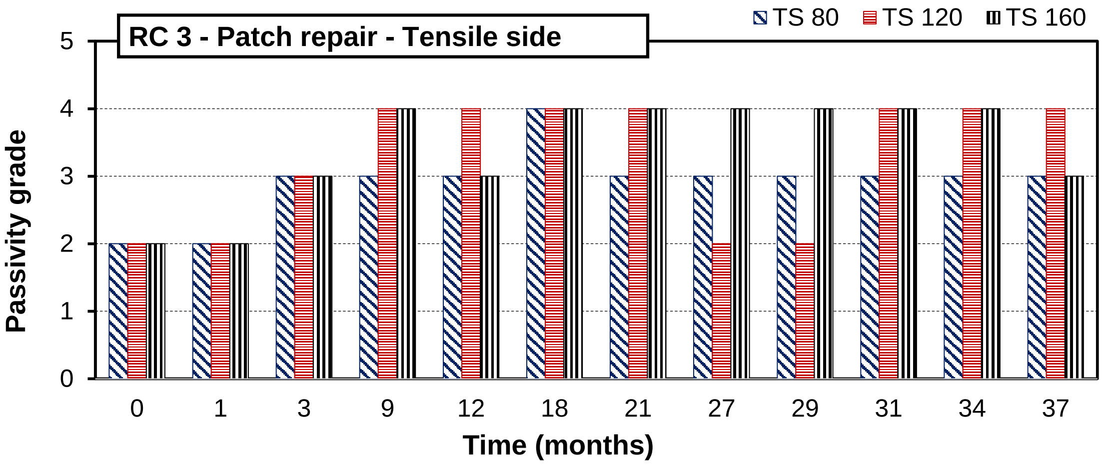

Figure 6.25 Development of the passivity film in the tensile steel (RC3)

Concerning the anodic and cathodic of beam RC4, the grade of passivity was 4 (presence of good passivity film) since the starting of the repair. A slight decrease was recorded around the 9 and 18 months, however, it recovered afterward and was maintained until the 37th month. In the 9 first month, the tensile rebar of RC4 was in grade 2 (presence of some passivity film) and gradually recovered. In the 37th month, the tensile steel of RC4 presents good to excellent passivity film (grade 4 to grade 5). It is distinguished as well that the diffusion of oxygen is recovering with the grade of passivity of the steel. Similarly, to the results shown from the half-cell potential measurement, RC4 shows better results.

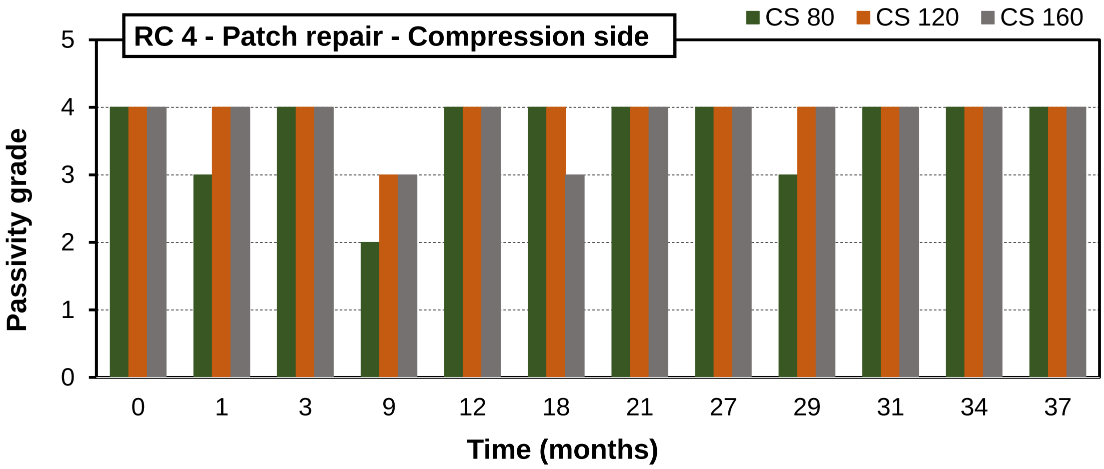

Figure 6.26: Development of the passivity film in the compressive steel (RC4)

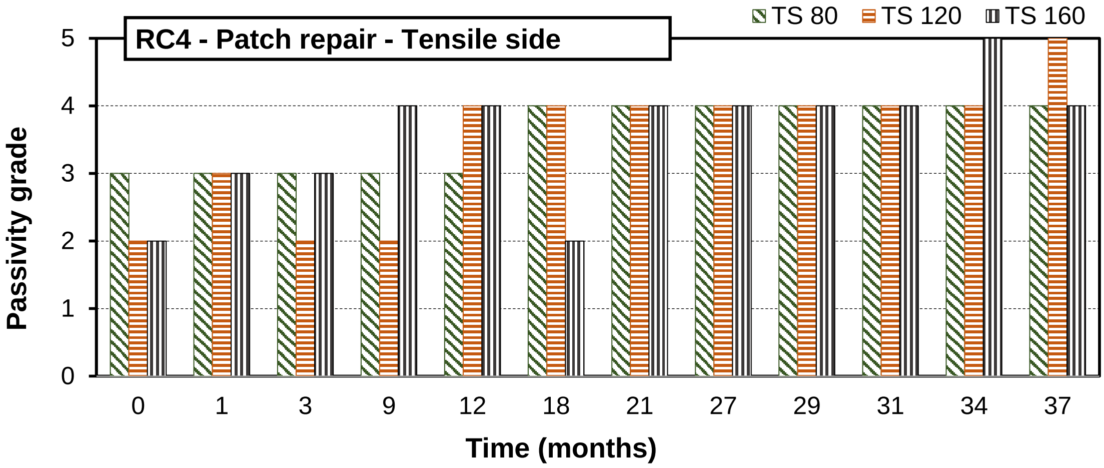

Figure 6.27: Development of the passivity film in the tensile steel (RC4)

6.3.3 Corrosion current density

The corrosion current density of the rebar in the parent concrete, the boundary, and the patch repair are recorded in *Figure 6.28* and Figure *6.29*. The current densities of the concrete are beyond the criterion until the 9 months and moved to the passive corrosion zone until the 21rst month. At the 37 months, the current density of the steel in the patch repair for both beams are in a passivity state and the steels in the boundary of the repair and the parent concrete have slightly higher though it is still under the corrosion current density of passivity (0.2µA/cm^2) per the CEB standard [CEB, 1998].

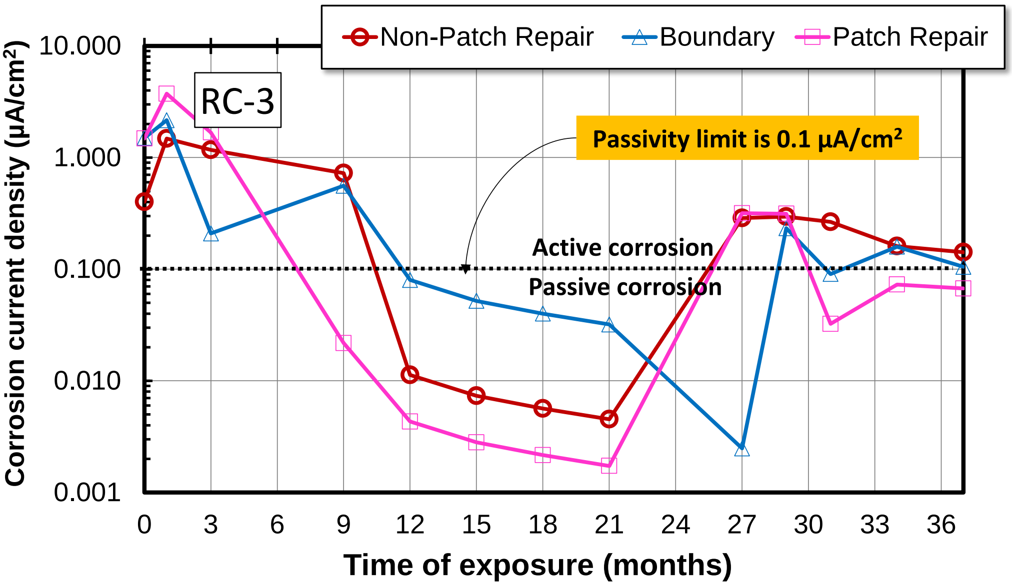

Figure 6.28: Current density of the tensile rebar (RC3)

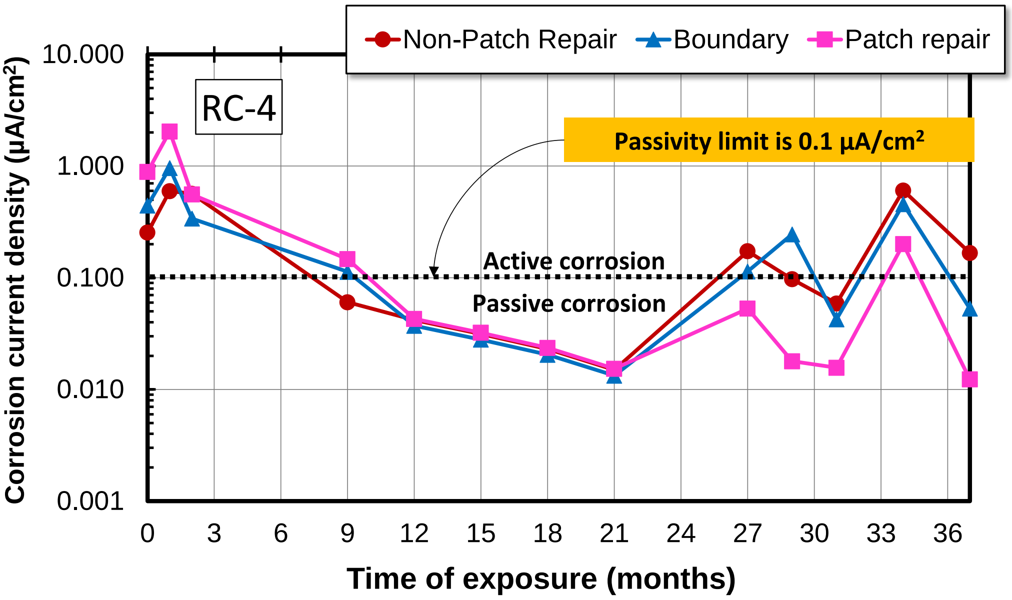

Figure 6.29: Current density of the tensile rebar (RC4)

6.3.4 Protective current density

Figure 6.30 and Figure 3.31 show the time dependent change in the protective current density of the anode in RC3 and RC4. Previous data about this result was published by Astuti et al. [Astuti et a., 2018, Astuti et a., 2019b]. The protective densities were monitored for each specimen. The British standard ISO 12696 limits the current density for cathodic protection in chloride contaminated concrete from 2mA/m^2 to 20mA/m^2 [ISO 12696, 2016; Bertolini et al., 2013].

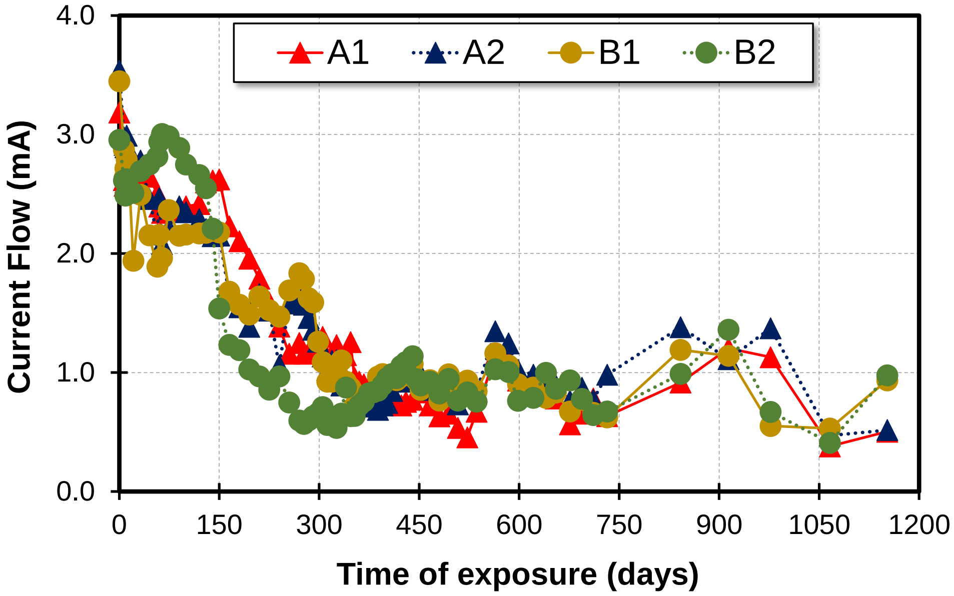

Figure 6.30: Current flow of sacrificial anode (RC3)

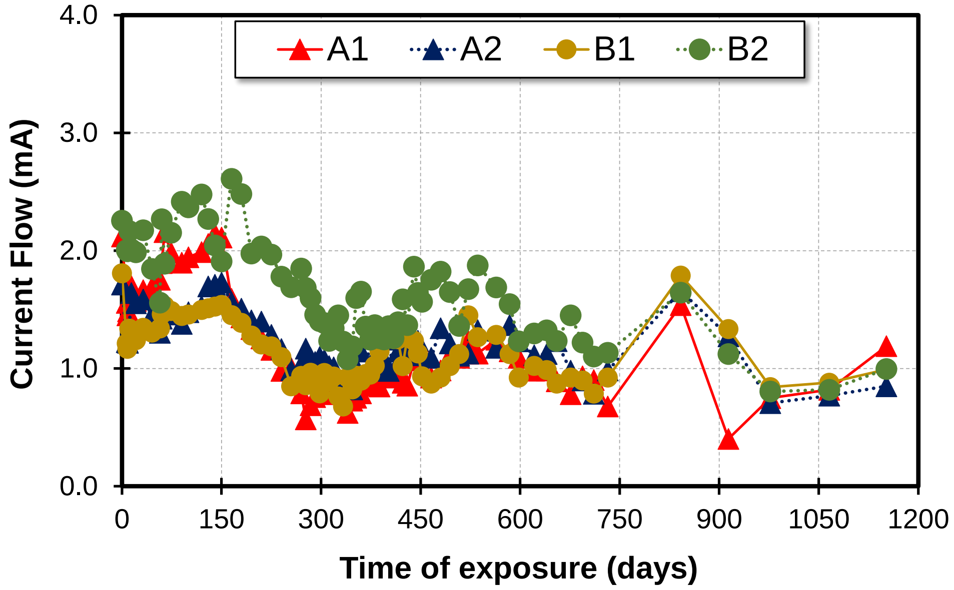

Figure 6.31: Current flow of sacrificial anode (RC4)

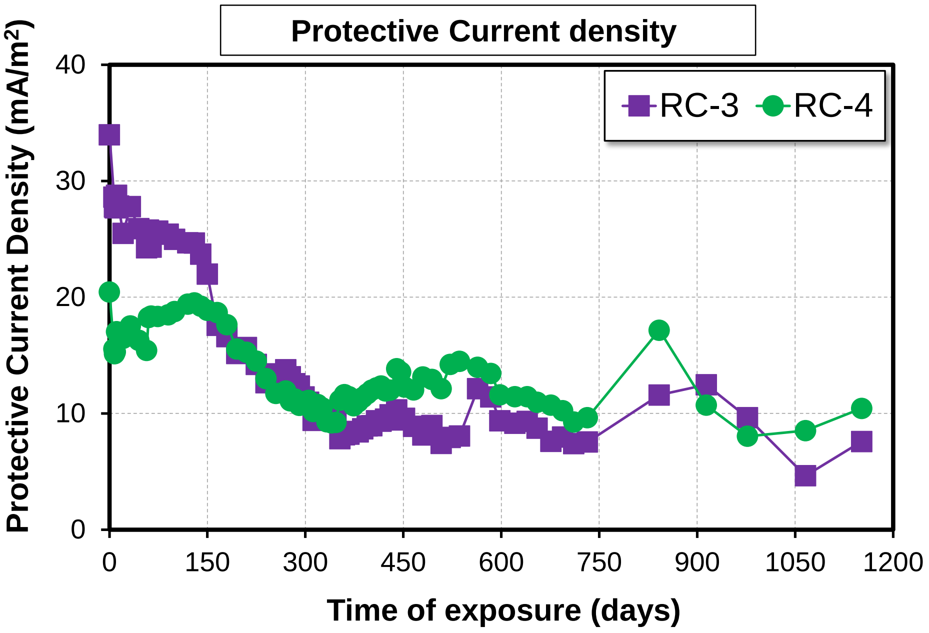

Figure 6.32 Protective current density of the sacrificial Anodes RC3-RC4

Figure 6.32 shows that the protective density of RC3 has excessively exceeded the 20mA/m^2 of the criterion set by the standard until 150 days after the application of the protection and gradually stabilizes at around 10mA/m^2. The current density in RC4 however was comprised between the 2mA/m^2 to 20mA/m^2 from the installation of the anode to the 37 months.

6.3.6 Potential development of sacrificial anodes

Figure 6.33 and *Figure 6.34* shows the development of the instant-off potential of the anode. The potentials were found around -400 mV to -1000mV and a sudden drop was observed until the 150th day for both beams before the potential decreases again. A faster recovery of the potential was observed in RC3 compared to RC4 and at the 37th months the instant-off potential are about -400 mV for RC3 and -800 mV for RC4.

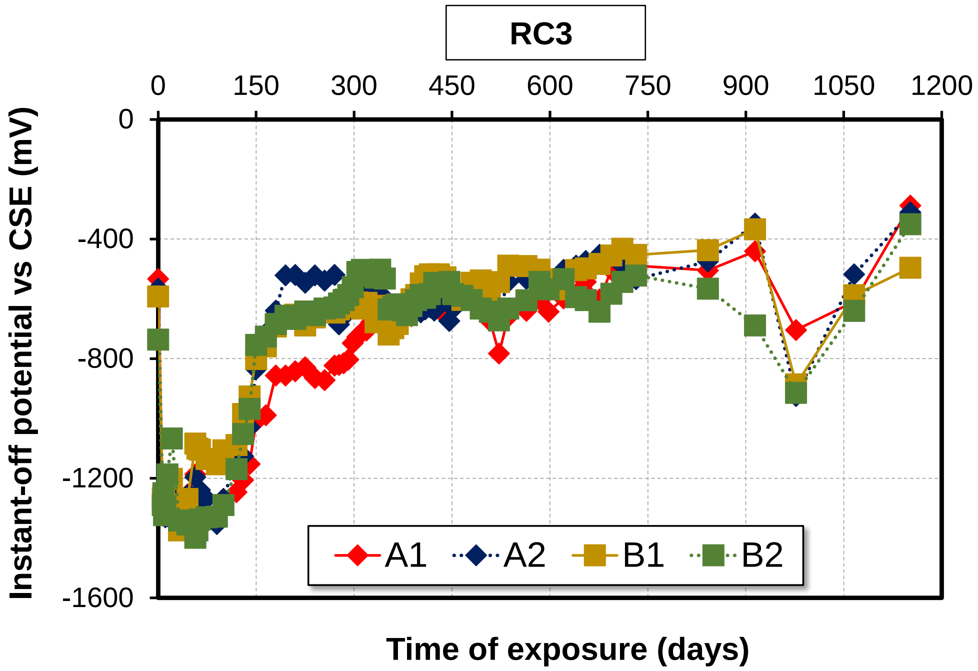

Figure 6.33 Instant-off potential of sacrificial anodes (RC3)

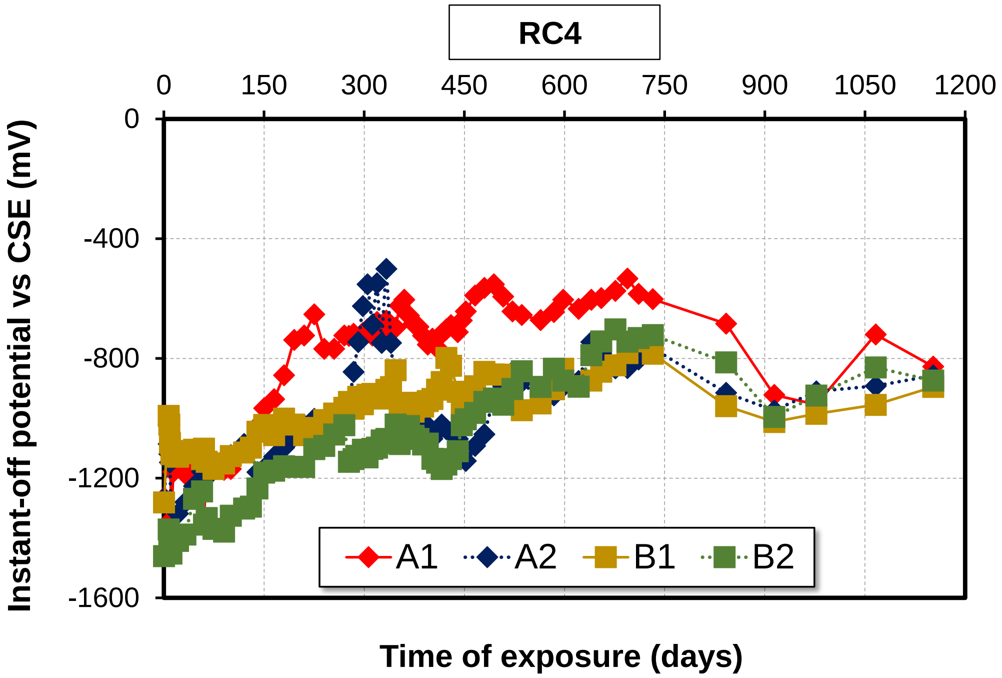

Figure 6.34 Instant-off potential of sacrificial anodes (RC4)

6.3.7 Anodic-Cathodic polarization curve of the anode

The anodic-cathodic polarization curve of the anode is also shifting to the left; it is recovering to a more noble, better passivity grade. It can be associated with the decrease in the protective current density.

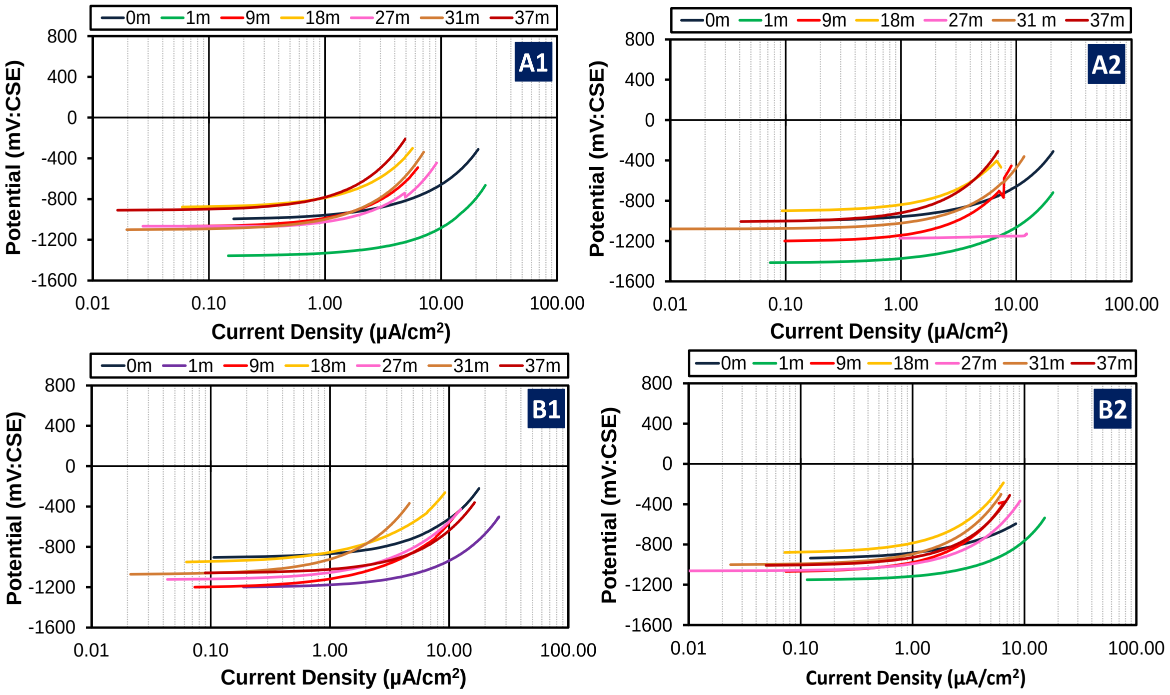

Figure 6.35: Anodic-cathodic polarization curve (RC3)

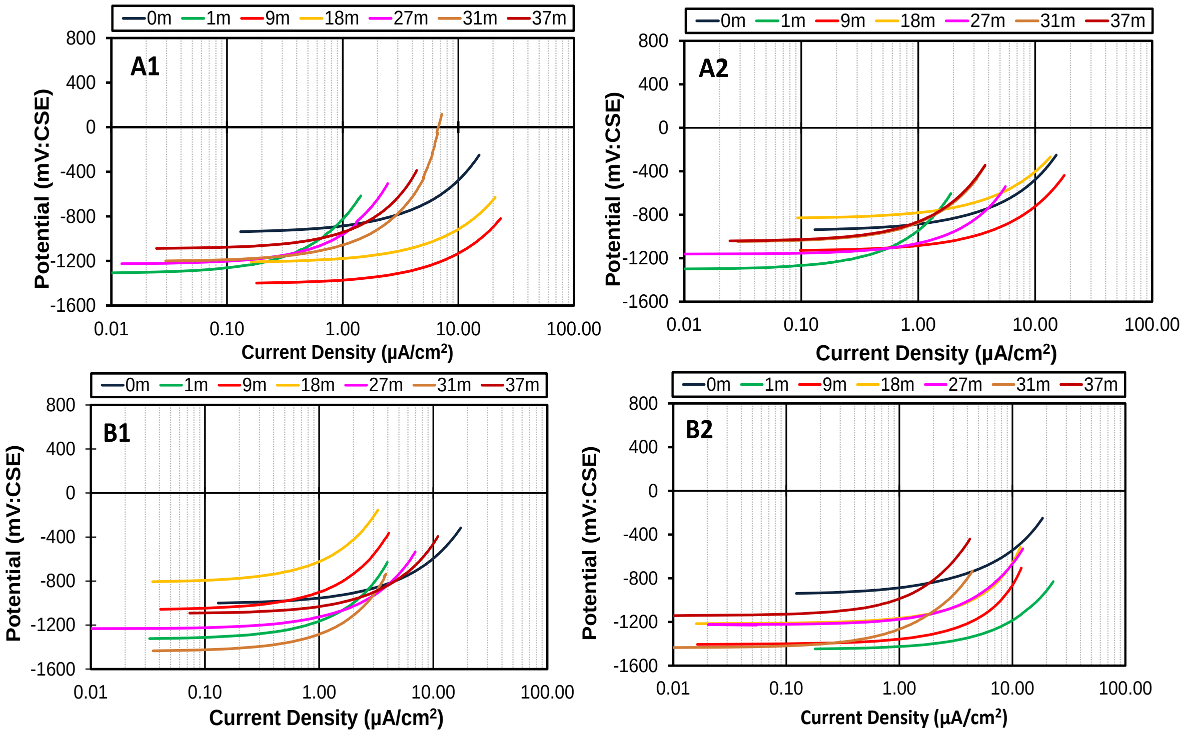

Figure 6.36: Anodic-cathodic polarization curve (RC4)

6.4 CONCLUSION

In this chapter, the effectiveness of the use of corrosion inhibitor and Sacrificial anode cathodic protection was investigated. The results are summarized as followed:

- The effectiveness of the used sacrificial anode was confirmed; however, it was shown that the area affected is relatively small in this surrounding. Therefore, the concrete in the patch area was not affected.
- The protective current in both RC3 and RC4 has decreased with time, nevertheless, it still meets the requirement set by the BS standard (2 to 20mA/m^2), with an average value around 10mA/m2.
- The depolarization value of the beam RC3 was almost zero after 37 months however, the concrete condition is steel improving. In RC4 as well, meeting the 100mV depolarization along the rebar was difficult, nonetheless, the performance of the sacrificial anode is still observed.
- After 37 months of the application of the repair, some sections of the steel in RC4 have reached the “90% no corrosion” zone set by the ASTM standard. Besides, the potential gradient started to disappear in both specimens which is among the primary goal in the use of cathodic protection. In addition, the formation of “Halo effect” [Sergi and Page, 1999; 2000] caused by the application of patch repair (chloride-free) concrete could be avoided as no sign of macrocell corrosion was observed from the electrochemical results.
- On one hand, the less performance of the beam RC3 can also be associated with the high chloride content measured in the beam (6.05kg/m^3) compared to RC4 (3.08kg/m^3). Previous studies showed that the effectiveness of the cathodic protection and the achievement of the 100mV depolarization is highly correlated to the concentration of chloride in the concrete [Oleiwi, 2018].
- On the other hand, the performance of RC4 could be attributed to the application of corrosion inhibitor on the rebar in the section of the patch repair.

6.5 REFERENCE

ACI Committee 222.2R-01, (2001): Corrosion of prestressing steels, American Concrete institute.

Ahmad, I., Suksawang, N., Sobhan, K., Corven, J.A., Sayyafi, E. A., Pant, S., and Martinez, F., (2016): Develop Epoxy Grout Pourback Guidance and Test Methods to Eliminate Thermal/Shrinkage Cracking at Post-Tensioning Anchorages: Phase II, Final Report, Contract No. BDV29-977-13, Florida Department of Transportation.

Ann, K.Y., Ahn, J.H., and Ryou, J.S., (2009): The Importance of Chloride Content at the Concretesurface in Assessing the Time to Corrosion of Steel in Concrete Structures, Construction and Building Materials,23, pp. 239–245.

Belletti, B., Rodrìguez, J., Andrade, C., Franceschini, L., Sànchez, J., and Vecchi, F., (2020): Experimental tests on shear capacity of naturally corroded prestressed beams, *Structural Concrete*, 21, pp. 1777–1793.

Belletti, B., Vecchi, F., Bandini, C., Andrade, C., Sanchez, J., (2020): Numerical Evaluation of the Corrosion Effects in Prestressed Concrete Beams without Shear Reinforcement Structural Concrete., 21 , pp.

Bertolini, L., Elsener, B., Pedeferri, P., and Polder, R.P., (2004): Corrosion of Steel in Concrete, (1st ed.), WILEY-VCH, Morlenbach.

Burdekin, F. M., ant Rothwell, G. P., (1981): Survey of Corrosion and Stress Corrosion in Prestressing Components used in Concrete Structures with Particular Reference to Offshore Applications, Publication 15.632, Cement and Concrete Association.

CEB, (1998): Strategies for Testing and Assessment of Concrete Structures, Bulletin No. 243, 183 pp.

Coronelli, D., Castel, A., Vu, N., and François, R.,(2009): Corroded Post-tensioned Beams with Bonded Tendons and Wire Failure, Eng. Struct., 31 , pp.1687-1697.

Di Prisco, M., (2019): Critical Infrastructures in Italy: State of the art, case studies, rational approaches to select the intervention priorities, Proceedings of the fib symposium: Concrete-Innovations in Materials, *Design and Structures*, Krakow, Poland, pp.49–58.

Dickson, T. J., Tabatai, H., and Whiting, D. A., (1993): Corrosion Assessement of a 34 Years old Precast Post-tensionned Concrete Grider, PCI Journal, 38, No. 6, pp. 44-51.

Domaneschi, C., Pellecchia, M., De Iuliis, E., Cimellaro, G.P., Morgese, M., Khalil, A.A. et al., (2020): Collapse Analysis of the Polcevera Viaduct by the Applied Element Method, Engineering Structures, 214, p. 110659,

Elsener, B., Andrade, C., Polder, R., and Raupach, M., (2003): RILEM TC 154-EMC - Electrochemical for Measuring Metallic Corrosion Materials and Structures, 36, pp. 461-471.

EN 12504-4. Testing concrete- Part 4: Determination of ultrasonic pulse velocity; 2004.

Essamin, O., Holley, M., Great Man Made River Authority (GMRA), (2004): The Role of Acoustic Monitoring in the Management of the World’s Largest Prestressed Concrete Cylinder Pipe Project, In: Proceedings of the ASCE pipeline division specialty congress – Pipeline engineering and, construction, pp.283–290.

Freyermuth, C. L., (1991): Durability of Post-tensionned Prestressed Concrete Structures, Concrete International, 13, No. 10, pp. 58-65.

Hamada, H., Haramo, M., and Otsuki, N., (1987): Ten Years Test on the Effects of Joints on the Durability of Concrete in Marine Environment, Japan Concrete Institute, 9, pp. 147-154.

hmad, I., Suksawang, N., Sobhan, K., Corven, J.A., vallier, R., Sayyafi, A. E., and Pant, S., (2018): Developing Guidelines for Epoxy Grout Pourback Systems for Controlling Thermal/Shrinkage Cracking at Post-Tensioning Anchorages: Full-Scale Testing and Numerical Analysis, Transportation Research Record, pp. 1-10.

Japan Society of Civil engineers (JSCE), (2007): Standards spec-ifications for concrete structures-design, No.15, pp 128-145.

JIS A 1108, (2018): Method of Test for Compressive Strength of Concrete, Japanese Standard Association.

JIS A 1154, (2020): Methods of Test for Chloride ion content in Hardened concrete, Japanese Standard Association.

Jones, R., (1969): Proceedings, International Symposium on Nondestructive Testing of Concrete and Timber, Institution of Civil Engineers, London, pp.1-7.

Lambert, P., Page, C. L., and Vassie, P. R. W., (1991): Investigations of Reinforcement Corrosion Electrochemical Monitoring of Steel in Chloride-contaminated Concrete Materials and Structures, 24, 143, pp. 351-358.

Li, F., and Yuan, Y., (2013): Effects of Corrosion on Bond Behavior Between Steel Strand and Concrete, Construction and Building Materials, 38, pp. 413-422.

Li, F., and Yuan, Y., Li, C.Q., (2011): Corrosion Propagation of Prestressing Steel Strands in Concrete Subject to Chloride Attack, *Construction and Building Material*, 25, pp. 3878-3885,

Manning, D. G.: Durability of prestressed concrete highway structures, NCHRP Synthesis of Highway Practice 140, Transportation Research Board, 1988.

Miyazato, S., (2021): Countermeasure by shielding against macrocell corrosion after patch repair, Concrete J., Vol.59, No.5, pp.452-455. (in Japanese)

Nagataki, S., Otsuki, N., Moriwake, A., and Miyazato, S., (1996): Experimental Study on Corrosion Mechanism of Reinforced Concrete at Local Part, Journal of Materials, Concrete Structures and pavement, n. 544, pp. 109-119 (in Japanese).

Oleiwi, H.M., Wang, Y., Curioni, M. et al., (2018): An Experimental Study of Cathodic Protection for Chloride Contaminated Reinforced Concrete Materials Structure,51, 148.

Otsuki, N., (1985): A Study of effectiveness of the Chloride on Corrosion of Steel Bar in Concrete, Report of Port and Harbor Research Institute, 127-134.

Pfeifer, D., McDonald, D. and Krauss, P., (1994): Rapid Chloride Permeability Test and its Correlation to the 90-day Chloride Ponding Test, PCI J., pp. 38-47.

Schupack, M., (1994): Durability Study of a 35 Years Old Post-tensioned Bridge, Concrete International, 16, No, 2, pp. 54-58.

Singh, S.K., (2000): Corrosion Studies on Prestressing Steel Wire, Ph.D. thesis. Imperial College, University of London.

Soutsos, M.N., Breysse, D., Garnier, V., Goncalves, A., and Monteiro, A.V., (2011): Estimation of on-site Compressive Strength of Concrete, Non-Destructive Assessment of Concrete Structures: Reliability and Limits of Single and Combined Techniques-State-of-the-Art Report of the RILEM Technical Committee 207-INR, 1, pp.119-186.

Takaya,S., Sato, S., Shiomi, H., Yamamoto, T., (2021): Maintenances method focusing on environmental dependence of corrosion products, Concrete J., Vol.59, No.5, pp.398-403. (in Japanese)

Whitehurst, E.A., (1951): Sonic tests concrete structures, Ameri-can Concrete Institute, J. proc., Vol. 47, pp. 433-444.

Yamaoka, Y., and Tanaka, Y., (1993): Comparison of the mechanisms of hydrogen embrittlement and stress corrosion cracking of high carbon steel wire, Int. Workshop on Prestressing Wire, Denver, Colo.

Sergi, G., Page, C.L., (1999): Sacrificial Anodes for Cathodic Protection of Reinforcing Steel around Patch Repairs applied to Chloride-contaminated Concrete, Proc. Eurocode 99, European Corrosion Congress, Aachen, Germany.

Page, C.L., Sergi, G., (2000): Developments in Cathodic Protection applied to Reinforced Concrete. Journal Materials in Civil Engineering, Sp. Issue, Durability of Construction Materials, pp. 8-15.

CONCLUSION AND RECOMMENDATIONS

Summary

Concrete is the material of first preference when it comes to construction and particularly in marine environments. Nevertheless, concrete production is energy intensive and demands outrageous resources, in materials and particularly water. In addition, the emission of carbon dioxide caused by the production of concrete is exorbitant, (or exorbitantly) leading to severe environmental pollution. In addition, in high chloride and severe environments, the performance of concrete structures is diminished as their primary consequences is the corrosion of the reinforcement in concrete. Therefore, providing durable and environmentally friendly concrete structures is of high importance.

The objective of this study is to assess the behaviors and parameters influencing the corrosion of reinforced concrete exposed to marine environment and come up with durable but economically and environmentally friendly concrete structures. Studies related to the effect of joint treatment on the corrosion of concrete structures exposed to a severe environment for more than 30 years were performed highlighting the importance of the use of the appropriate joint. In addition, the effect of initial defects in concrete with different chloride concentrations is investigated.

Contributions and conclusions

Chapter 1. introduces the study, gives an overview of the research, announces the objectives of this research, and outlines the arrangement of the dissertation. The overall purpose of this work is to contribute to the extension of the service life of concrete structures by understanding their behavior due to initial defect, namely the effect of bleeding water and the presences of joint. Beams exposed to severe marine environments for a long-term were investigated. In addition, suggesting an economical and environmentally sustainable preventive and repair method is the ultimate purpose of this study. The studies were centered on the use of electrochemical techniques.

Chapter 2. presents existing and previous studies related to corrosion in reinforced concrete structures exposed to severe environmental conditions. The mechanism of corrosion is detailed, some essential parameters affecting the corrosion of steel reinforcement are described. In addition, an existing and established method used to monitor and assess corrosion is detailed. Moreover, preventive and repair technologies established through previous research were presented. Understanding of previous studies highlights the importance of long-term exposure in the body of literature and are important in order to provide adequate measure regarding the durability of concrete.

Chapter 3. describes the investigation of the prestressed beams exposed to marine environments for more than 30 years. The study aimed at investigating the effectiveness of different joint treatments (mortar and epoxy resin treatments) on the corrosion of the prestressed beams. The beams were exposed to tidal marine environments. Bending loads were applied to the beams during the exposure time (0.1mm and 0.2mm). The investigation showed that the specimen without treatment was in critical condition compared to other beams. The electrochemical results showed that both types of joint treatments are effective in preventing the corrosion of the beams, however, the specimen with wider crack width showed less performance. The visual observation revealed that fracture of the prestressing bar has already occurred in the beams targeting 0.2mm cracks, regardless of the type of treatment. The chloride concentration was significant in all specimens however, the influence of the type of joints used was not distinguished. The compressive strength tests revealed that the beams were classified as high strength even after more than 30 years of exposure to severe environments. The formation of macrocell was observed with a distance between anodic and cathodic area of 5 cm to 10 cm. Further research is still required for a better understanding of corrosion of prestressed concrete in marine environments.

Chapter 4. investigates the effect of the bleeding water on the corrosion of reinforcing steel. Different level of concentration of chloride (0.2%-0.4% and 0.6%) and different shape of steel was used in this study. The rise of water caused the presence of gaps under horizontal steel bar. An increase in the potential and the rate of corrosion is observed with the increase of the height of the location of the steel. In addition, the interfacial gap creates the formation of macrocells between the upper and the lower steel bar. The results of the measurement of the void areas showed that the void is significant in the axial section of the rebar rather than the section nearing the mold during the casting. Water paths were also observed under the rebar. Regarding the effect of the shape of the rebar on the corrosion and the influence of bleeding water, it was observed that the round-shaped, and the square-shaped steel bars are more vulnerable to the effect of the bleeding. The visual observation confirmed that the upper section of the specimen showed larger voids and more corrosion.

Chapter 5. introduces a solution for the issues of corrosion of horizontal steel bars due to the interfacial gap and the problem of water scarcity by investigating the potential of the use of seawater as concrete mixing water. The aim of the study was to investigate the effectiveness of calcium nitrite used as in coating of rebar in seawater mixed concrete. OPC and GGBFS were used as binder. The effect of the concentration of calcium nitrite was distinguished only in the seawater mixed mortar (without coating). The calcium nitrite seems to show the opposite trend when used in GGBFS specimen. The use of coating was found to be effective in limiting the rate of corrosion and the diffusion of oxygen in the concrete, which highlights the effectiveness of the coating. Further study is necessary to investigate the performance of calcium nitrite in case the concentration is increased.

Chapter 6. shows the study done to provide an appropriate repair method using sacrificial anode cathodic protection. Two beams (RC3 and RC4) of more than 40 years were investigated. Sacrificial anodes were applied in the patch repair area of both beams and corrosion inhibitor was added to the one beam (RC4). The results after 37 months of monitoring showed that the chosen protection is still effective to recover the potential of the rebar. The gradient of potential is disappearing with time, and the instant off potentials of each rebar are higher than 1100mV, however, the depolarization for RC3 and RC4 has decreased. Those results are evidence of the effectiveness of the methods as well. The beam RC4 shows better performance compared to RC3 as some of its rest potential has reached -200mV threshold which signifies that the steel bars are starting to be passive to corrosion. The better condition of RC4 could be attributed to the use of a corrosion inhibitor as a coating for the rebar in the patch repair area. In addition, the concentration of chloride in RC4 is 50% less than the concentration of chloride in RC3.

Future work and recommendations

In this study, the durability of reinforced concrete in marine environment was investigated from old and new specimens. For sustainable several parameters need to be considered.

1. The presence of joints has a great impact on the early deterioration of concrete structures even in high strength concrete. Therefore, ensuring a good quality of joint is important for a long-lasting structure. Both epoxy and mortar are effective in mitigating corrosion.

2. The presence of void in the interface steel-concrete engendered by the bleeding in concrete is strongly affecting the corrosion of the steel reinforcement. Enhancing the density

of the concrete-steel interface significantly constraints the diffusion of oxygen and the ingress of the aggressive agents in the steel. Calcium nitrite shows better effectiveness when admixed with OPC binder.

3. The use of inhibitor was shown the enhance the effectiveness of sacrificial anode cathodic protection.

Corrosion has not yet occurred in the new specimens used in this study; therefore, long-term monitoring is yet required to assess their performance. In addition, in future work, a slight increase in the content of CNI could show better performance in the mortar coating of steel.